THE SEDIMENTOLOGY OF MID TO LATE MIOCENE CARBONATES AND EVAPORITES IN SOUTHERN CYPRUS

S. EATON

SUBMITTED FOR DEGREE OF DOCTOR OF PHILOSOPHY

UNIVERSITY OF EDINBURGH

1987

EX BIBL. UNIV. EDINBURGH

DECLARATION

The content of this thesis is the original work of the author and has not previously been submitted for a degree at this or any other university. Other peoples work is acknowledged by reference.

Simon Eaton
Grant Institute of Geology
University of Edinburgh

The copyright of this thesis rests with the author. No quotation from it should be published without his prior consent, and information derived from it should be acknowledged.

ACKNOWLEDGEMENTS

I would like to thank my supervisor, Alastair Robertson, for his enthusiasm and support during the course of this project, and the staff of the Grant Institute in general for making my three and a half years in Edinburgh an enjoyable and stimulating time. Friends and collegues, among them Phil Bentley, John Boyle, David Braunholtz, Alice Carter, Tristan Clube, Dave Cooper, Steve Farrell, Ken Greig, Andy Martin, Steve Rainey, Graham Shimmield, Pauline Smedley and Jo Taylor, provided a much appreciated non-academic environment.

In Cyprus, the Geological Survey Department, in particular Drs. Andreas Panayiotou and Costas Xenophontas, were very welcoming and helpful. Andreas and Melani of Governor's Beach, and the people of Pendakomo village, provided hospitality in the Cyprus tradition that will remain with me.

John Boyle, Tristan Clube, the late Steve Farrell, and Bram Murton all contributed to discussions in the field. In particular, Steve Farrell's enthusiastic reaction to the slumps in Cyprus has contributed to the interpretation of these exposures as presented in this thesis and is warmly acknowledged. He was a close friend and is missed.

Mr. Greig, Janis and an anonymous Cypriot on the Akamas peninsula all performed miracles with the field vehicle. My brother Mark accompanied me on two eventful return journeys across Europe and kept things moving despite a blown piston and failed clutch.

This work was funded by a NERC Research Studentship, which is gratefully acknowledged. Compilation benefited from computer hard- and software provided by my brother Mark and photographic equipment provided by Kevin Hird and Anne Wright.

Finally, I hold most valuable the deep support of my wife Alice, my father Jim, my late mother Mavis, my brothers Mark and Paul, and my sister Katharine.

CONTENTS

CHAPTER 1 INTRODUCTION

1.1 Scope of work 1
1.2 Geographical setting 1
1.3 General geological history of the Troodos Massif 4
1.4 Mesozoic rocks of southern Cyprus 7
1.5 Area of study and previous work 10
1.6 Methods 10
1.7 Layout 11

CHAPTER 2 STRATIGRAPHY

2.1 Introduction 13
2.2 Pakhna Formation 13
.1 Lithological characteristics 13
.2 Lithological subdivision by past workers 15
.3 Relationship to Lefkara Formation 15
2.3 The Koronia Limestone Member 19
.1 Status 19
.2 Lithological characteristics 20
.3 Relationship to underlying formations 20
2.4 Kalavasos Formation 22
.1 Status 22
.2 Lithological characteristics 24
.3 Relationship to Pakhna Formation 24
.4 Relationship to Koronia Limestone Member 25
2.5 Chronocorrelation of lithostratigraphic units 26
.1 Introduction 26
.2 Biostratigraphic framework 26
.3 Application of published data 30
.4 New data 34
2.6 Summary of revised stratigraphy 35

CHAPTER 3 LITHOFACIES OF THE PAKHNA FORMATION

3.1 Introduction 37
3.2 Lime mudstone lithofacies 38
.1 Occurrence 38
.2 Field character 38
.3 Petrology 39
.4 Discussion 40
.5 Interpretation 42
3.3 Marlstones 43
.1 Occurrence 43
.2 Field character 43
.3 Petrology 44
.4 Discussion 44
.5 Interpretation 46
3.4 Laminated calcilutites 46
.1 Occurrence 46
.2 Field character 46
.3 Petrology 47
.4 Discussion 47
.5 Interpretation 47
3.5 Calcarenites 48
.1 Occurrence 48
.2 Field character 48
.3 Petrology 50
.4 Discussion 51
3.6 Rudites 54
.1 Introduction 54
.2 Field description 55
.3 Discussion 58
.4 Interpretation 61
3.7 Slumps 62
.1 Introduction 62
.2 Description 62
.3 A model of slump fold development 63
.4 Discussion 70
.5 Interpretation 77
3.8 Comparison with the facies scheme of Walker & Mutti 77

CHAPTER 4 FACIES ASSOCIATIONS OF THE PAKHNA FORMATION

4.1 Introduction 81
4.2 General depositional setting 81
4.3 Environmental criteria 82
4.4 Perpheral sands association 83
4.5 Gullied slope association 83
.1 Introduction 84
.2 Hemi-pelagic sequences 84
.3 Channel-fill sequences 85
.4 Development history of channel-fill sequences 89
.5 Summary 90
4.6 The basin margin association 91
4.7 The basin plain association 92
4.8 Aprons versus fans 93
4.9 Summary 94

CHAPTER 5 BASIN RECONSTRUCTION

5.1 Introduction 97
5.2 Vertical trends 97
.1 Introduction 97
.2 Large scale coarsening upwards cycle 97
.3 Compositional variation of clastic material 99
.4 Compositional variation of calcilutites 99
.5 Ichnofacies 99
.6 Microfossil variations 100
5.3 Slumps as palaeoslope indicators 100
.1 Introduction 100
.2 Slump data 101
.3 Ayia Phylla 101
.4 Happy Valley 104
.5 Conclusions 104
5.4 Palaeocurrent data 107
5.5 Sedimentation rates 108
5.6 Spacial arrangement of facies 110
5.7 Evidence for the Akrotiri High 114
.1 Introduction 114
.2 Borehole and field data 114
.3 Mammonia chert pebbles in the Pakhna Formation 118
5.8 The Khalassa and Maroni sub-basins 124
.1 Introduction 124
.2 Structural considerations 124
.3 Clastic provenence and dispersal patterns 126
.4 Depocentres 127
5.9 Clastic source environments 130
5.10 A basin model for the Pakhna Formation 133

CHAPTER 6 THE KALAVASOS FORMATION AND ITS ENVIRONMENTAL INTERPRETATION

6.1 Introduction 136
6.2 The Messinian Event in the Mediterranean 136
6.3 Lithofacies of the Kalavasos Formation 140
.1 Introduction 140
.2 Parallel laminated gypsum 141
.3 Nodular laminated gypsum 142
.4 Graded gypsum 145
.5 Chaotic selenite 146
.6 Banded selenite 147
.7 Contorted gypsum 148
6.4 The onset of evaporitic conditions 149
.1 The transition to gypsum deposition 149
.2 Significance of some limestone conglomerates 152
6.5 Vertical sequences and associations 154
.1 The Maroni sub-basin 154
.2 The Khalassa sub-basin 157
.3 Other evaporites of the circum-Troodos belt 160
6.6 A depositional model 160
6.7 Other aspects 163
.1 Sedimentation rates 163
.2 The virtual absence of non-evaporitic input 167
.3 A final note on water depths 168

CHAPTER 7 THE YERASA FOLD AND THRUST BELT

7.1 Introduction 170
7.2 Deformation style 173
.1 The Moni Formation 173
.2 The Lefkara Formation 173
.3 The Pakhna Formation 175
.4 Basement lithologies 175
.5 Orientation of structures 176
7.3 A locally developed Miocene unconformity 176
7.4 Interpretation of observations 177
7.5 Tectonic significance of the Koronia Limestone Member 179
7.6 Structures of the Limassol Forest block 179
7.7 Evidence for earlier fault activity 181
.1 A parallel fault line in the Maroni sub-basin 181
.2 Evidence for earlier fault activity 183
.3 Possible influence on calciturbidite deposition 185
7.8 Summary 185

CHAPTER 8 SYNTHESIS

8.1 Introduction 187
8.2 Early development of the Troodos basement 187
8.3 Late Cretaceous reorganisation of basement 188
8.4 Tertiary uplift 191
8.5 Miocene tectonics on Cyprus 191
8.6 The plate tectonic setting of Cyprus 197
8.7 A plate tectonic related uplift mechanism 201
8.8 Contrasting deformation styles 202
8.9 Tectonics, sea-level changes, and evaporite deposition 204

CHAPTER 9 CONCLUSIONS 207

REFERENCES 210

PLATES 221

APPENDIX 1 Range charts 238
APPENDIX 2 Nannofossil extractions 245
APPENDIX 3 Isotope data 247
APPENDIX 4 Selected logs 248
APPENDIX 5 Published paper 259

ABSTRACT

This thesis is concerned with the sedimentological interpretation of the Pakhna and Kalavasos Formations in southern Cyprus. These comprise the Middle and Upper Miocene sedimentary cover of the Troodos ophiolite. Fieldwork has been concentrated in the Limassol and Larnaca Districts.

The sediments of the Pakhna Formation record the uplift and unroofing of the Troodos ophiolite, and were deposited in two structurally controlled sub-basins (the Khalassa and Maroni sub-basins). Basin geometries have been determined by a combination of slump, palaeocurrent and facies analysis. Sediments form a regressive basin-fill sequence of hemi-pelagic marls and clastic carbonates shed by gravity driven processes from a neritic environment into deeper water. Lithofacies are organised into four facies associations. These are, in proximal to distal order, peripheral sands, gullied slope, basin margin, and basin plain.

Uplift of basin-bounding blocks culminated in Late Miocene times with local steep thrusting over adjacent sediments, forming a narrow linear deformation zone known as the Yerasa fold and thrust belt. This episode was associated with the development of linear structural highs elsewhere on Cyprus and in the adjacent off-shore areas, and has been related to the convergence of the African and European plates.

Large quantities of bioclastic material, with admixed erosion products from emergent basement areas, were shed into the Maroni and Khalassa sub-basins during this episode.

Preliminary sea-level fluctuations prior to the Messinian desiccation of the Mediterranean Sea resulted in the development of refluxing evaporitic conditions in southern Cyprus, and the deposition of the gypsum sediments of the Kalavasos Formation. In the study area, these lithologies are of an entirely subaqueous origin,

and were deposited in relatively deep water conformably upon the Pakhna Formation. Down-slope reworking of clastic gypsum by gravity controlled processes was prevalent during the deposition of this unit.

With the continuing draw-down of the Mediterranean, the evaporite basins of southern Cyprus are inferred to have been isolated and completely dry before deposition of gypsum occurred on the abyssal plain of the Mediterranean.

CHAPTER ONE
INTRODUCTION

1.1 Scope of work

This project is primarily concerned with the study and interpretation of the Pakhna and Kalavasos Formations of southern Cyprus. These comprise the Middle and Upper Miocene *in-situ* sedimentary cover of the Troodos ophiolite.

Three field seasons were concentrated in the Limassol and Larnaca Districts on the south and southeastern side of the exposed ophiolitic basement (fig. 1.3). This work has involved geological mapping of key areas, lithological logging and sampling, with an emphasis on sedimentology in the first instance. Stereographic air photos were used to extend the mapping and facilitate basin analysis. Reconnaisance work on relevant formations in the Polis Graben (fig. 1.2) area has also been undertaken.

Some structural data have been collected and analysed using an adaptation of Nigel Woodcock's STATIS programme. Laboratory work at Edinburgh has included petrographic study of samples, X-ray diffraction of insoluable residues, and scanning electron microscope examination of the finer grained rocks. However, it should be stressed that this project has involved the study, over a relatively large area, of a series of sediments which have remained largely uninterpreted since the early sixties, and most of the conclusions of this study are based upon the findings of traditional fieldwork.

Results have been combined to produce the environmental and tectonic interpretation presented in this thesis.

1.2 Geographical setting

Cyprus is one of the larger Mediterranean islands, with a surface area of 9250 square kilometres. It lies in the northeast corner of the Mediterranean Sea, approximately centred on latitude 35 S and longitude 33 E,

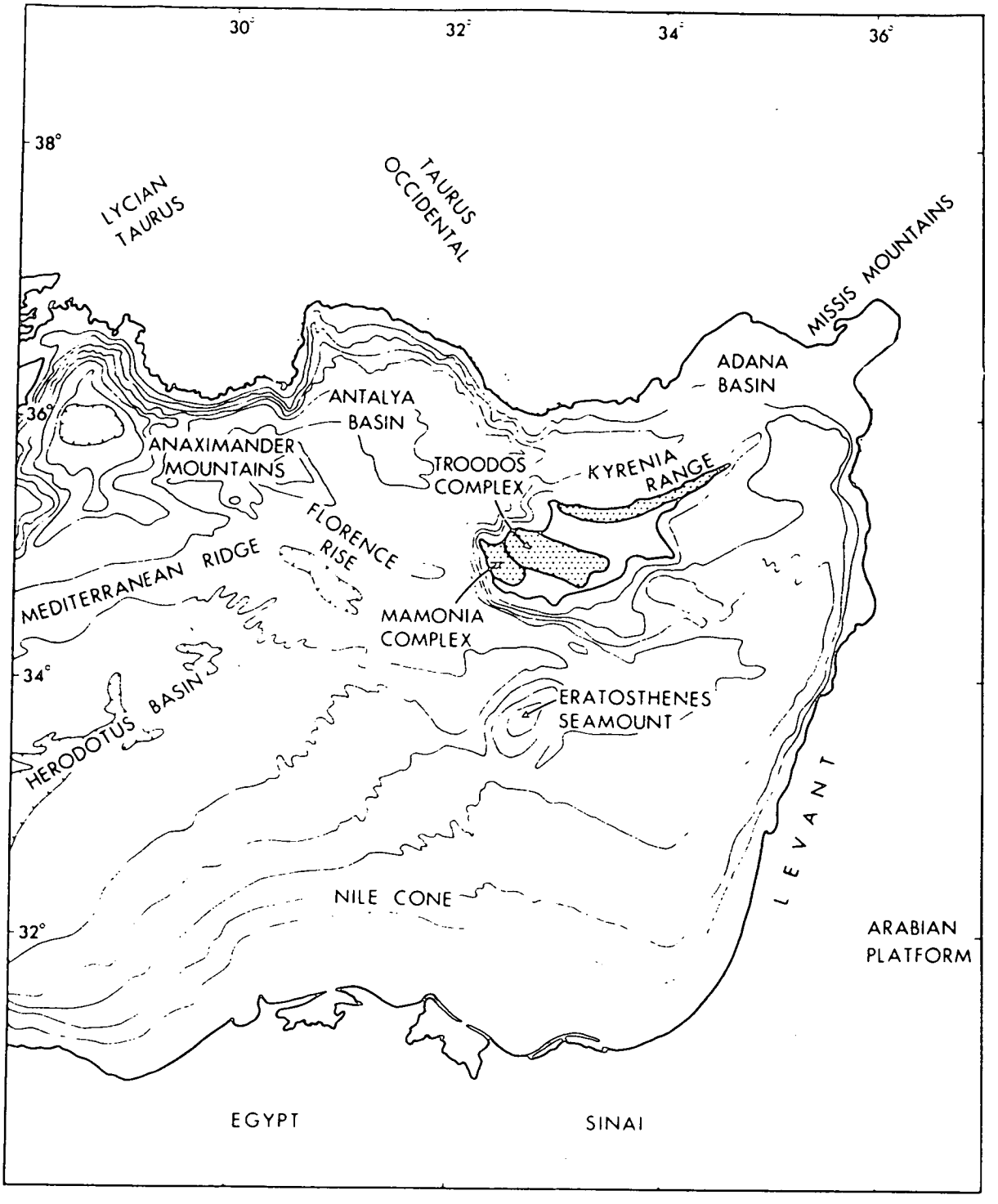

FIG. 1.1 Outline map of the Eastern Mediterranean. Bathymetric contours at 500 m intervals.

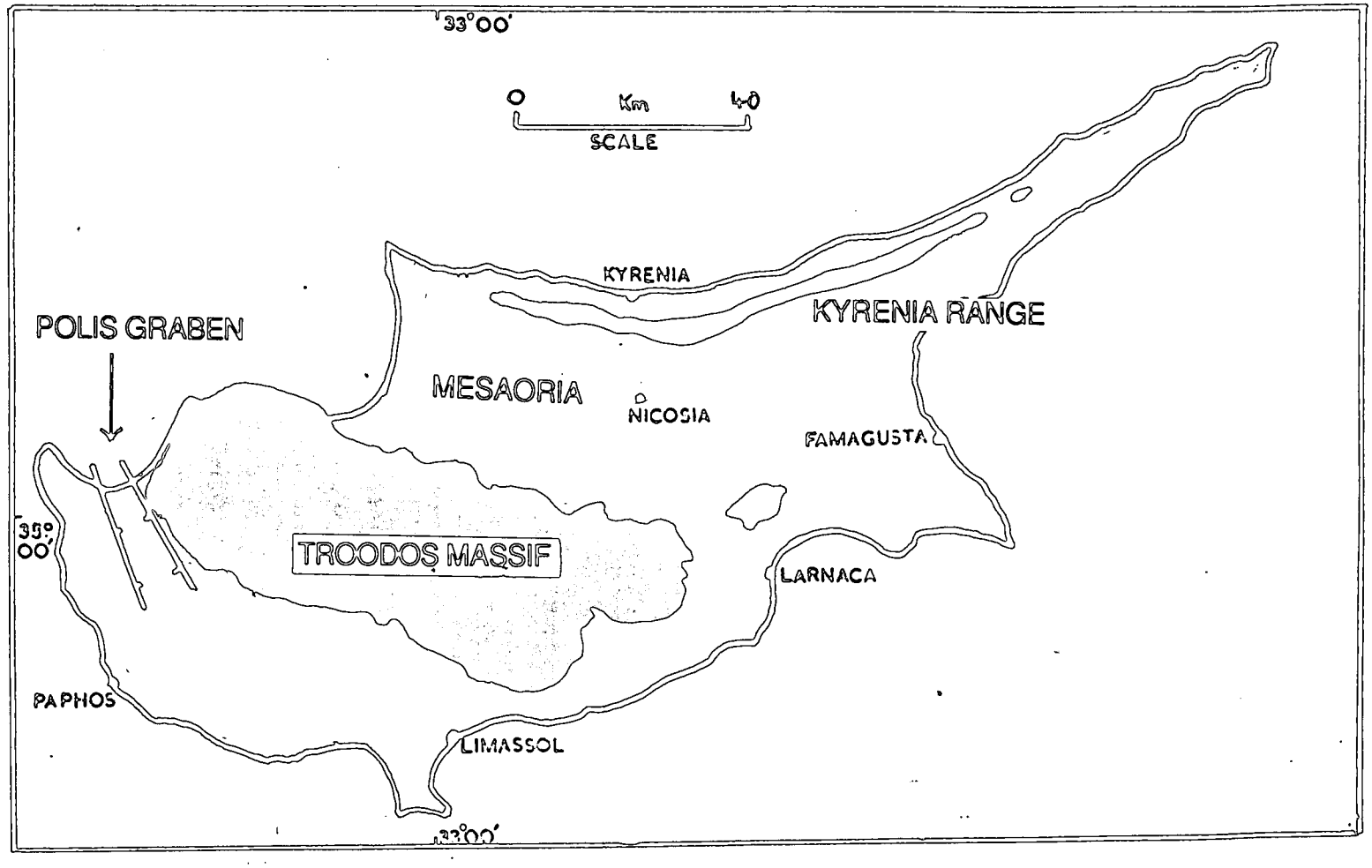

FIG. 1.2 Main topographic features of Cyprus.

and is only 65 km from the Turkish mainland to the north, and 95 km from the Syrian coast to the east (fig. 1.1). Topographically, it can be divided into three main regions; the Kyrenia Range to the north, the Troodos Mountains to the south, and the broad fertile plain of the Mesaoria inbetween (fig. 1.2).

The Kyrenia Range runs parallel to the north coast. It is a narrow, spectacular belt of mountains, rising to elevations approaching 1000 m. Geologically, it consists mainly of thrust slices of Permian to Cretaceous limestones, flanked by concurrent flysh deposits of Oligocene to Miocene age.

The Troodos Mountains are about 100 km east-west and 35 km north-south. They consist of basic and ultramafic igneous rocks, rising to a maximum height of 1951 m (Mount Olympos). Though steeply incised and rugged, the Troodos Massif is a broadly domal mountain region, in marked contrast to the narrow linear belt of the Kyrenia Range. The Polis Graben is a small northwest orientated Pliocene graben superimposed on the southwestern flank of the Troodos Massif (fig. 1.2)

The two mountain ranges are separated by the Mesaoria plain, which extends east-west across the middle of the island. This is formed of Pliocene to Recent sediments and is a lowland area.

1.3 General geological history of the Troodos Massif

The Troodos Massif is one of several ophiolitic complexes exposed in the Eastern Mediterranean area. These are widely accepted as having formed at oceanic spreading centres, and represent preserved fragments of Tethyan oceanic lithosphere.

The Troodos ophiolite is remarkably undeformed, and preserves a normal ophiolitic stratigraphy, with tectonised harzburgites, cummulate gabbros, sheeted dykes, and extrusive pillow lavas. These are overlain by an *in-situ* cover of Turonian (Blome & Irwin, 1985) to Recent sediments.

Stratigraphical nomenclature is based on the work of Henson et al. (1949). More detailed work, by officers of the Cyprus Geological Survey Department (eg. Wilson, 1959; Bagnall, 1960; Bear & Morel, 1960; Gass, 1960; Pantazis, 1967), and more recent studies (eg. Swarbrick & Robertson, 1980), have resulted in the more refined stratigraphy of current usage summarised in Table 1.1.

Immediately overlying the pillow lavas of the ophiolitic basement are metalliferous sediments (umbers) and deep-sea radiolarian mudstones of the Perapedhi Formation. These are developed locally , in hollows on the pillow lava surface, and are up to 60 m thick. They were deposited during, and immediately after, extrusion of the pillow lavas in an oceanic spreading zone.

The overlying Lefkara Formation is up to 700 m thick, and consists of pelagic chalks and calciturbidites. Occurrence of calciturbidites is largely limited to the Middle Lefkara Chalk-Chert unit. They contain pelagic foraminiferal material reworked by turbidity currents on an unstable deep marine slope (Robertson, 1976). Replacement by chert is partial and selective, and has occurred preferentially at the base of calciturbidite beds, resulting in bedding-parallel chert banding.

The Lefkara Formation is overlain by the Pakhna Formation, which is up to 300 m thick. Deposition was continuous with the sediments of the Lefkara Formation. It is characterised by chalks and hemi-pelagic marls, with an up-sequence increase in the content of fine terrigenous material. Reworked carbonates (the Koronia Limestone unit) and some ophiolite-derived clastics also occur. These deposits record the uplift and emergence of the Troodos ophiolite.

The Kalavasos Formation is a gypsum deposit up to 30 m thick (possibly more in the sub-surface). It is correlated on a lithological basis with the Messinian evaporites of the Mediterranean region. Previously, they were interpreted as shallow hyper-saline lagoonal deposits, but this study shows them to be of a deeper,

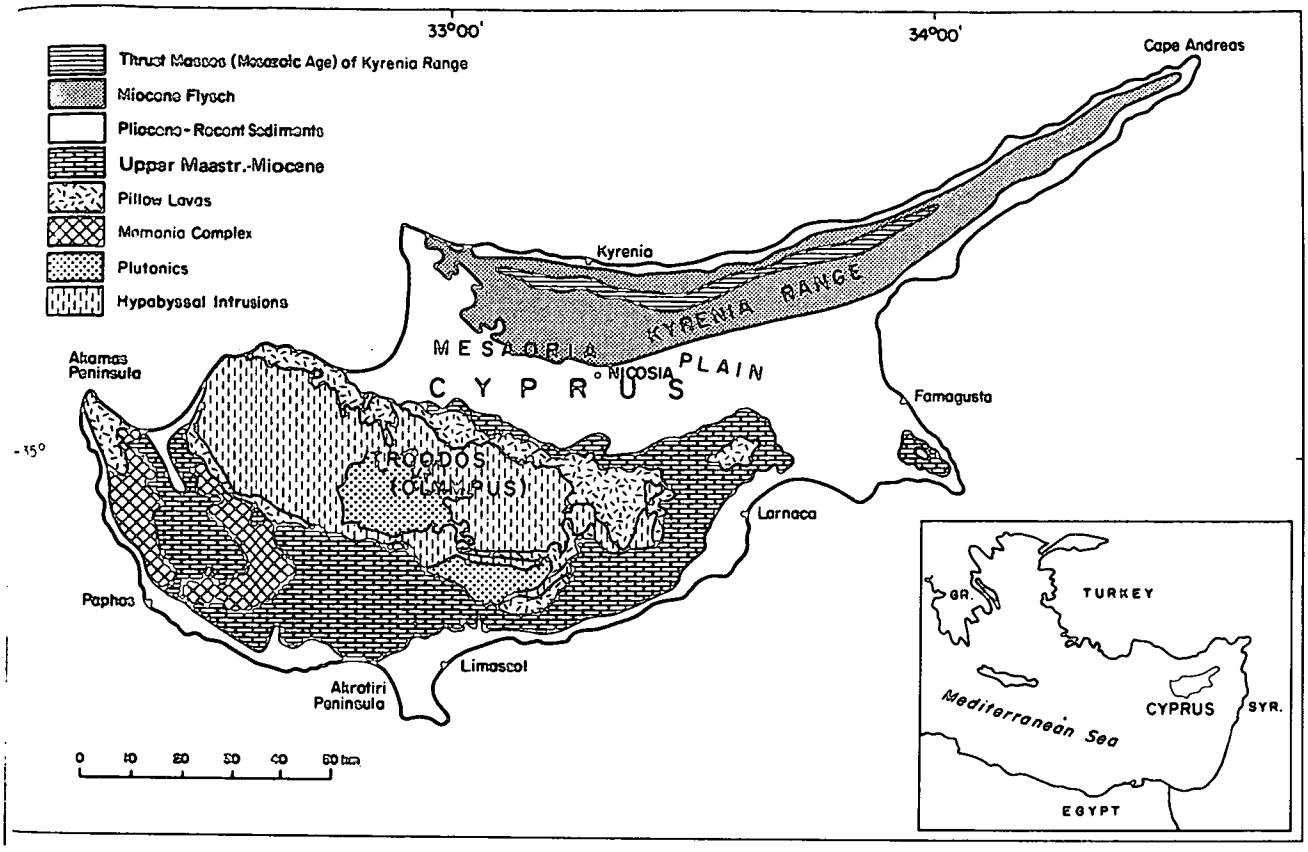

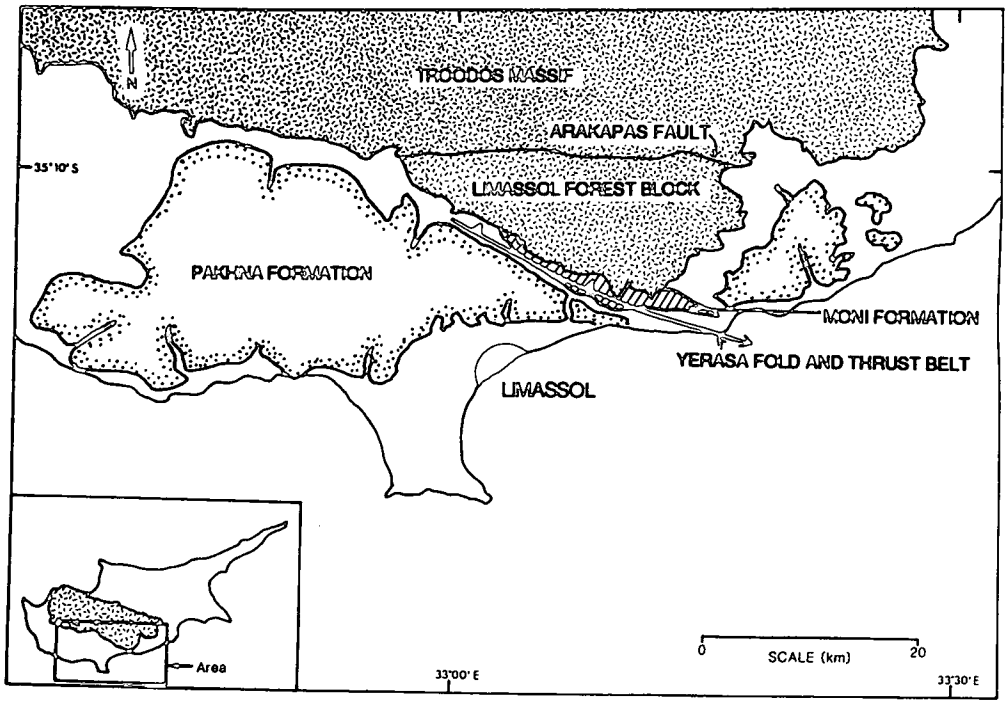

FIG.1.3 Outline geological map of Cyprus (above), and features in the study area (below).

permanently sub-aqueous nature. They mark the top of a mega-regressive sedimentary sequence overlying the Troodos ophiolitic basement.

A basal Pliocene transgression in Cyprus was followed by the deposition of marine marls and ophiolite-derived clastics of the Mirtou, Nicosia, and Anthalassa Formations. Pleistocene uplift of the island is marked by the deposits of the Fanglomerate unit, and by the development of a series of marine terraces.

Structurally, the Troodos Massif is anteformal, with an axis plunging to east and west. Pleistocene uplift, centred on a rising serpentinite diapir beneath Mount Olympos (Gass and Masson-Smith, 1963), has resulted in an annular outcrop pattern, with deepest structural levels exposed at the centre (Wilson, 1959). This is also seen in the outcrop pattern of the sedimentary cover, which is preserved on the flanks of the Troodos Massif and dips gently away from the exposed basement. This structure can be simply described as an eroded dome, elongated in an east-west direction (fig. 1.3).

In the southeast part of the exposed Troodos basement is a block of anomalous oceanic crust known as the Limassol Forest block (fig. 1.3). This is separated from the main massif to the north by a major east-west fault. This is the Arakapas fault, which has been interpreted as a fossil oceanic transform fault (Moores & Vine, 1971). To the south, the Limassol Forest block has been thrust over the adjacent sediments, producing a narrow linear zone of deformation known as the Yerasa fold and thrust belt. This tectonic episode is associated with the Miocene uplift history of the Limassol Forest block (Robertson, 1977a), which has been a major influence on sedimentation of the Pakhna Formation in the area of this study.

1.4 Mesozoic rocks of southern Cyprus

In southwestern Cyprus, a complicated series of Mesozoic rocks are exposed (fig. 1.3). These are collectively known as the Mamonia Complex, and comprise a

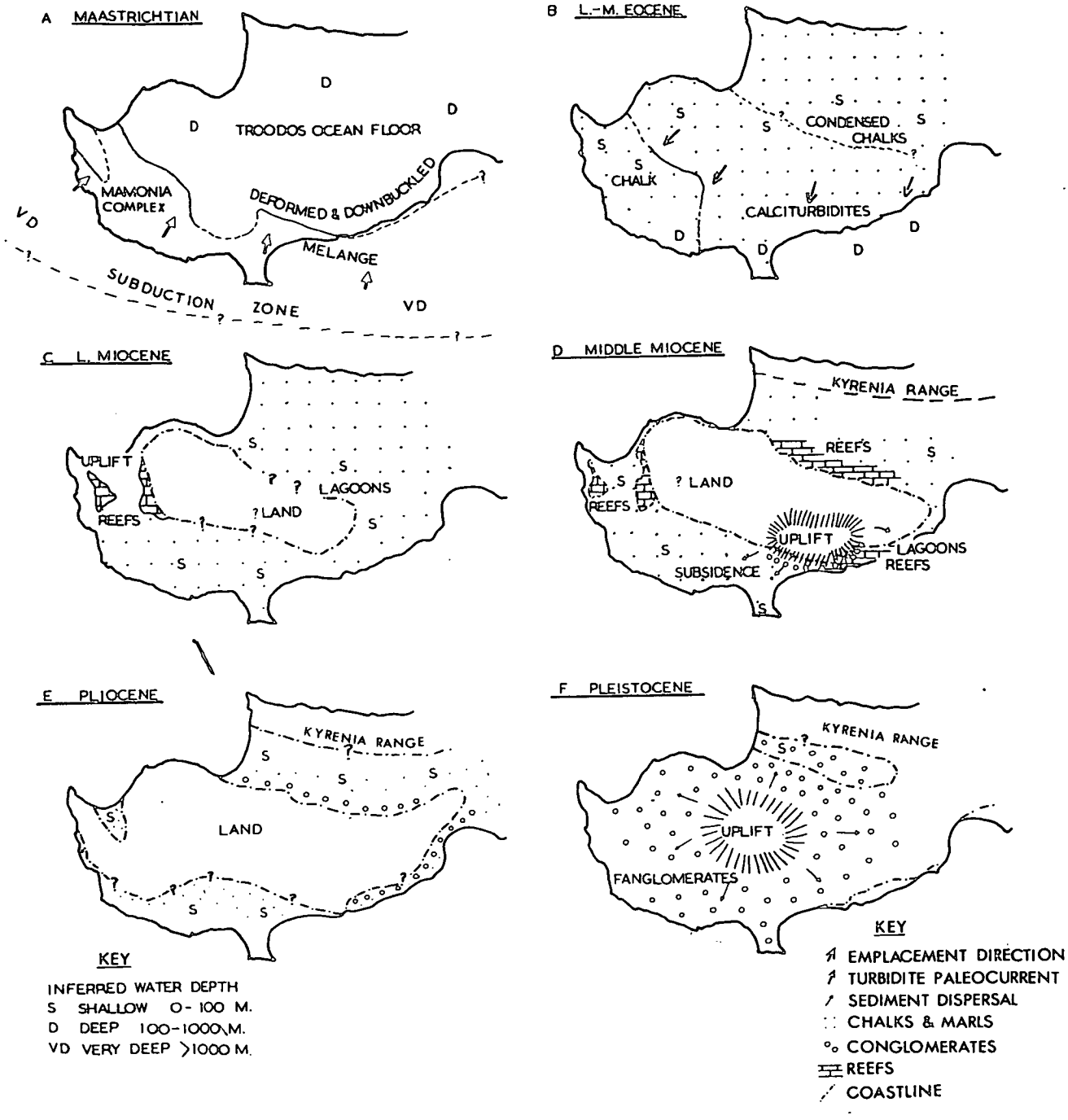

FIG 1.4 Reconstruction of chief features of Maastrichtian to Holocene palaeogeography of southern Cyprus. From Robertson (1977a).

series of passive continental margin type lithologies (the Ayios Photios Group) emplaced by low angle faulting upon a basement of oceanic lavas (the Dhiarizos Group), see Robertson & Woodcock (1979) for discussion. These lithologies are quite distinct from those of the Troodos ophiolite and its in-situ sedimentary cover. They are juxtaposed against Troodos-type crust by high angle faults (Swarbrick, 1980). This must have occurred in Late Cretaceous times as all units and structures are draped by pelagic chalks of the Lefkara Formation.

Mamonia-type lithologies are also exposed as exotic blocks in the Moni Formation of southern Cyprus. This occurs on the southern margin of the Limassol Forest block (fig. 1.3), and comprises Mamonia-type olistoliths in an in-situ matrix of bentonitic clays and radiolarian mudstones of Maastrichtian age (Robertson, 1977c). This unit thins northwards, from several hundred metres to nothing, wedging out completely against the pillow lavas and Perepedhi Formation of the Limassol Forest block. It is overlain conformably by the Lefkara Formation. The deposition of the Moni Formation is thought to be associated with the same phase of Late Cretaceous submarine tectonism that juxtaposed Mamonia- and Troodos-type units in southwestern Cyprus.

Palaeomagnetic work on Cyprus established that the Troodos ophiolite has undergone a 90 degree counter-clockwise rotation since its formation (Shelton & Gass, 1980). It was originally suggested that the most likely time for this to have occurred was during the Miocene. It was expected, therefore, at the outset of this project to find some indication of rotation-related strike-slip sedimentation in the Pakhna Formation. However, no such indication was found, and during the course of this study it became clear from detailed palaeomagnetic studies on a related project (Clube, 1985) that the rotation of the Troodos micro-plate was largely completed by early Tertiary times. It now appears that rotation was related to the Late Cretaceous tectonism involving also the

Mamonia Complex and the Moni Formation olistostrome.

Thus, an understanding of the complexities and structural relationships of the Mesozoic sequences is not directly relevant to an account of the Pakhna and Kalavasos Formations, and they can be regarded simply as a basement variation. Some reference is made to them in discussing source material for erosion products found in the Pakhna Formation (chapter 3), and the Moni Formation is a part of the Yerasa fold and thrust belt described in chapter 7.

1.5 Area of study and previous work

Fieldwork has been concentrated in the Limassol and Larnaca Districts, to the south and east of the Limassol Forest block (fig. 1.3).

Geological maps (at a scale of two inches to the mile) and accompanying memoirs of this area have been published by the Cyprus Geological Survey Department (Bagnall, 1960; Bear & Morel, 1960; Pantazis, 1967). Local hydrogeological surveys have also been reported (Greitzer & Constantinou, 1969; Hadjistavrinou & Constantinou, 1977). Robertson (1977a) published an account of the Tertiary uplift of Cyprus (fig. 1.4), which includes descriptions and interpretations of Middle and Upper Miocene sequences relevant to this work. However, detailed sedimentological work concentrating on an interpretation of the Pakhna and Kalavasos Formations and their sedimentary environments has not previously been reported.

1.6 Methods

The findings of this thesis are based largely upon conventional field mapping, section logging, and thin section examination of samples. Fine grained rocks have been examined under the scanning electron microscope. X-ray diffraction analysis of fine grained components was performed. Samples were disaggregated by mechanical grinding and the use of an ultrasonic bath before wet mounting and air drying. All samples were also glycolated.

The principles and techniques described by Brindley & Brown (1980) were adhered to.

Micropalaeontological analysis of nannofossil extractions has been undertaken by Hilary Stowe (London) on two samples, and results are recorded in Appendix 2. Micropalaeontological data have been referred to the correlation system used by the DSDP Scientific Party on Leg 42 (Hsu et al., 1978), and the time scale with which it is correlated is the one used throughout this thesis (see section 2.5.2).

A few selected samples were analysed for oxygen and carbon isotope ratios. These data do not form a significant contribution to this thesis, but are recorded in Appendix 3.

1.2 Layout

Chapter 2 discusses the stratigraphy of the Middle and Upper Miocene units in terms of field relationships and available micropalaeontological data.

Chapters 3, 4 and 5 are concerned with the sedimentological interpretation of the Pakhna Formation. Chapters 3 and 4 are largely descriptive, being concerned with the individual lithofacies and their vertical associations. An interpretation of the depositional environments, and a reconstruction of the basin geometry is undertaken in Chapter 5.

Chapter 6 describes and presents a depositional interpretation of the Kalavasos Formation evaporites.

Chapter 7 is concerned with the structure of the Yerasa fold and thrust belt, and relates the associated episode of deformation to its effects upon the sedimentation of the Pakhna Formation.

Chapter 8 synthesises the findings of previous chapters, and places them in the context of the plate tectonic setting of Cyprus in the Eastern Mediterranean.

The conclusions of this thesis are summarised in Chapter 9.

Ancillary data, including sedimentary logs, are

included in the appendices.

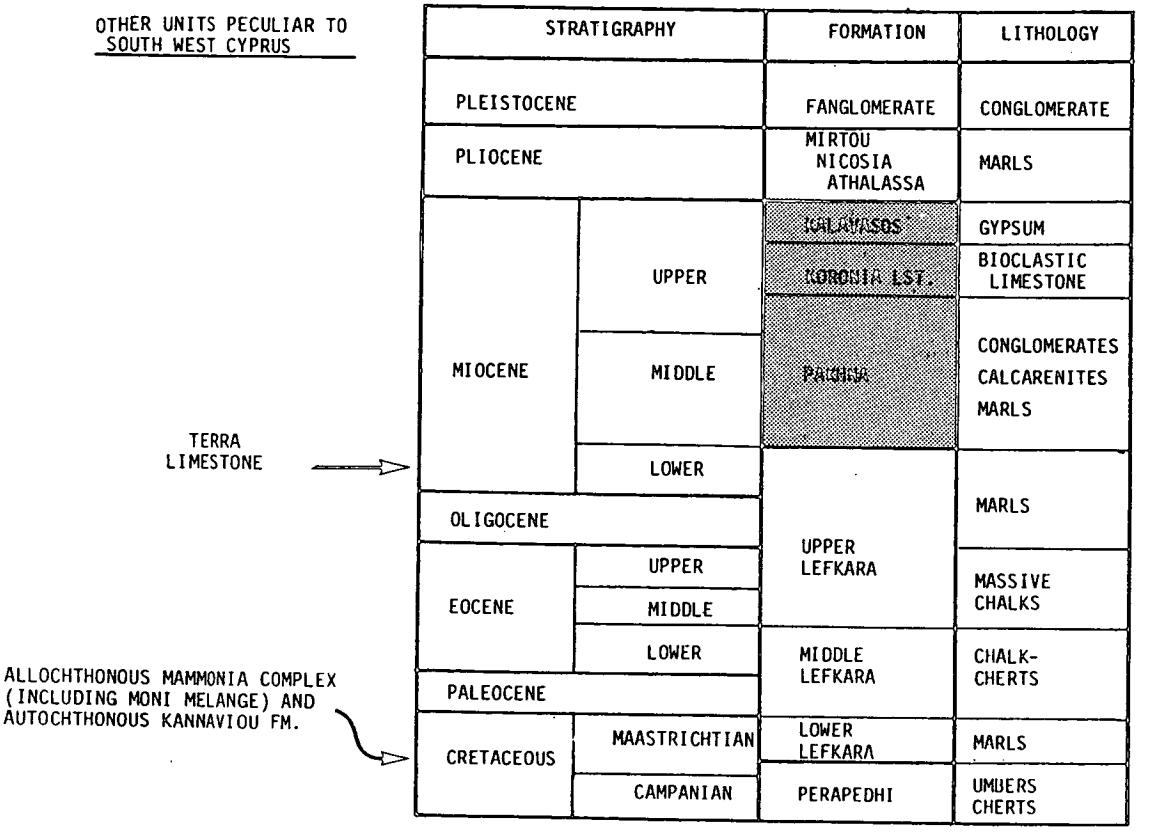

TABLE 1.1 Stratigraphic nomenclature of in-situ sedimentary cover of the Troodos ophiolite.

CHAPTER TWO
STRATIGRAPHY

2.1 Introduction

Stratigraphical nomenclature has been described in the previous chapter, and summarised in Table 1.1.

Further revision of the Miocene stratigraphy is proposed based on the work described in this thesis. Previously used names are retained but the relationships between the Pakhna, Koronia and Kalavasos stratigraphic units are redefined. Observed field relationships that form the basis for this revision are described. Since this represents a rationalisation of the existing stratigraphy, new type-sections are not presented. Detailed sedimentology is not relevant to this discussion and is considered in chapters 3, 4 and 5.

Micropalaeontological data from various sources are integrated with the new scheme. The principles laid down by Hedberg (1976) in the International Stratigraphic Guide are adhered to as far as possible.

Places and features mentioned in the text are located in figures 2.1, 2.4 and 2.5.

2.2 Pakhna Formation

2.2.1 Lithological characteristics

The Pakhna Formation consists of a sequence of marls, chalks, calcarenites and polymict conglomerates. The cream to buff-brown colour of the chalks and marls contrasts with the pure white chalks of the underlying Lefkara Formation. This feature, the more argillaceous nature and more obvious bioturbation of the Pakhna marls has been the basis of distinction in the field. The occurrence of graded, medium bedded bioclastic calcarenites within these deposits is a common feature. Polymict conglomerates and debris-flow deposits containing shallow water carbonate material and Troodos ophiolite-derived lava clasts are developed locally towards the top of this formation.

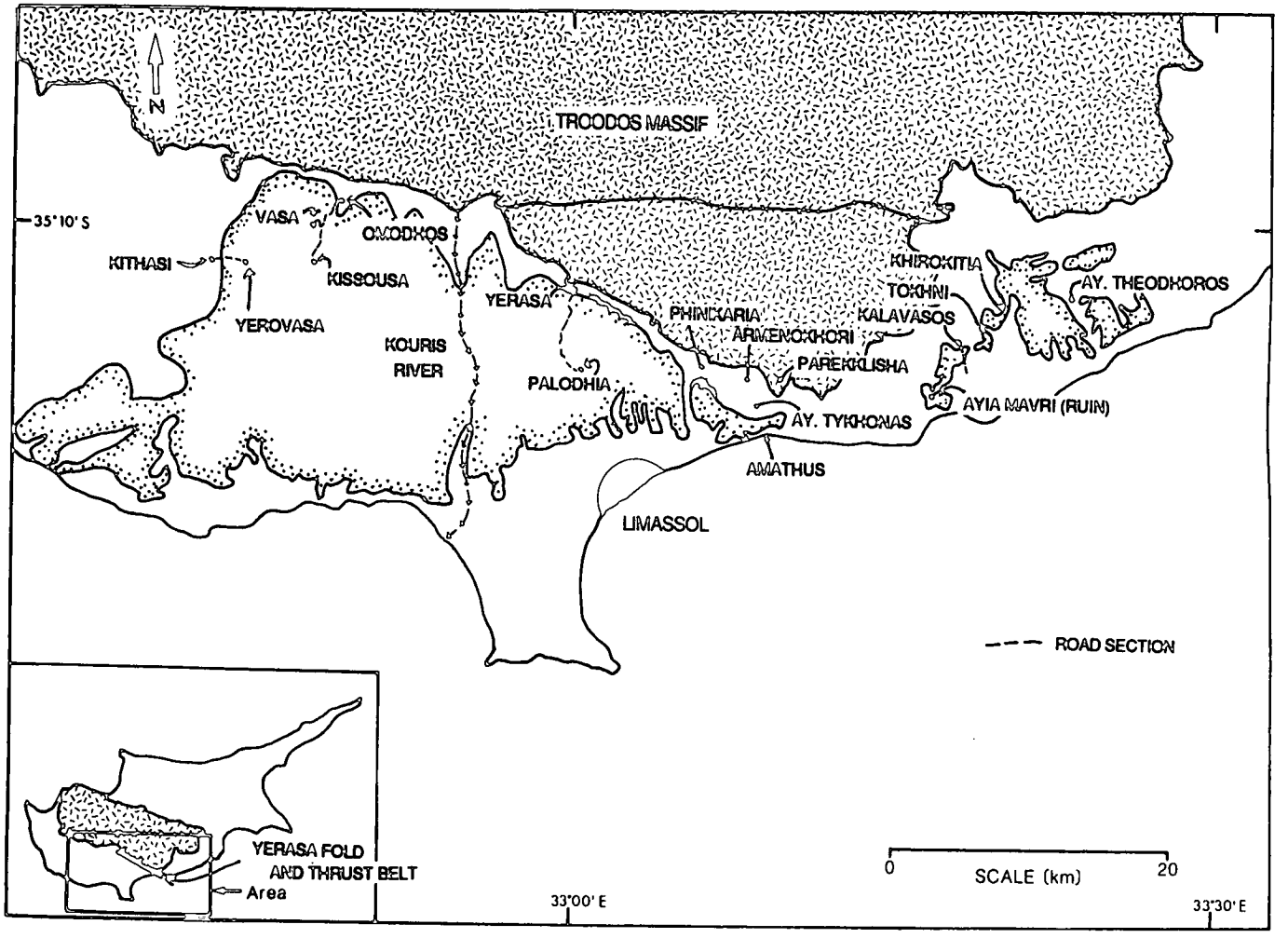

FIG.2.1 Location map for text section 2.2. Limit of Pakhna Formation outcrop area shown stippled.

2.2.2 Lithostratigraphic subdivision by past workers

2.2.2.1 Limassol-Larnaca area

Both Bagnall (1960) and Pantazis (1967) worked in adjacent areas in the Limassol and Larnaca Districts. They defined informally three members of the Pakhna Formation (see fig. 2.2). Although the names differ, the units concerned are lithological equivalents (see Pantazis 1967, pp. 66-67). However, the relationship interpreted between these members is contradictory. According to Bagnall, they are time-sequential whereas Pantazis, though unspecific, implies a significant degree of time-equivalence. The latter interpretation is confirmed in this study and, as noted by Robertson (1977a), lateral facies variations are a common feature in the Pakhna Formation of the Limassol and Larnaca districts.

In the absence of type sections for these members, and in view of the indefinite relationship between them, it is not proposed to incorporate these units into a formal stratigraphy.

2.2.2.2 Kouris River area.

Greitzer & Constantinou (1969) divide the Pakhna Formation in the Kouris River area (fig. 2.2) into five mappable lithological units above a 'Transition Zone' which overlies the Lefkara formation (fig. 2.3). This work was undertaken for a local hydrogeological survey and represents a more detailed examination of the sediments than in immediately adjacent areas. Extrapolation of the results into other regions, particularly if lithological correlation with other members was involved, would remain speculative. This work cannot at this stage, therefore, be incorporated into a formal stratigraphy.

2.2.3 Relationship to Lefkara Formation

Previous workers have stated that the Pakhna Formation is transgressive and that it laps over, and is unconformable upon, the Lefkara Formation (Henson *et al.*, 1947; Bagnall, 1960; Bear & Morel, 1960; Pantazis, 1967).

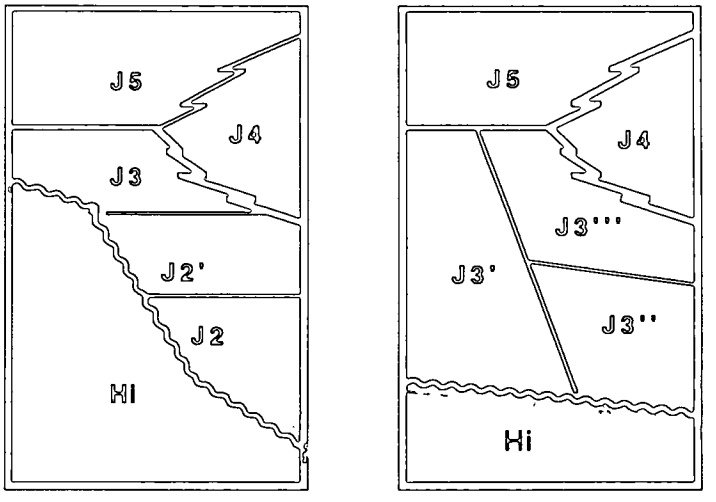

AFTER BAGNALL (1960)	AFTER PANTAZIS (1967)
J5 Gypsum facies	J5 Kalavasos Formation
J4 Koronia Limestone	J4 Koronia Formation
J3 Paper shales	J3''' Shaley limestone
J2' Fragmental Limestone	J3'' Massive limestone
J2 Wavy bedded Limestone	J3' Chalk-marls
Hi Lefkara Formation	Hi Lefkara Formation

Figure 2.2 Stratigraphic relationships and subdivision of the Pakhna Formation, as implied by the maps of Bagnall (1960) and Pantazis(1967). Heavy lines separate units of formation status. Thin lines separate members within formations.

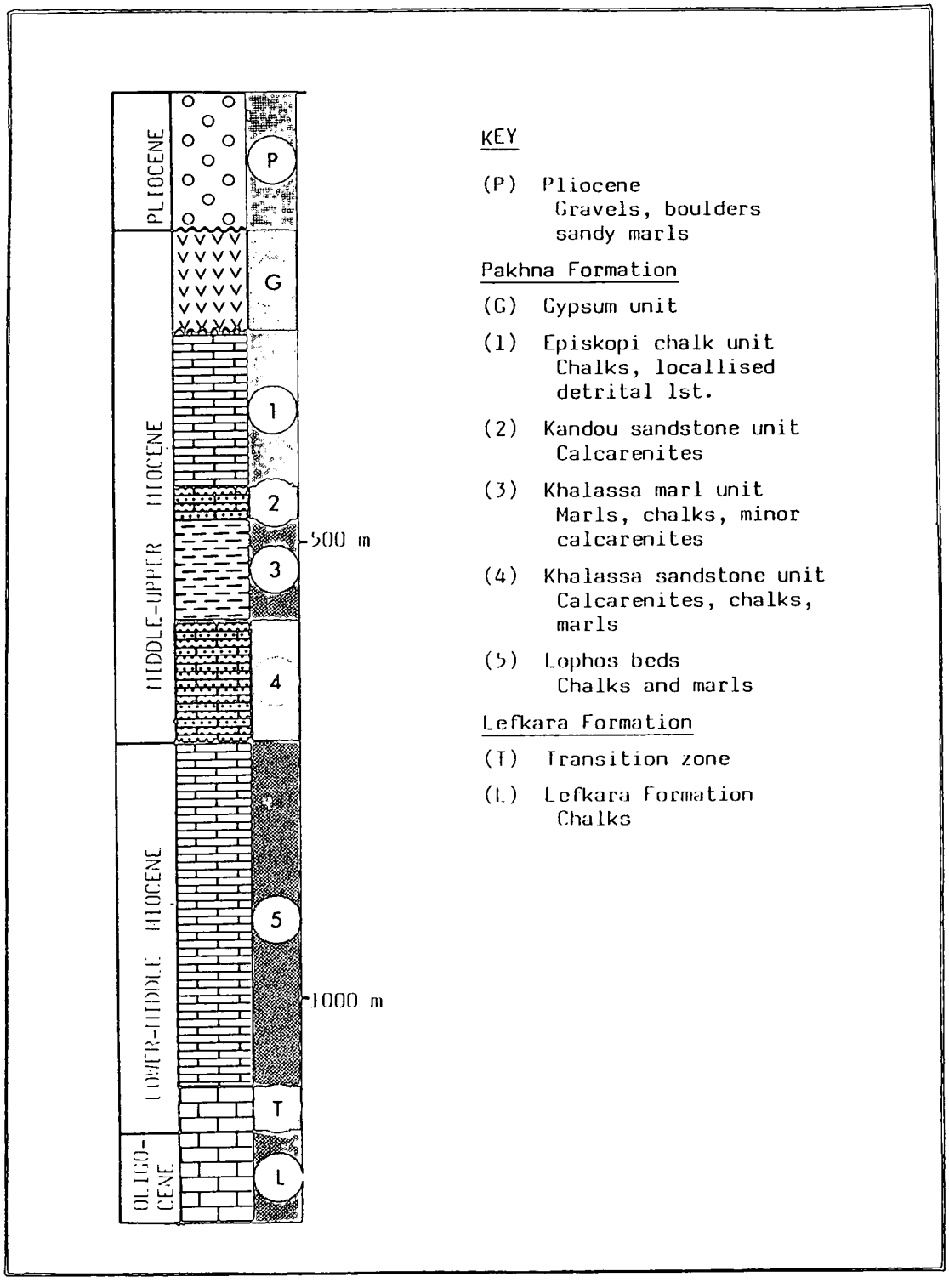

Fig. 2.3 Composite section showing lithostratigraphic subdivision of the Pakhna Formation in the Kouris River area (simplified after Greitzer & Constantinou, 1969).

That this unconformity is not of universal extent is recognised by some (Pantazis, 1967; Cleintaur et al., 1977; Robertson, 1977a) but without provision of geographic details. Contrary to this impression of a widespread unconformity, with only localised exceptions, this study shows that the Pakhna Formation on the south and southeast of the Troodos massif is generally conformable on the Lefkara chalks and that the transition is lithologically gradational and not marked by a sudden change in depositional environment. Notable exceptions to this are found immediately adjacent to the Limassol Forest igneous block in the Yerasa fold and thrust belt where onlap and unconformity do occur. Localities where these relationships can be examined are illustrated in fig. 2.1.

The gradational nature of the Lefkara/Pakhna boundary can be seen in the road sections of Yerovasa-Kithasi, Omhodos-Kissousa and Yerasa-Palodhia where Lefkara chalks pass upwards into Pakhna chalks and marls of a basinal facies. This relationship is also observed by Elion (1983) in similar sections between Omhodos and Vasa.

The localities between Ayios Tykhonas and Amathus are just to the south of the ESE-WNW trending Yerasa fold and thrust belt (fig. 2.1). The steep southerly dip of the Lefkara chalks decreases continuously up sequence to the south into the Pakhna Formation but no unconformity or sudden change in lithology occurs.

Along strike to the northwest, unconformity is observed where the boundary crops out closer into the axis of the fold belt. This is seen in the Armenokhori road section and on the hills immediately south of Phinikaria where shallowly dipping bioclastic deposits of the Pakhna Formation overlap onto more steeply dipping Lefkara chalks. Similar observations are made by Bear & Morel (1960) elsewhere in the fold belt. These overstepping bioclastic units are regarded as lateral equivalents of the Koronia Limestone Member (see section 2.3) which, in the area of Parekklisha, rests directly upon the pillow lavas of the Limassol Forest block.

To the east of the Limassol Forest block outcrops of the Lefkara-Pakhna boundary are conformable. This can best be examined in the road section immediately east of Kalavasos but is also demonstrable near Tokhni, south of Khirokitia, on the hills round Ayia Mavri and Ayios Theodhoros (fig. 2.1). The unconformable relationship suggested in places on maps of the Cyprus Geological Survey are found to be due to failure to recognise faulted contacts (e.g. Ayia Mavri), or to misinterpretation of the relationship between members of the Pakhna Formation. For example, Bagnall (1960) interprets the Kalavasos road section as representing only the uppermost Limestone-Shale member of the Pakhna, which has overlapped onto the Lefkara chalks from the east where the complete Pakhna sequence was deposited in a more basinal setting. This study finds that such sections represent a thinner, but complete, Pakhna sequence with no sedimentological evidence to suggest a depositional break.

2.3 The Koronia Limestone Member

2.3.1 Status

Originally described by Bellamy & Jukes-Browne (1905) from the north Troodos flank, the Koronia Limestone was interpreted to be a littoral facies of the Pakhna Formation and given member status by Henson *et al.* (1947). It was subsequently elevated to formation status by Bagnall (1960) and Pantazis (1967) on the basis of mapping on the south-eastern Troodos flank. Bagnall included gypsum deposits as a lateral equivalent of the same formation, whereas Pantazis separated the gypsum into the Kalavasos Formation (fig. 2.2).

Mapping and sedimentological work involved in this study shows that the Koronia Member consists of a range of lithologies which are not individually exclusive to this unit but occur to varying extents in other deposits of the Pakhna Formation. Collectively, however, the Koronia Member lithologies define a distinctive rock unit which occurs locally at the top of the Pakhna Formation and is

laterally equivalent to other Pakhna deposits. Its contacts are usually sharp and well defined but sometimes the up-sequence and lateral transitions to Koronia Member lithologies occur through progressive change in the relative proportions of associated lithologies. For these reasons the Koronia Limestone is here included as a member at the top of the Pakhna Formation, in accordance with the original designation by Henson et al. (1947).

The gypsum deposits are found to succeed the Pakhna (and Koronia) deposits with no overlap and are retained as a separate formation (section 2.4).

2.3.2 Lithological characteristics

The Koronia Limestone member of the Pakhna Formation forms a resistant capping of coarse reworked carbonate deposits which protect the underlying marls from erosion. It contains conglomerates, debris-flows and coarse calcarenites with minor marls and silts. Components are of a dominantly neritic origin and include fragments of bivalves, coralline algae, bryozoans, echinoids, benthic foraminifera, serpulids, sponge spicules and corals. Clasts of globigerinid chalks, marls and cherts are also common and occasional grains derived from the Troodos lava sequence are also found.

Outcrops near the neolithic settlement at Khirokitia (fig. 2.4) are of recrystallised limestone with no primary textures preserved. Perhaps significantly, these also show in-situ brecciation, probably due to post-Miocene faulting.

No in-situ reefal material is found, all lithologies being clastically derived. This is in contrast to the Koronia Limestone in the type area on the northern flank of Troodos (Bear, 1960; Carr & Bear, 1960).

2.3.3 Relationship to underlying formations

The Koronia Limestone at Amathus (fig. 2.4) rests with sharp contact on the marls of the Pakhna Formation. Though channel development has produced significant relief

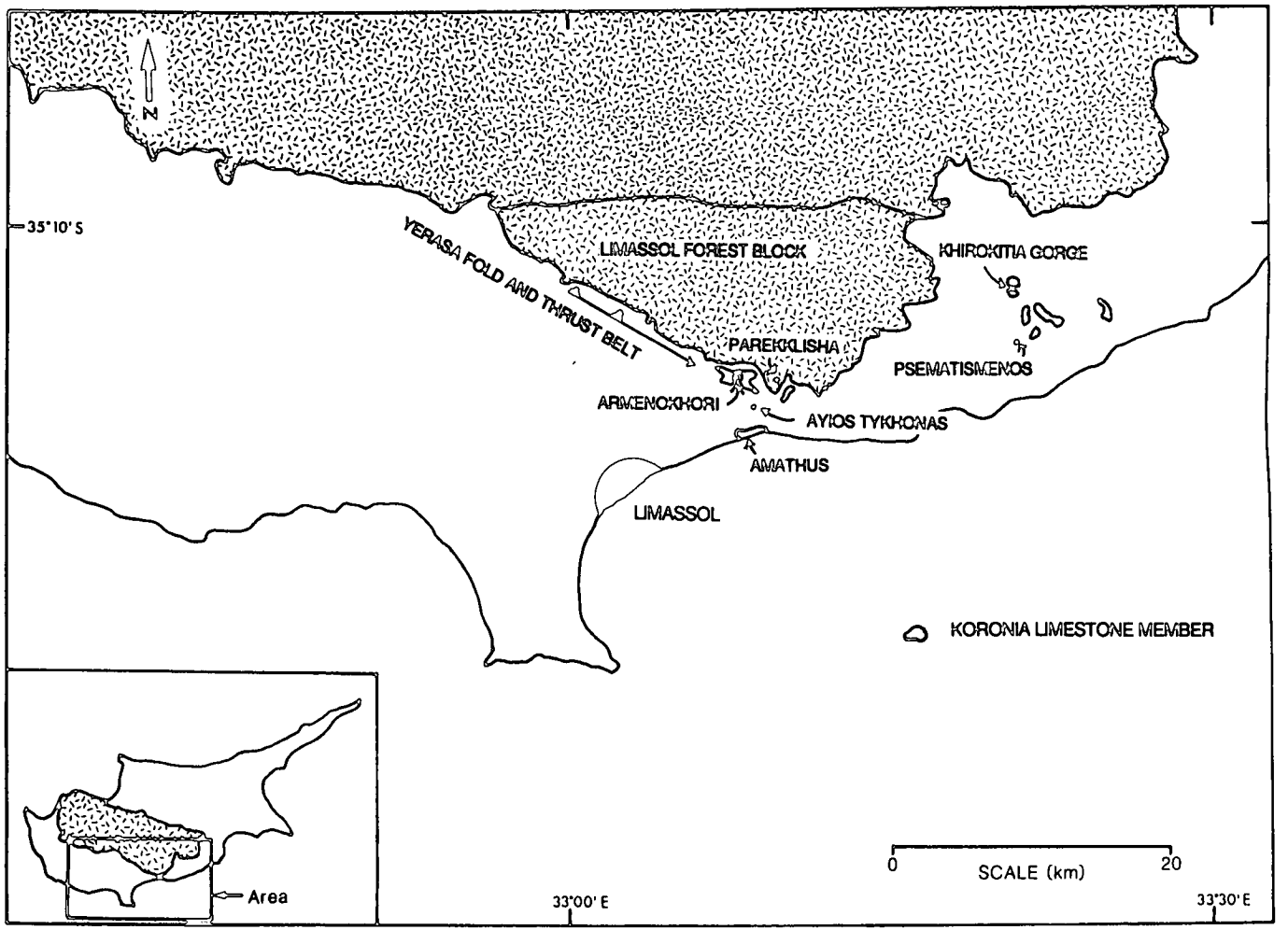

FIG. 2.4 Location map for text section 2.3, Koronia Limestone member .

on the contact, the channel-fill of the Koronia Limestone is conformable with the bedding of the underlying marls. Laterally, the Koronia Limestone grades into thinner sheets of unchannellised bioclastic material that are interbedded with marls.

To the north, in the Yerasa fold and thrust belt, the Koronia Limestone Member rests unconformably on the Moni Melange, as at Armenokhori and Ayios Tykhonas, and further north, in the region of Parekklisha, directly on the pillow lavas of the Limassol Forest block (fig. 2.4). The Koronia Limestone is therefore conformable on Pakhna sediments in basinal areas but transgressive unconformably over increasingly older sediments and onto uplifted igneous basement on the north basin margin.

To the east of the Limassol Forest block the Koronia Limestone is in all cases conformable on Pakhna marls and calcarenites. This can be seen in the hillsides to the east of Psematismenos where carbonate conglomeratic sheets succeed Pakhna sediments. At some localities closer to the Limassol Forest area, such as in the gorge section at Khirokitia, the base of the Koronia Limestone Member has considerble relief. As at Amathus, this is due to channel development.

The Koronia Limestone occurs only locally. Laterally it thins and disappears and is equivalent to the uppermost marls and calcarenites of the Pakhna Formation.

2.4 Kalavasos Formation

2.4.1 Status

The Kalavasos Formation was recognised as a mappable lithological unit by most workers, but was only given formation status by Pantazis (1967), who proposed the inclusion of all circum-Troodos evaporite deposits within this unit.

Sedimentological considerations (chapter 3) indicate that the gypsum was originally deposited over an extensive area, blanketing previous lithologies. This is evidenced by the widespread exposure of the Kalavasos Formation to

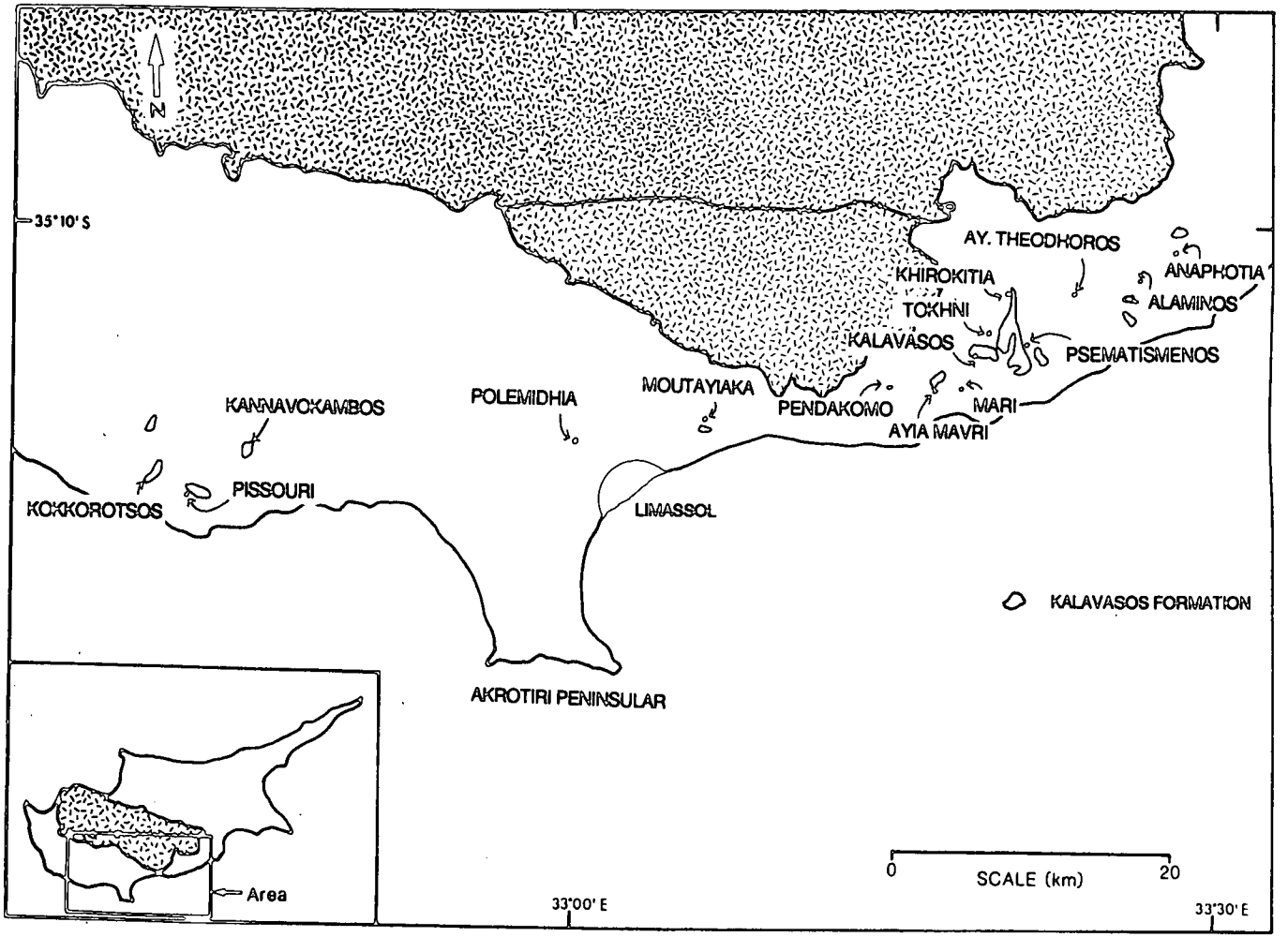

FIG. 2.5 Location map for text section 2.4, Kalavasos Formation.

the east of the Limassol Forest area (fig. 2.5), where lateral continuity is broken only by faulting and erosion. To the south of the Limassol Forest block, exposure is patchy and outcrops are absent westwards from Polemidhia to Pissouri. This is due to erosion prior to the deposition of marine terrace deposits (Bear & Morel, 1960, p. 64). However, borehole data from the Akrotiri peninsula (Hadjistavrinou & Constantinou, 1977) reveal the subsurface continuation of the Kalavasos Formation, where it has been protected from post-evaporite erosion.

The Kalavasos evaporites are thus both laterally extensive and lithologically distinctive. Formation status, as proposed by Pantazis, is therefore appropriate.

2.4.2 Lithological characteristics

This formation consists of a variety of gypsum lithologies with minor gypsiferous marls occurring at some localities. These lithologies are more fully described in chapter 6. Anhydrite and higher evaporites are absent and no sabkha-type deposits occur, the gypsum being entirely of subaqueous origin.

2.4.3 Relationship to Pakhna Formation

The Kalavasos evaporites are invariably found to be conformable on Pakhna Formation deposits. Figure 2.5 shows localities referred to in the text.

In the Pissouri area this contact can be seen, for example, where an unmarked track crosses a gully at grid reference 697383. Here a sequence of brown laminated marls and medium bedded chalks pass up through a metre of gypsiferous marls into finely laminated gypsum. Elion (1983) describes sections at Kannavokambos and Kokkorotsos in the same area which demonstrate a similar relationship.

At the Moutayiaka gypsum pits the basal contact is not seen. The northern pit, now infilled with rubbish, is at a lower topographic level than adjacent Pakhna deposits but this appears to be due to down-faulting of the gypsum along northeast striking faults.

To the east of the Limassol Forest block the Kalavasos Formation often caps scarps, with laminated gypsum overlying laminated Pakhna marls. This is seen between Tokhni and Khirokitia, on the scarps immediately northwest of Kalavasos quarry (see also Rouchy & Monty, 1979), and near the Ayia Mavri ruin half way between Pendakomo and Mari (fig. 2.3). The same relationship is found in areas where the uppermost Pakhna sediments are of a different facies as, for example, immediately southwest of Tokhni where a gypsum surface overlies Pakhna polymict channellised conglomerates.

Elsewhere, generally, the contact is not exposed but in all cases field observations suggest a similar stratigraphic relationship.

2.4.4 Relationship to Koronia Limestone

Previous authors have consistently suggested some degree of lateral equivalence between the Kalavasos Formation and the Koronia Limestone (Bagnall, 1960; Pantazis, 1967; Cleinteur et al., 1977). This study finds that no such equivalence exists in the areas covered and that the Kalavasos Formation wholly post-dates the Koronia Limestone. This is consistent with the implications of sections 2.3.1 (status of the Koronia Limestone) and 2.4.3 (relationship between the Pakhna and Kalavasos Formations).

Outcrops in which the Kalavasos evaporites are adjacent to Koronia Limestone are found to be faulted as at Khirokitia and in the hills between Psematismenos and Ayios Theodhoros. Faulting also accounts for the juxtaposition of gypsum against Lefkara chalks described by Bagnall (1960, p. 53) at Kokkines north of Anaphotia.

At other localities, and within individual fault blocks, Koronia Limestone is found to underlie the evaporites. The small Koronia Limestone outcrop described by Bagnall (1960, p. 52) north of the Kalavasos gypsum quarry grades southward into the evaporites and is found to be a limestone debris-flow which underlies the

Kalavasos Formation. It is probably equivalent to the intraformational conglomerate described by Rouchy & Monty (1979) in the same area. Similarly, to the south of Alaminos a dip slope of Koronia Limestone, again a limestone conglomerate, is in fact overlain by the Kalavasos evaporites which crop out in a quarry to the south (grid reference 394507). Sedimentological aspects of these exposures are discussed in section 6.4.2.

On the hill about one kilometre northeast of Psematismenos, spot height 276 m, the calcirudites mapped by Bagnall (1960) as Koronia Limestone overlie post-evaporite marls and are probably of Pliocene age.

The non-equivalent nature of Kalavasos evaporites and the Koronia Limestone, as suggested by these observations, is further supported by sedimentological considerations (section 6.4) and faunal studies (Adams, 1976, p.56; Hadjistavrinou, 1975, pp.33-37).

2.5 Chronocorrelation of lithostratigraphic units

2.5.1 Introduction

The determination of the relative ages of rock strata from different areas and the chronostratigraphic correlation of sequences are fundamental to basin analysis. Relative age relationships between lithostratigraphic units are often determinable from field relationships. Chronostratigraphic correlation, however, requires the identification and application of time-diagnostic criteria. The most convenient and widely used criterion is fossil type. This is true in Cyprus where correlation is achieved, as with most Neogene sedimentary sequences, by micropalaeontological studies and interpretation of results within the framework of established microfossil biozonation schemes.

2.5.2 Biostratigraphic framework

The first systematic biozonation of the circum-Troodos sedimentary succession was proposed by Mantis (1970a). Subsequent work (Mantis, 1970b; Hadjistavrinou,

1974; Hadjistavrinou, 1973) has produced the scheme illustrated in fig. 2.6, taken from Pantazis (1978) after Mantis (unspecified source). This system is based upon foraminiferal assemblages, mostly planktonic, but benthic species are also used, particularly for the Neogene zones. Benthic foraminiferal age ranges recorded are shorter than those established elsewhere in the Mediterranean region (e.g. Bizon et al., 1978). This reflects control by sea-bottom environments over the temporal distribution of these species and suggests that duration of appropriate benthic conditions for these species varied in Cyprus on a shorter time-scale than their true age ranges. The application of first and last appearence criteria of these species to biozonation should therefore be treated with caution.

Baroz & Bizon (1977) applied a different biozonation, previously established for the Western Mediterranean (Bizon & Bizon, 1972), to the sequences of the north Troodos flank. This scheme was also used on Leg 42A of the Deep Sea Drilling Project (Hsu et al., 1978) for which correlations with the absolute time scale (after Ryan et al., 1974) and the biozones of Blow (1969) (foraminifera) and Martini (1971) (nannoplankton) are also made (fig. 2.7). This is the biostratigraphic framework and chronostratigraphic correlation to which micropalaeontological data are referred in this study. Range charts are included in Appendix 1.

The relative paucity of keeled globorotalids in the Eastern Mediterranean during the Miocene limits the stratigraphic resolution of foraminiferal studies in Cyprus during this period (Prof. F.T. Banner, pers. comm., 1983). This is particularly true in the upper part of the Pakhna Formation where generally poor preservation and increasing proportions of longer ranging benthic species relative to planktonics add to the problem. In the uppermost Pakhna sediments low diversity assemblages and barren beds, reflecting stessed environmental conditions, extend up to the base of the Kalavasos evaporites. This

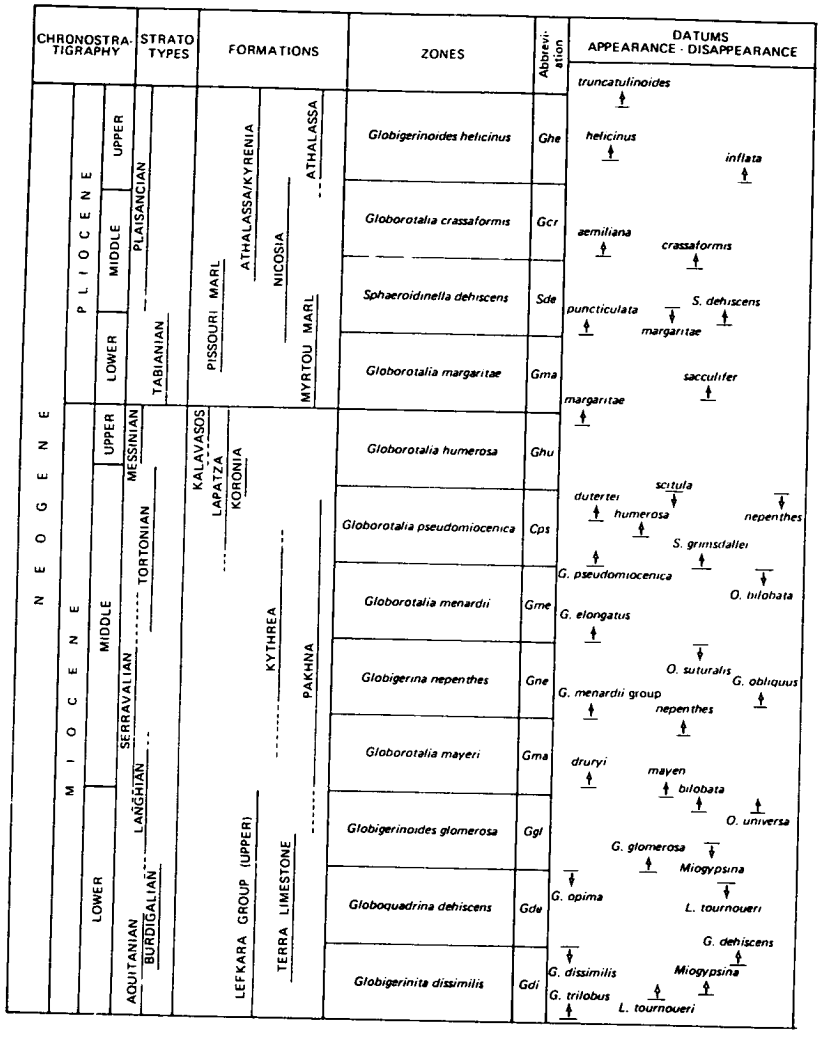

FIG. 2.6 *Cyprus Neogene foraminiferal zoning by M. Mantis.*

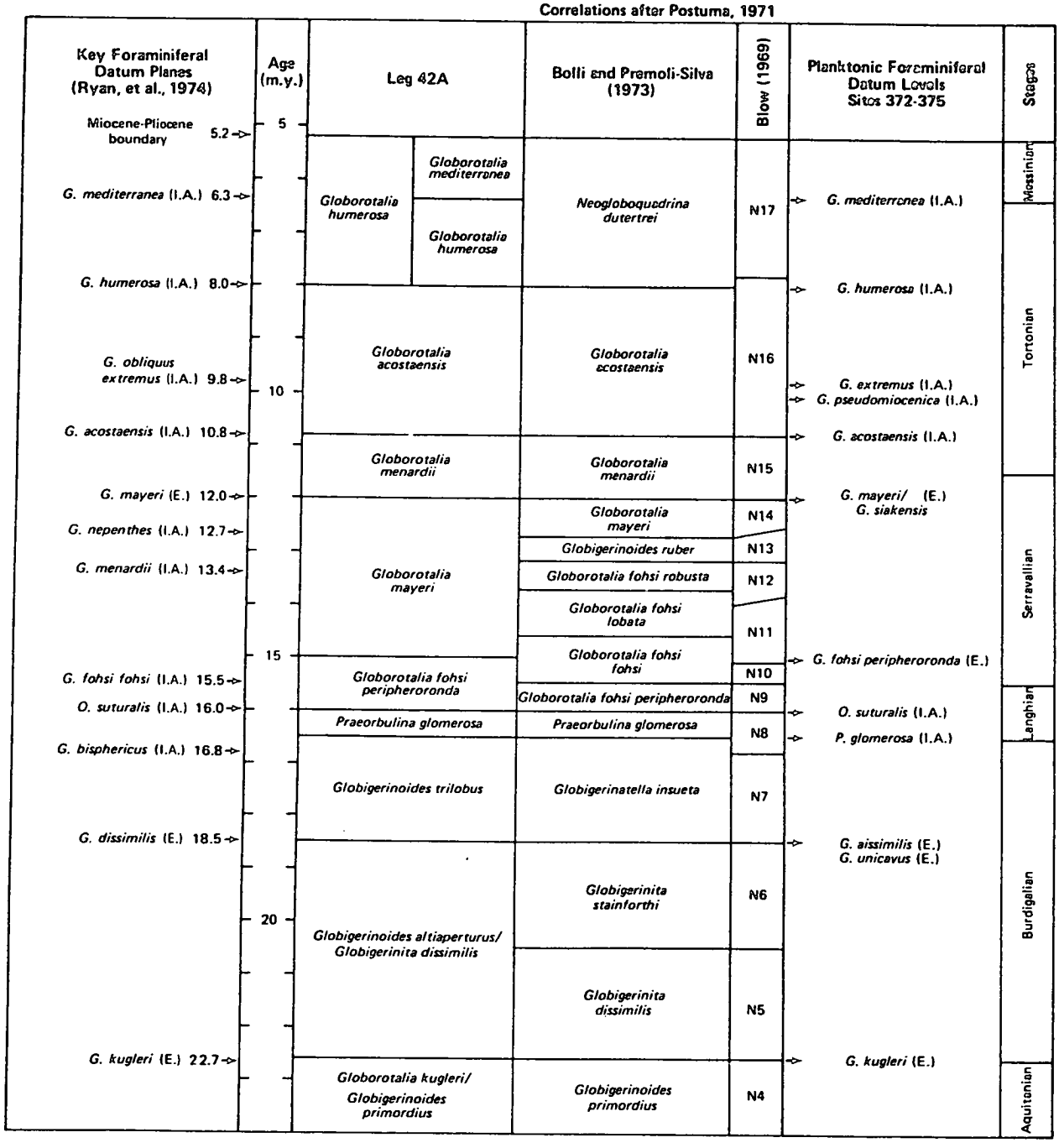

FIG. 2.7 Miocene biozonation, as used on DSDP Leg 42A.

transition is taken to occur during Messinian times by analogy with other areas and through sedimentological considerations (see chapter 6). The base of the evaporites is thus a useful intra-Messinian marker horizon.

2.3.3 Application of published data

A laterally extensive marker horizon of chalks characterised by its content of the large foraminifera Discospirina italica occurs in the upper part of the Pakhna Formation and is included on the geological maps of Bagnall (1960) and Pantazis (1967). This species is extant today in the Mediterranean and the North Atlantic (Adams, 1959). Adams (1976) indicates a first appearance of this species in the Mediterranean during the Tortonian, and Hadjistavrinou (1973) suggests correlation of a Discospirina italica zone with the Globorotalia menardii zone (Serravallian-Tortonian). However, where detailed biostratigraphic work has been undertaken on Cyprus, Discospirina has only been reported from inferred lower Messinian sediments (Baroz & Bizon, 1977; Orszag-Sperber et al., 1980; Elion, 1983). Close association of the Discospirina band in southern Cyprus with the Messinian evaporites of the Kalavasos Formation suggests a similar stratigraphic position. Nevertheless, the possibility of significant diachroneity should not be discounted.

Useful micropalaeontological data exist for several localities in the Miocene sequences to the south and west of the Limassol Forest area (Greitzer & Constantinou, 1969; Heguera, 1982; Ortiz, 1982; Elion, 1983; Haskett, 1984; Philpott, 1984; Urquhart, 1984). These localities are shown in fig. 2.8, to which the following paragraphs refer.

(1) Microfossil determinations from the Pakhna sediments of the Kouris River area are given by Greitzer & Constantinou (1969) in which data are referred to the locally used subdivisional units, see section 2.2.2.2 and fig. 2.3. These determinations suggest a position for the

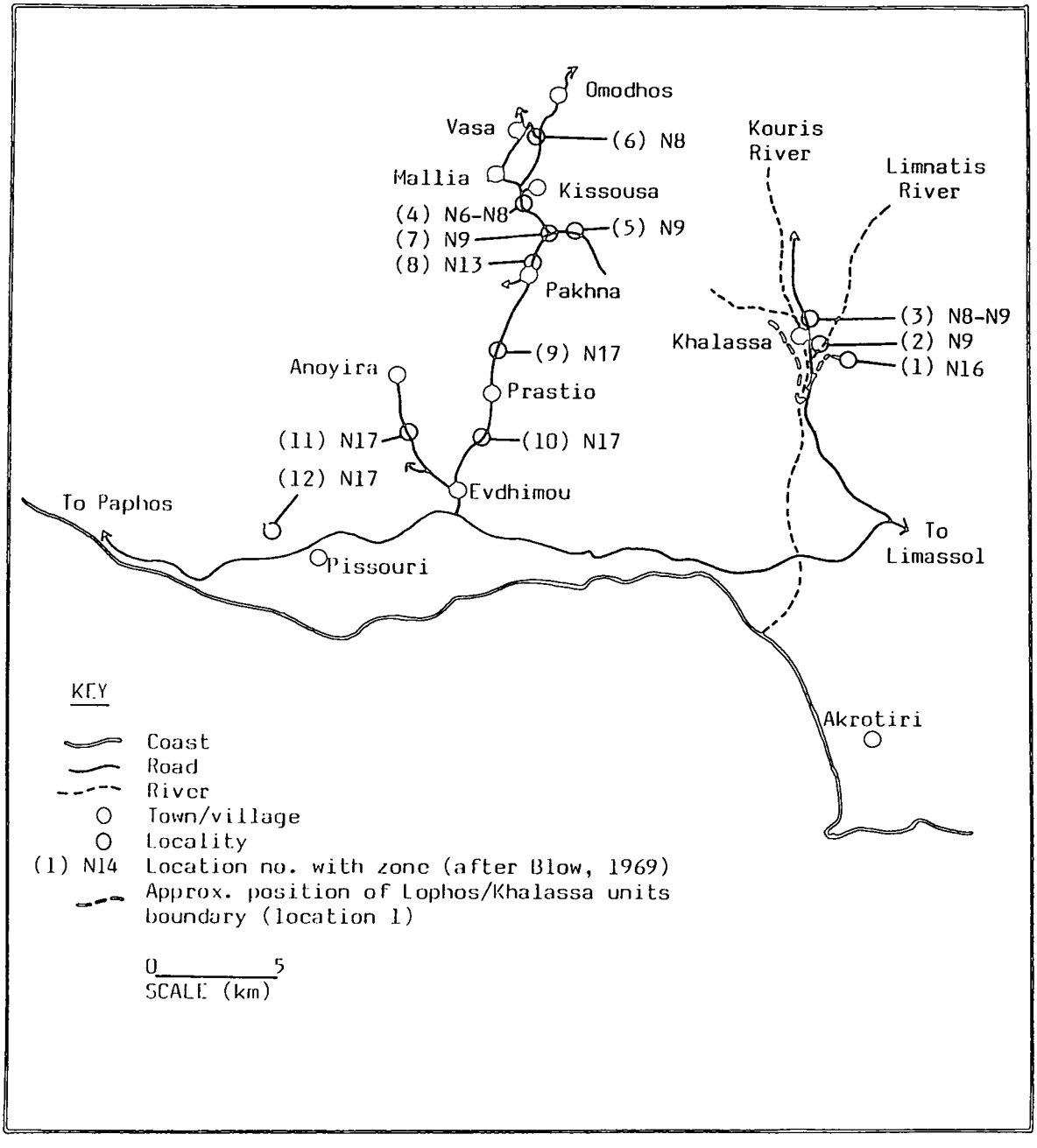

Fig. 2.8 Location map and zonal determinations for area south and west of Limassol Forest block (see text).

Lophos Beds/Khalassa sandstone unit boundary between mid N16 zone of Blow (1969) (Globigerina bulloides in Lophos Beds) and top N16 (Globoquadrina dehiscens in overlying units; range taken from Postuma, 1971). No further useful biostratigraphic conclusions can be drawn from the data.

(2) Herguera (1982) records foraminiferal assemblages from road cuts on the old road between Khalassa village and the confluence of the Limnatis and Kouris rivers. Species include Globorotalia fohsi fohsi, Orbulina universa, Orbulina bilobata, Globorotalia mayeri, Globorotalia scitula praescitula and Globigerinoides transitoria. These indicate a Langhian age, zone N9.

(3) Ortiz (1982) examined foraminifera from two sections near the Limnatis bridge on the new Limassol road and suggested a Late Langhian age for these deposits, zones N8 and N9.

(4) This cutting, from the Kissousa bridge south to the bend (grid ref. 807313) on the Kissousa-Pakhna road, was examined for foraminifera by Urquhart (1984). Data indicate mid N6 (Globigerinoides sacculifera) to mid N7 (Globigerina connecta) correlation for the lower part of the section (north end) ranging up-sequence to N8 (Globigerinoides sicanus and Praeorbulina transitoria).

(5) This locality, a road cut at grid ref. 830306, was also examined by Urquhart (1984). The identification of Orbulina universa and Praeorbulina glomerosa circularis indicates mid to late N9 zonation.

(6) This is the "Niveau 7" locality of Elion (1983) and is located below Vasa where the road splits between the Mallia and Omhodos/Limassol routes. Two nannoplankton assemblages are recorded. The first contains Helicosphaera ampliperta, H. carteri, Sphenolithus heteromorphus, Reticulofenestra pseudoumbilica, Cyclicargolithus floridanus, C. pelagicus and Discolithina multipora and is attributed to zone NN4 (of Martini, 1971). The second assemblage contains Coccolithus pelagicus, Cyclicargolithus abiscetus, C. floridanus, Sphenolithus heteromorphus, S. abies, Discoaster exilis and

Helicosphaera euphratis and is attributed to zone NN5. The NN4/NN5 boundary is correlated with the N8 zone of Blow (1969).

(7)(8) Haskett (1984) studied outcrops on the road section to Pakhna from the T-junction on the Omhodos-Limassol route. As at locality (5), an N9 age is attributed to the sediments at the base of the section, locality (7), with younging up the scarp towards Pakhna, to locality (8) with an age equivalent to N13 inferred from the absence of Globorotalia praemenardii and the presence of highly evolved Globigerina druryi.

(9) This locality, 4 km south of Pakhna on the Evdhimou road, was also examined by Haskett (1984) who assigned an early to mid N17 correlation to it on the finding of highly evolved Globorotalia tumida merotimida and Globorotalia tumida plesiotumida.

(10) This is the "waterfall sequence" of Philpott (1984) and the "Prastio ravine" locality of Elion (1983). Both authors record poor preservation of microfossils but attribute the sediments to late Tortonian/early Messinian (N17). Elion cites the presence of Globorotalia dutertrei and the Messinian nannoflora Sphenolithus abies.

(11)(12) These are, respectively, the Kannovokambos and Kokkorotsos localities of Elion (1983). The presence of Globorotalia dutertrei and the nannofossil Sphenolithus abies indicate Late Tortonian or Early Messinian ages (N17). Locality (12) is capped by Messinian gypsum.

To the east of Limassol, Pantazis (1967, pp. 68-69) lists some microfossil assemblages for samples from the Amathus area. Reasonable stratigraphic resolution can be made if the proposed last appearance of Globigerinoides triloba immatura (now G. globoquadrina immatura after Banner & Blow, 1960), in the Globorotalia mayeri zone (up to top N14) is correct, as indicated by Mantis (1970). However, this species is also reported from the Pakhna sediments above the Lophos Beds in the Kouris River area (Greitzer & Constantinou, 1969) indicating that it ranges

up to atleast zone N16 in Cyprus (see locality (1) in previous section and figs. 2.3 and 2.8). This N16 upper limit is assumed in the age determinations made below, but it must be pointed out that even this assumption is questionable (see Blow, 1969). The sample numbers, with suggested biozone and zone-diagnostic species, are as follows:

83Ø2	N13	(Globorotalia aff. menardii) to
	N16	(Globigerinoides triloba immatura)
83Ø3	NIØ	(Globorotalia foshi foshi) to
	N11	(Globorotalia foshi foshi)
83Ø3A	N9	(Orbulina universa) to
	N16	(Globigerinoides triloba immatura)
83Ø3B	N13	(Globorotalia menardii) to
	N16	(Globigerinoides triloba immatura)

Sampling points are not well located but would appear to be close to the base of the Koronia Limestone which crops out in the immediate area.

The micropalaeontological determinations listed for the Pakhna Formation deposits to the east of the Limassol Forest block in Bagnall (196Ø) have little biostratigraphic application, but the reported occurrence of Orbulina universa in two Lefkara Formation outcrops (p.32) has important implications for the chronostratigraphic nature of the Lefkara/Pakhna formations boundary. This species indicates an Upper Langhian age (N9) or younger. Other localities in southern Cyprus of the same biozone or older (localities (2),(3),(4),(5),(6) and (7) in fig. 2.8) have been mapped as Pakhna Formation. The Lefkara/Pakhna formations boundary would therefore appear to be significantly diachronous across southern Cyprus.

2.3.4 New data

Unfortunately, it has not been possible to have collections of rock samples dated by micropalaeontological methods during the course of this work. The only new data come from two samples, collected from chalk beds high in the Pakhna succession, from near the villages of Kalavasos and Moutayiaka. Nannofossil assemblages from these samples

have been described by Hilary Stowe of University College, London. Full details are given in Appendix 2. The results are not particularly useful due to poor preservation, and the absence of diagnostic species.

2.6 Summary of revised stratigraphy

The stratigraphic relationship of the Middle and Upper Miocene lithostratigraphic units (Pakhna Formation, Koronia Limestone member, and Kalavasos Formation), as determined by this study, are illustrated in figure 2.9.

Field observations indicate a conformable relationship between the Pakhna and underlying Lefkara Formations, except at rare locations in the Yerasa fold and thrust belt. Micropalaeontological considerations indicate that the conformable boundary is diachronous as mapped, ranging at least in age from Blow's N6 to N9 zones (Burdigalian to top Langhian).

The Koronia Limestone unit is laterally equivalent to marls in the Pakhna Formation, and being developed only locally, is attributed member status.

The Kalavasos Formation is found to be conformable upon the Pakhna Formation, including locally the Koronia Limestone member, and is of Messinian age. No evidence for a diachronous boundary is found. This formation can be related to other Messinian evaporites in the Mediterranean area (see chapter 6).

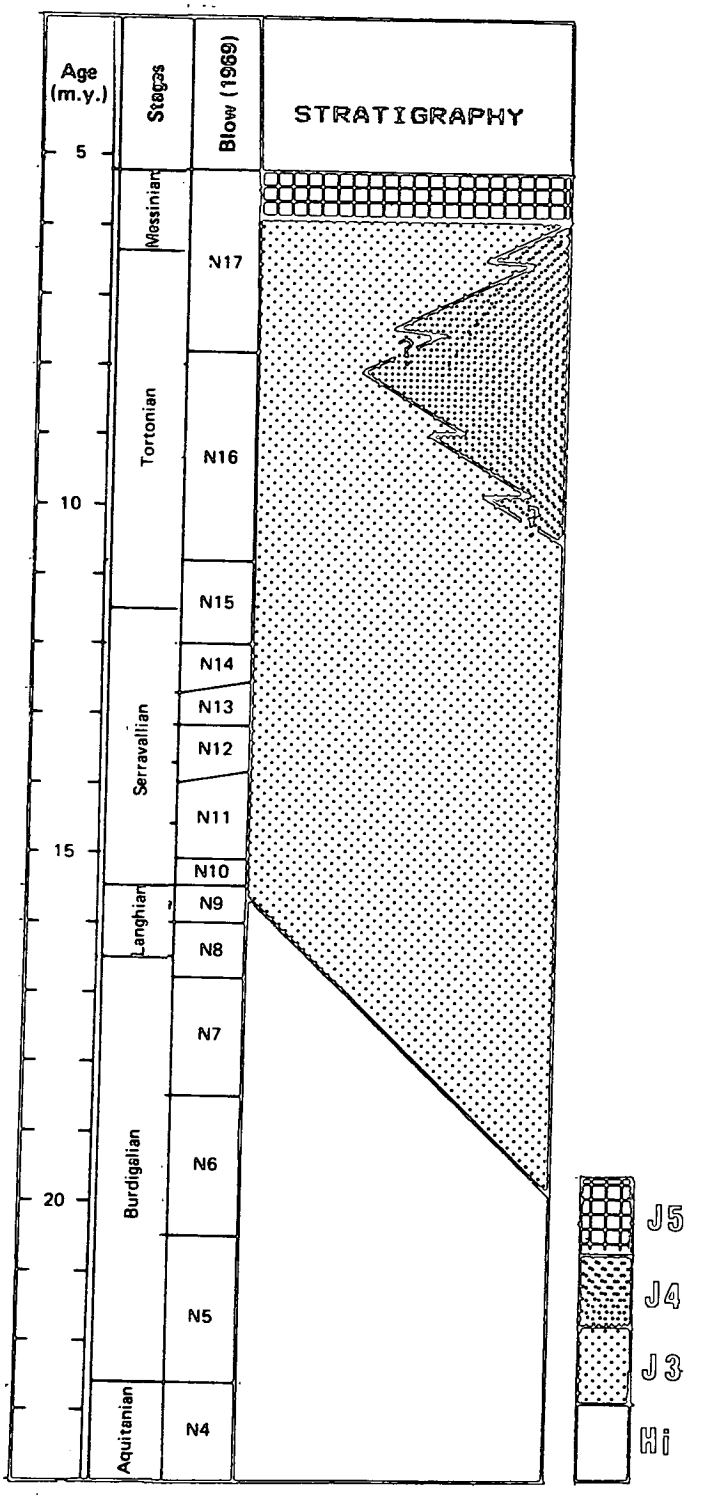

FIG. 2.9 Stratigraphy of Middle and Upper Miocene units in the study area. Hi = Lefkara Formation, J3 = Pakhna Formation, J4 = Koronia Limestone member, J5 = Kalavasos Formation. Note diachronous Pakhna-Lefkara Formation boundary.

CHAPTER THREE
LITHOFACIES OF THE PAKHNA FORMATION

3.1 Introduction

The division of Pakhna Formation lithologies into a series of lithofacies, as presented in this chapter, is used to present descriptive field data in a way that avoids repetition as much as possible. These lithofacies are rock units defined on the basis of outcrop characteristics including colour, bedding, composition, texture, fossil content and sedimentary structures.

Field observations are supplemented with the results of laboratory studies, principally thin section examination of representative samples.

For each lithofacies the main geographical and stratigraphical occurrences are described, and other commonly interbedded lithofacies types are listed. References to other lithofacies defined in this chapter, where made, are emboldened.

Variations within each lithofacies are described. In some cases lithological characteristics are variable continuously between two lithofacies. Classification of intermediate type lithologies, which is necessarily subjective when assessed on field criteria, may result n an "overlap" of lithofacies, e.g. a marly chalk (Lime Mudstone) might otherwise be described as a chalky marl (Marlstone). Ideally, however, the lithofacies described in the following sections are intended to be mutually exclusive.

In this chapter the interpretation of lithofacies is limited to genetic processes, without the resolution of a specific depositional setting. Full interpretation of depositional environments involves assessment of associated lithologies in vertical sequences, and recognition of facies associations which is the subject of Chapter 4.

The lithofacies described are; lime mudstones, marlstones, laminated calcilutites, calcarenites, rudites and slumps.

3.2 Lime Mudstone Lithofacies

3.2.1 Occurrence

This is volumetrically the most abundant lithofacies of the lower sequences of the Pakhna Formation, immediately above the Lefkara Formation. Due to the broadly anticlinal nature of the Troodos massif and its sedimentary cover, this lithofacies most commonly crops out closest to the exposed ophiolite. It is often interbedded with marlstones, thin bedded calcarenites and graded calcarenites.

3.2.2 Field character

This lithofacies consists of white to light grey, grey-green or grey-brown homogenous lime mudstones. The white lime mudstones are similar to the chalks of the underlying Lefkara Formation, but the dominantly off-white colour, due to traces of argillaceous material, distinguishes them from the Lefkara Formation. When fresh, these lime mudstones are hard, but the more argillaceous lithologies are preferentially softened and weathered with exposure. Beds are laterally continuous, generally 20-50 cm. thick with no thinning or thickening at outcrop scale (over 100 metres laterally). Thicker units, in excess of 2 metres, are probably the result of bedding homogenisation through intense bioturbation. This is consistent with the slightly mottled appearence of these beds and the ubiquitous presence of *Planolites*, *Chondrites*, and rarer *Zoophycos* and *Teichichnus* trace fossil types. Destruction of bedding structures by burrowing is further suggested by the occurrence of partially obliterated thin bedded calcarenite interbeds and 10 cm thick horizons of dispersed carbonate sand in lime mudstones (obliterated thin bedded calcarenite interbeds, see Plate 6B).

In some outcrops lime mudstone beds contain a network of interconnecting, but essentially bedding-parallel, millimetre-thick marl seams. In some cases this can give the appearence of flaser structures and small scale lenticular bedding, but is related to stylolitization and burial-related pressure solution (see discussion).

Macrofossils extracted from this lithofacies include thin-shelled epi-pelagic bivalves and echinoids. With the aid of a hand lens it is usually possible to distinguish microfossils on freshly weathered surfaces.

Towards the top of the Pakhna Formation clean indurated white chalks occur. These are medium bedded, compact and hard, with two approximately perpendicular vertical joint sets imparting a blocky fracture. Black staining, probably by MnO2, of joint surfaces is common. Trace fossils are absent, except for discontinuous thread-like goethite staining which picks out rare burrows. Some of these blocky chalk beds contain stunted bivalves and the large benthic foraminifera Discospirina (Adams, 1959), and form part of the "Discospirina band" of Bagnall (1960) and Pantazis (1967). Though generally structureless, one notable occurrence (at Moutayiaka) shows fine parallel laminations and contains well preserved fossil fish.

3.2.3 Petrology

In thin section the lime mudstones are globigerinid wackestones and mudstones with a micrite matrix (Plate 2A). Burrow fills contain a high proportion of globigerinid tests, sometimes resulting in grain-supported foraminiferal sand pockets. Globigerinids are well preserved, uncrushed, and variously unfilled, internally cemented with calcite or mud filled. No siliceous replacement is seen. Occasionally, limonite is found within foraminiferal tests. Unfilled foraminifera tests which are cut by solution seams are partially or completely dissolved.

This lithofacies has a very low clay mineral content, but traces of kaolinite, montmorillonite and palygorskite

were detected by XRD in some samples, and are concentrated along solution seams if developed. Small amounts of quartz were also detected.

Examination of samples with the SEM shows the matrix to consist of coccolith shields (Plate 2B). Diagenetic processes which are seen to have affected both the nannofossils and the foraminifera include solution welding and calcite overgrowth.

The compact white chalks of the "Discospirina band" are found to be finely recrystallised to microspar. Nannofossils have been extracted from them but are generally so poorly preserved as to make identification impossible. However, a few species have been recorded (Appendix 2).

3.2.4 Discussion

The association of globigerinid (pelagic) foraminifera with a matrix of coccolithic micrite is indicative of an open marine pelagic or hemi-pelagic origin for this lithofacies. The lack of primary sedimentary structures is attributed to the homogenising effect of bioturbation.

The Chondrites-Planolites trace fossil association, with subordinate Zoophycos and Teichichnus, is a common one in deep-sea cores from around the world. Despite reservations held by some authors on the bathymetric significance of these ichnogenera in Palaeozoic sediments (Seilacher, 1964; Hantzschel, 1975; Osgood & Szumuc, 1972), Ekdale (1978) concludes that in Mesozoic strata it is safe to assume a deep-sea origin for this trace fossil assemblage (see also Kennedy, 1975 and Scholle et al., 1983). This conclusion is in agreement with the palaeobathymetric interpretations based on foraminiferal assemblages taken from sequences dominated by this lithofacies within the area of this study (Herguera, 1982; Ortiz, 1982). These microfossil assemblages are dominated by pelagic species (85-99%) which is in itself indicative of deep water. Herguera also compared the extracted benthic foraminifera populations with the present day

depth distribution of similar populations in the East Mediterranean (as documented by Parker, 1958) and concluded that the faunal content indicates open marine conditions of mid-bathyal depths (700-1100 m).

Observed variations from sample to sample in the proportion of mud-filled to hollow or cemented foraminifera tests probably reflects variations in bioturbation intensities. The generally uncrushed nature of the foraminifera attests to the preferential compaction and flowage of the micitic matrix under burial.

Anastomosing, but essentially bedding-parallel, marl-rich solution seams seen in this lithofacies, and reported by Pantazis (1967) from the Upper Lefkara chalks, are also a product of burial diagenesis. These features are similar to those described by Garrison & Kennedy (1977), Einsele (1982) and Ricken & Hemelben (1982) and are attributed to localised concentration of clay minerals by clay-enhanced migration of carbonate, dissolved by pressure solution, in unlithified chalks. This process is insignificant at burial depths less than 300 m (Garrison & Kennedy, 1977). SEM examination shows that burial was also sufficient to promote solution welding of impinging grains in the matrix. Intra-stratal redistribution of dissolved carbonate by grain boundary diffusion and reprecipitation in strain shadows is inferred and would account for the overgrowths on coccoliths (Plate 2B) and the void-filling calcite cements and overgrowths of foraminifera tests (Scholle, 1977; see also Plate 1D, 1E). This process results in the progressive lithification of hemi-pelagic and pelagic oozes. Substantial lithification, producing a compact lime mudstone as with this lithofacies, requires burial depths in excess of 1000m under normal circumstances (Neugebauer, 1974; Schlanger & Douglas, 1974).

The "Discospirina band" type microspar chalks that occur towards the top of the Pakhna Formation have undergone significantly more recrystallisation than the pelagic chalks that characterize the sequence lower down

(Plate 2C). This can not be explained by burial history alone since these recrystallised chalks overlie the diagenetically more stable lower pelagic chalks. It would be reasonable to suggest that the more intensive recrystallisation reflects a greater "diagenetic potential" of the primary sediment (Schlanger and Douglas, 1974) as found in peri-platform oozes. The composition of such sediments is more strongly influenced by platform derived aragonitic and Mg-calcite rich muds (Schlager and James, 1978).

Modern Discospirinids have a deep habitat, ranging well down into the bathyal zone (Sturani, 1978). Since the fauna in the "Discospirina band" chalks does not appear to be reworked this implies a similar depth of deposition for these sediments in Cyprus. However, Adams has cautioned (discussion in Sturani, 1978) that primitive Discospirinids may not have occupied the same depth zone as modern varieties.

3.2.3 Interpretation

The composition, texture, faunal and trace fossil content of this lithofacies indicates deposition in an open marine pelagic environment in an outer shelf to bathyal position. There is little indication of terrestrial influence apart from traces of detrital quartz and clay minerals (wind blown?). The absence of hardgrounds, silicified burrows, and *Thalassinoides* type trace fossils (all indicative of shallow shelf environments) supports this interpretation. Preservation of coccolith plates and foraminifera tests indicates deposition above the calcite lysocline. Diagenesis is burial related and involves remobilisation of carbonate by pressure solution and its intra-stratal redistribution, producing marl-rich solution seams where removed, and overgrowths and cements where redeposited. This diagenesis is inferred to indicate burial depths in excess of 1000 metres.

3.3 Marlstones

3.3.1 Occurrence

Marlstone lithologies occur throughout the area of study. They are subordinate in volume to lime mudstone in the lower parts of the Pakhna Formation. Up sequence, the general pattern is towards increasing proportions of marlstones at the expense of lime mudstone lithologies. Dark organic-rich mudstones, as described in the following sections, are found at several localities where exposure is fresh. With weathering, however, they become brown and yellow as in other organic-poor marlstones. Since fresh exposures are only found in a few newly cut road sections it is difficult to accurately assess the extent of these organic-rich marlstones on the basis of field observations alone.

3.3.2 Field Character

At outcrop, this lithofacies occurs as thin to medium-thick (5-50cm), laterally continuous, beds of marls and silty marls. They are distinguished from the lime mudstone lithofacies by their stronger colours (greys, green-browns and yellows) and by their softer, more friable, nature, such that the marlstones are usually weathered more recessively than associated lithologies. Both these features are due to the higher argillaceous content of this lithofacies.

Basal contacts appear to be sharply transitional where not obscured by bioturbation. Some marlstones contain abundant fine-grained plant material and occasional carbonised wood, and may be the weathered equivalents of the dark organic-rich marlstones. Bioturbation is prevalent, with common *Planolites* and *Chondrites* type trace fossils. Anastomosing, but essentially bedding-parallel, solution seams, as described for the lime mudstone lithofacies, also occur in this lithology.

In the area between Ayia Mavri and the Kalavasos road section there is a 1.3m band of red and pink marlstone.

Mapping indicates that this is a laterally continuous feature confined to a particular position in the sequence. This implies that the red colouration is due to a primary compositional feature, that is not common to other parts of the sequence.

As with the lime mudstones, dispersed microfossils can be seen in rocks of this lithofacies with the aid of a hand lens.

3.3.3 Petrology

The marlstones are texturally similar to the lime mudstones in thin section, i.e. globigerinid wackestones and mudstones, but with a more argillaceous micritic matrix. Globigerinid tests are generally uncrushed and variably hollow or infilled with mud or calcite cement. Clay mineral responses on XRD traces for samples from this lithofacies are stronger than for the lime mudstone lithologies. Kaolinite is always found, with significant quantities of montmorillonites and palygorskite in most. Chlorites and illites occur in traces. Quartz is also common.

SEM examination shows various degrees of calcite overgrowth on globigerinids, and a matrix containing ubiquitous coccolith plates. Dark organic-rich marlstones contain abundant plant material with pyrite framboids (Plate 2F). Pyrite is also found within foraminifera tests (Plate 2E).

The red marlstones of the Ayia Mavri-Kalavasos area are globigerinid mudstones coloured by poorly crystalline hydrated iron-oxides (limonite) dispersed through the matrix. XRD analysis reveals trace amounts of muscovite, kaolinite, quartz and feldspar. The absence of sharp peaks for iron-oxide minerals is consistent with the amorphous nature of limonite.

3.3.4 Discussion

The marlstones are in many respects similar to the lime mudstones. They are globigerinid carbonate mudstones

with a nannofossil-rich matrix, and have similar trace fossil assemblages. The marlstone lithologies have a greater proportion of fine-grained silicate minerals, but all those which occur as traces in the lime mudstones are found in the marlstones. These similarities are not surprising in view of the intimate association of these two lithofacies in the lower parts of the Pakhna succession. A hemi-pelagic origin is proposed for the marlstones.

The distinguishing feature of the marlstones is the greater dilution of their biogenic carbonate component with silicate minerals, and this may be of environmental significance. The presence of marl-filled burrows, extending down from marlstone lithologies into underlying lime mudstones, indicates a primary origin for the distinguishing characteristics of this lithofacies. However, the presence of marl-rich solution seams suggests that diagenetic remobilisation of carbonate may have enhanced primary compositional variations.

The increased silicate content of the marlstones (as compared with the lime mudstones) may be due to any of the following processes:

a) syndepositional dissolution of carbonate due to a raised lysocline

b) reduced carbonate production and/or input

c) increased detrital silicate supply

Dissolution of nannofossils and foraminifera prior to incorporation in the sediment, that could reflect a rise in the lysocline, is not apparent from SEM examination of these sediments (Plate 1). Foraminifera are generally well preserved or overgrown. Reduced carbonate production cannot be ruled out on the basis of this study. However, Einsele (1982) concluded that for limestone-marl sequences generally "cyclic productivity can be regarded only occasionally as the principal controlling limestone-marl rhythyms". Furthermore, the occurrence of woody (terrestrial) organic matter and silt grade detrital quartz (and feldspar) within the marlstones suggests a

significant terrigenous contribution to the sediment. This would be consistent with the higher clay mineral content and clay mineralogy, since kaolinite is a characteristic weathering product in tropical soils and montmorillonites can also be derived by weathering of mafic igneous terrain.

3.3.3 Interpretation

In many respects the marlstones are similar to the lime mudstones. They have the same texture, faunal and trace fossil assemblage and similar composition. The higher proportion of silicate minerals and the inclusion of woody organic matter in the marlstones suggests a greater terrestrial influence on this lithofacies. It is possible that influx of this material into the basin reflects tectonic control in an emergent source area. Sedimentary structures have been destroyed by bioturbation. Deposition would therefore appear to have been in an open marine hemi-pelagic environment.

3.4 Laminated calcilutites

3.4.1 Occurrence.

Laminated calcilutites are generally found in the uppermost parts of the Pakhna succession, and continue up to the base of the overlying Kalavasos Formation.

3.4.2 Field character

Exposure is generally poor, as these lithologies are soft and readily break down to produce a soil cover. Best exposures are found on scarp slopes, where water run-off has cleaned the face. They are equivalent to the "paper shales" of Bagnall (1960) and Pantazis (1967), consisting of marls and silts parallel laminated on a millimetre scale. Commonly, they are brown or grey in colour. They are fissile, and often show fossil plant material and fish scales on the lamination surfaces. Other components discernable with a hand lens include sponge spicules and foraminifera. Bioturbation is rare. In some sections,

especially close to the base of the Kalavasos evaporites, gypsum veins occur. These are thin (1 cm or less), filled with fibrous gypsum orientated approximately perpendicular to the vein margins, and cut across bedding in an apparently unsystematic manner.

3.4.3 Petrology

The laminated nature of this lithofacies is sometimes compositional (marly/silty laminations) but is also defined by a preferental parting along surfaces rich in detrital plant material. Compositionally, these beds consist of micro-crystalline argillaceous carbonate, with silt-grade material composed of foraminiferal tests (benthic and pelagic varieties), opaline silica sponge spicules, with lesser detrital quartz and feldspar grains. An abundant, but poorly preserved nannofossil assemblage has been extracted from samples of this lithofacies (Appendix 2).

3.4.4 Discussion

The micro (and macro) fauna of this lithofacies indicates a marine depositional setting (sponge spicules, coccoliths, foraminifera, fish scales). Lamination suggests deposition below storm wave base, or in quiet, protected waters. Absence of bioturbation structures, a scarcity of benthonic macro-fauna, and good preservation of detrital plant material all suggest poorly oxygenated bottom conditions at the time of deposition.

The absence of current structures suggests that the silt-grade terrigenous components, and possibly also the argillaceous components, have been deposited from suspension, and may have been introduced by dilute turbidity currents.

3.4.5 Interpretation

The laminated calcilutites represent deposition in a marine environment with pelagic and terrigenous components. Bottom conditions were probably oxygen

deficient, resulting in supressed benthic activity.

3.3 Calcarenites

3.3.1 Occurrence

Calcarenites occur throughout the Pakhna Formation. However, in lower parts of the sequence, outcropping closer in to the Troodos massif, their occurrence is sporadic and their contribution to the sedimentary column relatively minor. Up sequence, the calcarenites are increasingly abundant, so that at some localities the entire succession consists of this lithofacies.

3.3.2 Field Character

The calcarenites can be usefully subdivided into three types on the basis of bedding character; a) thin-bedded b) medium-bedded and c) massive.

a) Thin-bedded calcarenites

These occur as laterally extensive 2-10 cm thick parallel beds of silt- to sand-grade carbonates or, more rarely, thin and lenticular pebbly beds. Bioturbation often obliterates primary depositional textures, and in extreme cases completely disemminates component calcarenite grains throughout adjacent lithofacies (Plate 6B), destroying bedding completely. However, where bioturbation is not so severe, the thin-bedded calcarenites have sharp bases, and may show normal grading. Tops may be marly or bioturbated. Sometimes outsize elliptical rip-up clasts of lime mudstone or marl occur at the base.

Pebbly thin-bedded calcarenites occur at some localities towards the top of the Pakhna succession. Pebbles are of angular to well-rounded chert and are admixed with coarse to granular bioclastic material. They also differ from the normal thin-bedded calcarenites in that they lens out in one direction (over 10 m or so) and may thicken in the other up to 15 cm. Thus, in this lithofacies scheme, they grade laterally into medium-

bedded calcarenites (see below). Tops may be rippled or exhibit weak parallel- or cross-lamination.

b) Medium-bedded calcarenites

These are 10-30cm thick bioclastic deposits that may be up to pebbly grade at the base and fine upwards to coarse, medium or fine sand. Bedding is parallel and laterally extensive, or channelised (Plate 6D). Some beds have erosive down-cutting bases and may be amalgamated with others of the same type (Plate 6E). Sorting is generally good, though outsize soft marl clasts at the base, and trains of large marly clasts within beds, do occur.

In some cases, scour and erosion at the base of a bed may have resulted in a step-like down-cutting into underlying marlstones or lime mudstones. Adjacent to these erosive lateral bed margins the calcarenites contain a very high density (over 80%) of soft marl rip-up clasts. Away from the bed margin, marl clast size and density fall off rapidly (Plate 6C).

Bases of beds commonly exhibit scours. Loading and flame structures are common. Sole marks, such as grooves and flutes, are found, but bedding surfaces are rarely adequately exposed. Tops are occasionally asymmetrically rippled, or with a trace of parallel- or low angle cross-lamination.

Calcarenite components identifiable at outcrop include bivalve fragments (especially pectinids and oysters), coralline algae, coral fragments, sponge spicules, large foraminifera, chert pebbles and chalk lithoclasts. At many localities these calcarenites are friable and appear to have undergone exsolution of aragonitic components.

Infaunal escape burrows and Thalassinoides-type trace fossils are sometimes found.

c) Massive calcarenites

These occur as thick-bedded (over 30cm) units of well

sorted but ungraded buff-brown to white calcarenites (Plate 7C). Grain size may be up to granule grade. Thickening of individual beds is not apparent at most outcrops, but in the larger quarries lensing and broad channelling can be seen (Plate 8).

Beds are generally massive and structureless. Rarely, however, rippled upper surfaces or parallel laminated tops are developed. De-watering pipes have been observed but dish structures are not seen. Large (10 cm) elliptical marl clasts may be found near the base or entrained within these beds.

Some beds consist of a coarse bioclastic matrix containing moulds of whole and fragmented shelly material up to 2cm across. Moulds are of originally aragonitic bivalve shells, gastropods and corallites. Undissolved fragments include oyster and coralline algae debris. Many fossils show evidence of boring by macro-organisms (gastropods or sponges) prior to sedimentation. Dispersed chert granules and pebbles are also present.

The extreme thickness of some of these units, sometimes in excess of 5m, is probably due to an amalgamation of several depositional units that is difficult to detect due to uniformity of grain size and lack of structures or interbeds.

3.5.3 Petrology

The calcarenites are carbonate grainstones with a sparry calcite cement, or a mud matrix. Composition varies with position in the Pakhna succession. Lower down, calcarenites consist of well sorted globigerinid sands with small amounts of silt grade quartz grains (Plate 3A). Up sequence, large benthonic foraminifera (mostly discorbaceans, orbitoids and rotaliaceans) become increasingly common at the expense of pelagic varieties (Plate 3B). Concomitant with this change in foraminiferal composition is the inclusion of increasing amounts of neritic bioclastic material. This shallow water-derived component contains fragments of coralline algae (branching

and encrusting varieties), bivalves, echinoids, bryozoans, gastropods, serpulid worm tubes, sponge spicules, corals, micritised peloids, and, rarely, relic ooids. Some clasts have micritic envelopes. See Plates 3C, 3D, 4A, 4B, 4C, 4D.

Towards the top of the sequence there is a significant siliciclastic component, containing detrital feldspars, pyroxenes, and quartz grains, and rock fragments of chert, globigerinid chalk, micritic limestone and basaltic lavas (Plate 5A).

Burial compaction effects are variable. Some samples show bedding-parallel compaction and crushing of thin-walled components and inter-penetration of more competent grains. Chambers, such as in uncrushed foraminifera tests, are infilled with calcite spar or lime mud.

Neomorphism of carbonate grains is common, and is generally associated with a mosaic calcite cement.

Lava fragments are usually degraded, limonite and chlorites being common products.

3.5.4 Discussion

The different bedding characteristics of the three types of calcarenite lithology, as described in section 3.5.2, requires that they are discussed separately.

Thin-bedded calcarenites

Sharp bases, bioturbated tops, lateral continuity, grading, cross-bedding, rippled tops, and the inclusion of soft rip-up clasts are all indicative of deposition from a turbidity current. Thin-bedded turbidites can be deposited in a variety of settings, ranging, for example, from basin plain to inter-channel, channel mouth or lobe fringe settings in an ideal deep sea fan (Mutti, 1977; Walker, 1978); or in basin margin settings involving sheets or broadly channelled thin-bedded turbidites as part of a distal apron sequence along a carbonate margin (Cook & Mullins, 1983; Mullins *et al.*, 1984). Distinguishing between the various possible settings requires an

EX BIBL. UNIV. EDINBURGH

interpretation of the facies assemblage within which this lithofacies occurs, and this is undertaken in chapter 4.

The pebbly thin-bedded turbidites are unusual, since most "distal" or "proximal" thin-bedded turbidites are relatively fine grained. However, this type of lithology may correspond to the "proximal limb" of a turbidite deposited in the relatively short proximal "feather edge" of an asymmetrically lenticular turbidite (Engel, 1974; Sadler, 1982). This would be consistent with the observation that these beds grade laterally into medium-bedded calcarenites.

Medium-bedded calcarenites

These are also interpreted as turbidite deposits. Turbiditic features include sharp bases with scour and sole marks, grading, and continuous parallel bedding or bedding thinning against channel margins. The poor development of classic Bouma sequence structures, with only rare parallel or cross lamination preserved, may reflect rapid decay of stream power during deposition, or it may be due to the control of grain size on depositional mechanisms as suggested by Mutti & Ricci-Lucchi (1975) who observed that turbiditic medium to very coarse grained sandstones generally lack internal lamination except near the top. Grain density may also be important (see Robertson, 1976). It is also possible that grain shape may be inhibiting development of these structures, since bioclastic skeletal fragments are more irregular and generally less equidimensional than the siliciclastic components in most classical turbidites. In this respect, the different hydrodynamic behaviour of bioclastic grains has been reported by Maiklem (1968).

The inclusion of soft marly rip-up clasts is brought about by erosion of the substrate during transport and deposition of this lithology. Local derivation and minimal transportation of these rip-up clasts is demonstrable at some outcrops. Plate 6C, for example, shows a step-like portion of a graded calcarenite margin which has been

eroded into the underlying marlstone lithology. Laterally, within the calcarenite, the concentration of substrate derived marly clasts decreases from over 80% close to the margin to much lower values away from the stepped edge, where marly clasts are more dispersed and have been transported further. Erosion of the substate, which appears to have behaved in a cohesive manner, involves initial disaggregation into large blocky angular "clasts". Further break-up and rounding of these soft clasts only comes with incorporation into, and transport within, the calcarenitic material of the turbidite.

As with the thin-bedded calcarenites, these medium bedded calciturbidites could be deposited in a wide range of environments. Resolution relies on interpretation of facies assemblages and is attempted in the following chapter.

Massive calcarenites

These bear many similarities to the massive sandstones of Walker (1978). Sharp bases and tops , with occasional de-watering pipes and infaunal escape burrows suggest rapid deposition in a single event by a process in which the final grain support mechanism is the upward flow of pore fluid (Lowe, 1976). Field evidence and lithofacies associations (chapter 4) show that these massive calcarenites were deposited in marine channel-fill sequences, and it seems likely, therefore, that sediment transport was by high density turbidity currents. Under the Bouma terminology these would be described as A-unit only turbidites (B,C,D units absent).

The uniform grain size suggests derivation from a previously sorted sediment body. It may be that these deposits represent material from carbonate sand shoals in a shallow-water wave-influenced environment that have subsequently been redeposited into deeper water by mass flow processes.

Compositional variations in the calcarenites are similar for each of the different bedform types. These variations represent changes in the source environment. Globigerinid turbidites indicate reworking of unconsolidated pelagic or hemi-pelagic sediment. Calciturbidites composed largely of large benthonic foraminifera normally associated with symbiotic algae suggest a source within the photic zone. Coralline algae are not normally found below 150m water depth (Wray, 1983). Other carbonate skeletal components are generally shallow water types and indicate ultimate derivation from a neritic environment with a diverse normal marine fauna.

The non-skeletal components, which are particularly common in this lithofacies towards the top of the Pakhna Formation, are characteristic of the Troodos ophiolite and sedimentary cover lithologies, and may be derived from an adjacent uplifted portion of the ophiolite. The cherts and globigerinid chalk lithoclasts are similar to Lefkara Formation lithologies. An alternative source for the chalk clasts would be by erosion and down-slope reworking of sediment which had undergone early submarine cementation on the upper portion of a carbonate slope (see Mullins et al., 1984). Lava fragments may have been eroded from the Troodos pillow lavas, though it is also possible that they could be from the Dhiarizos Group of the Mamonia Complex which crops out in southwest Cyprus. Palaeogeographic reconstructions based on facies analysis is helpful in resolving these possibilities and is undertaken in chapter 5.

3.6 Rudites

3.6.1 Introduction

Two lithological subdivisions of rudites are recognised: clast-supported conglomerates and matrix-supported conglomerates. They are generally found only in the uppermost sequences of the Pakhna Formation, where they are frequently associated with calcarenites .However, matrix supported conglomerates occur sporadically

throughout the whole succession, particularly in the area to the east of the Limassol Forest block.

3.6.2 Field description

Clast-supported conglomerates occur in beds varying from less than a metre to over 4 metres thick. Bases are sharp, often with scour and erosion, sometimes with loading structures. Bedforms may be channellised, with channel margins directly observed in outcrop (Plate 7A), or inferred from the limited lateral continuity of beds. Otherwise conglomerates occur in extensive sheets with planar bases. Clasts are well rounded and vary in size up to 30 cm across, though rarely outsize 'rafts' over 2 m in length are found. The matrix is of sand to pebble grade material.

The clast supported conglomerates can be divided into two types, based on composition:

a) carbonate conglomerates

b) polymict conglomerates

The carbonate conglomerates have a globigerinid chalk matrix with admixed echinoid fragments and shallow water bioclastic grains supporting clasts of compound corals, chalks and marls, recrystallized limestone, and carbonate lithoclasts of shallow marine origin.

The polymict conglomerates contain cobbles and boulders of chalk, poorly preserved compound corals and igneous material comparable with the pillow lavas and dolerites of the Limassol Forest block (Plate 7B). No ultra-mafic type igneous clasts are found. The matrix is of sand to pebble grade bioclastic material (including corals, vermetid gastropods aggregates, bivalve fragments, gastropods, coralline algae, large foraminifera and echinoid debris) admixed with chert and degraded igneous pebbles.

Internal organisation of these conglomerates is variable, ranging from well organised with grading, imbrication and stratification to completely disorganised. Where imbrication occurs it is with the long (a-) axis

dipping in an up-stream direction and the intermediate (b-) axis lying transverse to flow. This is the "resedimented conglomerate" fabric of Walker (1975), and the four re-sedimented conglomerate models presented therein apply well to these sediments (fig. 3.1).

Bed thickness of matrix-supported conglomerates range from 0.3 to 4 metres, and may vary substantially on outcrop scale. Bases are non-erosive, and planar except where loading has occurred. Channelling of these deposits is sometimes evident, with beds thinning against channel margins. In the Happy Valley road section (GR 839369, in Episkopi Sovereign Base) drag folds are developed in the sediments immediately underlying matrix-supported conglomerates, and thrusting has occurred in sediments at the toe of the deposit (see section 3.3.4). Both features can be related to deceleration of the debris-flow during the final stages of emplacement.

Bed tops are usually planar, with occasional upward projecting blocks. Where relief was developed it has been locally planed off and ponded with later sediments.

Clast composition of the matrix-supported conglomerates varies. Some, especially those occurring in channel-fill sequences cut into marls and chalks, are monomict with clasts of material similar to the local substrate. These clasts are irregular in shape, with rounded edges and sometimes folded back on themselves in a manner suggestive of slumpballs. They appear to have been soft but coherent when incorporated into the sediment and the implication is that they have been derived by erosion of the substrate on the channel margins or elsewhere in an up-current direction, possibly very locally. The matrix is of marly carbonate sand which may be normally graded toward the top of the unit.

Another distinctive type of deposit consists of angular platy limestone clasts up to 50 cm in length. These clasts are of irregularly laminated pelsparites (Plate 5B) set in a micritic matrix with scattered pelagic forams or rarer admixed bioclastic debris. Encrustation of

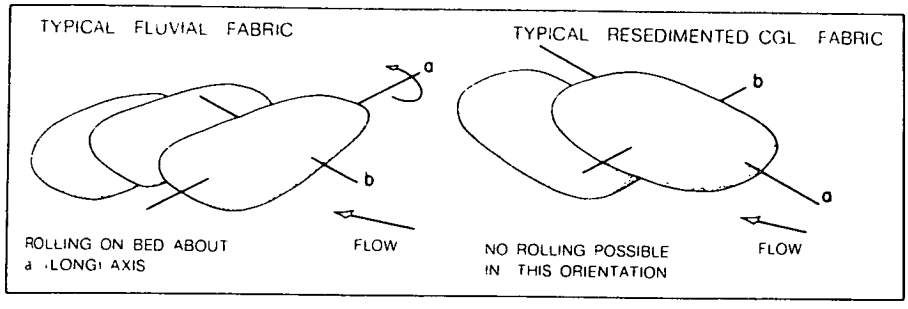

Contrast between conglomerate fabric produced by rolling clasts on the bed (long axis transverse to flow) with typical fabric in resedimented conglomerates (no rolling, long axis parallel to flow).

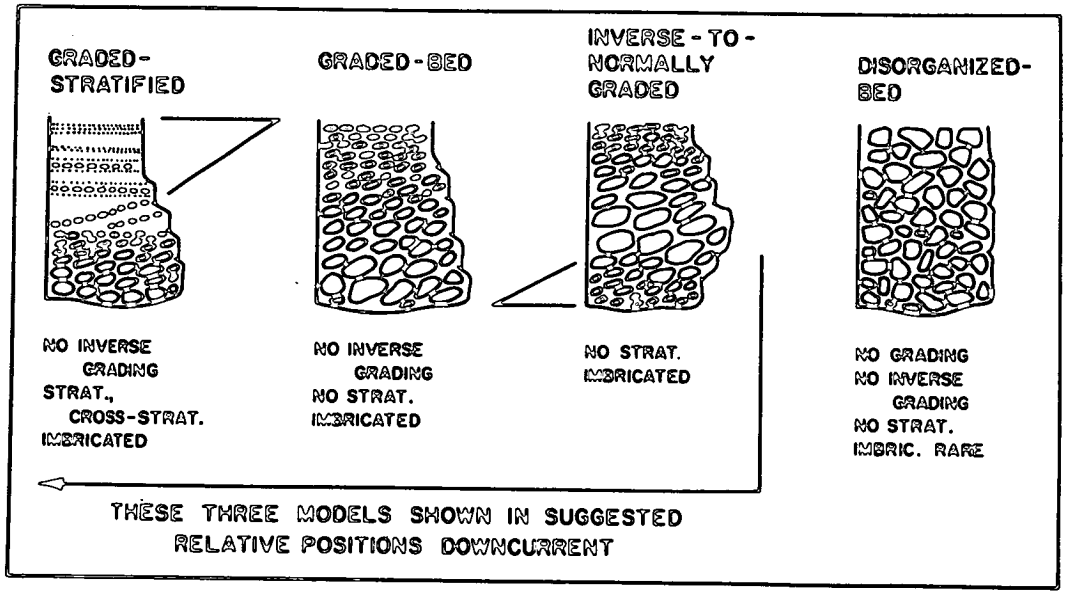

FIG. 3.1, showing (above) the resedimented conglomerate fabric of Walker (1975), and (below) the clast supported conglomerate models of Walker (1979) based on internal organisation.

clasts by serpulids has been observed (Plate 4A), suggesting that the matrix originates by post-depositional infiltration. Preferred orientation of clasts is sometimes evident.

Other conglomerates consist of rounded cobbles and boulders of finely recrystallised limestones, compound corals, chalks and lithified muddy calcarenites with neritic debris. Matrix is chalky with pelagic foraminifera.

3.6.3 Discussion

Several factors indicate a marine depositional setting for the rudites:

a) lithofacies associations

b) matrix composition

c) internal organisation

Interbedding with marls and siltstones of undisputable marine origin is the most obvious environmental indication and is commonly observed at outcrop with this lithofacies (see chapter 4).

Matrix composition is essentially of two types: substrate-similar and substrate-dissimilar. A substrate-similar matrix is one which is compositionally similar to the underlying lithology and is most commonly micritic with dispersed globigerinid foraminifera (e.g. Happy Valley). These are interpreted as having been incorporated into the rudite by turbulent mixing during transport across the substrate, producing a richer micrite-water mix and enhancing bouyancy-lift and cohesion of rudite clasts (Lowe, 1982). Mixing of unlithified globigerinid micrites in this way would indicate a marine setting.

Substrate-dissimilar matrices consist of pebbles and gravels of terrigenous derivation (lava fragments) with skeletal material of shallow marine origin. Aragonitic components (notably coral and gastropod clasts) have been dissolved subsequent to deposition creating a mouldic porosity. As a gravity deposit, therefore, these rudites must be deposited down-slope of a neritic marine

environment.

The internal organisation of the clast-supported conglomerates compares well with descriptions from Walker (1979), summarised in figure 3.1. These are thought to be deposited by high density turbidity currents. Inverse grading, where it occurs, is normally in the lower part of a conglomerate bed and is equivalent to the R2 unit of Lowe (1982) (fig. 3.2). He interprets this as representing the freezing of a highly concentrated traction carpet due to a drop in flow velocity below that necessary to maintain dispersive pressure. This may then be followed by direct sedimentation of suspended material producing a graded layer (R3) which may then be reworked by the now waning but relatively steady sandy high density turbidity current producing stratification structures as found in the graded stratified conglomerate model (fig. 3.1).

Disorganised grain-supported conglomerates probably result from cohesive flow processes (Lowe, 1982). The matrix/water mixture provides bouyant lift, thereby reducing the effective weight of clasts, and lubricates grains, thereby preventing frictional locking (Rodine and Johnson, 1976). These deposits are similar to debris-flows except that clast support during transport is by lubricated intergranular dispersion (ie. by rolling, sliding and bouncing in a bouyant, lubricating matrix/water mixture).

With a more cohesive and denser matrix, clasts can be fully supported, and a true debris-flow results. These are structureless except in the lower boundary layer where simple shear occurs due to frictional resistance with the substrate. This may rotate non-spherical clasts into a preferred orientation with short axes perpendicular to the base, imparting an imbrication to the deposit. Platey clasts of lithified irregularly laminated pelsparites show preferred orientation in some Koronia Limestone deposits which can be related to the palaeoslope down which the debris flow travelled (see chapter 5 for integration of palaeoslope data).

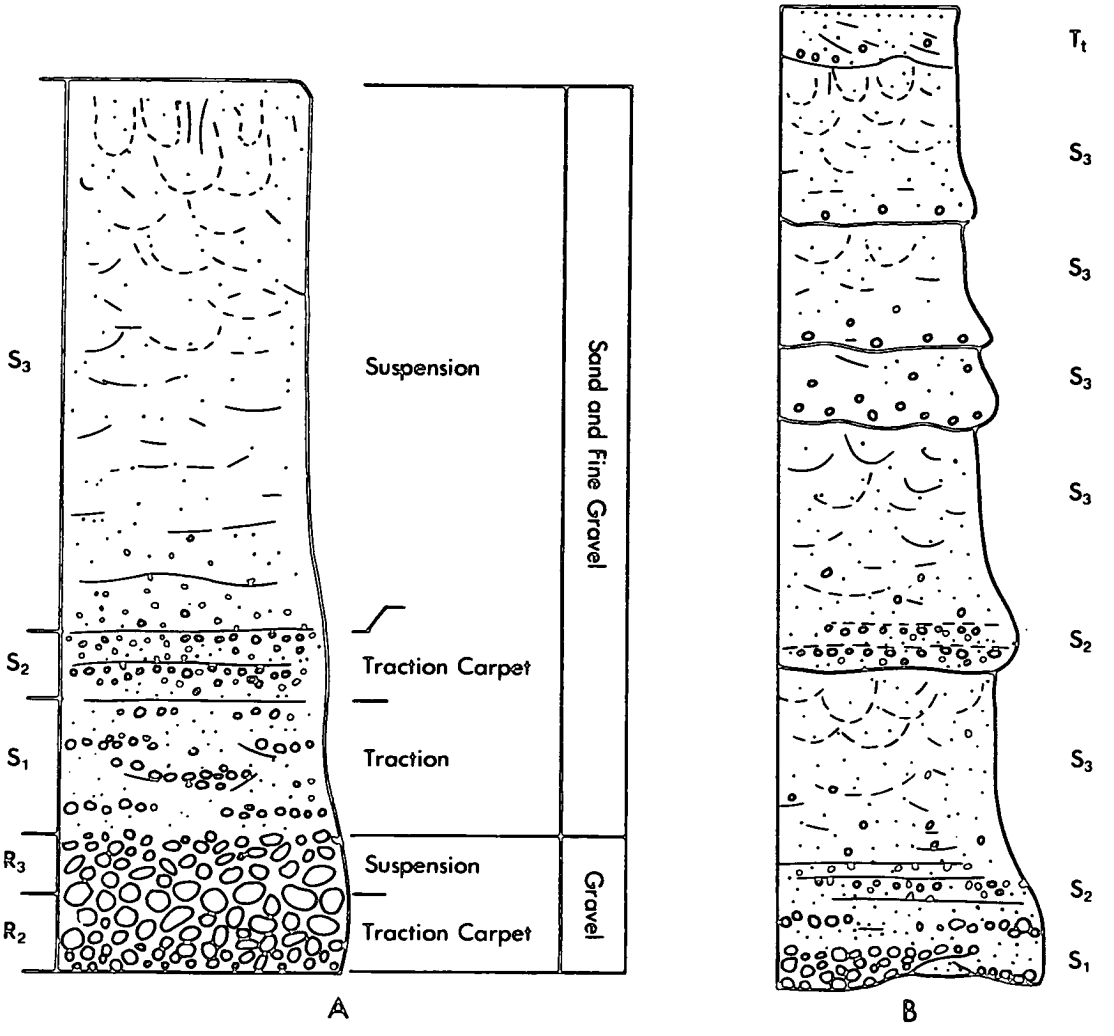

A) Ideal sequence of divisions deposited by a single high-density turbidity current declining through discrete gravelly and sandy sedimentation waves. Because of downslope separation of gravel and sand depositional stages, complete high-density sedimentation units such as this are rarely formed. B) Complex sedimentation unit deposited by surging sandy high-density turbidity current.

FIG.3.2 From Lowe (1982)

Many workers have speculated theoretically (eg. Hampton, 1972), or postulated from field evidence (Gawthorpe and Clemmey, 1985), that marine debris-flows may be generated from the break up of sedimentary slides. Field observations from this study strongly suggest that such a mechanism is valid (see section 3.7.4).

As with the calcarenites, the different components in the rudites can be interpreted as having been derived from different portions of an emergent land-mass to basin transect. Cherts, chalk lithoclasts and Troodos-type lava clasts have been eroded from an emergent block of the ophiolite. Micritised peloids, skeletal material, miliolid foraminifera etc. may be derived from protected marginal marine areas, possibly in a back-reef environment. Compound coral boulders, coralline algae, bryozoans etc. may represent reef talus.

There is a marked contrast in the rounding of component clasts of different derivation. Terrigenous material is generally well rounded whereas matrix skeletal material is often whole and unbroken. This may reflect differing transport histories as would be expected if land-derived erosion products were mixed with neritic carbonate material prior to down slope reworking by gravity driven processes.

3.6.4 Interpretation

The rudites of the Pakhna Formation are all marine deposits comprising clasts reworked down-slope and incorporated into channel-fill sequences or as planar sheet deposits. Clasts have been derived from uplifted basement and associated sedimentary cover units and have been mixed with neritic and reefal carbonate material and slope deposits during transport history. Transport mechanisms are gravity controlled and dominated by high density turbidity currents with a significant amount of grain interaction. Internal organisation and consideration of theoretical models suggests that deposition involves variously traction or suspension sedimentation or

frictional and/or cohesive freezing.

3.7 Slumps

3.7.1. Introduction

The terms "slide" and "slump" are here used in the manner suggested by Woodcock (1979b) i.e. slide refers to a failed sediment body which may contain rotated and unrotated elements, slump refers to a unit which displays only rotated characteristics (internal deformation, angular discordance between failed and unfailed units).

The most reliable criterium for the identification of sedimentary slides is their intraformational nature, i.e. that they are bound above and below by normally bedded units. This is only apparent when looking at slumped portions of a slide, or where dissimilar lithologies are juxtaposed against a glide plane which can be shown to have developed intraformationally.

Sliding can affect any of the lithologies described, and can produce a range of deformational styles within the slide unit. Exposure is frequently inadequate for meaningful detailed interpretation. However, several outstanding exposures do occur and these are important not only for their implications for basin reconstruction, but also for their relevance to an understanding of the processes involved in the development of marine slides.

3.7.2 Description

Units of this lithofacies range in thickness from 0.8 m to over 12 m. Lateral extent in some instances may be limited, of the order of tens of metres, but the more spectacular slump sheets can be traced at individual outcrops for hundreds of metres and may extend over several tens of kilometres (see discusion). Lithologies involved vary from medium bedded chalks and foraminiferal sands to graded calciturbidites and silts. Debris flows may also be incorporated into the failed unit.

Slumped lithofacies usually have a planar or slightly undulating base corresponding to the lower detachment

surface, but this may be modified by syn-or immediately post-emplacement dewatering from underlying beds. Upper surfaces may be planar or irregular. Irregular surfaces are ponded and/or eroded by succeeding units.

Internally, slumped lithofacies show a range of deformational styles and intensities, ranging from undeformed portions to complete disaggregation. Slump folds are gently to steeply inclined, with short limb lengths ranging from a few centimetres to over 2 m. Hinge thickening and limb thinning is sometimes apparent. Axial planes may be straight or refolded. Refolding can result in upright open folds with sub-vertical axes, or non cylindrical approximately co-axial refolded folds with flat lying axial surfaces.

Apart from the basal glide plane, other faults may cut into the slump unit isolating recumbent intra-folial folds or terminating as tip lines in the cores of folds. In other cases, faults may cut up to the upper surface, separating coherent units within the slump body.

Some fold limbs display micro-faulting, usually extensional (Plate 9B), but on some short limbs with a reverse off-set (contractional, Plate 9C).

3.7.3. A model of slump fold development

Slumps are produced by gravity driven slope failure in the sediment pile, resulting in the downslope transport of a coherent or semi-coherent unlithified sediment body. Much of the work on slumps has concentrated on the relationship between fold attitude and palaeoslope orientation (Hansen, 1965; Lajoie, 1972; Stone, 1976; Woodcock, 1979a). More recently, workers have become interested in the detailed internal organisation of sedimentary slides and an understanding of the processes involved in their generation (Farrell, 1984; Gawthorpe and Clemmey, 1985; Farrell and Eaton, in press). This section discusses a model for slump fold development. The major slump bodies observed in southern Cyprus are then discussed within the context of this model.

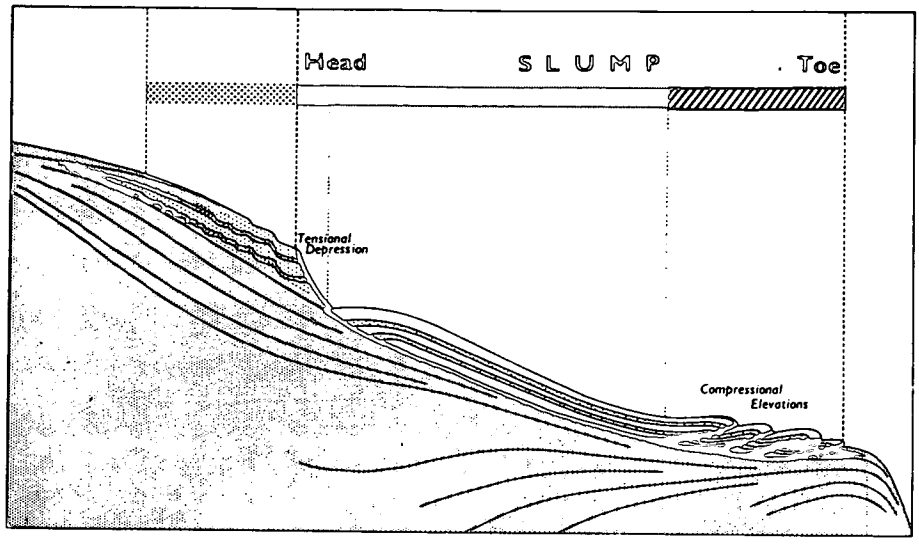

Diagrammatic cross-section of a slump on a gentle slope. Unstippled beds have slumped; sparsely stippled beds have been disturbed perhaps by intrastratal movement; densely stippled beds have not been disturbed. Cross-hatching overlies a zone of compressional folding and thrusting at toe of slump. Vertical hatching overlies a zone of undeformed or slightly deformed beds in the middle of the slump. Solid black overlies an exposed glide plane in a zone of tension at the head of the slump. Large stipples overlie disturbed beds beneath smooth seabed.

FIG 3.3 Cross-sectional geometry of a modern slump, from Lewis (1971).

Studies on modern submarine slides (eg. Lewis, 1971) show that they are characterised by having a basal failure above which the unit has undergone contractural strain in its forward (downslope) region and extensional strain in its rear (upslope) portion (the head, fig. 3.3). This is similar to the cross section predicted for the initial failure of a sedimentary slump by the dislocation propagation model of Farrell (1984). The basal failure is initiated as a point dislocation and propagates as a fault tip line (sense of Boyer & Eliot, 1982). Strain in the material above this dislocation loop depends on the relationship between the fault propagation direction and the slip direction. With sedimentary slides the slip direction is controlled by the orientation of the (palaeo-) slope. Thus upslope from the initial failure point strain in the overlying material is extensional, whereas downslope it is contractional (fig. 3.4). Extensional stain may be accommodated by faulting or ductile thinning. Contractional strain, it is argued, produces upright buckle folds by pure shear deformation of anisotropic (i.e. bedded) sediments during slump initiation (Farrell & Eaton, in press). Fold hinges are developed sub-parallel to the palaeoslope strike (Jones, 1940), although some initial curvature may be generated by the radial propagation of the basal failure surface. Hence the average fold axis orientation is normally used as an indication of the palaeoslope strike (Woodcock, 1976).

If the basal failure surface cuts up and intersects the sediment-water interface, the faulted unit is completely detached and may travel downslope as a coherent unit. This may happen on slopes as low as 2 degrees (Lewis, 1971). If there is significant frictional resistance on the detachment surface (which may be enhanced by dewatering) then simple shear is imparted on the slide during transport. This has the effect of rotating linear elements into the transport direction. Thus, with increasing simple shear, upright symmetrical buckle folds, with fold axes grouped closely around the

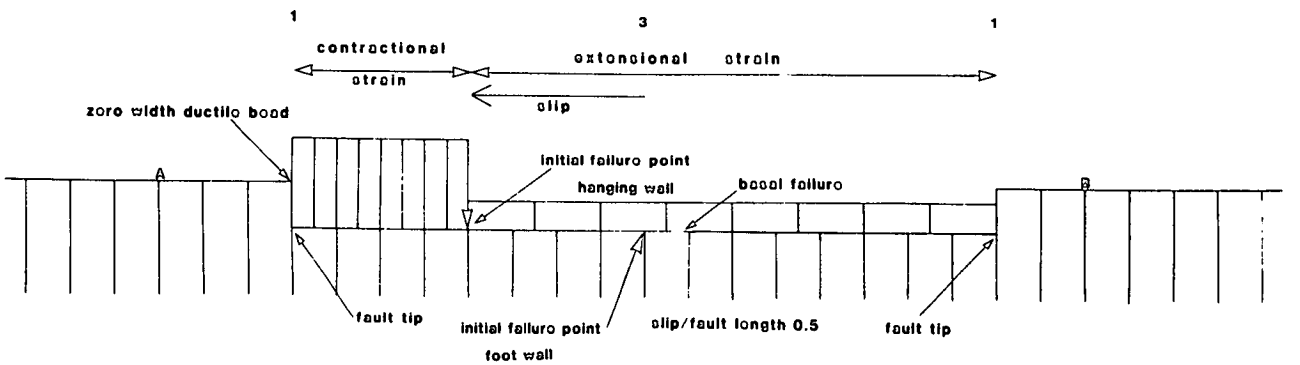

FIG. 3.4 Strain relationships developed during slump initiation, from theoretical considerations (Farrell, 1984). Down slope direction is to the left.

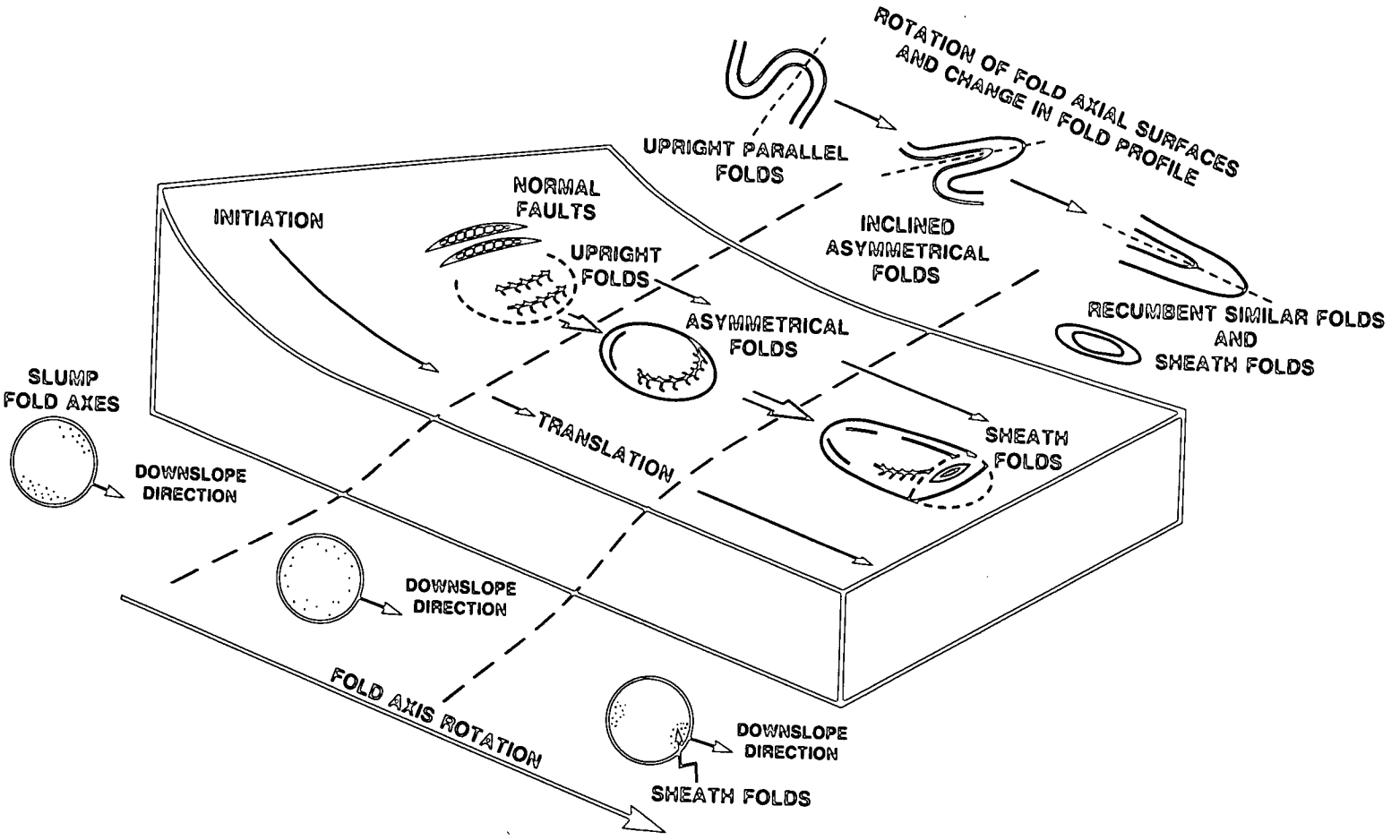

FIG. 3.3 Modification of slump geometries during translation. See text.

palaeoslope strike direction, evolve into recumbent or isoclinal folds with shallowly dipping axial surfaces and fold axes scattered towards the gross transport direction (downslope), see figure 3.5. Plots of axial surface dip against fold hinge azimuth for slumps from Cyprus are plotted in fig. 3.6 and demonstrate this relationship. For a population of folds from within each individual slump unit, rotation of the hinge azimuths toward the gross transport direction is accompanied by a tendancy towards recumbence (shallower dip of axial planes). Initially curvilinear hinges may be accentuated into sheath folds by this process.

Deceleration and termination of movement may result from translation onto a reduced slope, or by regaining of shear strength across the basal failure surface (Farrell, 1984). The former would result in deceleration of the slide from front to back (upslope propagation of an "anti-dislocation"), over-printing a contractional strain on the unit which may result in late stage upright buckle folds refolding earlier structures.

An increase in shear strength across the basal failure surface would be promoted by a drop in pore fluid pressure due to de-watering. Fluid escape is easiest at the rear of the slide where normal faulting occurred during the initial failure event. This would promote deceleration from the rear, with the forward propagation of an "anti-dislocation" and extensional strain over-printing. This would involve increasing friction on the basal failure surface and increased simple shear immediately prior to movement termination. Clastic dyke development and sediment injection structures could also be associated with this late stage extensional event. By this process it would be possible for a slide to come to rest before reaching the base of slope.

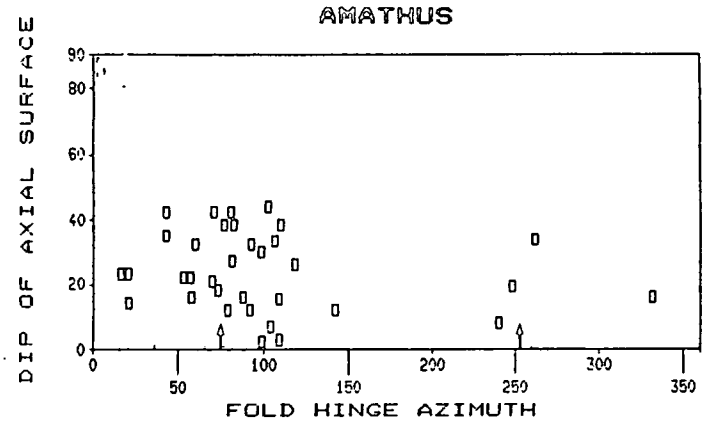

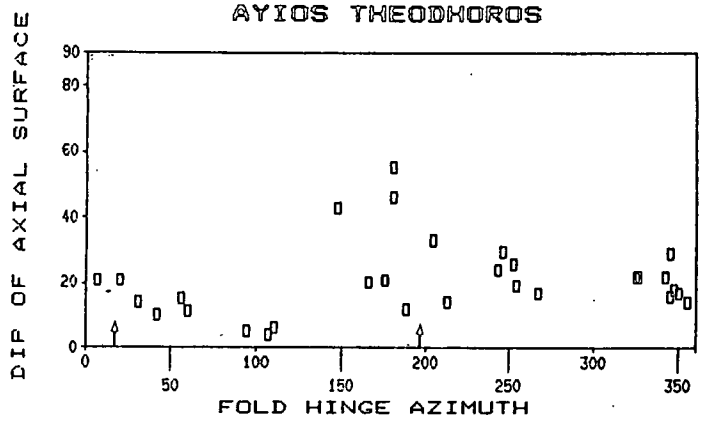

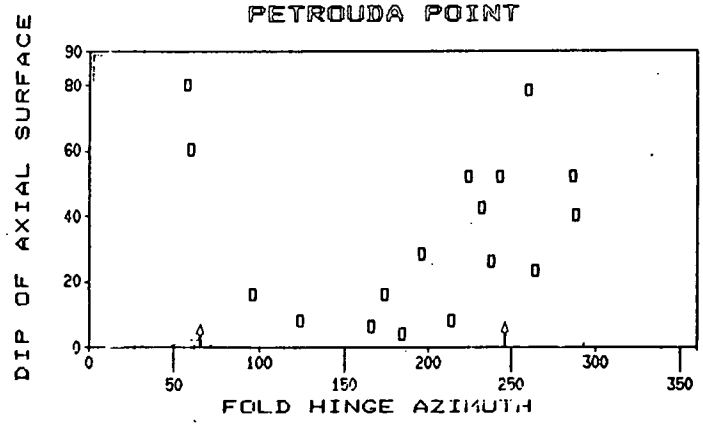

FIG. 3.6 Plots of axial plane dips against fold axis azimuth for populations from three slumped units in Cyprus (see section 5.3 for details). Arrows show mean axis azimuth. Note how the most upright folds generally occur with fold axis orientation close to mean axis orientation. All data corrected for regional dip.

3.7.4 Discussion

The various outcrops of slumped lithofacies of the Pakhna Formation in southern Cyprus, with their differing deformation styles, can all be interpreted within the framework of the model described above. Five major exposures are referred to, details of which are summarised in Table 3.1. Of the five, one is from the Kalavasos Formation but is referred to briefly in this section as the deformation style is relevant to the topic of slump processes. Another locality, Petrounda Point, was mapped by Bagnall (1960) as Lefkara Formation but is time equivalent to Pakhna Formation sediments (see section 2.5.3).

Slumps involving only layer parallel shortening by pure shear, as would be expected if slump development was arrested at an early stage, have not been found within the Pakhna Formation. However, a 0.8 m thick buckle folded gypsum unit of the Kalavasos Formation is found at Tokni Quarry (see section 6.3.7). The upright fold style (Plate 17D) and close clustering of fold axes (fig. 5.2) suggests that negligable translation related rotation of elements has occurred and that data from this site would provide an accurate estimate of palaeoslope orientation (see section 5.3.2).

The slump folded horizons that are found in the Koronia Limestone Member at Amathus (see fig. 3.7) consist of finely interbedded carbonate sands and silts (calcarenite lithofacies). These occur within a channel-fill sequence of graded calcarenites and rudites. Slump thickness ranges from 0.8 to 1.0 m. Slump folds are generally asymmetrical, with axial surfaces inclined at angles ranging from a few degrees to 45 degrees with respect to the underlying bedding, indicating significant simple shear. This is also suggested by the scatter in fold axes orientations (chapter 5, fig. 5.2). Micro-faults, with cm scale spacings and throws of a few mm, are observed on fold limbs. Examination of polished sections across these faults shows them to be diffuse zones of

	TOKHNI	AMATHUS	AYIOS THEODHOROS	PETROUDA POINT	AYIA PHYLA
Thickness of slump unit	1.5 m	1.0 m	5 m	Over 12 m	4 m
Upright to inclined folds	YES	YES			
Recumbent isoclinal folds			YES	YES	YES
Sheath folds		YES		YES	
Refolded folds				YES	
Late upright folds				YES	

Table 3.1. Summary list of features observed at five slump exposures discussed in the text. See fig. 3.7 for locations.

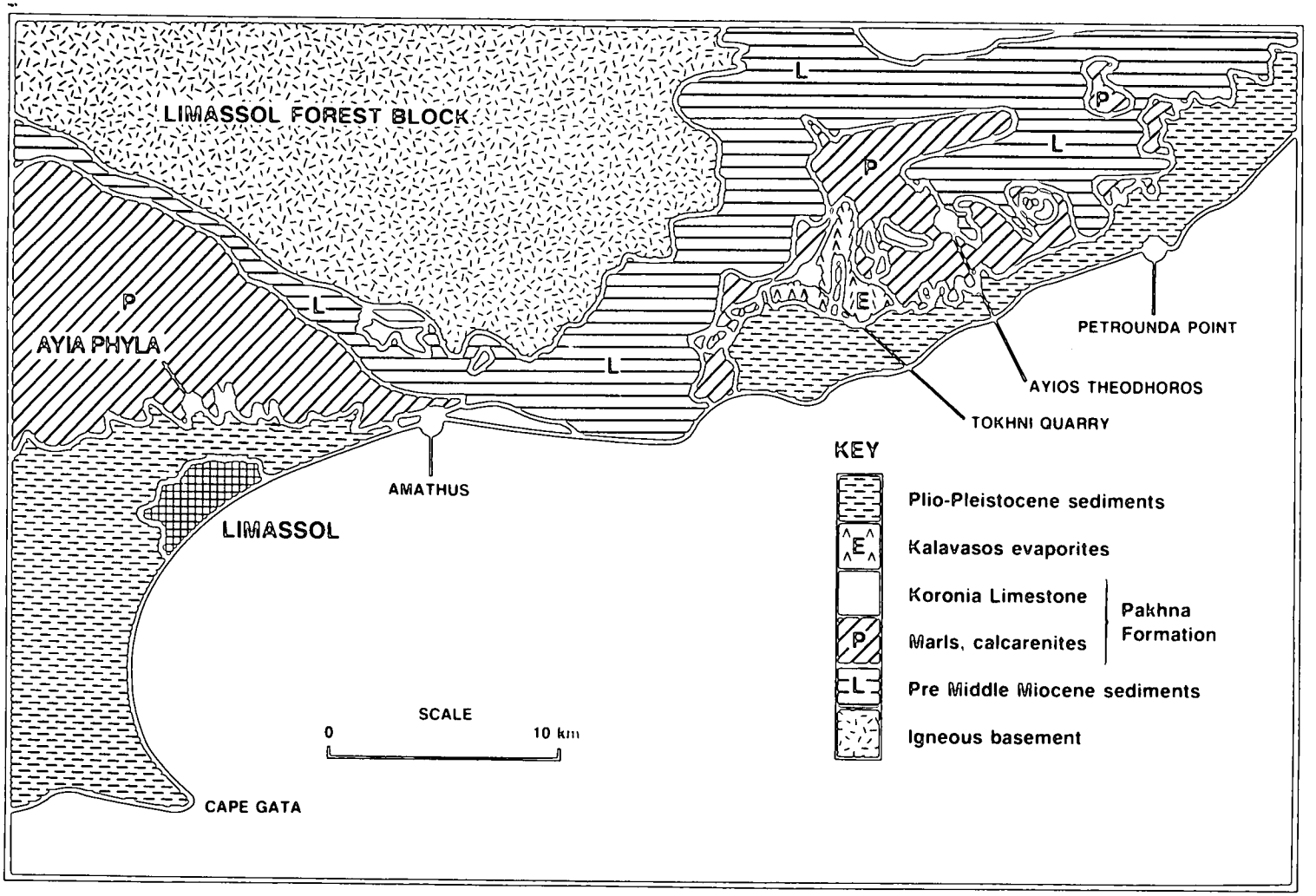

FIG. 3.7 Location map for text section 3.7.4, showing slump localities.

grain re-packing. Micro-faults may show a reverse sense of displacement (contractional strain) on some steep limbs, but are more usually extensional. They may be developed during simple shear of early buckle folds. Elements such as fold limbs lying within the contractional field of the incremental strain ellipsoid will shorten and develop reverse micro-faults, whereas other elements will be extensionally strained. A brittle response to strain may reflect competancy, or could be promoted by high pore fluid pressures.

Ubiquitous fluid injection structures, piercement structures, and clastic dykes, often exploiting pre-existent slump faults (fig. 3.8), testify to rapid de-watering from the substrate. Clastic dyke orientations are roughly parallel to the palaeoslope strike (as estimated from the slump fold data) and their termination at the top of the slumped unit demonstrates their (immediately) post-emplacement origin. It is possible that de-watering from the basal detachment surface and the consequent drop in pore fluid pressure contributed to the termination of slump movement.

The slumped unit at Ayios Theodhoros (fig. 3.7, Plate 9F) consists of a 5 m thick unit of medium bedded foraminiferal chalks with thin marly interbeds, which have been deformed into asymmetrical recumbent folds with shallowly dipping axial surfaces and curvilinear hinges. Many folds are isolated by internal glide planes. The basal detachment surface is planar with no fluid injection structures or signs of rapid de-watering. These features suggest that substantial simple shear has been imposed during transport, and that this slump may be relatively far travelled.

The cliff exposure at Petrouda Point consists of chalks, marls, foraminiferal sands and lignitic marls which have all been incorporated into a slump horizon in excess of 12 m thick (Plate 9D). The unit includes early thin slumps and debris flows which have been refolded into open to tight upright large scale folds with limb lengths

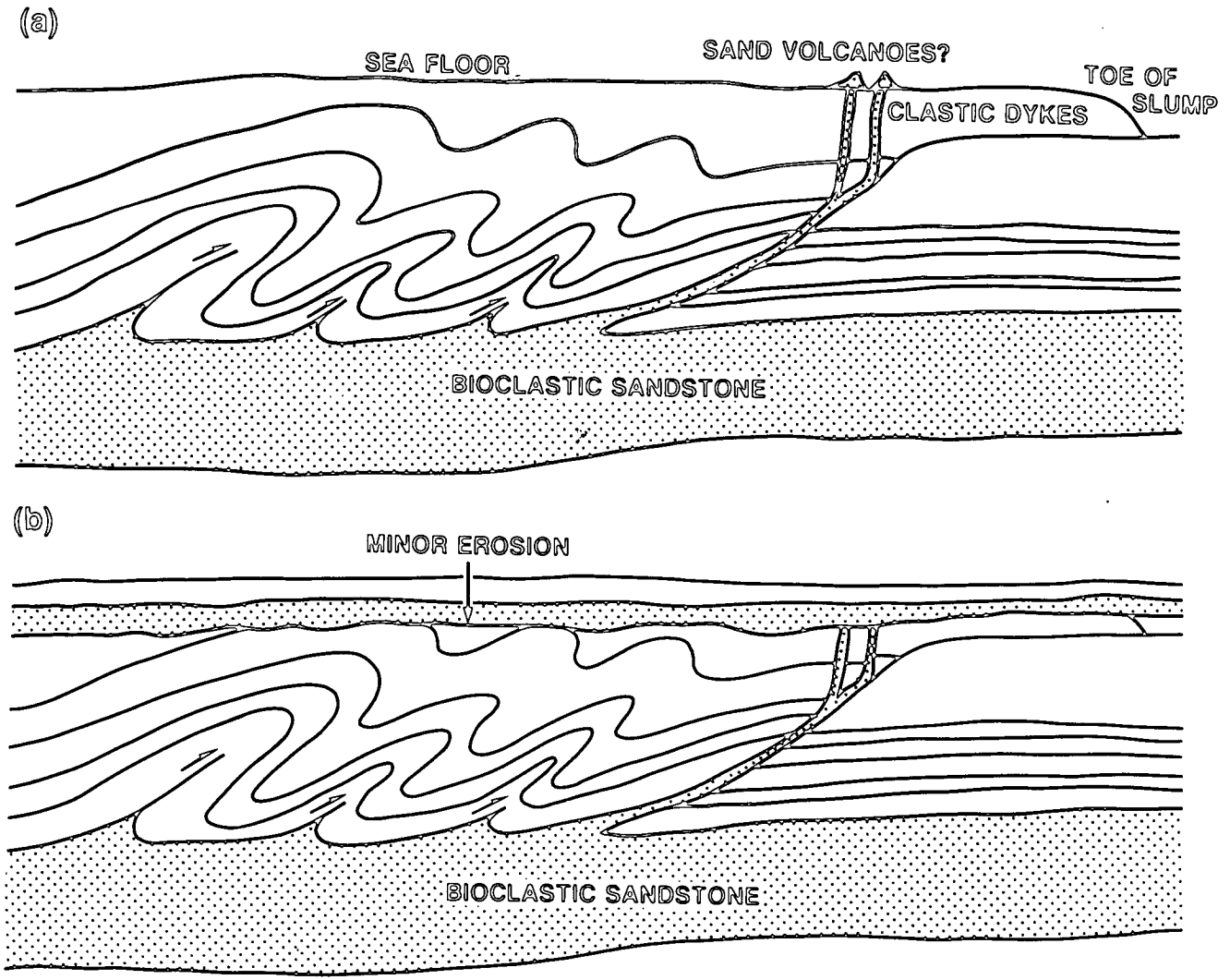

FIG. 3.8 Slump unit at Amathus showing (a) immediately post emplacement geometry and (b) post burial geometry (interpreted). Note fluid injection structure exploiting slump fault.

up to 8 m. The early folds include refolded "hook" folds and sheath folds (Plate 9E), testifying to substantial simple shear and polyphase folding. The late large-scale upright folds are interpreted as having formed during termination of movement due to a decrease in slope gradient. Similar slump units are described in the same stratigraphic position from Cape Kiti and inland at Mazatos (Bagnall, 1960) and have also been examined in cliffs 3 km west of Cape Dolos (G.R. 218407). This suggests extensive slope failure during this interval.

Exposed in the quarry face at Ayia Phyla (fig. 3.7) is a 4 m thick slumped unit containing rotated and unrotated sections of medium bedded calcarenites separated by low-angle slump faults (Plate 8). Towards the north end of this exposure the slump unit passes through a recumbent folded "toe" into a debris-flow deposit containing isolated fold hinges and blocks of bedded calcarenites in a sandy matrix. A mechanism for the generation of debris-flows by disaggregation of a moving slump sheet has been suggested by previous authors (Cook & Taylor, 1977; McIlreath & James, 1979; Crevello & Schlager, 1980; Stanley, 1982). Hampton (1972) suggested that "jostling" in the toe of a slide was an important process in breaking it up and mixing in water. Farrell (1984) cited slope related increases in slide velocity as a means of disaggregation. Gawthorpe and Clemmey (1985) suggest that slide sheet break-up occurs preferentially at the leading margin due to increased differential displacement rates associated with variable drag effects, ramp climbing and thinning over culminations. The implication is that slide generated debris-flows are deposited down slope from the arrested slide (fig. 3.9). Continued motion of the slide sheet, however, can lead to over-riding of the upslope portion of the debris flow, as seen in the Ayia Phyla exposure.

It may be that debris-flow formation involving dewatering from the basal glide surface promotes shear coupling with the substrate. Additionally, cohesion and

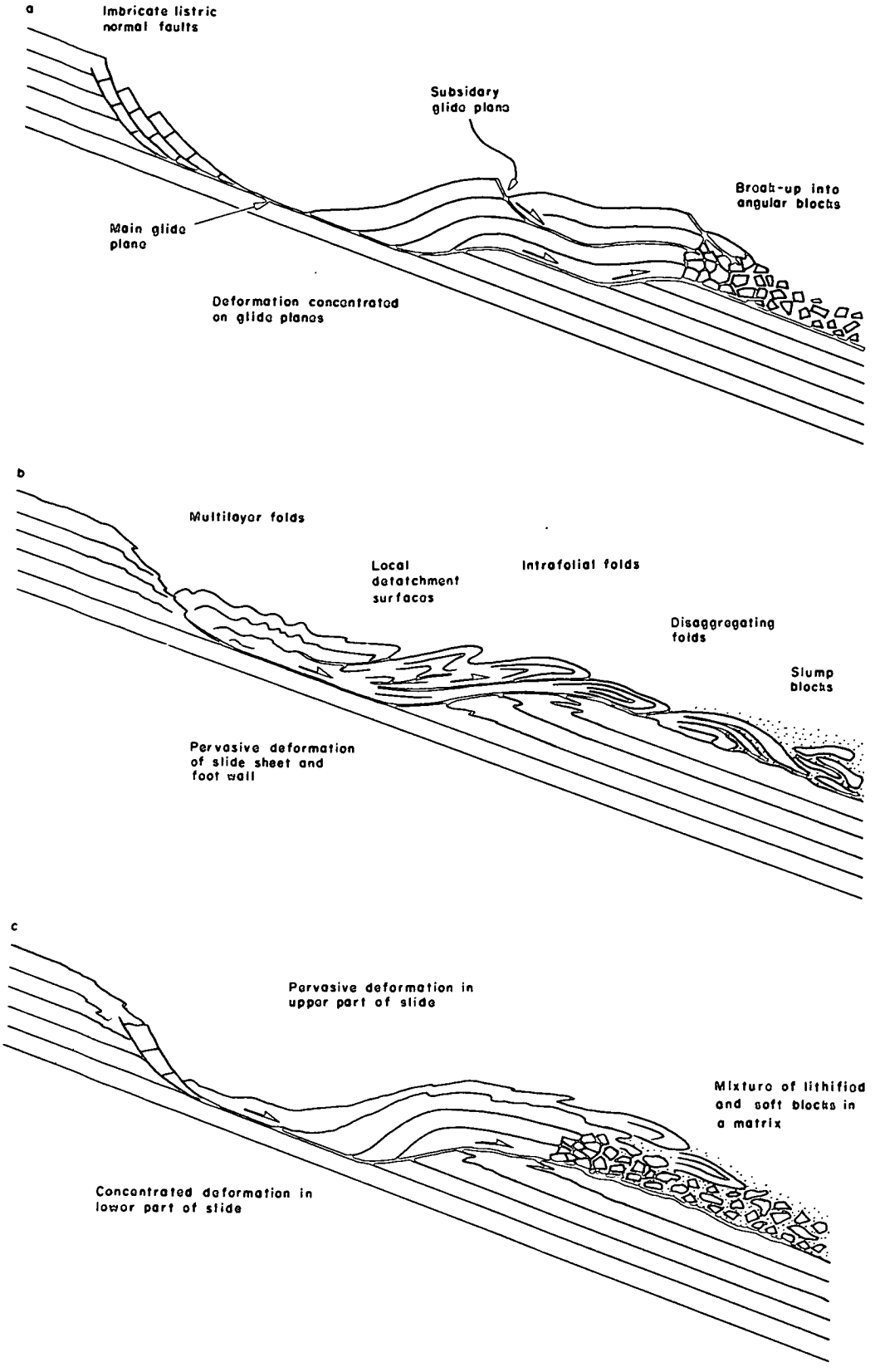

FIG. 3.9 Simple models showing internal anatomy of slide sheets, and their relationship to debris-flows. (a) Slump in competent lithified material. (b) Slump in coherent soft sediments. (c) Composite slump unit made up of upper soft sediments and lower lithified sediments. From Gawthorpe & Clemmey (1985).

turbulence within the debris-flow would further decelerate the leading disaggregated portion of a slide, imposing a backward propagating strain wave on the trailing slide.This would account for the internal folding and thrusting of the slide at Ayia Phyla, and for its over-riding of upslope portions of the debris flow.

3.7.5 Interpretation

Slumps generated by gravity induced submarine slope failures give rise to intraformational disturbed horizons which may appear chaotic in limited exposures but inwhich organised and interpretable collections of structures can be found at more extensive outcrops. These structures can be interpretated in terms of a dislocation model for slump genesis (Farrell, 1984) and a consideration of the processes involved in slide translation and deceleration (Farrell & Eaton, in press). Ubiquitous development of slumps is indicative of slope instability, which may be brought about by tectonic processes, over-steepening by rapid sedimentation, or by erosion of channels and the creation of gravitationally unstable channel margins (Stanley, 1982).

Slumps may sample any lithology found in these environments. Emplacement environments are interpreted from associated (autochthonous) deposits, and needn't be at base of slope or basin plain position since dewatering may lead to termination on the slope.

Disaggregation of slides during transport can give rise to debris flows and, by inference, turbidites.

3.8 Comparison with the facies scheme of Walker & Mutti

The lithologies of the Pakhna Formation, as described in this chapter, are similar to the types of lithologies discussed by Walker & Mutti (1973) and incorporated into their facies scheme. This scheme (Table 3.2) has received general acceptance. Its continuing use in the literature demonstrates the validity of the original work, and confirms the successful achievement of its original

purpose - to facilitate comparison between basins and to provide a descriptive framework as an aid to rapid communication. Furthermore, although this scheme was originally based on the study of siliciclastic sequences, it has been successfully applied to many clastic carbonate systems (eg. Price, 1977;, Ruiz-Ortiz, 1983;, Wright & Wilson, 1984).

Correlation of the lithofacies of the Pakhna Formation (as presented here) with the scheme of Walker & Mutti (1973) is made in Table 3.3.

Under the Walker & Mutti (1973) scheme, the first order descriptor for the basic classification is the applicability of the Bouma sequence. For reasons discussed elsewhere (section 3.4), Bouma sequences are not well developed in the calcarenites of the Pakhna Formation, despite evidence supporting their interpretation as turbidites. This fact accounts for the main differences between the two lithofacies schemes. Thus the distinction between base-absent and base-present turbidites (distinguishing Walker & Mutti's facies C and D) is not made for the Pakhna Formation deposits, being all included as graded calcarenites. Similarly, a thin facies D lithology becomes indistinguishable from a facies E lithology, and both would be equivalent to the thin-bedded calcarenite lithofacies (this study).

Wherever pebbly sandstones are observed in the Pakhna Formation, they are always organised (ie. there are no A3 equivalents found) with a volumetrically small proportion of pebbles at the base of a graded calcarenite unit. Thus A4 lithologies are included within the graded calcarenite lithofacies of this work. Thin-bedded pebbly calcarenites have no equivalent in an unmodified Walker & Mutti (1973) type facies scheme, since they are too thin to be included in the pebbly sandstone facies (A3 or A4).

BASIC CLASSIFICATION OF TURBIDITE AND OTHER RESEDIMENTED FACIES, BASED UPON MUTTI AND RICCI LUCCHI (1973)

BOUMA SEQUENCE NOT APPLICABLE	FACIES A -- Coarse grained sandstones and conglomerates A1 Disorganized conglomerates A2 Organized conglomerates A3 Disorganized pebbly sandstones A4 Organized pebbly sandstones. FACIES B -- Medium-fine to coarse sandstones B1 Massive sandstones with "dish" structure B2 Massive sandstones without "dish" structure.
BEDS CAN REASONABLY BE DESCRIBED USING THE BOUMA SEQUENCE	FACIES C -- Medium to fine sandstones -- classical proximal turbidites beginning with Bouma's division A. FACIES D -- Fine and very fine sandstones, siltstones -- classical distal turbidites beginning with Bouma's division B or C. C-D FACIES SPECTRUM -- can be described using the ABC index of Walker (1967). FACIES E -- Similar to D, but higher sand/shale ratios and thinner more irregular beds.
BOUMA SEQUENCE NOT APPLICABLE	FACIES F -- Chaotic deposits formed by downslope mass movements, e.g. slumps. FACIES G -- Pelagic and hemipelagic shales and marls -- deposits of very dilute suspensions.

TABLE 3.2

LITHOFACIES (THIS STUDY)	EQUIVALENT FACIES (WALKER & MUTTI, 1973)
RUDITES	
Clast supported	A1, A2
Matrix supported	
Sandy matrix	A1, A3
Muddy matrix	F
CALCARENITES	
Massive	B
Graded	C, D, A4
Thin bedded (#)	E
CALCILUTITES	
Lime mudstones	G
Marlstones	G
Laminated calcilutites	G
SLUMPS	
Slumps	F

(#) Thin bedded pebbly calcarenites have no equivalent.

TABLE 3.3 Correlation of the lithofacies scheme of this study with that of Walker & Mutti (1973), (see Table 3.2).

CHAPTER FOUR
FACIES ASSOCIATIONS OF THE PAKHNA FORMATION

4.1 Introduction

Facies associations are "groups of facies considered to be genetically or environmentally related" (Reading, 1978, page 5), and their recognition is fundamental to environmental interpretation. Four facies associations of the Pakhna Formation are described in this chapter, and are named according to the environment under which they are interpreted as having been deposited. These associations are peripheral sands, gullied slope, basin margin and basin plain associations. They are illustrated with reference to field observations and sedimentary logs, and are described in terms of composite sequences of lithofacies types. Important logged sections are illustrated in Appendix 4, which also contains a fold out location map covering places mentioned in this chapter (fig. A4.1).

In the previous chapter the lithofacies described are compared with the facies scheme of Walker & Mutti (1973). As pointed out (section 3.8), this scheme was developed for and applied to clastic and carbonate fan models. It must be stated, however, that similarity of facies type represents similarities of depositional processes only (in this case marine sediment gravity flows), and these processes in themselves do not control the larger scale distribution geometry of the depositional system. Distributional geometry is considered in section 4.8

By way of introduction to the description of these associations a brief review is now made of the general depositional setting of the Pakhna Formation as described by previous authors.

4.2 General depositional setting

The Tertiary evolution of the Troodos ophiolite and its sedimentary cover is characterised by generally continuous uplift from abyssal plain depths to emergence

(Cleintuar et al., 1977; Robertson, 1977a). Localised emergence of the Troodos massif as early as Oligocene/Lower Miocene times is indicated by the Terra Limestone Formation, a shallow algal/coral/shell detrital limestone with basement erosion products resting directly on Troodos pillow lavas (Cleintuar et al., 1977; Robertson, 1977a). Middle to Upper Miocene times are characterised in southern Cyprus by uplift centred on the Limassol Forest block (Robertson, 1977a, see fig. 1.4). Subaerial exposure may have extended beyond the Limassol Forest block, but certainly no further than the present day limit of basement outcrop, as Miocene sediments surrounding the ophiolite are marine.

Lithofacies of the Pakhna Formation include rudites and calciturbidites, shed into a marine basin with background pelagic sedimentation (chapter 3). Reworked components in the clastic sediments include varieties derived from reefal, back reefal and terrestrial environments. It is suggested, therefore, that the uplifted Limassol Forest block was fringed with reefs and neritic carbonate environments which fed material into the Pakhna basins (Robertson, 1977a).

4.3 Environmental criteria

The four facies associations described for the Pakhna Formation in this study are named according to their interpreted environment of deposition. These environments (peripheral sands, gullied slope, basin margin and basin plain) can be distinguished in modern examples often on the basis of submarine topographic profile, each being separated by a break in slope (Crevello & Schlager, 1980; Schlager & Chermak, 1979). In ancient examples distinction has to be made on the basis of lithological characteristics, which may change gradationally between environments, especially between basin margin and basin plain environments (Cook & Mullins, 1983). Of particular importance in this respect are the clastic lithologies (calcarenites and rudites). The presence or absence of

parts of the Bouma sequence in the calciturbidites (graded calcarenite lithofacies) can not be used as criteria since, for reasons discussed in section 5.4, Bouma divisions are not well developed. Instead, dominant grain size, bed forms (channellised or sheet-like), and proportion of clastic material in vertical sequences are used as the basic criteria by which the different facies associations are distinguished.

4.4 Peripheral sands association

This facies association is not extensively preserved in the area of study. The only exposures are those of the Koronia Limestone member which crop out discontinuously in a narrow belt running through the villages of Armenokhori, Ayios Tykhonas and Parakklisha (fig. A4.1). This excludes the Koronia Limestone outcrop at Amathus, which is part of the gullied slope association.

The peripheral sands association consists of amalgamated massive calcarenites in sections up to 12 m thick. Due to the massive nature of the lithology, bedding is difficult to define except where a slight grading is present, which is on a scale of 50-100 cm. These deposits are homogenous clean coarse bioclastic grainstones, containing pectinid and oyster fragments, serpulid, echinoid, bryozoan and coralline algae debris, with micritised peloids (Plate 3C). Small ammounts of detrital quartz and feldspars are found. At some localities graded calcarenites occur in laterally continuous parallel beds 30-50 cm thick. Occasionally, Thalassinoides-type burrows are observed.

All units of this association lie unconformably upon the Moni Formation (Upper Cretaceous) or, as NE of Parakklisha, directly upon the pillow lavas of the Limassol Forest block. The calcarenites have gentle southerly dips except where flowage of the underlying Moni clays has resulted in landslip.

The sediments of this facies association are well washed shallow marine carbonate sands deposited as sheet-

like bodies in a high energy environment. Their unconformable relationship with the underlying rocks suggests that they may represent a transgressive sand unit. The basal contact is not exposed. It seems likely that the soft nature of the Moni Formation clays would not lend themselves to the generation of clasts, so that a basal conglomerate may not exist

The peripheral nature of this lithofacies association refers to its position adjacent to, and overlapping upon, the Limassol Forest basement block. It is the most proximal facies association preserved and is laterally continuous in a basinward direction with the gullied slope association.

4.5 Gullied slope association

4.5.1 Introduction

The gullied slope asociation is dominated by silty calcilutites (hemi-pelagic sequences) which are "condensed" relative to more basinal sequences. Locally, towards the top of some sections, calcarenites and rudites may occur in well defined channel-fill bodies.

4.5.2 Hemi-pelagic sequences

These consist of interbedded bioturbated foraminiferal chalks, silty marlstones and, becoming more significant towards the top of the Pakhna Formation, laminated calcilutites. Rare graded calcarenites containing reworked neritic and pelagic components may also occur. In many areas, these hemi-pelagic lithologies comprise the entire Pakhna succession, passing directly into the gypsum deposits of the Kalavasos Formation, and having a lithologically gradational and conformable relationship with the underlying Lefkara Formation chalks.

Hard-grounds and nodular horizons are absent, indicating that early sea-floor lithification did not take place, and suggesting that, in contrast to the slope model of Cook & Mullins (1983), contour currents were not active during deposition. This would suggest that the condensed

nature of these hemi-pelagic sequences is primarily a result of low sedimentation rates due to bypassing, rather than by submarine winnowing and erosion (see also Schlager & James, 1978).

Precise thickness comparisons of time-equivalent sequences are difficult to give as it requires more detailed biostratigraphic control than is available, but on the basis of lithological mapping (see fig. 7.2) the gullied slope associations are less than 100 m thick. This represents a time span of 10my (15-5 mybp, see section 2.3.1) assumming no intraformational erosion surfaces. Thus, without correcting for decompaction, a reasonable figure for sedimentation rate of this facies association is 1 cm/ 1000 yrs. By comparison with other ancient examples (eg. Scholle et al., 1983, their fig. 17) this is a low figure and indicates sediment starvation.

Towards the top of the hemi-pelagic sequences of this association, bioturbation of calcilutites diminishes and laminated calcilutites predominate. These are interbedded with occasional compact white discospirinid-type chalk bands and continue up section to the base of the overlying Kalavasos Formation.

4.3.3 Channel-fill sequences

Locally, within upper sections of the gullied slope hemi-pelagic sequences, well defined channels are found, filled with massive and graded calcarenites, clast and matrix-supported conglomerates and rarer slumps and interbedded marlstones.

Development of major channel-fill sequences is limited to three localities in the area of study: Khirokitia, Tokhni and Amathus (fig. A4.1).

Channel-fill lithologies thin systematically away from the channel axis and pinch out against the margins (Plates 7A, 10C). Where channel margins are not exposed the channelised nature can be inferred from the limited lateral continuity of these fill features and their replacement over short distances along strike with

bioturbated hemi-pelagic lithologies

Multiple fill events demonstrate that channel cut and fill were separate events, and it is likely that these channels existed as eroded features acting as sediment transport routes for some time before being filled. Axial depth of channels, as seen in outcrop, range from 5m (Amathus) to over 20m (Khirokitia, Plate 7A).

Compound channelling, with new channels being cut into partially filled older ones, can be observed in the outcrops at Amathus, and is inferred from relationships at Khirokitia and Tokhni.

These three localities are now described separately.

1) Khirokitia

The best exposure demonstrating the channellised nature of the coarse clastic deposits at Khirokitia (fig. A4.1) is found in the river gorge beneath the village immediately east of the water tower (GR 307512). Here, a channel filled with coarse clast-supported conglomerates occurs with steep channel margins (up to 45 degrees) cut into silty marlstones (Plate 7A). The channel margin, and by inference the axis, strikes approximately NW-SE. The fill consists of cobbles generally 20-30 cm across but with rarer boulders up to 2 m in length, set in a pebbly coarse sand matrix. Sorting is poor, imbrication not well developed but where it does occur it indicates derivation of clasts from the north-west (direction of the Limassol Forest block). Stratification of the conglomerates into units of 1.5 to 4 m thickness is defined by thin pebbly bands at the top of each unit.

Cobbles are well rounded Lefkara-type chalks and cherts, Troodos-type lavas and dolerites (but no coarse ultra-mafics) and poorly preserved compound corals and recrystallised limestones. Some cobbles have been bored (0.5 by 2 cm deep), probably by bivalves although the organism is not preserved.

Matrix components include plagioclase-phyric lava pebbles, pyroxene and plagioclase grains, globigerinid

chalk clasts, peloids, superficial ooids and bivalve, echinoid, bryozoan, coral, coralline algae and benthic foraminifera debris. Much of the coarser originally aragonitic material is exsolved resulting in a mouldic porosity.

Conglomerates in the upper half of the exposure do not cut as steeply into the surrounding marlstones. They are also less coarse, better sorted, and contain significantly less igneous material as both framework clasts and matrix constituents. A coarse "lag" of imbricated chalk boulders occur at the base of this unit. Lateral continuity of this upper unit to the south is limited as it is lost in outcrops in that direction. These features suggest that the upper portion of the exposure is an approximately longitudinal section through a second, upper, fill sequence in a channel that was cut into the earlier, lower, channel-fill sequence.

2) Tokhni

At Tokhni Quarry (fig. A4.1) approximately 30m of vertical exposure shows a sequence of massive calcarenites, clast supported polymict conglomerates and minor thin marlstones (Plate 10D). Although channel margins are not observed, sections along strike to the northeast (towards Khirokitia) and to the southwest (towards Tokhni) are calcilutite dominated hemi-pelagic sequences. The Tokhni calcarenites and rudites are inferred to be channel confined.

The east face of the quarry consists of a single thinning upwards series of massive coarse calcarenites interbedded with silty marls (Plate 7C). This is interpreted as representing channel-fill and abandonment (see Mutti & Ghibaudo, 1972; Walker, 1978). Above this, exposure is discontinuous, reflecting domination by marlstone lithofacies, but shows at a higher level the development of another small channel sequence with a basal clast-supported rudite of chalk cobbles and boulders in a bioclastic matrix. The base of this fill sequence (ie the

channel floor) cuts down through 5 m of underlying lithologies over a distance of 20 m towards the south. The top of this section is capped with a small exposure of clinty, vuggy limestone mapped as Koronia Limestone by Bagnall (1960). This is a clastic deposit containing fossil serpulids, bryozoan fragments, coralline algae, and coral clasts. Many fragments were encrusted with foraminifera, algae and serpulids prior to incorporation in the deposit. Aragonitic components have been dissolved out at an early stage during marine diagenesis (Plates 4A, 4C) leaving a mouldic porosity. The matrix is of micrite and peloids. No Troodos derived material is found.

Similarities between the Tokhni and Khirokitia channel-fill sequences are:

a) multiple channel fill events

b) compound channel development

c) lower fill units contain significant amounts of Troodos derived igneous and associated sedimentary cover erosion products

d) upper fill units show an increase in the proportion of carbonate (neritic derived) over terrigenous (Troodos erosion products) components.

3) Amathus

This locality is about 10 km east of Limassol on the old Nicosia road. It is mapped by Pantazis (1967) as Koronia Limestone capping a sequence of Pakhna Formation marls. Best exposures of the channel-fill sequence are found in the old quarry north of Ayia Vavara monastery. Channel fills are made up of clast supported conglomerates, matrix-supported mudstone intraclast conglomerates, slumps and minor silty marlstones. Channels are cut with well defined bases into Pakhna marls (hemi-pelagic sequence, see Plate 10C), or, as at Khirokitia and Tokhni, into each other as compound units. Channel relief is in excess of 5 m.

An important difference from both Tokhni and Khirokitia is the absence in the Amathus sediments of non-

carbonate clastic components, i.e, there are no Troodos erosive products. These limestones are composed almost entirely of clastic neritic carbonate clasts with only traces of detrital quartz, feldspar and rare radiolarian chert fragments. Also, channel axis orientations (180, 235, 252 degrees) are all towards the south or south-west, in marked contrast to the easterly orientation of the channels at Tokhni and Khirokitia.

The lowest lithology in the channel fill sequences is a conglomerate of marlstone clasts. These are rounded and elliptical, or folded into slump balls and are probably of local derivation being eroded from the channel floor or margin. Matrix is carbonate sand and gravel compositionally similar to the graded calcarenites which make up the bulk of the channel fill sequence. There is a thinning and fining upwards tendancy accompanied by a decrease in the marl intraclast content. Towards the top of each fill sequence carbonate sands and silts predominate, often thinly interbedded and sometimes with well developed loaded sand ripples. These beds become less confined up sequence. Lithological equivalents of the Amathus channel fill sequences can be mapped westwards beyond Moutayiaka and towards Phinikaria, thinning in places to a 2m amalgamation of laterally continuous graded calcarenites.

4.5.4 Development history of channel-fill sequences

On the basis of observations at the three outcrops described the following summary of events can be made:

(1) Pelagic chalk sedimentation and chert formation (Lefkara Formation), followed by;

(2) Hemi-pelagic slope sedimentation, with low net sedimentation rates. Then;

(3) Channel cutting takes place, truncation surface developed, followed by;

(4) Channel-fill and abandonment.

Each channel-fill sequence can be interpreted as recording the upslope migration of the transition line

between erosional and depositional regimes on the slope ultimately leading to complete channel choking and the deposition of broadly lenticular clastic carbonate sheets.

The channel is initiated in an erosional regime upslope from the depositional area (basin margin or basin plain), where it acts as a bypass channel. With time the line dividing erosional from depositional regimes migrates upslope. The first sediments deposited in the channel are under the regime occurring closest to this divide and consist of mudclast conglomerates eroded locally and deposited rapidly. Subsequent sediments are the coarsest fraction of the slope sediments (conglomerates) followed by progressively finer sediments as the erosional regime retreats further upslope. This cycle may be repeated, resulting in compounding of channel-fill sequences.

4.3.3 Summary

The gullied slope association is thus defined to include the complete condensed sequence which is capped locally with channel-fill units. Because of the localised nature of these units some sections will show no gully development. These can be identified as belonging to this facies association by the following;

(1) their condensed nature

(2) marl dominant make-up, with clastic input as occasional parallel thin to medium bedded graded calcarenites or as horizons of clastic carbonate bioturbated into the marls.

(3) demonstrable lateral equivalence along strike with channel-capped condensed Pakhna sequences

These features compare well with those described for a modern gullied slope by Schlager & Chermak (1979) and Mullins *et al.* (1984). The absence of hardgrounds or other indicators of early cementation on erosional surfaces such as gully margins is consistent with the findings of Mullins *et al.* (1984) that gullies tend to form on the lower parts of slopes where hemi-pelagic sediments have less diagenetic potential than bank derived aragonite rich

muds found more proximal to the carbonate source environment. Furthermore, the fact that Cyprus was a carbonate fringed emergent island rather than a true platform means that production and supply of aragonitic muds with a high diagenetic potential would be reduced in comparison.

4.6 The Basin Margin Association

The basin margin association is characterised by slumps, matrix supported conglomerates (debris flows), clast supported conglomerates, and calcarenites (massive, graded and thin bedded types) interbedded with chalks and marls. Some channelling of the clastic lithofacies is observed, but it is generally of a broad and shallow nature. Beds tend to occur as lenticular or sheet-like bodies in amalgamated packets. This is in marked contrast to the discrete channellised clastic bodies of the gullied slope association.

In between clastic packets the sequences comprise bioturbated marls and chalks with sporadic thin to medium bedded fine-grained graded calcarenites.

As explained in section 4.3, distinction between basin plain and basin margin associations on the basis of the Bouma subdivisions in calciturbidites is not possible. Instead, the distinction is made on the basis of the proportion of clastic material contained in a vertical sequence. For this study, the basin margin association is defined as containing >35% clastic material (calcarenites and rudites). This is found to vary upwards to 82% (Ayia Phyla section, Appendix 4).

Slumps and matrix supported rudite sheets are also found in some basin margin sequences, eg. Ayia Phyla, Happy Valley (fig.5.5). Although regarded as distinctive basin margin features by Cook and Mullins (1983), unchannellised debris sheets occur in basin plain environments aswell.

Small scale thinning/fining or thickening/coarsening upwards sequences within the basin margin association are

not convincingly apparent. Figure 5.1 shows a plot of bed thickness for clastic lithologies in the Kouris River section. No systematic variation occurs and the only valid observation is that thicker bedded units tend to occur in the packets of amalgamated beds. A similar result is found for other basin margin sequences.

The inclusion of slope derived clasts (globigerinid mudstone clasts) in the calcarenites of this facies association is also a typical feature of reworked carbonates in a basin margin environment (e.g. Crevello & Schlager, 1980; Mullins et al., 1984).

The up-sequence evolution of clastic component composition suggests unroofing of an uplifted portion of Troodos type basement, as indicated by other considerations (see sections 3.5.4, 5.10, 7.8). It is likely therefore that tectonic controls had a considerable influence on sedimentation. Pulsed uplift of the source area might reasonably account for the packeted nature of the calcarenite sheets in the basin margin sequences.

Appendix 4 contains logs from the basin margin association, which show many of the features described.

4.7 The Basin Plain Association

Sediments of the basin plain association are dominantly pelagic and hemi-pelagic chalks and marls. Occasional medium thick, fine grained parallel bedded and laterally continuous calcarenites occur. Thin bedded calcarenites are more common, but are usually partly or substantially obliterated by bioturbation (Plate 6B). The chalks and marls are globigerinid nannofossil mudstones, typical of pelagic and hemi-pelagic environments (sections 3.2, 3.3) with a trace fossil assemblage characterised by Zoophycos, Chondrites and Planolites. These sediments tend to be "cleaner", with less argillaceous material than in other facies associations, reflecting the the more distal location of the basin plain environment. Logged sections at Kisoussa and Ayios Therapon illustrate the essential monotony of these sequences (Appendix 4).

Basin margin and basin plain environments can grade into each other laterally and vertically (Mullins & Neuman, 1979). Basin plain sequences are distinguished from basin margin sequences in this study by their lower redeposited carbonate content, less than 35% (see sections 4.3 and 4.6). Transition from basin margin to basin plain is marked by decreasing thickness, grain size, and frequency of clastic carbonate lithologies (Crevello & Schlager, 1980; Schlager & Chermak, 1979), and by a rapid decrease in the scale and frequency of slumps, slides and debris flows basinward from the margin slope (Cook & Mullins, 1983).

The Happy Valley road section (Appendix 4) is interpreted as showing this transition in a vertical sequence, from basin plain in the lower, chalk dominated, part to basin margin in the upper section containing rudites, calcarenites and slumps. The rudites are cobble and boulder conglomerates occuring as thick irregular sheets with loaded bases. Clasts include coral debris of shelf derivation supported in a matrix of lime mud with comminuted echinoid and bivalve debris. Frictional coupling between debris flow and substrate is evident from drag folding along the base, and thrusting of the substrate at the toe (Plate 8, fig. 5.4). These features are related to the emplacement of the debris flow, and might reflect rapid decceleration due to decreasing slope gradient over the transition from margin to basin plain.

The slumped unit in this section involves chalk lithologies and indicates failure of pelagic deposits on the basin margin. The irregular top has been planed off in places, and ponded with chalks in the hollows.

4.8 Aprons versus fans

Although description and process interpretation of lithofacies has involved comparison with facies schemes normally applied to submarine siliciclastic fan models, this is not meant to imply an application of a fan model to the sediments of the Pakhna Formation. Indeed, Cook

(1982), Cook & Mullins (1983), and Mullins et al., (1984) suggest that carbonate submarine fans rarely develop, and that most carbonate debris is reworked downslope as a series of coalescing aprons fringing the shallow water source area.

Several observations support the debris apron model for this study (see Cook, 1983). These are:

(1) Lack of convincing small scale thickening or thinning upwards cycles in basin margin or basin plain sequences.

(2) Identification of small channel fill sequences in the gullied slope association. These indicate that clastic sediment was bypassing the upper slope through a series of small gullies as opposed to a larger fan feeder canyon. Along strike separation of these gullies is of the same scale as described from a gullied slope in the Tongue of the Ocean, Bahamas (Schlager & Chermak, 1979).

(3) As argued further in the following chapter, the spatial arrangment of facies associations indicates a concentric series of facies belts, similar to those found in small off-platform basins of the Bahamas (Schlager & Chermak, 1979; Mullins et al, 1984) implying a line source (coalescing series of point sources) for the sediments.

(4) The scale of the basin (see chapter 5) is inadequate for the development of a major fan system as observed in modern examples (see Shanmugam et al., 1985).

Full discussion of depositional models and reconstruction of sedimentary environments is undertaken in the next chapter.

4.9 Summary

Four facies associations have been recognised in the Pakhna Formation of southern Cyprus. By interpretation of depositional processes and environments, and by comparison with ancient and modern examples, these have been identified as peripheral sands, gullied slope, basin margin and basin plain associations. Their distinctive features are summarised in Table 4.1, which also lists

some comparable associations from various studies on modern basins. Figure 4.1 shows schematic typical logs for each association. Relative thicknesses are proportional to the approximate sedimentation rates as calculated in section 5.5.

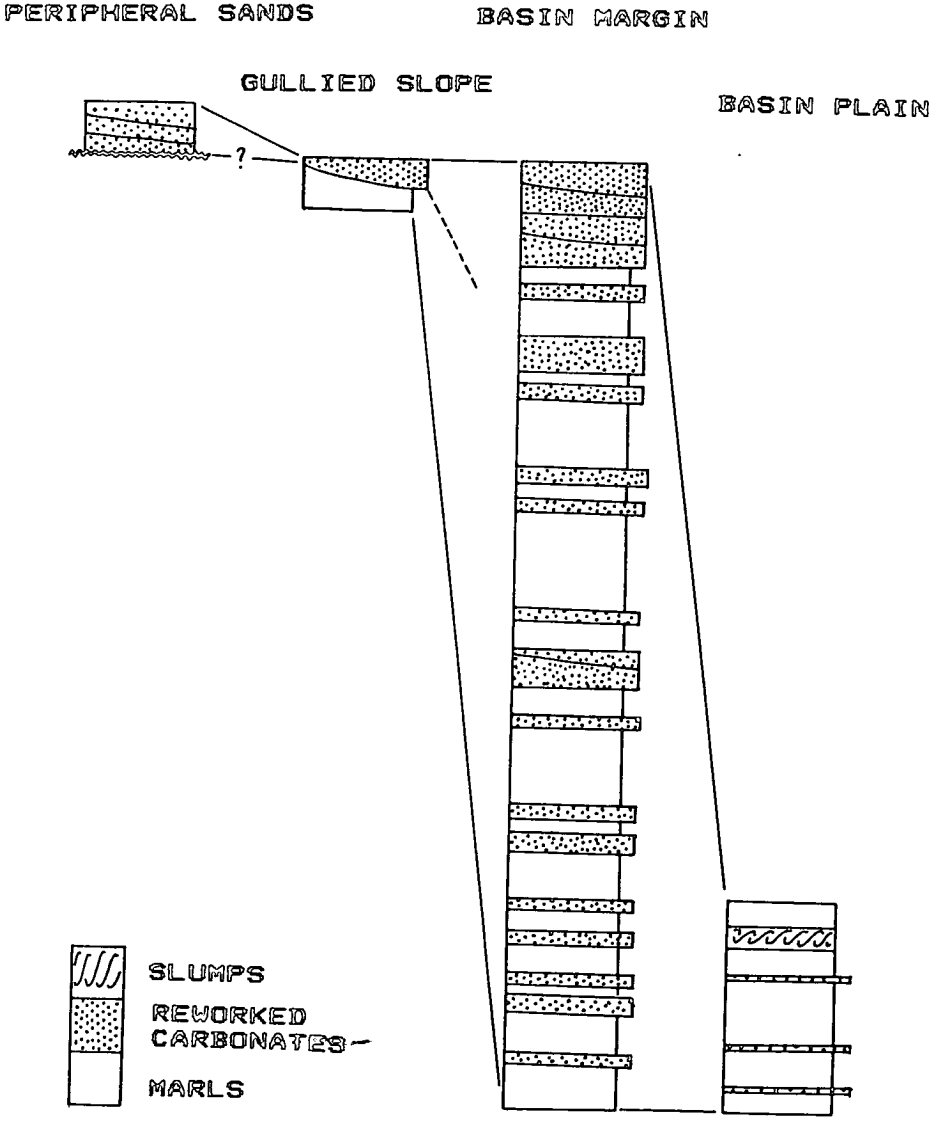

FIG. 4.1 Schematic representation of sequences of different facies associations, with total thickness proportional to estimated sedimentation rates.

FACIES ASSOCIATION	CHARACTERISTIC LITHOFACIES	COMPARABLE ENVIRONMENTS(other authors), and MAIN DIFFERENCES
PERIPHERAL SANDS	Massive calcarenites Graded calcarenites	Peri-platform Sands, isolated platform (Read, 1985) No true carbonate platform on Cyprus
GULLIED SLOPE	Lime mudstones Marlstones Calcarenites (channels) Rudites Slumps	Gullied Bypass, isolated platform, Read, 1985) Gullied Slope (Schlager & Chermak, 1979) Upper Slope (Mullins et al., 1984) Lower diagenetic potential of fine fraction on Cyprus
BASIN MARGIN	Calcarenites Rudites Marlstones Lime mudstones Slumps	Lower Slope or Basin Margin, isolated platform (Read, 1985) Basin Margin (Schlager & Chermak, 1985) Lower Slope (Mullins et al., 1984) Base of Slope Apron (Cook, 1982)
BASIN PLAIN	Lime mudstones Marlstones Thin bedded calcarenites	Basin Plain (universal)

Table 4.1 Comparison of the facies associations of the Pakhna Formation with depositional environments described by other authors.

CHAPTER FIVE
BASIN RECONSTRUCTION

5.1 Introduction

In this chapter the evidence used to reconstruct the depositional environments of the Pakhna Formation is presented and discussed. The model arrived at is geologically realistic and accounts for the observations and data gathered in this study and from previous work. It represents a new and more detailed model than any yet produced for this area, and may serve as a useful framework or starting point for any further work that might be undertaken.

5.2 Vertical trends

5.2.1 Introduction

The Pakhna Formation can be regarded in broad terms as a single regressive sequence deposited between the pelagic marine chalks of the Lefkara Formation and the evaporites of the Kalavasos Formation. Several uni-directional up-sequence changes in sedimentology reflect this. These are described below. They are all interpreted as indicating an increasing influence of shallow water environments with time, and are consistent with the general model of uplift and exposure of basement blocks during the Miocene (Robertson, 1977a).

5.2.2 Large scale coarsening upwards cycle.

Lowermost Pakhna sediments are similar in character to the Lefkara chalks. Up-sequence, increasing proportions of reworked sand and silt grade carbonate material are found in the sediments. In most areas studied, the uppermost Pakhna sediments contain significant quantities of rudites or coarse calcarenites. This is well illustrated in the transect from Kissousa through the Kouris River valley to Ayia Phyla (fig. 5.1).

Vertical sections which do not show this trend are from the inter-gully areas of the gullied slope association. Absence of coarse material in these instances

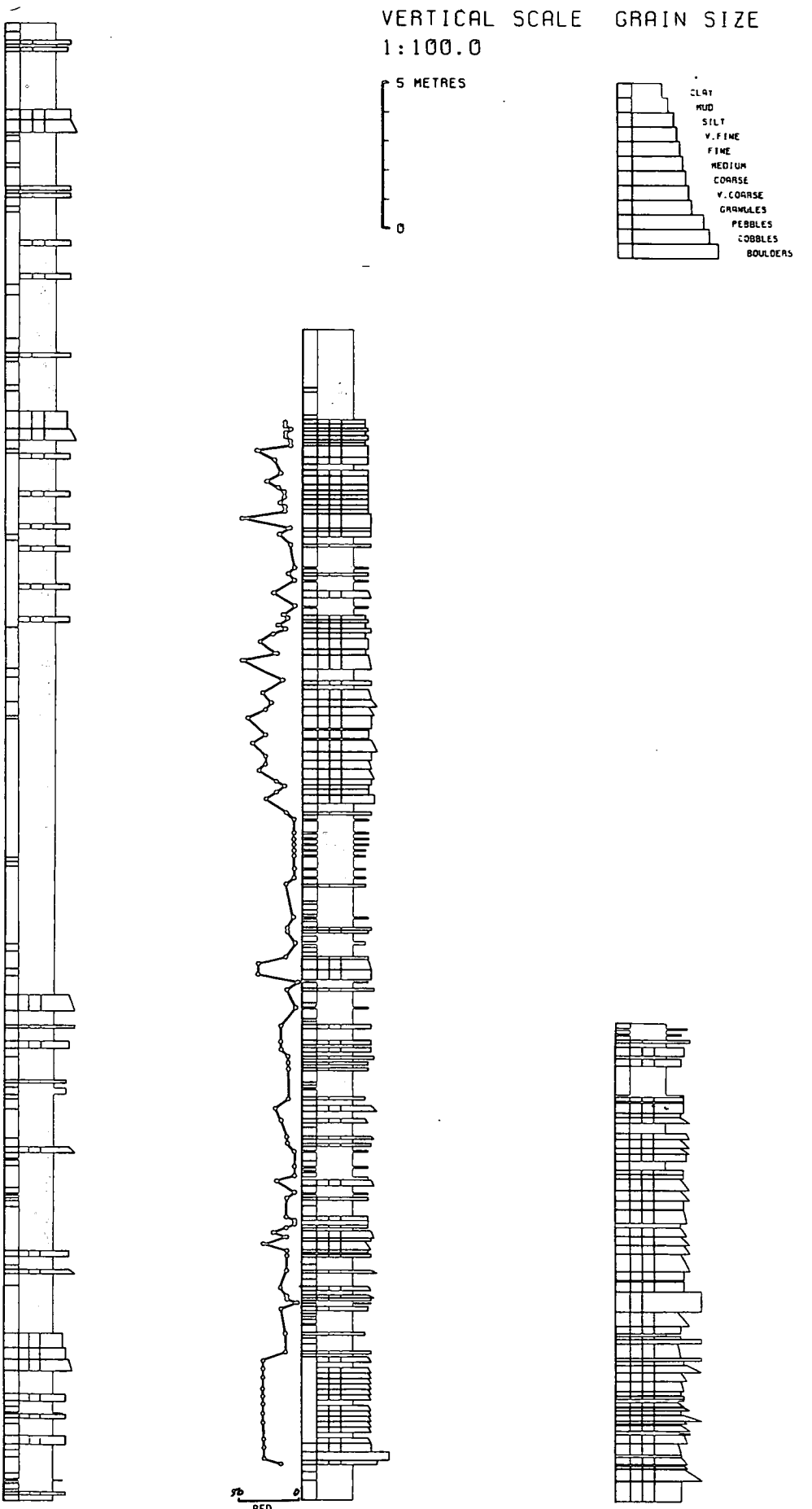

FIG. 3.1 Computer drawn logs showing representative sections from the Khalassa sub-basin. Kissousa (lowest in stratigraphy) is lime mudstone and marlstone dominated. Kouris River has packeted clastic lithologies (no systematic bed thickness variations). Ayia Phyla (highest in stratigrahy) is dominantly coarse carbonate sands. See

is due to sediment by-passing on a starved slope.

3.2.3 Compositional variation of clastic material.

As discussed in section 3.5.4, there is a general upward change in clastic composition from reworked pelagic to neritic biogenic carbonate, to terrigenous derived erosion products. This reflects uplift, exposure and erosion of the basement and basin margins.

3.2.4 Compositional variation of calcilutites

Early Pakhna calcilutites are clean pelagic and hemi-pelagic chalks with traces of kaolinite and montmorillonite (see section 3.2). Up-sequence the clay mineral content increases and chlorite, illite, and traces of detrital feldspars occur, and the proportion of quartz silt increases, suggesting increasing terrestrial influence.

Occasionally this trend is reversed, as when clean homogenous white cacilutites of the "Discospirina band" are found near the top of the Pakhna Formation (see section 3.2). These "chalks" are markedly different from those lower in the sequence as they are found in thin section to be almost completely recrystallised to microspar. This may reflect an increasing proportion of shallow water-derived aragonitic and Mg-calcite mud, which is more prone to diagenetic recrystallisation (Schlager & James, 1974).

Calcilutites from the upper parts of the Pakhna Formation also contain abundant plant debris.

3.2.5 Ichnofacies

Zoophycos, Planolites and Chondrites characterise the sediments in the lower parts of the Pakhna Formation, and indicate a relatively deep palaeo-bathymetry (see section 3.2.4). Up-sequence these give way to Thalassinoides as the predominant trace fossil, usually occurring in calcarenites, and characteristic of shallow shelf environments. The uppermost lithologies of the

Pakhna Formation are free of bioturbation structures, indicating a stressed benthic environment.

5.2.6 Microfossil variations

Microfossil populations extracted from the Pakhna Formation contain increasing proportions of benthic foraminifera up-sequence, and a rapidly declining content of pelagic genera. This is reflected also in the selection of benthonic species as zone indicators in the Upper Miocene foraminiferal stratigraphic scheme of Mantis (1969).

5.3 Slumps as palaeoslope indicators

5.3.1 Introduction

Slump fold orientation data can be used to estimate palaeoslope orientation (Jones, 1940; Woodcock, 1979). The most commonly used technique is based upon the assumption that slump folds initiate with their fold axis parallel to the strike of the palaeoslope. Since acceleration, translation and deceleration can reorientate slump fold axes (Farrell & Eaton, in press) a mean axis method on large data populations is the most reliable method. Downslope direction is indicated by fold asymmetry, with axial planes dipping in the upslope direction (Woodcock, 1979). One advantage of this method is that the three dimensional orientation data can be analysed statistically (Watson, 1960) and confidence limits for estimates can be calculated.

Statistically useful amounts of slump data have been collected from localities at Amathus, Ayios Theodhoros, Petrouda Point, and the Tokhni gypsum quarry (fig. 3.7). Lithological aspests of these outcrops have been described in section 3.6.

Petrouda Point is mapped as Lefkara Formation but regarded as time equivalent to Pakhna Formation deposits (see section 2.5.3) and is therefore relevant to basin reconstruction. The outcrop at Tokhni gypsum quarry is of Kalavasos Formation evaporites. As discussed later, basin

morphology does not appear to change much between Pakhna and Kalavasos Formation times. Data from this exposure are included here for convenience of discussion.

Soft sediment deformation structures which can be related to palaeoslope orientation have been observed at Happy Valley and Ayia Phyla and are also discussed in this section.

5.3.2 Slump data

The Amathus, Ayios Theodhoros, Petrouda Point and Tokhni quarry data sets are shown as contour plots of slump fold axis orientations in fig. 5.2. Data has been processed by a version of Nigel Woodcock's STATIS program. This involves:

(1) rotation of all data points for correction of regional dip.

(2) statistical calculation of the mean orientation using the Watson method (Watson, 1960).

(3) calculation of the cone of confidence semi-angle for the mean at the 95% confidence limit.

(4) production of equal area contour plots

The down palaeoslope direction is taken to be at 90 degrees from the mean fold axis attitude in the direction indicated by the dominant fold vergence. The slumped unit at Amathus occurs in a channel fill sequence and may thus be influenced by local channel topography.

These slumped units all indicate a Miocene palaeoslope directed away from the Limassol Forest block (fig. 5.5).

5.3.3 Ayia Phyla

The quarry face at Ayia Phyla shows a slump and debris flow unit within a sequence of massive calcarenites of the basin margin facies association (Plate 8). The southern end of the exposure shows a slump unit with rotated beds and internal thrust faults defining triangular pop-up zones (fig. 5.3). Towards the north, increasing rotation and breakup of the unit is seen as it

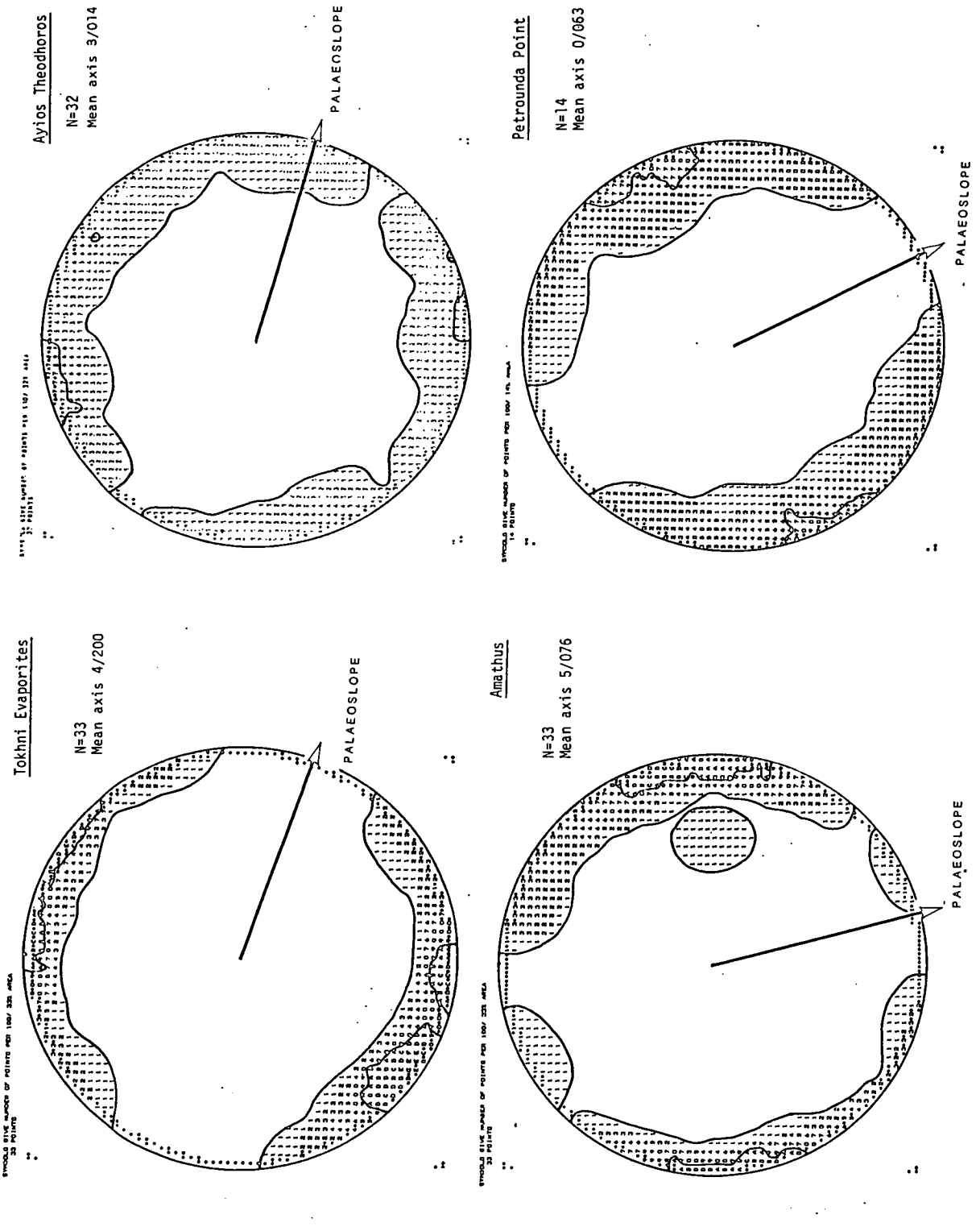

FIG 5.2 Computer contoured plots of slump fold axes orientations from four slumped units in Cyprus (see fig. 3.7 for location). Diagrams are orientated with north towards the binding margin. Alpha-numeric symbols on plot indicate contoured density value ranging from 1 (1) to 35 (Z). All data corrected for regional dip.

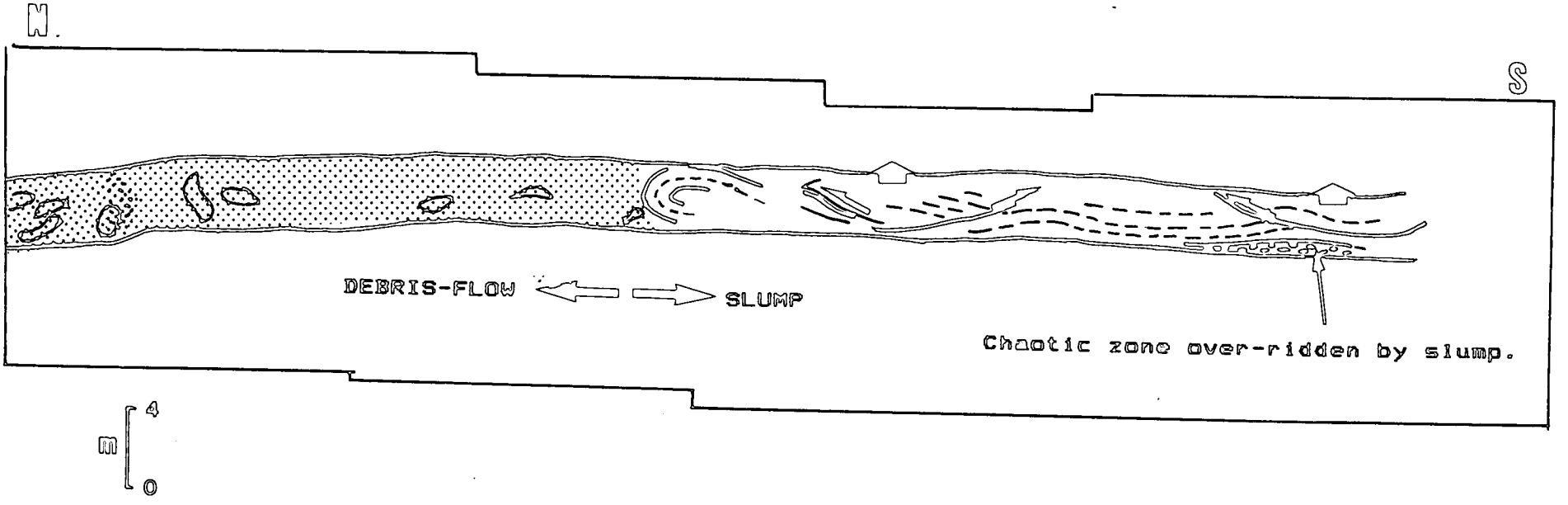

FIG. 3.3 Line drawing of intra-formational slump unit at Ayia Phyla (taken from Plate 8). Slump unit is 4 m thick, and its upper and lower surfaces are parallel with associated bedding. Thrust bounded "pop-up" zones shown with thick arrows. Dashed lines show bedding within the slump. Slump passes northwards into debris-flow.

passes into a disorganised matrix-supported debris-flow. This intimate relationship between the slump and the debris-flow shows that they were formed as part of the same depositional event. The process of debris flow generation by disaggregation of slumps has been discussed previously (3.3.4), and implies that this unit was derived from the south and was transported northwards. As a mass flow deposit, this suggests a northward dipping palaeo-slope at this locality.

5.3.4 Happy Valley

The Happy Valley road section is interpreted as showing a transition from basin plain to basin margin environments (see section 4.7). Plate 8 shows a debris-flow from the top of this section, in the basin margin association. Dip-slip movement on the two thrust faults in the substrate at the toe of the flow is indicated by bedding off-set (fig. 5.4). Beneath the body of the flow small-scale soft-sediment folds occur with vergence towards the north. These deformation features within the substate have relatively minor displacements and provide more reliable directional data than deformation structures within the debris-flow. Fault orientations and fold geometries are consistent with having been formed during emplacement from south to north.

5.3.5 Conclusions.

The data presented in this section provide useful constraints for modelling the basin morphology around the Limassol Forest block during Miocene times. Interpretation of the Ayia Phyla and Happy Valley sections indicates a northward dipping palaeoslope in the southern areas. This is in contrast to the palaeoslope orientations calculated from slump data at the four other slump localities which dip south and southwestward away from the Limassol Forest block. Thus Ayia Phyla and Happy Valley sections suggest a basin margin or local high to the south of the area studied, in the region of the Akrotiri Peninsular.

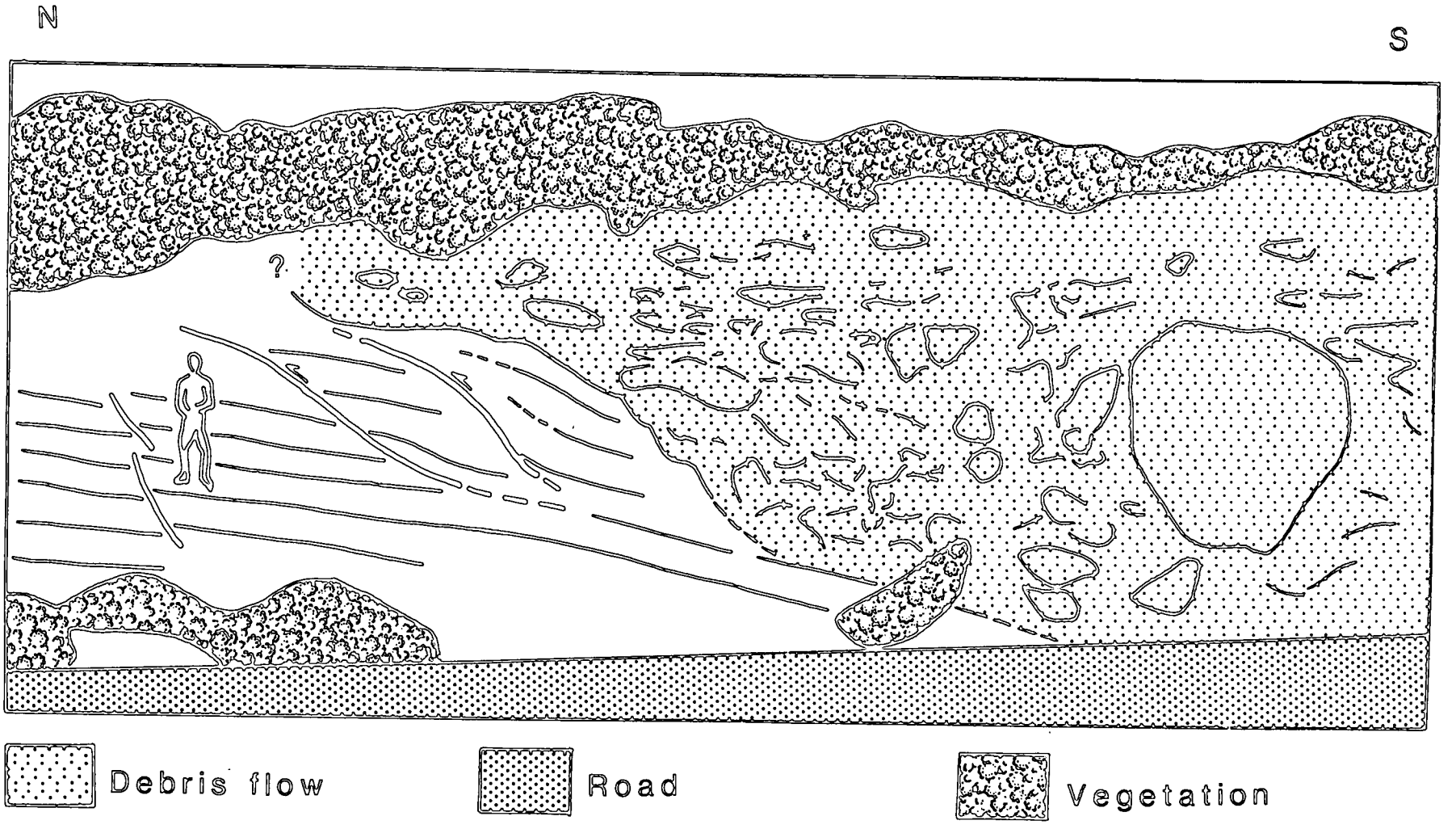

FIG. 5.4 Line drawing of toe of debris-flow at Happy Valley. See also Plate 8.

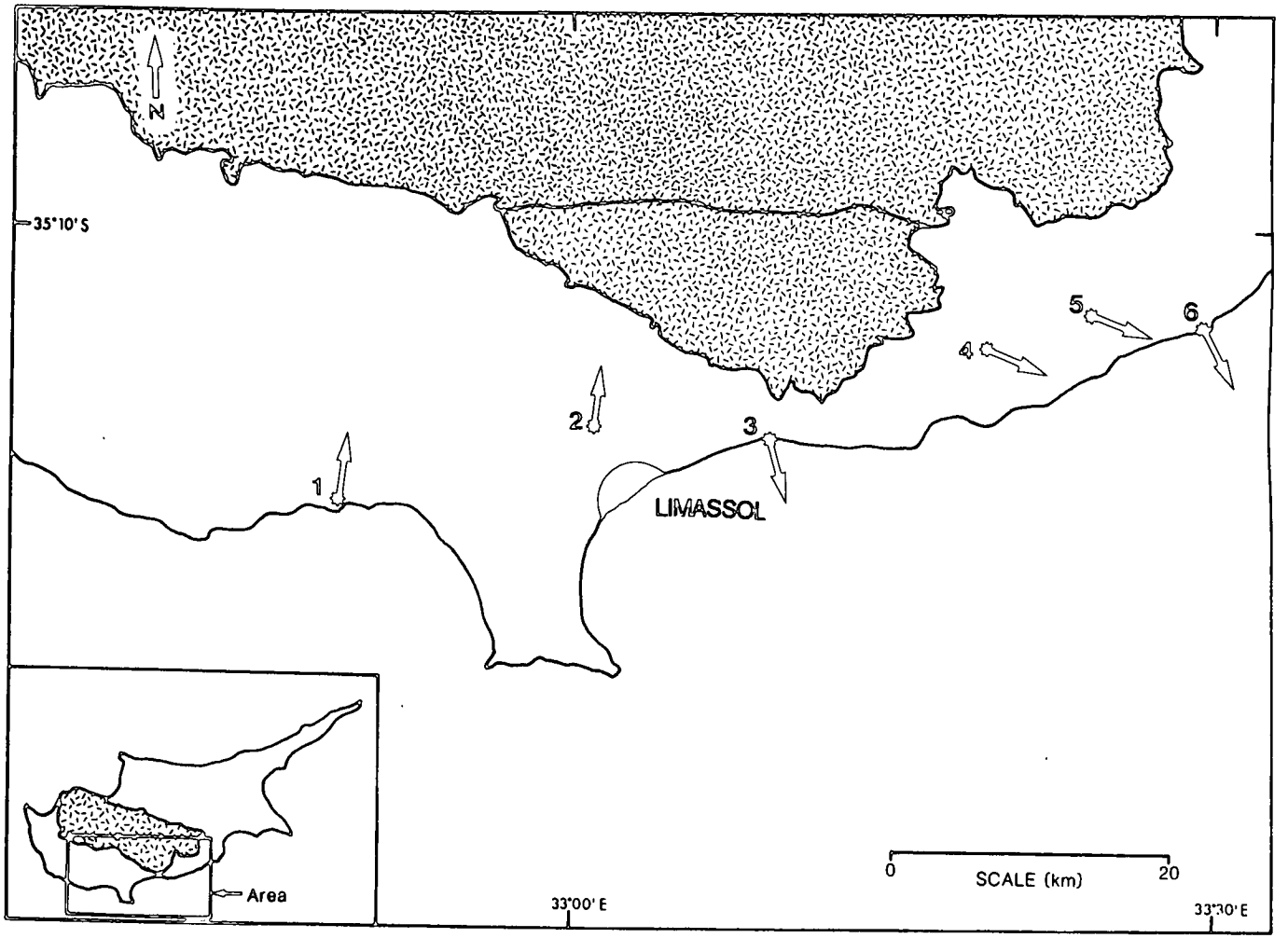

FIG. 5.5 Palaeoslope determinations from localities in the study area. 1 Happy Valley, 2 Ayia Phyla, 3 Amathus, 4 Tokhni, 5 Ayios Theodhoros, 6 Petrouda Point.

5.4 Palaeocurrent data

Reliable palaeocurrent indicators are not commonly found in the sediments of the Pakhna Formation. This is due to a variety of factors:

(1) Bouma sequences containing the cross bedded Bouma C-unit are not well developed in sediments regarded as turbidites (graded calcarenites). This may be due to the inhibiting effect of coarse grain size, rapid deposition, or the control of grain density. Another factor is that of grain shape, these beds being composed of irregular shaped bioclasts. It may be significant that most occurrences of well-developed Bouma subdivisions recorded for coarse calcarenites are for beds made up of equidimensional clasts (pelagic foraminifera, ooids, peloids, eg Robertson 1974, Cooper 1986).

(2) Rock exposures are usually two dimensional, making the directional interpretation of any cross-bedding or ripple cross lamination difficult. It is not possible therefore to compensate for scarcity of data with quality of data.

(3) Sole marks are not commonly found. Rarity of sole marks in carbonate sequences has been remarked upon by other authors (eg. Enos & Moore, 1983, pg 535). Furthermore, their detection is made difficult by the limitations of the exposures (see (2) above).

(4) Bioturbation is extensive and destroys primary structures.

The palaeocurrent data which have been collected are shown in fig. 5.6. Most data are from ripple-cross-lamination, but some clast-imbrication has also been found in the coarser sediments. Sole marks have only been collected from one locality. At some localities the azimuth for a palaeocurrent direction has been determined, but in most cases it has only been possible to make a general statement such as "towards the south" due to the limitations of a planar outcrop.

With these limitations in mind, the palaeocurrent data are consistent with having been generated by processes associated with mass flow travelling downslope from an uplifted Limassol Forest Block, and it compares well in this respect with the slump data. An interesting feature is the occurrence in the southern part of the basin (Kandou, Ayia Phyla, Ypsonas, see fig. 5.6) of northward travelling palaeocurrents. Palaeoslope data from this area (localities at Happy Valley, Ayia Phyla, see fig. 5.5) suggest that these areas are on the southward margin of the basin with a derivation from upslope to the south. The question of a southern high is discussed in section 5.7.

5.5 Sedimentation rates.

Poor chronostratigraphic control means that sedimentation rates can only be approximated. An estimation for the gullied slope deposits was made in section 4.5.2, and a figure of 1.0 cm /1000 years was arrived at. An estimation for the basin margin and basin plain associations can be made using information from the Kouris River area. The top of the Lophos Beds (Greitzer & Constantinou, 1969), which mark the transition from basin plain to basin margin associations, is dated as top N16 (section 2.5.3), i.e 8 mybp (figure 2.3). The Lophos beds are 350 m thick (fig. 2.3) and extend down section to the top of the Lefkara Formation (first appearence of Orbulina Universa at 16 mybp). Thus a rough average for the sedimentation rate of the basin plain association is:

$$350 / (16-8) \times 100 / 1000 = 4.4 \text{ cm} / 1000 \text{ yrs.}$$

Likewise, the basin margin association extends up-sequence from the top of the Lophos Beds (8 mybp) to top Pakhna Formation (5.5 mybp, taken as base Messinian salts) and is 450 m thick (fig.2.3). This gives:

$$450 / (8-5.5) \times 100 / 1000 = 18.0 \text{ cm} / 1000 \text{ yrs.}$$

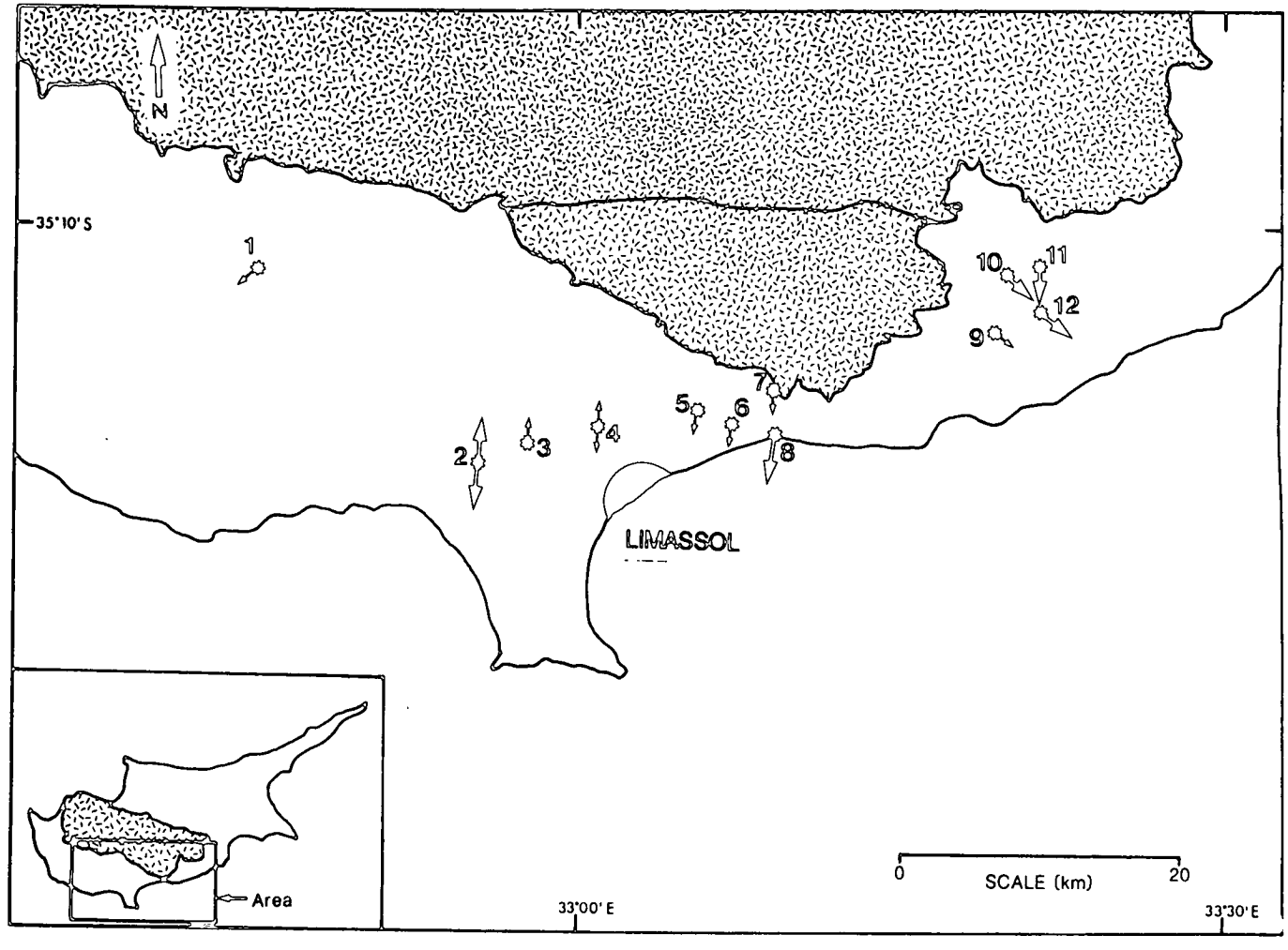

FIG. 5.6 Palaeocurrent determinations from localities in the study area. 1 Yerasova, 2 Kandou, 3 Ypsonas, 4 Ayia Phyla, 5 Yermasoyia, 6 Moutayiaka, 7 Parakklisha, 8 Amathus, 9 Tokhni, 10 Khirokitia, 11 Kophinou, 12 Psematismenos. All data from cross-lamination except (2) from flutes, (10) & (11) from clast imbrication. Large arrows show well constrained determinations (10<N<20).

It must be emphasised that these estimates are calculated from data for one area only, and that thickness measurements are taken from composite vertical sequences which are off-set laterally by up to 17 km. They are therefore less than ideal, but all that can be done in the absence of borehole data and refined chronostratigraphic correlation. They are given here as a first approximation to the relative average sedimentation rates of the different facies associations.

No attempt is made to estimate sedimentation rates for the peripheral sands association.

5.6 Spatial arrangement of facies.

By analogy with studies of modern settings (Read, 1985; Mullins et al., 1984; Schlager & Chermak, 1979) the expected lateral relationships between the facies associations of chapter 4 at any given instant in time would be as illustrated in figure 5.7.

As previously discussed, the Limassol Forest block was a centre of uplift during Miocene times, and one would therefore expect the facies associations of the Pakhna Formation to be arranged as a series of linear belts about the uplifted block (figure 5.8). The present day outcrop pattern of the facies associations is shown in fold-out figure A4.1. Divergence from the "simple ideal" of figure 5.8 is brought about by three factors:

(1) Lateral migration of facies belts with time. This results in the superposition of adjacent facies belts in a vertical sequence (Walther's Law of Facies, 1894, as presented in Blatt, Middleton and Murray, 1980).

(2) The outcrop surface cuts through the stratigraphy.

(3) There is an indication from palaeocurrent and slump data, and from distribution of facies associations, of the development of a southern high during Miocene times in the area of the Akrotiri peninsular.

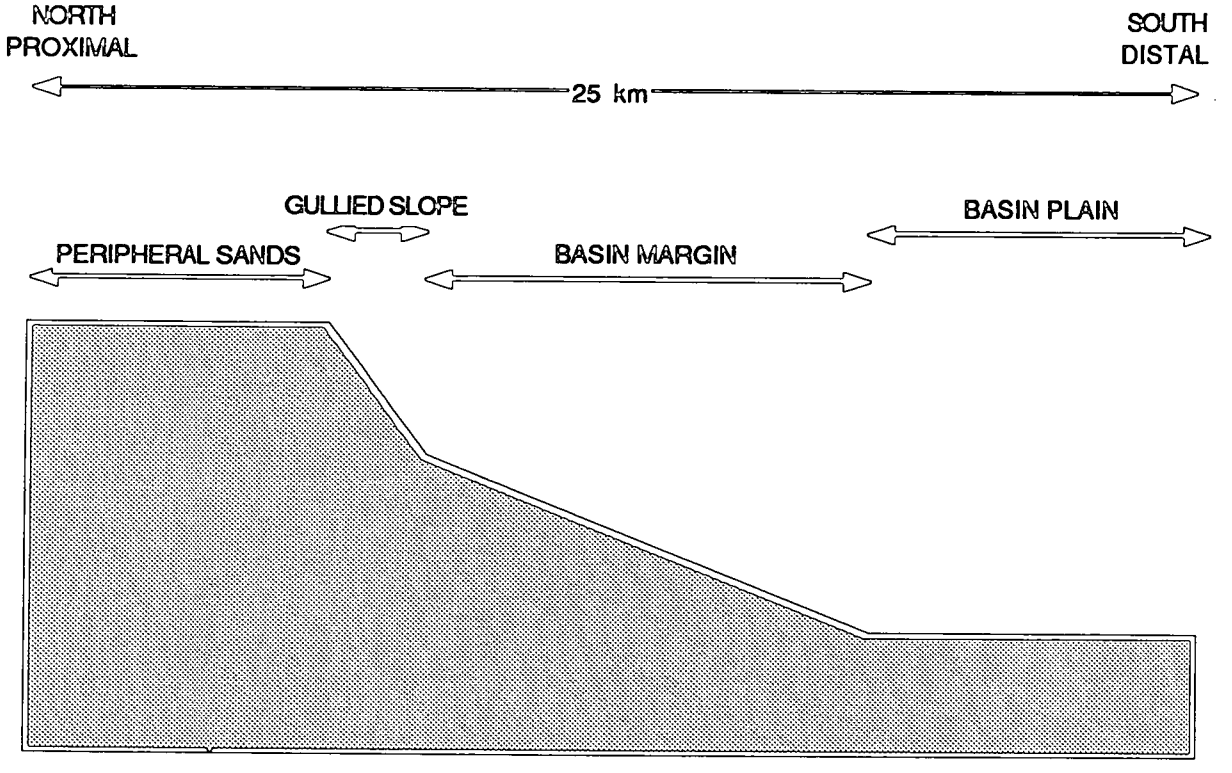

FIG. 5.7 Schematic representation of lateral relationships between the facies associations at any one point in time.

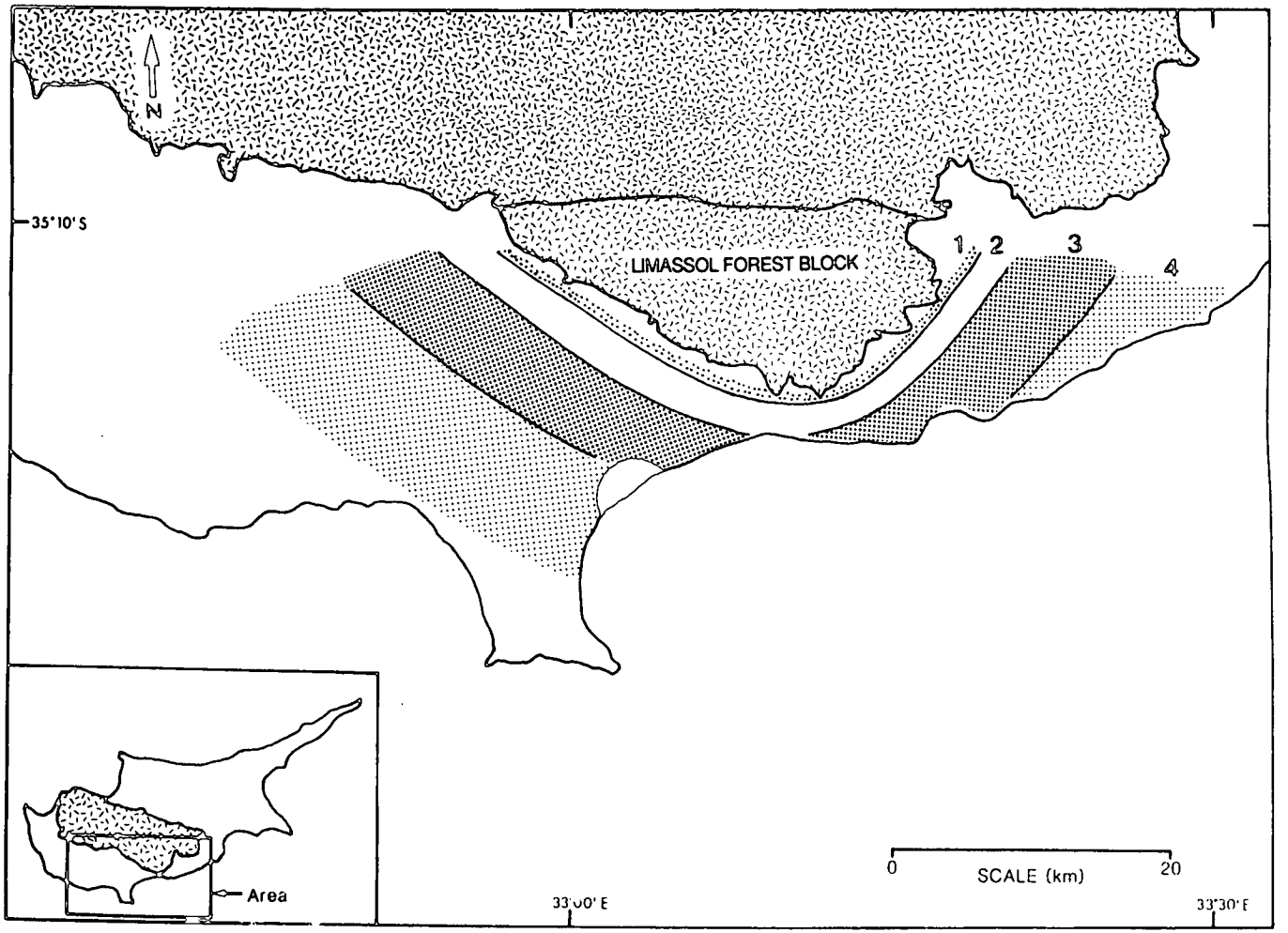

FIG. 5.8 Expected simple radial distribution of facies belts about uplifted Limassol Forest block. 1 = Peripheral sands, 2 = Gullied slope, 3 = Basin margin, 4 = Basin plain.

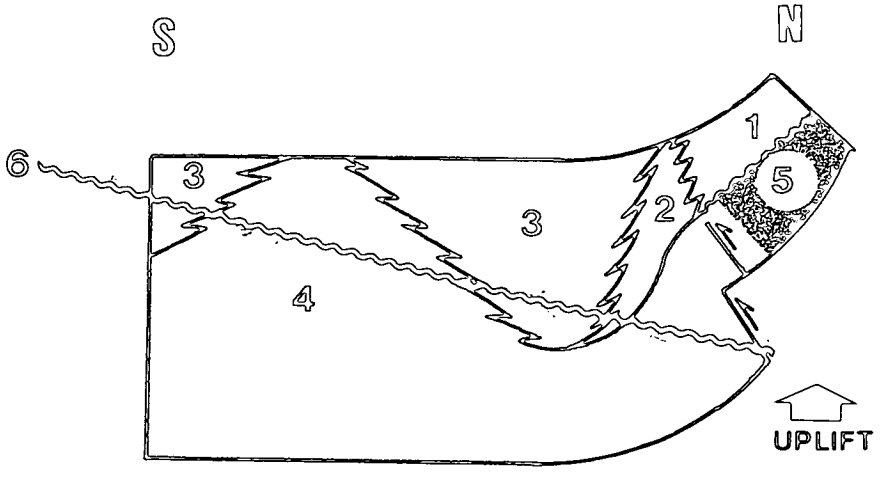

FIG. 5.9 Schematic basin profile showing relationship of facies associations. 1 = Peripheral sands, 2 = Gullied slope, 3 = Basin margin, 4 = Basin plain, 5 = Uplifted basement, 6 = example present erosion surface.

Vertical trends (section 5.2) suggest a generally regressive nature of the Pakhna Formation, implying migration of the facies belts towards the basin centre with time. This is coupled with the present day outcrop surface and distribution pattern of facies associations to arrive at the schematic cross-section shown in figure 5.9.

5.7 Evidence for the Akrotiri High.

5.7.1 Introduction

Palaeocurrent data (section 5.4) and slump data (section 5.3) hint at the existence of a southern high in the region of the Akrotiri Peninsula during the Miocene. These data, being from only a couple of points, are inconclusive on their own. However, several other lines of evidence suggest quite strongly that a structural high running approximately east-west through the position of Akrotiri Peninsula defined the southern margin of the Pakhna basin. This additional evidence comes from borehole and field data.

5.7.2 Borehole and field data

Hydrogeological boreholes were drilled across the Akrotiri Peninsula by the Cyprus Geological Survey Department and the results, including borehole records, were published by Hadjistaurinou & Constantinou (1977). Of particular interest are boreholes EB50 and EB44 (figs. 5.10, 5.11, 5.12). Borehole EB50 drilled through 150 m of Plio-Pleistocene sands and gravels into Lefkara chalk, with no Pakhna Formation deposits present. EB44, some 3 km to the south, drilled through 100 m of Plio-Pleistocene gravels into 230 m of shales, radiolarites and umbers of the Mamonia Complex (Mesozoic).

Mamonia sediments (Ayios Photios group) crop out in the cliffs beneath the RAF hospital at Cape Zevgari (see fig. 5.10), where they occur as folded red radiolarian cherts unconformably overlain by Pliocene deposits (see also Morel, 1960). Thus, in the Akrotiri area, Mamonia basement and Lefkara chalks have been uplifted and eroded

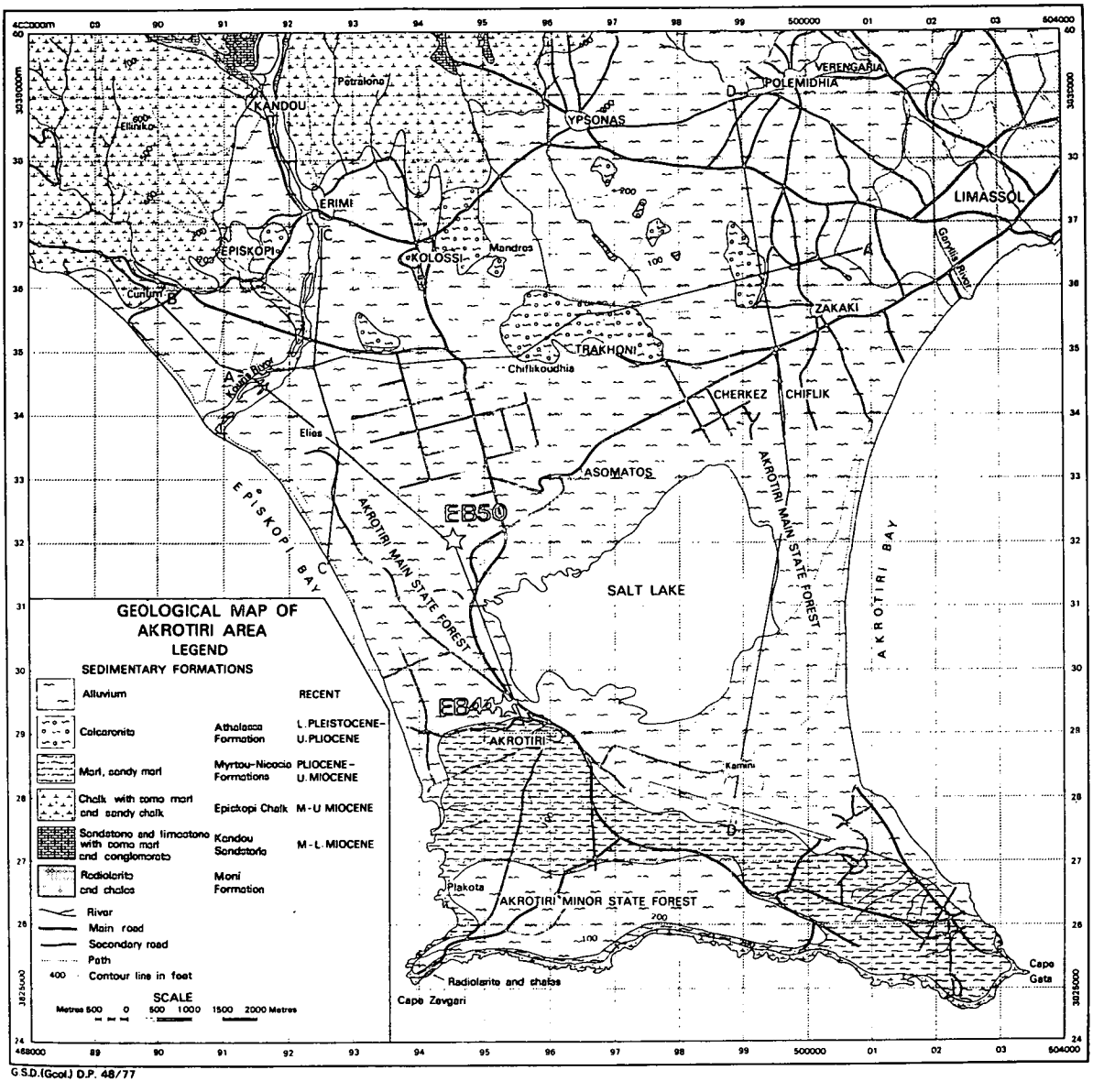

FIG 5.10 Borehole location map, Akrotiri Peninsula.

BOREHOLE RECORD

No. OF SAMPLE

VILLAGE & No. AKROTIRI

OWNER: Government

N. 3829160 m E. 495600 m

GROUND ELEVATION: 61.06 Ft.

SERIAL No. EB 44

HYDR. SERIAL No.

L.R.O. SHEET No. LVIII/39

L.R.O. PLOT No. 63

Airlift + PUMPING TEST

DATE:	25/7/68		
YIELD G.P.H.	10000		
DRAWDOWN: Ft.			
G.P.H/Ft.			
Cl. p.p.m.	22000		

+ Before observation pipes were inserted

DRILLING DATA

DRILLER: Theologou

RIG: Mayhew

METHOD: Rotary

DATE: 18/7/68-15/8/68

WATER STRUCK AT DEPTH Ft.	DEPTH OF WATER TABLE Ft.
35-320	47

PUMPING EQUIPMENT

TYPE OF PUMP:

PUMP SUCTION AT Ft.

PURPOSE OF D.H. Observation

SAMPLES EXAMINED BY

Chr. Constantinou - Y. Graitzer

G.S.D. (Hydr.) D.P. 7/77

AGE	FORMATION	DESCRIPTION	LITHOLOGY	DEPTH Ft. 1" 2"
Pliocene to Recent		Calcareous sandstone with coral gravel		20
		Gravel mostly rounded max. 3cm diameter 47		80
		Grey sandy marl with gravel		100
		Gravel with sandstone max. 2cm diameter		200
		Marl, sand with gravel		220
		Very fine sand with marl		270
		Dark grey sandy clay		280
		Coarse sand with marl		320
		Dark grey sand with gravel and marl		
	Mamonia	Grey brown radiolarite with shales and umber		460
		Grey marl		480
		Sholos and umber with radiolarites		1075

Cement plug

FIG. 5.11 Borehole record, EB44.

BOREHOLE RECORD

No. OF SAMPLE

VILLAGE & No. PHASOURI

OWNER: Government

N. 3831925m E. 494550m

GROUND ELEVATION: 4.69 Ft.

SERIAL No. EB 50

HYDR. SERIAL No.

L.R.O. SHEET No. LVIII/30

L.R.O. PLOT No. 1/1

PUMPING TEST

DATE:			
YIELD G.P.H.			
DRAWDOWN: Ft.			
G.P.H/Ft.			
Cl. p.p.m.	210		

DRILLING DATA

DRILLER: St. Avraam

RIG: Mayhew

METHOD: Rotary

DATE 16/8/68-12/9/68

WATER STRUCK AT DEPTH Ft.	DEPTH OF WATER TABLE Ft
3.5-420	3.5

PUMPING EQUIPMENT

TYPE OF PUMP:

PUMP SUCTION AT Ft.

PURPOSE OF B.H. Observation

SAMPLES EXAMINED BY

Chr. Constantinou - Y. Greitzer

G.S.D. (Hydr.) D.P 10/77

AGE	FORMATION	DESCRIPTION	DEPTH: Ft.
Plio - Pleistocene		Soil 3.5 V	10
		White grey sandy marl with some small gravel	60
		Gravel mostly of igneous origin	80
		Grey sandy marl with some gravel	120
		Gravel of igneous and sedimantary origin	160
		Grey sandy marl and some gravel	170
		Gravel of igneous and sedimentary origin	216
		Grey sandy marl and gravel	230
		Gravel of igneous and sedimentary origin	270
		Grey sandy marl	280
		Gravel, mostly of igneous origin	330
		White grey sandy marl with gravel	340
		Gravel mostly of igneous origin	380
Lapithos	Ayia Mavri Chalk	White grey chalk with some chert	420

Borehole diameter 8 3/4"

FIG. 3.12 Borehole record, EB50.

prior to deposition of the Pliocene sediments.

That this occurred during Pakhna Formation times seems likely in view of the subcropping Lefkara Formation beneath the Pliocene deposits (borehole EB5Ø). Miocene uplift would also be suggested by analogy with the uplift of the Limassol Forest block just 3Ø km to the northeast.

If this is correct then it ought to be possible to distinguish Mamonia-type erosion products within the clastic sequences of the Pakhna Formation. Significant quantities of such material would suggest derivation from a southern margin (the Akrotiri High) since no Mamonia basement occurs on the northern margin of the basin (see geological map, fig. 1.3)

3.7.3 Mamonia chert pebbles in the Pakhna Formation

Notable at localities on the southern limit of Pakhna Formation outcrop close to the Akrotiri peninsula is the inclusion in graded calcarenites of well to very well rounded grey and yellow chert pebbles, up to 1 cm across. These pebbles are concentrated as pebbly bases to these lithologies. The degree of rounding is in contrast to the angular nature of the coarse carbonate material with which they are mixed, which also contains moulds of unbroken bivalve and gastropod shells.

The pebbles have been extracted and examined petrogaphically. The following eight types have been identified:

(1) Well rounded pebbles of yellowish translucent microcrystalline quartz, up to 1Ø mm across. Very common. (Plate 11A).

(2) Angular to well rounded grains of unstrained monocrystalline quartz, up to 3 mm across. Very common. (Plates 11B, 12D).

(3) Well rounded pebbles of translucent yellow radiolarian cherts. Radiolarians are preserved as micro-quartz but rarely with chalcedony. Up to 1Ø mm across. Common. (Plate 11C).

(4) Well rounded argillaceous quartz siltstones with sub-angular silt grains. An original depositional lamination is sometimes visible. Up to 10 mm across. Common.

(5) Mature quartzite intraclasts with well compacted sub-angular to rounded quartz grains and silica cement. Up to 5 mm across. Rare. (Plate 11D)

(6) Aggregates of strained and sutured micro and mega quartz, rounded to angular. Sometimes showing a preferred grain orientation. Up to 3 mm across. Rare. (Plate 12A).

(7) Black metalliferous chert (manganese rich ?). Well rounded. Rare. (Plate 12B).

(8) Well rounded chert with relict peloidal texture preserved as micro-quartz and chalcedony. Very rare. (Plate 12C).

Notably absent in these cherts is isotropic silica.

None of these pebble types can be confidently matched with chert bearing lithologies from the in-situ sedimentary cover to the Troodos type basement. Chert occurrences and reasons for their rejection as erosional source are listed in Table 5.1.

Petrographic equivalents of pebble types 5, 6 and 8 have only been recorded from sandstones of the Ayios Photios Group of the Mamonia Complex. These sandstones also contain large amounts of material of pebble types 1, 2, 3 and 4 (Plate 13). Therefore, the quartz pebbles found in the Pakhna Formation calcarenites local to the Akrotiri Peninsula are petrographically indistinguishable from Mamonia lithological material. Reworking of Mamonia quartz bearing sandstones and conglomerates involving transport through a neritic carbonate environment would also explain the well rounded nature of the pebbles and their association with "immature" bioclastic grains.

To further corroborate this conclusion, samples of the Pakhna chert pebbles were analysed by XRD. The results are shown in figure 5.13, and can be compared with XRD traces from Lefkara Formation cherts in figure 5.14.

FORMATION	CHERT TYPE and REASON FOR REJECTION
LEFKARA	Granular and vitreous cherts, containing opal C-T. Incomplete replacement of carbonate (Robertson & Hudson, 1974). These cherts do not match petrographically.
MONI	Akamas sandstones have much associated feldspar. Parekklisha sandstone olistoliths could provide some loose rounded quartz grains, but otherwise does not match chert pebbles petrographically (see Robertson, 1977c).
PEREPEDHI	Metalliferous umbers and radiolarian cherts with isotropic matrix (Robertson & Hudson, 1974). Does not match petrographically with Pakhna chert pebbles. Would also expect large quantities of associated eroded lava clasts to be included.
TROODOS IGNEOUS	Clear quartz occurs in stockwork pipes (Boyle, 1984). Volumetrically insignificant, and no eroded lava clasts are found, as would be expected if stockworks were being eroded.

TABLE 5.1 Outlining main occurrences of chert and quartz in the Troodos *in situ* sedimentary cover, and reasons for rejection as source material for chert pebbles of the Pakhna Formation sediments.

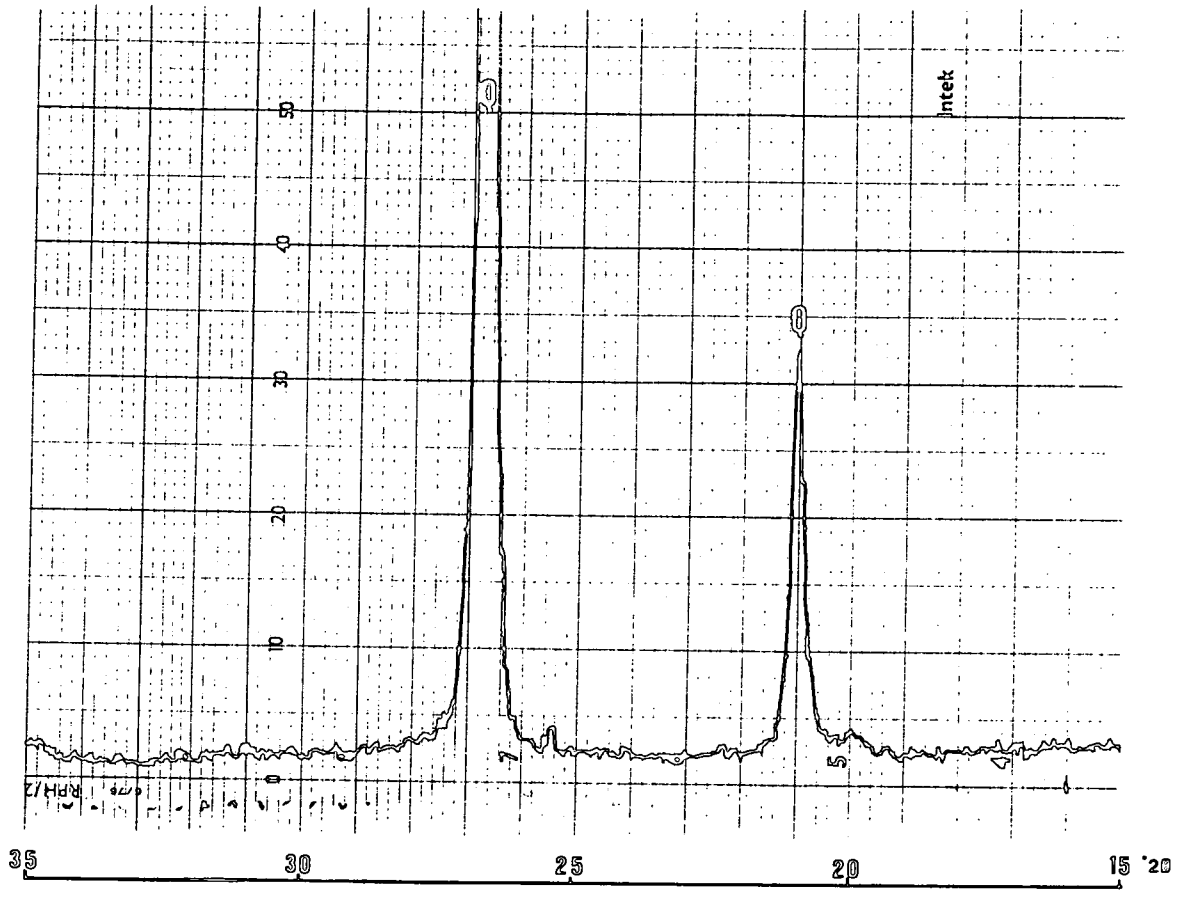

FIG. 5.13 XRD results for quartz pebbles discussed in section 5.7.3. Q = Quartz peak. For comparison with Fig. 5.14.

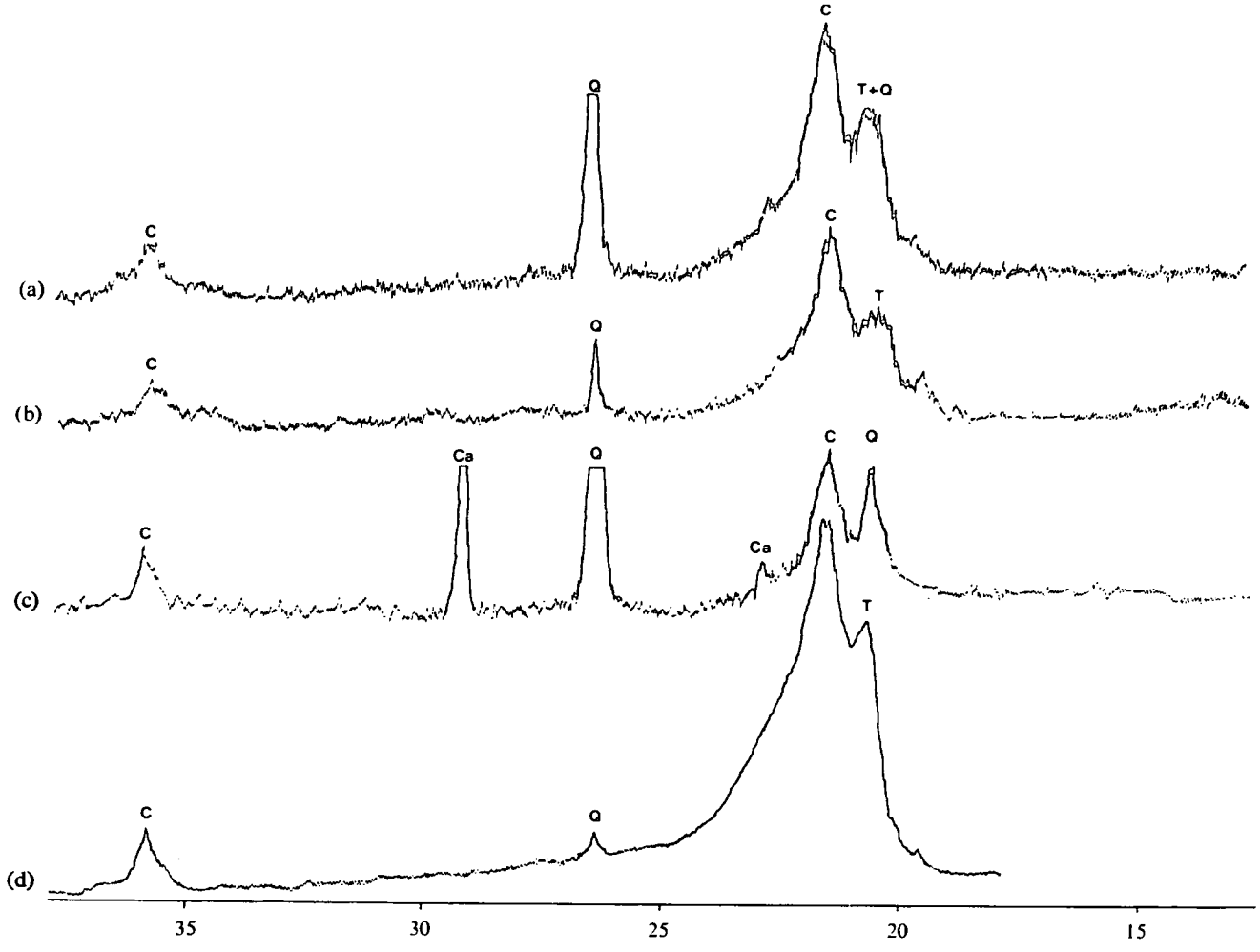

Fig. 7. X-ray powder diffractometer traces of cherts. (a) Radiolarite, Pyrga; (b) radiolarite, Troulli; (c) partially silicified chalk (Granular Chert), Tremithios River; (d) Opal C–T (Type D) from Jones & Segnit (1972) for comparison. Cu Kα radiation. C, Cristobalite; Ca, calcite; Q, quartz; T, tridymite.

FIG. 3.14 XRD results for Lefkara and Perepedhi Formation cherts (from Robertson & Hudson, 1974).

(taken from Robertson & Hudson, 1974). Pakhna Formation pebbles contain quartz only, whereas the cherts from the Lefkara Formation contain quartz and opal-CT. An Ayios Photois Group source for the pebbles is again suggested.

Axial derivation of these components, possibly from the west where most of the present day exposures of the Mamonia Complex are found, cannot be ruled out completely. However, the following observations argue for derivation from an Akrotiri High, running approximately east-west through the Akrotiri Peninsula, and eroded down to Mesozoic basement (Mamonia Complex) during the Middle and Late Miocene:

(1) Calcarenite lithologies of the Pakhna Formation containing coarse pebbly Mamonia-derived material are found only in close proximity to the Akrotiri Peninsula.

(2) Palaeoslope and palaeocurrent data suggests down-slope sediment transport on a northward dipping palaeoslope in the area where the Mamonia derived pebble lithologies are found.

(3) Borehole data shows marked unconformity between Pliocene and Mesozoic lithologies near Akrotiri village, i.e. south of where the reworked Mamonia type pebbles are now found.

The sea cliffs on the south coast of the Akrotiri Peninsula are mapped by Morel (1960) as Pakhna Formation, and contain a boulder bed interpreted as a Miocene submarine fault scarp deposit. If correct, this would imply that the southern margin of the Miocene Akrotiri High lies to the north of these cliffs. This would be difficult to reconcile with the outcrop of Mamonia lithologies at Cape Zergavi. However, blocks of recrystallised limestone with vugs pseudomorphous after selenitic gypsum have been found in the boulder beds, indicating that these deposits post date the Messinian evaporites. It seems likely, therefore, that the southern limit of the Miocene Akrotiri High lay off-shore from the present Akrotiri Peninsula, and that no Pakhna Formation deposits occur in the sub-surface south of borehole EB44

(near Akrotiri village).

3.8 The Khalassa and Maroni sub-basins

3.8.1 Introduction

Two sub-basins for the Pakhna Formation deposits are distinguished in the area of study. These are the Maroni sub-basin, to the east of the Limassol Forest block, and the Khalassa sub-basin, to the south and west of the Limassol Forest block (fig. 3.15). These sub-basins are distinguished primarily on the basis of two factors; structural considerations, and sediment provenance and dispersal patterns.

3.8.2 Structural considerations.

Miocene uplift of the Limassol Forest block was accompanied by steep overthrusting onto the sediments of its southwestern margin, producing the Yerasa fold and thrust belt (Robertson, 1977a). Sediments in the fold belt are locally overturned. This deformation took place prior to the deposition of the Koronia Limestone Member (Late Miocene), which transgresses the structure with angular unconformity (see section 7.3). Structural details are more fully presented in chapter 7, but the important conclusion is that uplift culminated prior to Koronia Limestone times and defined the northern margin of the Khalassa sub-basin.

Structures of the Yerasa fold and thrust belt plunge at low angles to the southeast, where continuation is marked by a broad anticlinal feature in the Lefkara chalks and the Moni Melange. Evolution of this structure during the uplift of the Limassol Forest block would have created a gently plunging anticlinal rise on the Miocene sea floor, separating the Maroni sub-basin (east of the Limassol Forest block) from the Khalassa sub-basin (south and west of the Limassol Forest block).

The southern margin of the Khalassa sub-basin is defined by the Akrotiri High, a feature which also evolved during the Miocene and interpreted by analogy with the

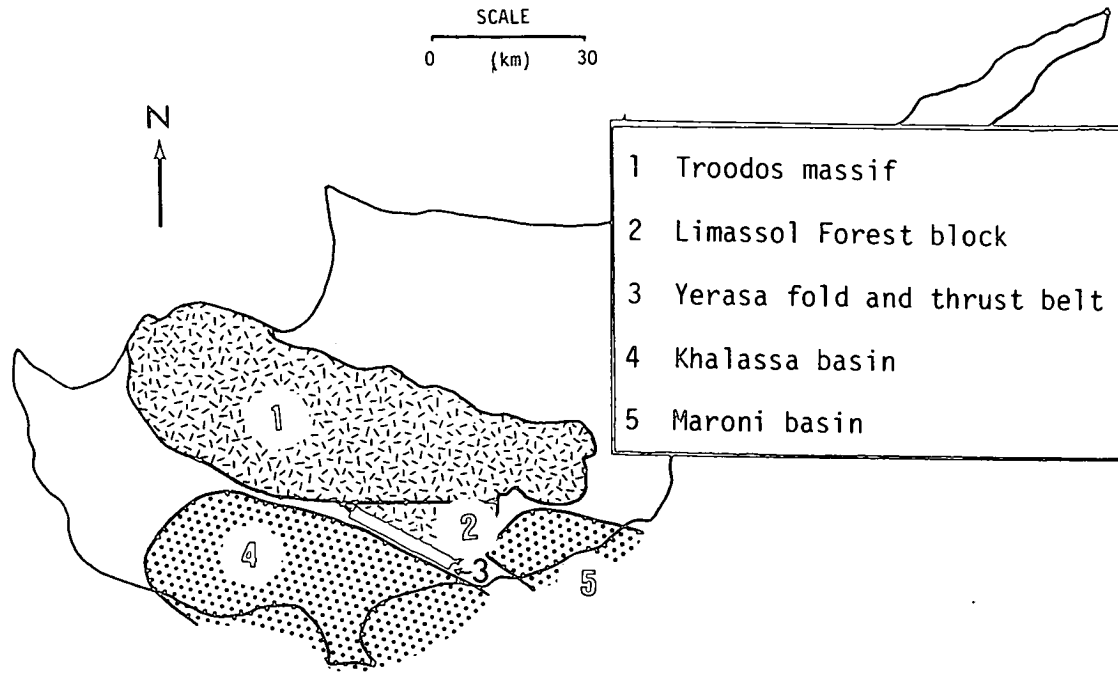

FIG 5.15 MAP SHOWING LOCATION OF RELEVANT BASINS IN SOUTHERN CYPRUS

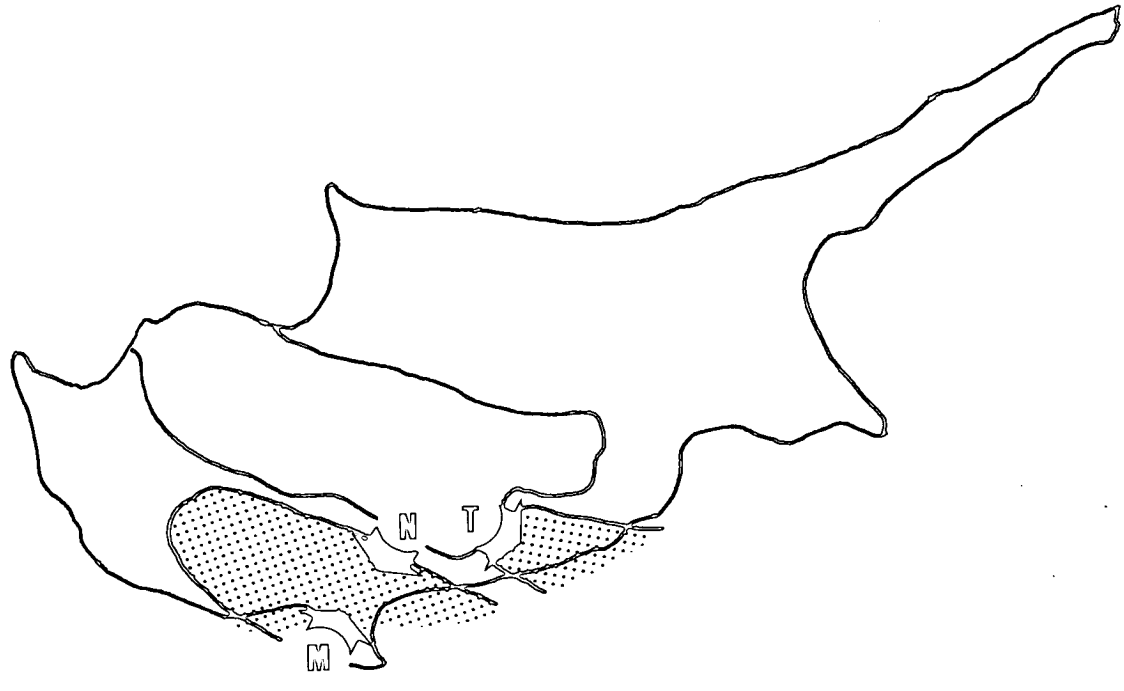

FIG. 5.16 Clast provenances and dispersal directions. T = Troodos province, M = Mamonia province, N = Neritic intra-basinal province.

Limassol Forest block as being structurally controlled.

In summary, structural considerations suggest that the two sub-basins were brought into existence and isolated from each other by the tectonic processes that uplifted the Limassol Forest block and the Akrotiri High.

5.8.3 Clastic provenance and dispersal patterns

Three different clast provenances can be identified.

(1) Troodos province.

(2) Mamonia province.

(3) Neritic intra-basinal province.

The clastic material in each of these three groupings is dominated by reworked neritic bioclasts. This component is similar for all these provinces and is derived from a circum-littoral zone fringing the basin margins (see section 5.9).

Sediments of Troodos provenance also contain a non-carbonate fraction of weathered lava clasts, feldspar aggregates, and clinopyroxene grains. Rare clear quartz is found, sometimes containing inclusions of epidote. This latter component is similar to jasper dscribed by Boyle (1984) from stockworks and fault zones within the ophiolite sequence. Sediments of Troodos provenance are found exclusively in the Maroni sub-basin to the east of the Limassol Forest block.

Mamonia province sediments are found close to the Akrotiri High (section 5.7) in the southern most part of the Khalassa sub-basin. These sediments contain quartz sandstone and chert clasts, derived from eroded Mamonia basement on the Akrotiri High, mixed with neritic bioclastic material.

Sediments deposited to the south of the Limassol Forest block, in the northern part of the Khalassa sub-basin, are almost completely clean of non-carbonate clastic components. Minor amounts of silt grade quartz do occur, but, in contrast to sediments of the Troodos province, lava clasts are very rare. This material is essentially of intra-basinal origin.

It seems, therefore, that three different dispersal systems were delivering sediments into two sub-basins (fig. 5.16). In the north, erosion products of the Troodos basement (Limassol Forest block) were being transported eastward down a gullied slope (chapter 4) into the Maroni sub-basin. South of the Limassol Forest block very little of this material is evident and it appears that only neritic carbonate of intra-basinal origin was being reworked southwards into the Khalassa sub-basin. The third dispersal system was transporting erosion products of uplifted Mamonia basement (Akrotiri High) northwards into the southern part of the Khalassa sub-basin.

5.8.4 Depocentres

An isopach map for the Pakhna Formation in the Maroni sub-basin, based on field mapping, is published by Bagnall (1960) which shows maximum thickness near the villages of Ayios Theodhoros and Psematismenos (fig. 5.17). The base of the Pakhna Formation in this region is not isochronous (section 2.5.3), so this isopach map is not for a time-equivalent body of sediment. Rather, thicknesses should be increased towards the south east where Lefkara Formation chalks are contemporaneous with early Pakhna sediments.

Evaporites of the Kalavasos Formation, deposited in the same basin, show considerable thickening to the south east (e.g. borehole EB22, fig. 5.18), and it may be that the true depocentre lies near Maroni village ,or possibly off-shore.

Without more extensive and deeper borehole data than is available it is not possible to construct an isopach map for the Pakhna Formation in the Khalassa sub-basin. However, the linear structural grain of the area, and the sediment dispersal patterns (section 5.8.3) suggest that this sub-basin was elongate between the Troodos Massif to the north and the Akrotri High to the south, with a depositional axis running approximately towards the ESE inbetween.

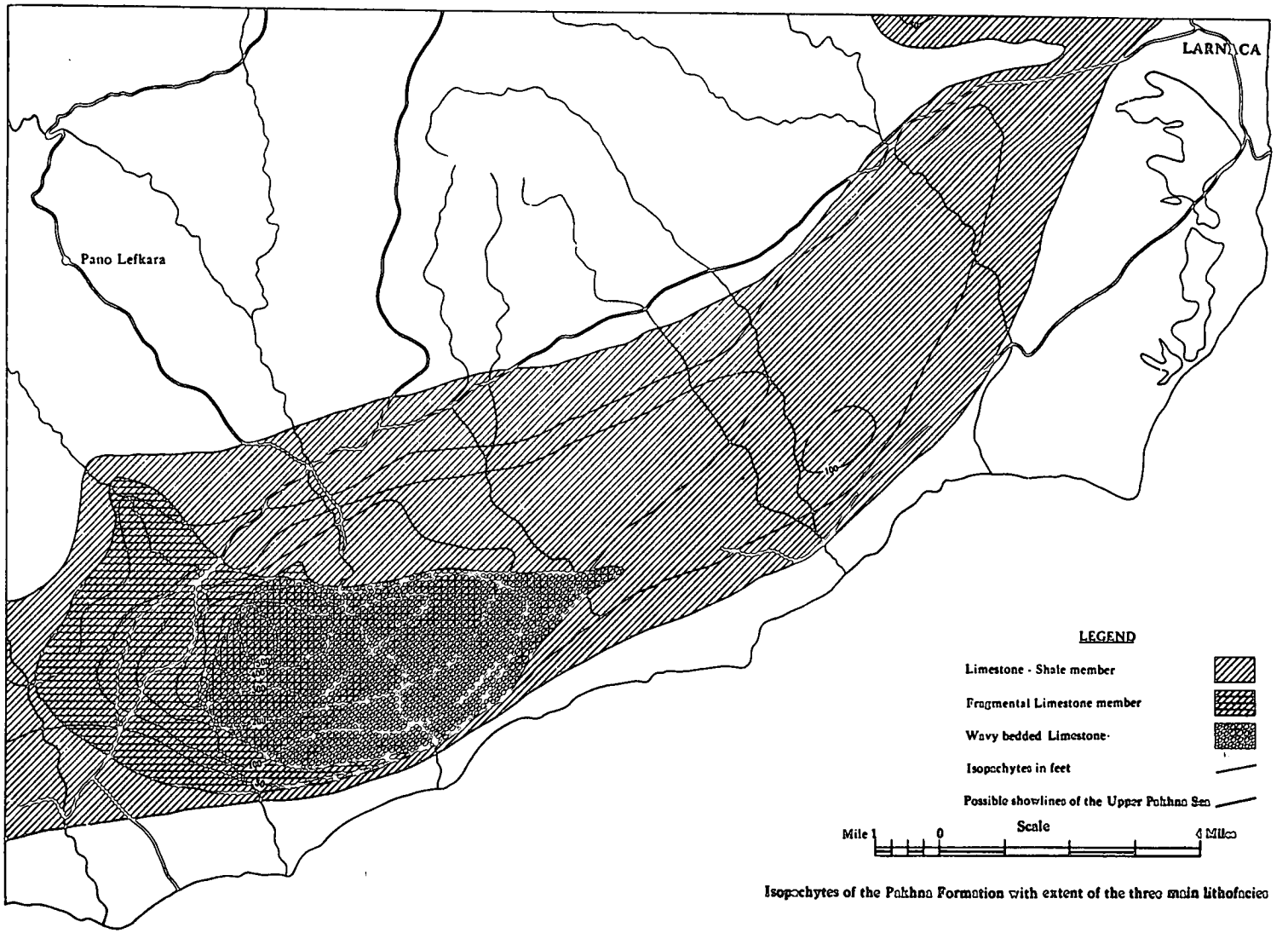

FIG. 5.17 Pakhna Formation isopach map, from Bagnall (1960).

AGE	FORMATION	DESCRIPTION	LITHOLOGY	DEPTH Ft.
Most likely Upper Miocene	Myrtou Marls	Yellowish Marl with little Sand Subangular Gravels		30 33
		Grey Marl		699
Middle to Upper Miocene	Pakhna	Sands and Sandstones Grey Marl		717 750
		Gypsum		001

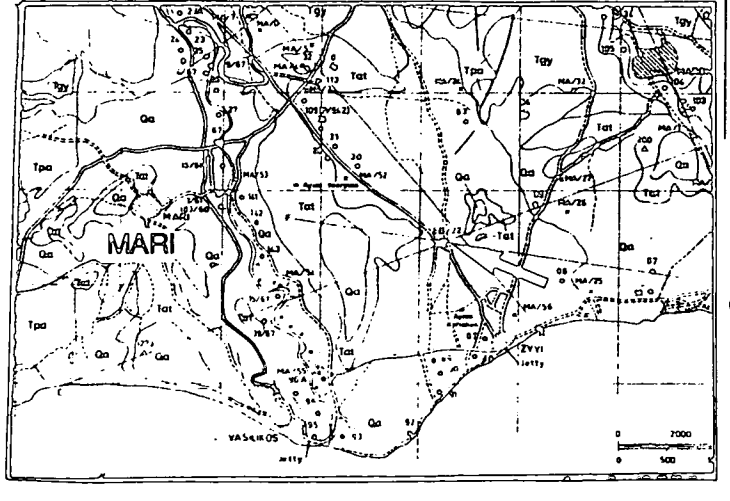

BOREHOLE RECORD

No. OF SAMPLE EB/22

VILLAGE & No. Tokhni (Zyyi)

OWNER: Government

N. 120500 m. E. 201250 m.

GROUND ELEVATION: 796 Ft.

SERIAL No. EB/22

HYDR. SERIAL No.

FIG. 5.18 Borehole record, EB22, and location map relative to Mari village (see Fig. 2.5).

5.2 Clastic source environments

The composition of reworked carbonate material in the Pakhna Formation sediments shows increasing influence of neritic source environments up sequence (section 5.2.3). These source areas are no longer preserved in the geology of southern Cyprus due to erosion. However, components in the reworked sediments provide some clues to the nature of these source environments, and possible analogues from both ancient and modern examples can be found.

The large amounts of red algae in association with bryozoan and bivalve debris is suggestive of a temperate reefal assemblage, such as found in Miocene sequences on the Atlantic coast of southwest Europe and Morocco (Chevalier, 1961). In the present day Mediterranean, coralline algae are also found to construct build-ups ranging in position from the intertidal zone (the "trottoir zone" of Peres, 1967), down to depths of 150 m ("coralligene plateau" of Laborel, 1961). The uppermost (youngest) clastic lithologies of the Pakhna Formation also contain compound coral debris, often mouldic in preservation, and with affinities to Porites. This is of particular interest as it is consistent with the concept of the Mediterranean as a "Messinian coral refuge" in which coral reefs persisted long after their demise at equivalent latitudes on the Atlantic coast (Esteban, 1980).

Pedley (1979) describes build-ups of red algae from the Upper Coralline Limestone Formation in Malta. This is of Tortonian or possibly Messinian age and thus contemporaneous with the Pakhna sediments of Cyprus. The Maltese deposits contain biostromes of Porites, crustose coralline algae, serpulids, bivalves, gastropods, miliolid and encrusting (Homotremtinae) foraminifera and peloids. Boring of Porites patch reefs by sponges and bivalves is common. These deposits are interpreted as representing a high energy shallow water marine setting (Pedley, 1979). The Upper Coralline Limestone Formation of Malta, therefore, contains in there original environment many of

the skeletal elements found in the calcarenites and calcirudites of the Pakhna Formation.

A similar age-equivalent formation is also found in Sicily (Pedley, 1983). This is the Carlentini Formation, which contains build-ups of coralline algae and corals, including Porites. Faunal assemblages also contain Clypeasteroid echinoderms, miliolid foraminifera, and pectinids in the more turbulent, reef dominated environments. Abundent rhodoliths and bryozoans are found on the fore-reef slope. Water depth is interpreted as 1 to 50 m for these assemblages.

It is likely that the emergent Limassol Forest block and Akrotiri High were fringed with neritic environments similar to those described from the Miocene of Sicily and Malta.

An important difference is that the Pakhna Formation deposits also contain erosion products from the emergent basement units. Introduction of terrigenous clastic material into a reef belt would locally modify reef development. This has been described by Haywood (1982, 1983) with examples from the ancient (Miocene, Turkey) and the modern (the Red Sea). Coastal alluvial fans are constructed by the surface drainage system and prograde out into the marine environment. Reefs grow as arcuate belts about the fan margins (fig. 5.19). Siliciclastic and bioclastic material is mixed in the protected area behind the reef belt, and may be organised into sand bars by wave action. Gravel lobes prograde out though fluvial channels cutting the reef belt, and flash floods may periodically result in the seaward transport of material beyond the reef barrier. Uplift of the land area, as envisaged for the Limassol Forest block and Akrotiri High, would promote marine progradation of the alluvial fan system and result in reworking of alluvial, lagoonal and reefal components into deeper water. These deposits would be analagous to graded calcarenites found in the Pakhna Formation.

A final note concerns the apparent low diversity of coral species found as reworked clasts in the Pakhna

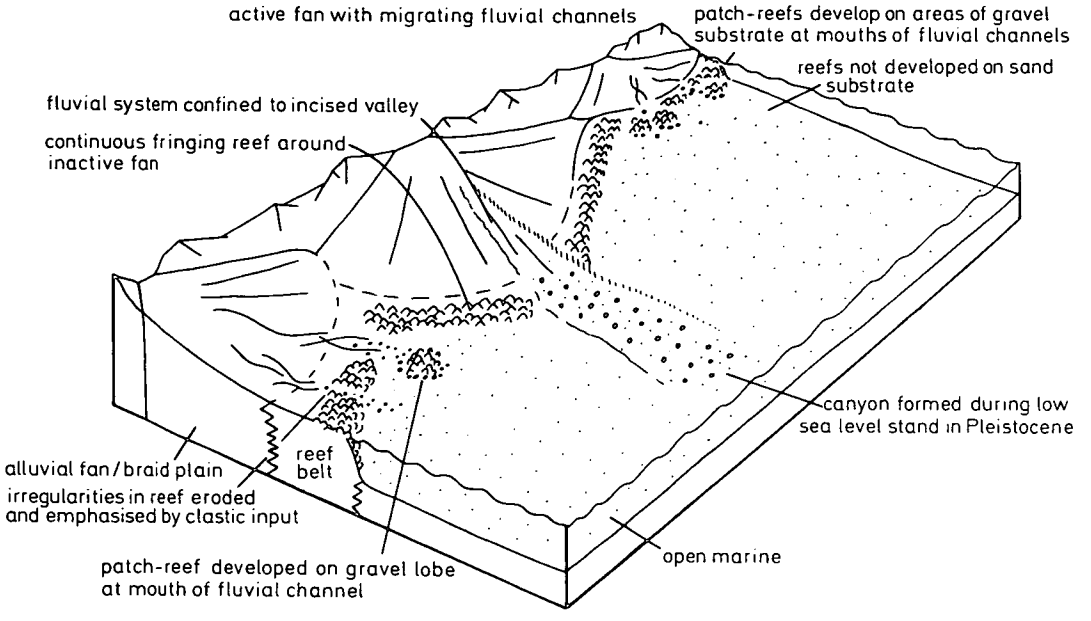

FIG. 5.19 Schematic model showing influence of clastic sediments on reef development and morphology, coastal alluvial fan, Red Sea. From Hayward (1982).

Formation. Though preservation is poor, coral debris from around the Limassol Forest block appears to be of a single genera, tentatively identified as Porites. Messinian coral reefs of south east Spain show an "aberrant" ecology, in that they consist of a monospecific coral framework (Porites) associated with bryozoans and serpulids (Esteban, 1980; Dabrio et al., 1981; Santisteban & Taberner, 1983). This has been interpreted as due to progressive environmental stress imposed by increasing salinities prior to the Mediterranean evaporite event (Esteban, 1980).

The same association, but in reworked material, is found in the uppermost calcarenites of the Pakhna Formation, in particular in the Koronia Limestone Member. It may be that "stressed" reefal communities, similar to those described from Spain, also developed in Cyprus prior to the Messinian evaporitic draw down of the Mediterranean.

5.10 A basin model for the Pakhna Formation

A reconstruction of depositional environments for the Pakhna Formation of the Limassol District in southern Cyprus is illustrated in fig. 5.20. This accounts for observations and available data in a geologically realistic manner. Implicit features of this model include:

(1) Uplift of the Limassol Forest block was probably concommitant with uplift of the Akrotiri High. These two structural features define the northern and southern margins of the Khalassa sub-basin. Uplift culminated in Koronia Limestone times.

(2) The Maroni and Khalassa sub-basins are separated by the easterly continuation of the Yerasa fold and thrust belt.

(3) By analogy with the Limassol Forest block, the Akrotiri High is also shown as a thrust related feature.

(4) The easterly dispersal direction for the erosive products of the Limassol Forest block (Troodos province of section 5.8) is structurally controlled.

(5) A consequence of (4) is that most clastic material from the northern margin of the Khalassa sub-basin is derived from an intra-basinal source in the neritic zone (neritic intra-basinal province of section 5.8).

(6) Basement and cover lithologies, and uplifted fringing reefs are eroded and transported into coastal alluvial fans, where mixing with neritic carbonate occurs prior to down slope reworking.

(7) Numerous point sources in the neritic zone contribute sediment to the lower slope apron (basin margin facies association) through by-passing of the upper slope (gullied slope facies association).

(8) The development of linear structural highs bounding the basin restricted bottom water circulation. This accounts for reduced bioturbation, and preservation of large amounts of plant remains in the uppermost calcilutites, which mark the transition up sequence to the evaporites of the Kalavasos Formation.

FIG. 5.20

SCHEMATIC RECONSTRUCTION OF DEPOSITIONAL ENVIRONMENTS
LIMASSOL DISTRICT, LATE MIOCENE TIMES

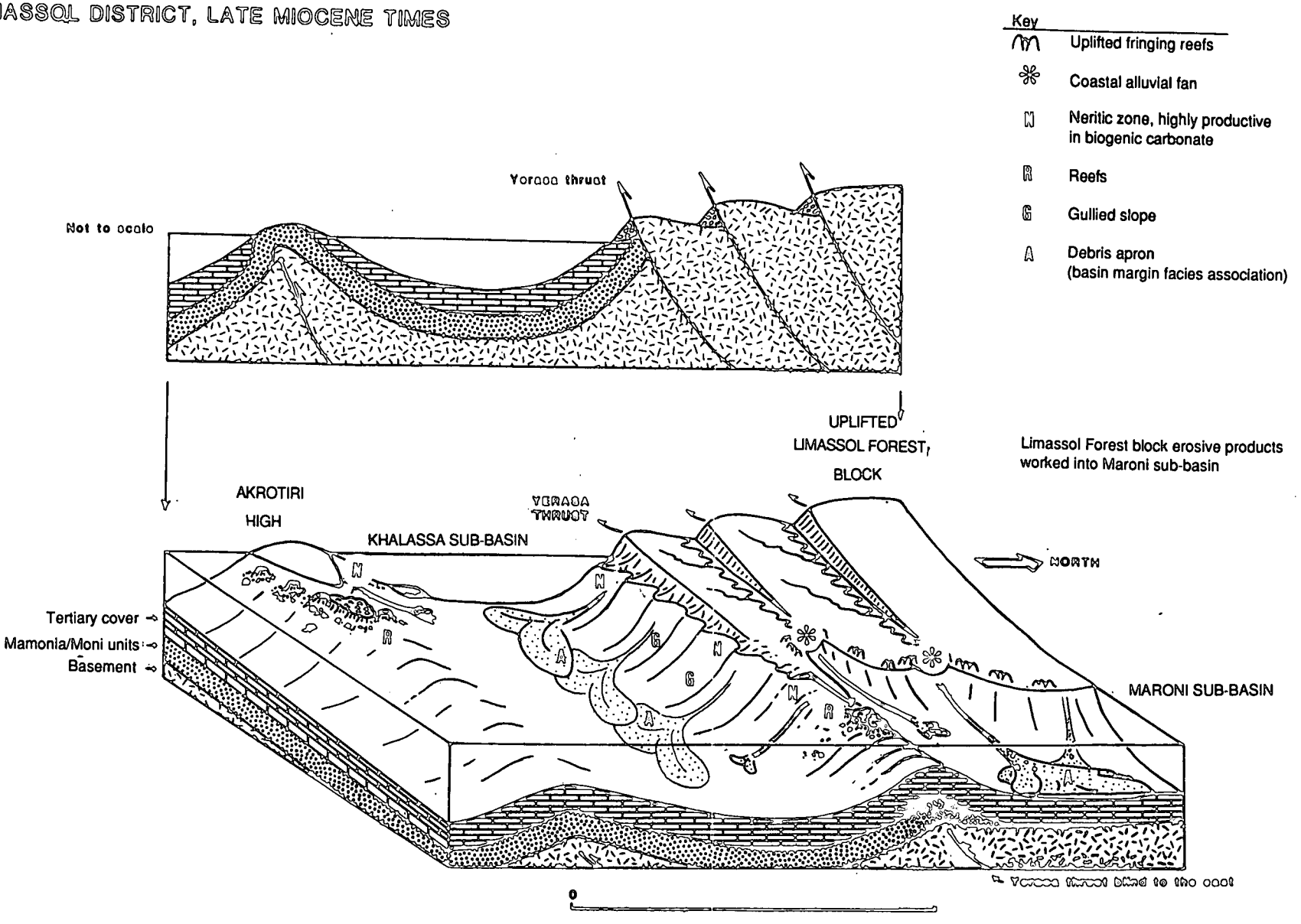

CHAPTER SIX

THE KALAVASOS FORMATION AND ITS ENVIRONMENTAL INTERPRETATION

6.1 Introduction

The Kalavasos Formation comprises all the outcrops of Late Miocene evaporites located around the Troodos massif, and consists almost entirely of gypsum, with minor gypsiferous marls. Outcrop area and field relationships with underlying formations have been described in section 2.4. These observations indicate that the Kalavasos Formation has no lateral equivalence with the Koronia Limestone Member, and that it wholly post-dates the Pakhna Formation in the area of study.

Weathering of the Kalavasos Formation results in poor quality exposure. On the whole, the outcrop area is represented by a scrubbily vegetated, friable, weathered gypsum soil. Full lithological examination is generally only possible in relatively fresh quarry faces. Four such quarries have been examined: Tokhni, Kalavasos, and Maroni quarries in the Maroni sub-basin, and Moutayiaka quarry in the Khalassa sub-basin. A hillside outcrop north of Pissouri village in the Khalassa sub-basin was also logged (G.R. 716381). Gypsum outcrops in the Polis Graben area and on the Troodos north flank were also examined for comparison.

Exposures exhibit a wide range of gypsum lithologies, which are described and interpreted in the following sections.

6.2 The Messinian Event in the Mediterranean

Extensive evaporite deposits in excess of two kilometres thick beneath the present day abyssal plain of the Mediterranean Sea were first discovered during the Deep Sea Drilling Project (DSDP) Cruise Leg 13 (Ryan, Hsu *et al.*, 1973). These deposits contain sabkha facies evaporites which are sandwiched between deep water open marine sediments, with deep marine Pliocene sediments above. The geographical distribution of the evaporites, as revealed on seismic data (fig. 6.1), bears a close

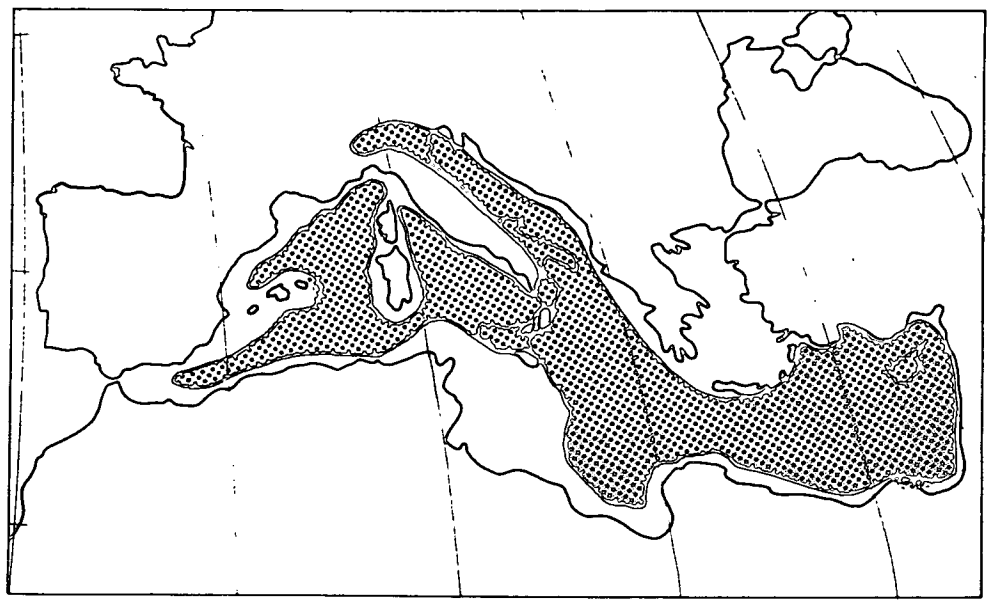

Fig. 2. Distribution géographique des évaporites messiniennes en Méditerranée. Tentative de reconstitution. Les dépôts de la Mer Rouge n'ont pas été représentés (d'après Nesteroff 1973).

FIG. 6.1 Distribution of Messinian halite in the Mediterranean (from Nesteroff, 1973).

relationship to the present bathymetry. This suggests that the Mediterranean, as a whole, was already developed to its present configuration by Messinian times. Pliocene subsidence could not, therefore, account for the present position of thick halite deposits several kilometres below sea-level. A desiccated deep basin model was proposed to explain the origin of these deposits (Hsu, Ryan & Cita, 1973). According to this model, isolation of the Mediterranean Sea about 5.5 mybp was followed by evaporitic draw-down and precipitation of thick gypsum and halite sequences from salt lakes whose brine levels were dropped to thousands of metres below the Atlantic sea level. This was accompanied by cutting of erosion surfaces to several kilometres below present base-level (see Ryan & Cita, 1978). Subsequent flooding of the Mediterranean through the "Iberian Portal" (Adams et al., 1977) restored open marine conditions. This desiccated deep basin model was supported by the findings of further DSDP investigations (Hsu, Montadert et al., 1978) and by a wealth of subsequent research throughout the Mediterranean region (see Cita, 1983 for an excellent review). It is now a widely accepted model for the origin of most of the Messinian Mediterranean evaporites.

On-shore exposures of Upper Miocene evaporites have long been known from around the Western Mediterranean. For example, in Spain (Gignoux & Fallot, 1927), the Italian Appenines (Pareu & Ricci Lucchi, 1972), Sicily (Ogniben, 1957), and Algeria (Perodon, 1957). They clearly occur at a structurally elevated level (compared to equivalent deposits beneath the sea floor), and in contrast to the thick halite-dominated successions encountered during DSDP drilling, comprise thinner sequences of gypsum and anhydrite. Hsu (1973) recognised the possibility that gypsum deposition in these shallower marginal basins could be explained by assuming the presence of topographic barriers creating local hyper-saline basins prior to the main phase of evaporitic draw-down (fig. 6.2). This limits the suitability of many of the on-shore exposures as

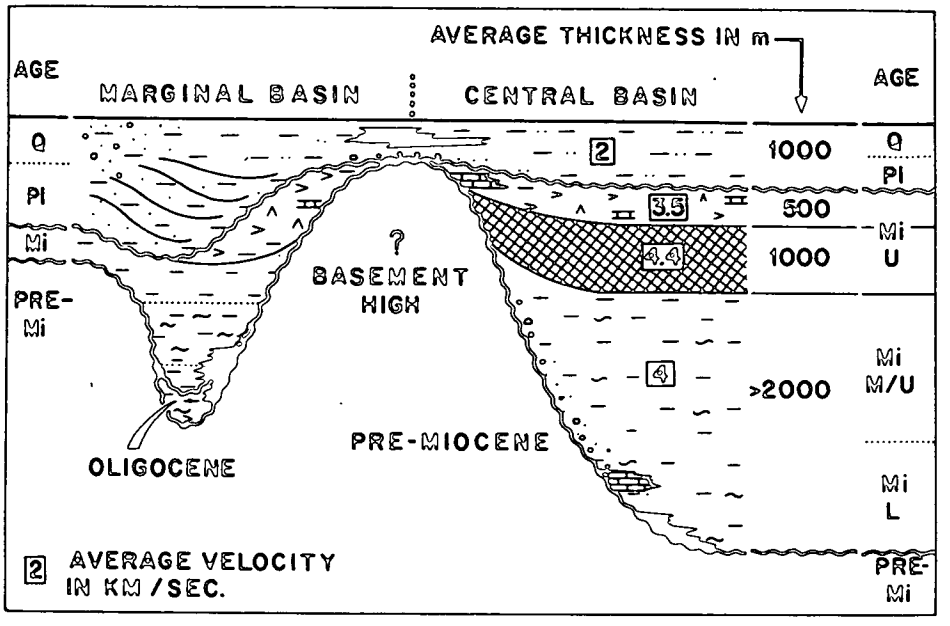

This generalized post- to late tectonic Upper Cenozoic stratigraphic scheme of the Mediterranean basins is largely based on the situation in the Balearic area, but also applies to other parts of the Mediterranean. Two unconformities which correspond to major pre-Miocene phases of Alpine orogeny are shown below Lower or Middle Miocene pelagic and Oligocene continental sediments. Late Miocene tectonic movements led to evaporite deposition in restricted basins and to erosion on the margins of these basins. This phase was followed by strong Plio-Quaternary subsidence and marine transgression.

FIG. 6.2 Relationship of marginal and deep Mediterranean evaporite basins (from Mulder, 1973).

analogues for the drilled sequences of the DSDP holes. Never-the-less, studies on land exposures, particularly on the Messinian evaporites of Sicily (Hardie & Eugster, 1971; Decima & Wezel, 1973; Richter-Bernberg, 1973; Schreiber et al., 1976) have led to the environmental interpretation of a wide variety of gypsum and halite lithologies, and have contributed enormously to evaporite sedimentology in general, and to an understanding of the Mediterranean Messinian deposits in particular.

In the Eastern Mediterranean, the existence of a thick sub-sea Messinian halite deposit is well established (Evans et al., 1978; Hsu, Montadert et al., 1978; Mulder et al., 1975). However, few on-shore evaporite exposures have been described. On the Ionian islands of Western Greece gypsum lithologies are interbedded with up to 200 m of marls and re-worked carbonates (Braune et al., 1973; Underhill, 1985; Schilling et al., 1978). On Crete, a poorly exposed thin development of shallow marine gypsum is reported, inter-bedded with marls (Meulenkamp & Zachariasse, 1973). On Cyprus, the Kalavasos Formation consists almost entirely of gypsum, is well developed (easily mapped as a single unit over a relatively large area), and can be examined in detail at several disused quarries.

Thus the Kalavasos Formation is one of only a few formations in the Eastern Mediterranean where Messinian evaporites are accessible for study.

6.3 Lithofacies

6.3.1 Introduction

Sabkha-type lithologies (nodular or enterolithic gysum in association with laminated algal carbonate) have not been developed or have not been preserved in the area studied. Instead, the gypsum lithofacies of the Kalavasos Formation compare well with subaqueous gypsum deposits described by, for example, Schreiber et al., (1976) and Vai & Ricci Lucchi (1977). These include: parallel laminated gypsum, nodular laminated gypsum, graded gypsum

beds (turbidites), banded selenite (primary and *in situ*), chaotic selenite (debris-flows), and contorted gypsum (slumps). These are described in detail in the following sections, and are compared with other examples described by Schreiber *et al.*, (1976) in fig. 6.3.

It was commonly observed that the best preserved gypsum features were in the freshest exposures. Weathering produces a progressive textural modification of the rock. Compare, for example, the lower (fresher) and upper portions of Plate 15C (parallel laminated gypsum). Also, in the Maroni gypsum quarry, textural modification becomes progressively stronger up sequence towards the original weathering surface (fig. 6.8).

In thin section (Plate 5D), crystals are commonly euhedral and with tightly interlocking irregular boundaries. Therefore, weathering appears to promote recrystallisation. Ultimately, this process can obliterate all detail and produce a homogeneous granular gypsum rock (alabaster).

6.3.2 Parallel laminated gypsum

Locally known as "mamara" and previously quarried as flagstones, this lithofacies consists of 1-5 mm thick alternating light and dark coloured gypsum laminae (Plate 15C). Individual laminae are parallel, and can be traced across the extent of the outcrop (over 5 m) without lensing out, merging, or being cut. Unlike similarly laminated gypsum lithologies described elsewhere (eg Hardie & Eugster, 1971) in which lamination is defined by gypsum/carbonate couplets, these deposits are composed entirely of gypsum.

With a hand lens it is possible to see that the rock is made up of fine acicular gypsum crystals randomly orientated in the plane of bedding

Thin section examination shows very fine interlocking subhedral crystals with occasional acicular gypsum laths up to Ø.5 mm long (Plate 5D). No clear distinction between light and dark laminae is seen. One uninvestigated

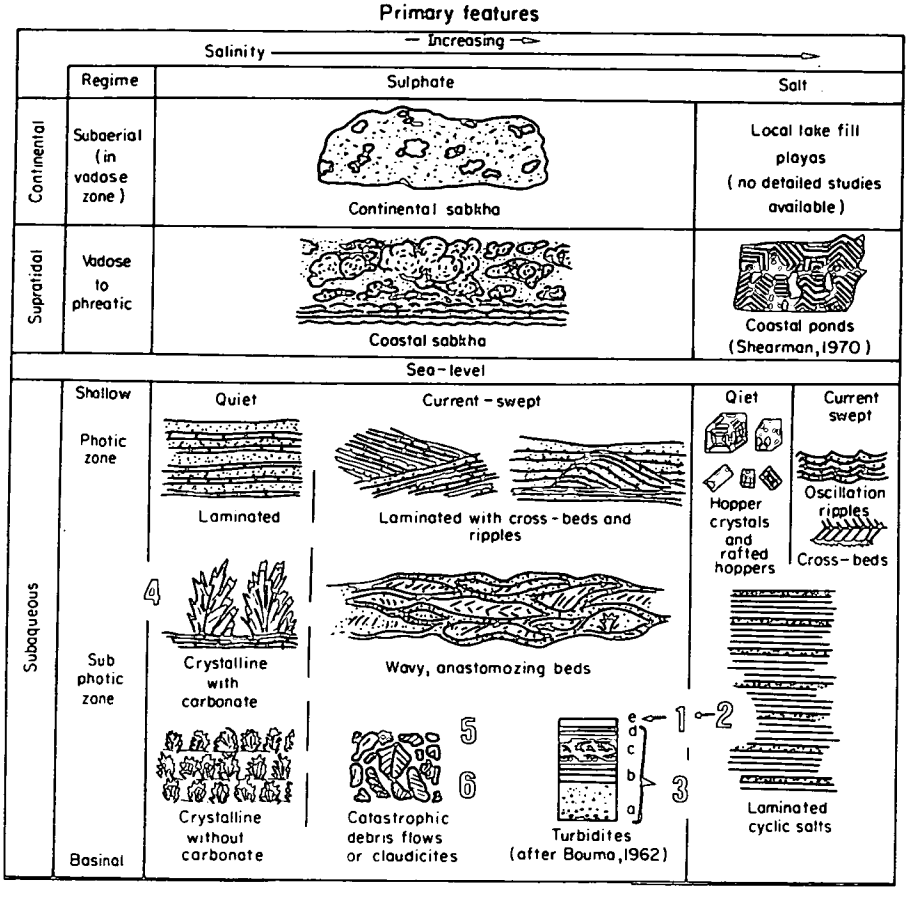

FIG. 6.3 Evaporite depositional environments after Schreiber et al., 1976, and correlation with evaporite facies described in this study. 1 = parallel laminated gypsum, 2 = nodular laminated gypsum, 3 = graded gypsum, 4 = banded selenite, 5 = chaotic selenite, 6 = contorted gypsum.

possibility is that laminations are defined by alternating levels of bituminous and/or clay material.

This lithofacies occurs in Cyprus in rock units up to 2 m thick. It sometimes grades into a nodular facies (nodular laminated gypsum), but otherwise has sharp well defined boundaries with other lithofacies.

Continuous parallel lamination, and the absence of desiccation features, anhydrite relics or associated carbonate material all suggest gypsum deposition in a low energy continuously subaqueous environment. Fine, acicular crystal habit is characteristic of gypsum precipitated directly in the water column. Precipitation probably occurs in the uppermost water layers where evaporation takes place, and where oxygenation, due to atmospheric exchange and algal photosynthesis, is greatest. This is supported by Sloss (1969), who concluded on the basis of laboratory experiments that gypsum precipitation occurs above the interface between oxygenated surface waters and brine. Sonnenfeld (1969) also states that it is the lack of oxygen that restricts gypsum precipitation (in a hyper saline water body) largely to the photic zone. In deeper, density stratified, anoxic brines sulphate ions are prone to being stripped of their oxygen by anaerobic bacteria. This is also recognised by, for example, Schreiber & Decima (1978), who show primary precipitation of gypsum essentially restricted to the photic zone (fig. 6.4).

It is likely, therefore, that the parallel laminated gypsum is deposited by the settling of a fine gypsum precipitate from in uppermost layers of the water column.

6.3.3 Nodular laminated gypsum

This is similar to the parallel laminated gypsum but contains interlaminar nodules of coarsely crystalline white gypsum. Nodules are up to 10 cm thick and generally elongated in the plane of lamination. Gypsum laminae pass over and around these nodules, suggesting early diagenetic interlaminar growth. Concentrated development can result in severe disruption of the parallel laminae, but

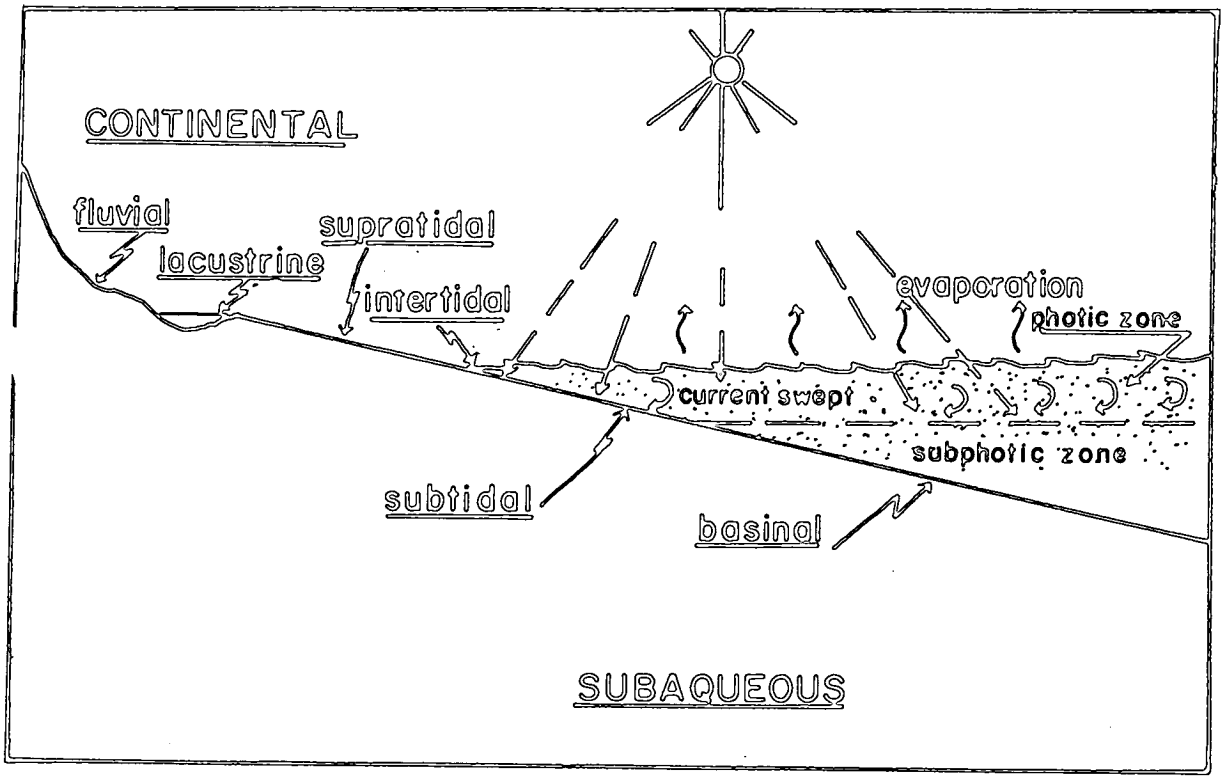

FIG. 6.4 Physical processes contributing to evaporite deposition, showing surface zone of direct precipitation (after Schreiber & Decima, 1978).

coalescing of nodules in a "chickenwire texture" is not observed.

Gypsum nodules are usually regarded as forming by rehydration of diagenetic anhydrite in a supra-tidal or otherwise exposed environment (Shearman, 1971; Schreiber et al., 1976). However, these deposits on Cyprus are monomineralic and do not show any evidence for emergence from a subaqueous environment.

The possibility of early diagenetic subaqueous growth of gypsum nodules has been suggested previously (Dean et al., 1975; Dean & Anderson, 1982). The lithological evidence from these deposits in Cyprus supports this possibility.

6.3.4 Graded gypsum

This lithofacies consists of normally graded beds of medium to coarse granular or acicular gypsum, or of larger selenite laths. In the Maroni sub-basin, continuous parallel normally graded beds up to 30 cm thick are found (Plate 16A). These contain coarse to fine acicular gypsum, sometimes with a coarse base of abraded selenite laths up to 2 cm long. Long axis orientation is invariably parallel to bedding and with a preferred orientation. Bases of beds are sharp.

Inclusion of non-gypsum lithoclasts or grains in these deposits is rare, and has only been observed at one outcrop. This is on the hillside to the west of Tokhni village at GR 292491. Here, carbonate clasts up to 5 mm long are included (Plate 5D). In thin section these are peloids, often oval or circular in section and with relict ooid-like concentric coatings and rare globigerinid foraminifera (Plate 5C).

In the Khalassa sub-basin, at Moutayiaka, and north of Pissouri (GR 716381) thicker and coarser graded beds are found (fig. 6.9). These contain large broken and abraded selenite clasts up to 30 cm long at the base and grade up to acicular gypsum needles of about 5 mm at the top. Bed thickness ranges up to 2 m. Clasts in the lower

halves of these beds are randomly orientated, but the finer grained material towards the tops show a preferred orientation with long axes aligned in the plane of bedding.

Abrasion of grains, grading, preferred orientation of acicular clasts, and continuous bedding all suggest deposition from suspension and current activity. Continuous grading suggests a single event for the deposition of each bed. This lithofacies is therefore interpreted as being deposited by turbidity currents.

Similar graded gypsum deposits, also interpreted as turbidites, have been described from the deep Mediterranean basins (Garrison *et al.*, 1978), Sicily (Schreiber *et al.*, 1976), the Italian Appenines (Vai & Ricci Lucchi, 1977) and the Zechstein of the North Sea area (Schlager & Boltz, 1977).

The lower coarse part of thick bedded units, in which clast orientation is random, may be due to rapid deposition and fluidisation in a equivalent way to the A division of the Bouma sequence.

6.3.5 Chaotic selenite

This lithofacies is characterised by poor sorting of clasts supported in a matrix of gypsum or carbonate.

The lowermost unit in the quarry at Maroni is a thick (over 2 m) unit of coarse abraded selenite laths up to 10 cm long. There is a rough normal grading in the upper half of this bed, where laths also tend towards parallelism with bedding. These aspects are similar to the thick coarse graded beds described above from the sections in the Khalassa sub-basin. However there are two differences. First, the unit at Maroni also contains occasional elliptical marl cobbles containing sponge spicules. Second, the selenitic body of the deposit supports a large boulder of banded selenite which is about 1 m across (Plate 16C).

At Tokhni and Kalavasos quarries, coarse selenite laths up to 15 cm long are supported in a micrite matrix.

The micrite is seen as microcrystalline under SEM examination, with no micro- or nannofossils found.

Both these lithofacies types are interpreted as deposited by debris-flows. This is based on the observed poor organisation, matrix support, and abraded and broken nature of some of the laths.

Deposits comparable with the carbonate supported selenite debris-flows have been described by Vai & Ricci Lucchi (1977), and interpreted similarly.

The large selenite laths and the block of banded selenite found in these units are derived from upslope shallower subaqueous environments.

6.3.6 Banded selenite

Banded selenite has been observed in two places, a badly weathered example on the gypsum surface south of Tokhni village (Plate 15B), and in the quarry at Moutayiaka. It consists of 5-30 cm high bands of vertically oriented and upward radiating twinned selenite blades. These bands are separated by thin (3 mm) layers of micrite, poorly exposed and washed out at outcrop.

Similar deposits have been described from Sicily by Hardie & Eugster (1971) and interpreted as primary subaqueous , mostly shallow water, gypsum deposits. This has been supported by study of salina analogues (Schreiber & Kinsman, 1975; Warren, 1982; West, pers. com. 1984), and by the interpretations of other evaporite workers (e.g. Vai & Ricci Lucchi, 1976). Pagnia (1978), concluded on the basis of field studies that similar lithologies in Spain were deposited at depths ranging down to 70 m.

Upward radiating growth of twinned selenite crystals from a horizontal nucleation surface is indicative of primary growth from saturated solution. A low to medium energy environment is required in order to allow crystal growth to continue without fragmentation. Direct precipitation requires oxygenated water (Sonnenfeld, 1979) and is generally regarded as being restricted to the photic zone (see section 6.3.2). It is likely, therefore,

that these deposits formed in shallow protected waters, or below wave base, but not significantly below the photic zone.

6.3.7 Contorted gypsum

At Tokhni gypsum quarry there is a 1.8 m intra-formational band of contorted gypsum (Plate 17D). This is composed of finely crystalline bands of opaque (white) and translucent (dark) gypsum. These bands are in the form of upright buckle folds. The unit is bound above and below by undeformed gypsum lithologies interpreted as subaqueous in origin. There are no indications of emergence such as desiccation cracks, and no textural evidence for alteration from anhydrite. Thirty three measurements of fold axis orientations were taken from this unit and found to cluster closely when plotted (fig.5.2). These fold geometries are therefore well organised, suggesting that the apparent deformation was by layer parallel shortening. These aspects can only be explained by slump initiation (sectipn 3.6.3).

Plate 17B shows a feature found in the exposure about 2 m below the contorted gypsum bed. Brittle disaggregation of a small slump fold in laminated gypsum has been preserved. Flakes of curled laminated gypsum are incorporated as clasts in the overlying graded gypsum bed. Continuation of the processes "frozen" in this exposure would produce gypsum slurries and turbidites downslope from this location, and it provides convincing evidence for slope instability during deposition of these gypsum lithologies. The vergence direction of this slump fold is consistent with the fold geometries in the contorted gypsum bed being produced on the same slope. These considerations support a slump origin for this lithofacies.

6.4 The onset of evaporitic conditions

6.4.1 The transition to gypsum deposition

Outcrop of the Kalavasos Formation is at its most extensive in the Maroni sub-basin (see fig. 2.5). Here it forms a continuous unit draping the Pakhna Formation. The contact can be examined at several points along the western margin of the sub-basin where it crops out in a line running approximately northeast near the villages of Kalavasos, Tokhni and Khirokitia. Figure 6.5 shows a series of schematic logs from along this line, and illustrates how the gypsum deposits overlie both hemi-pelagic and channel-fill sequences of the gullied slope association of the Pakhna Formation.

Near Ayia Mavri (ruin, GR 252443) gypsiferous laminated calcilutites pass up through a 50 cm band of soft structureless gypsiferous marls into selenite banded on a 1-7 cm scale (fig 6.6). At G.R. 292493, west of Tokhni, the gypsiferous marls of the laminated calcilutites contain small vugs (up to 5 mm long) which are pseudomorphous after gypsum. This passes up into a 5 cm band of well cemented micro-crystalline limestone, which is then overlain by laminated gypsum (fig. 6.6). At Anaphotia (GR 424555), the uppermost laminated Pakhna Formation marls contain abundant well preserved plant debris.

Similarly, in the Khalassa sub-basin, gypsiferous Pakhna Formation marls pass up through a laminated facies into apparently conformable gypsum deposits (north of Pissouri, G.R. 697385). Near Moutayiaka (GR 102425, see log Appendix 4) the uppermost laminated calcilutites contain small well preserved fossil fish.

Lamination and preservation of organic matter in the uppermost Pakhna marls is attributed to reduced benthic activity due to increasing salinities prior to the onset of gypsum deposition.

Thus in vertical sequence, marine bioturbated marls of the Pakhna Formation pass into laminated calcilutites, locally containing plant debris or fossil fish, and then

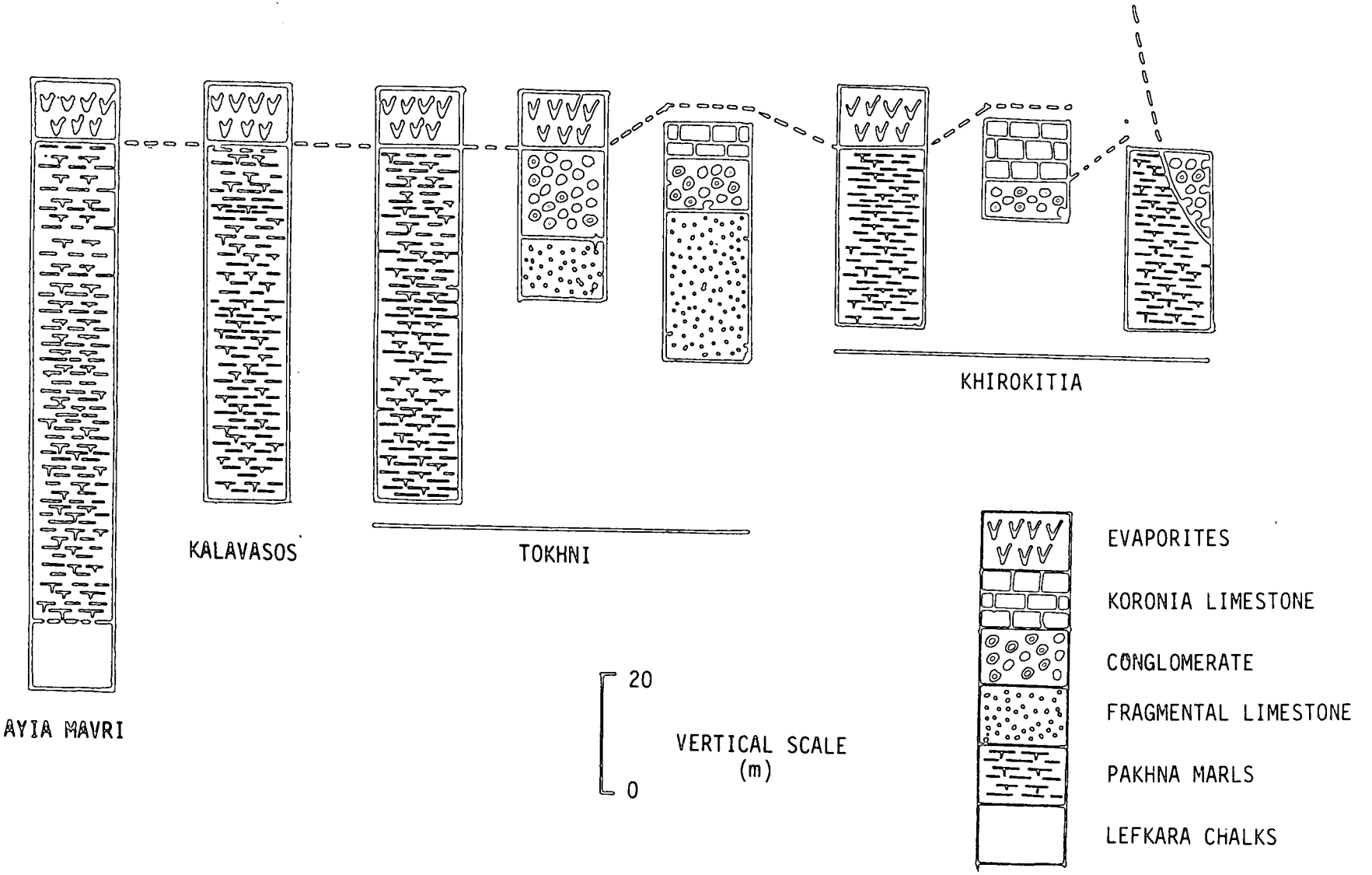

FIG. 6.3 Schematic logs from along the western margin of the Maroni sub-basin, showing relationship of evaporites to underlying units. See Fig. 2.1 for locations.

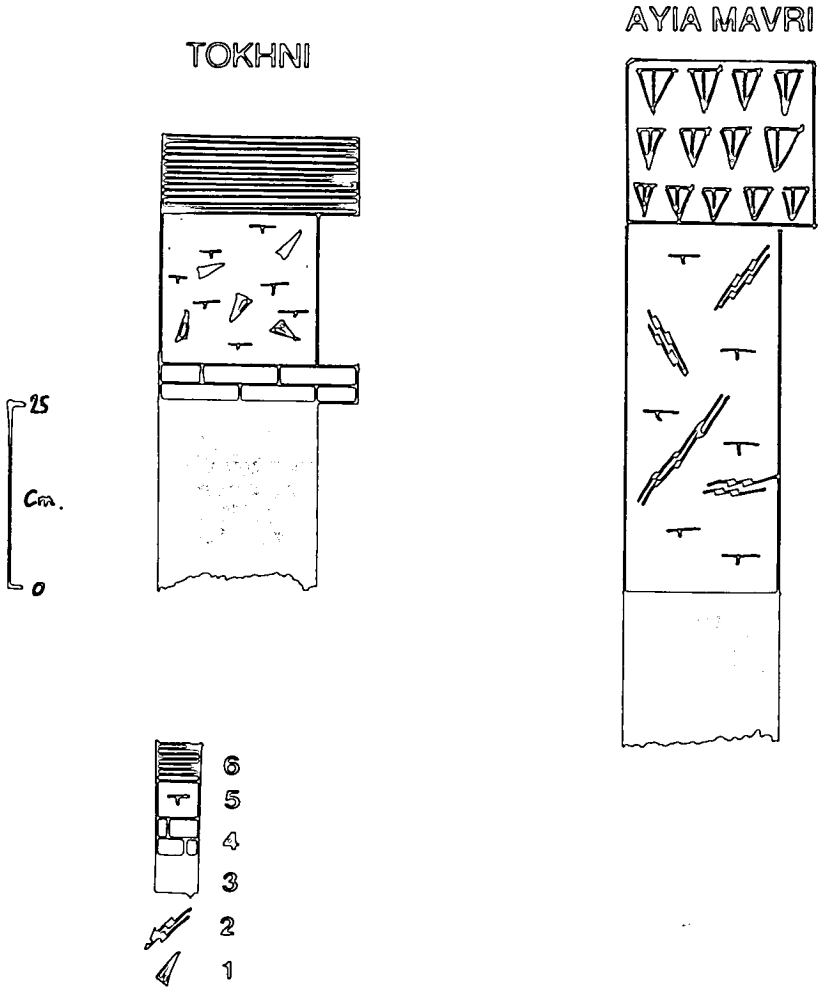

FIG. 6.6 Conformable Pakhna- Kalavasos Formation transition. 1 = selenite crystals, 2 = gypsum veins, 3 = laminated calcilutites (Pakhna Formation), 4 = crystalline limestone, 5 = gypsiferous marls, 6 = laminated gypsum.

into gypsum of a subaqueous origin. Features indicating emergence (rootlet horizons, scour features, fenestral porosity, curled mudflakes, desiccation cracks, anhydrite nodules, stromatolitic carbonate) are conspicuously absent. This suggests continuous sub-aqueous sedimentation across the Pakhna-Kalavasos Formation boundary.

Therefore, sedimentological considerations as well as field relationships (see section 2.4) indicate a conformable relationship between the Pakhna and Kalavasos Formations.

6.4.2 Significance of some limestone conglomerates

At several localities in the Maroni sub-basin a conglomeratic limestone deposit of the Koronia Limestone Member has been mapped as laterally equivalent to the Kalavasos Formation (Bagnall, 1960; Pantazis, 1967). Examples are found at Kophinou (GR 351532), Alaminos (GR 397514) and near Kalavasos (GR 277473). In each case, the Koronia Limestone Member crops out as a resistant cap above a steep scarp slope of softer Pakhna Formation marls. The Kalavasos Formation is exposed on the dip slope, and detailed mapping shows that in each case it is stratigraphically on top of the Koronia Limestone Member (fig. 6.7).

The limestone conglomerates are up to 3 m thick, and are notable in that they consist of platey clasts up to 30 cm long of laminated pelsparites (Plate 5B) in a matrix containing pelagic foraminifera, dispersed fragmented coralline algae, and peloids. At Kophinou, platey clasts show a preferred orientation (imbrication, see fig. 5.6) and have been encrusted by serpulids after deposition but prior to matrix in-filling and early cementation (see Plate 4B,D).

These deposits are at first glance similar to flat-pebble conglomerates commonly found in ancient strand-line deposits (Pettijohn, 1975, page 184), and on modern tidal carbonate flats (Shinn, 1983). However, serpulid encrustation, and the inclusion of globigerinids and

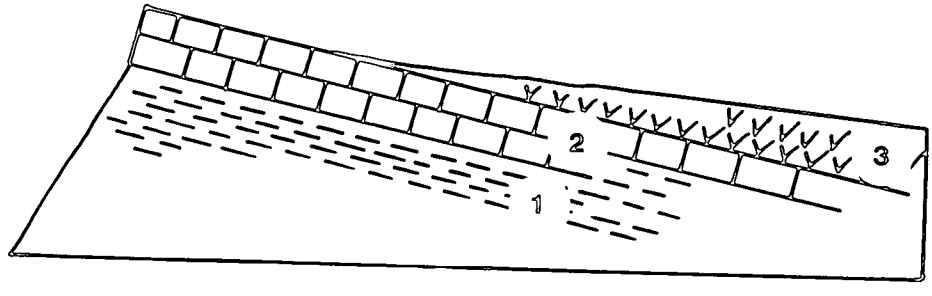

FIG. 6.7 Generalised field relationships at Koronia Limestone outcrops mentioned in the text. 1 = Pakhna Formation marlstones and laminated calcilutites, 2 = Koronia Limestone member, 3 = Kalavasos Formation evaporites stratigraphically above Koronia Limestone member.

peloids coated by early isopachous cement (Plates 4B, 4D) indicate conglomerate deposition occurred under normal marine sub-tidal conditions.

From the outcrop at Kalavasos (GR 277473) Rouchy & Monty (1981) reported traces of blue-green algae, indicative of fresh water, and inferred deposition in a fresh water marshy environment. It is difficult to reconcile this interpretation with an evolution from marine to sub-aqueous hyper-saline environments envisaged for the Pakhna and Kalavasos formations in this study. Limited new oxygen and carbonate isotope data from apparently in-situ laminated pelsparites collected at this locality favour a normal marine setting (Appendix 3).

Reworking of clasts, including fresh water limestones, into a marine environment might explain the observations. Indeed, Rouchy & Monty recognise that "intraformational conglomerates" are intimately bedded with the lithologies that they examined. Alternatively, the identification of fresh-water algal remains on the basis of poorly preserved morphological features in thin section may, perhaps, be erroneous.

It is possibly significant that these locally developed, and lithologically distinctive, platey clast limestones are only found immediately beneath clastic gypsum deposits. It may be that the preliminary lowering of sea-level prior to evaporite deposition resulted in the emergence, early lithification and downslope reworking of peloidal carbonates from the basin margin.

6.5 Vertical sequences and associations.

6.5.1 Maroni sub-basin

Figure 6.8 shows graphic logs of sections through the Kalavasos Formation from quarries at Tokhni, Kalavasos, and Maroni. These sequences are all dominated by mass-flow gypsum deposits (turbidites, slumps and debris-flows). A tentative lithological correlation is indicated.

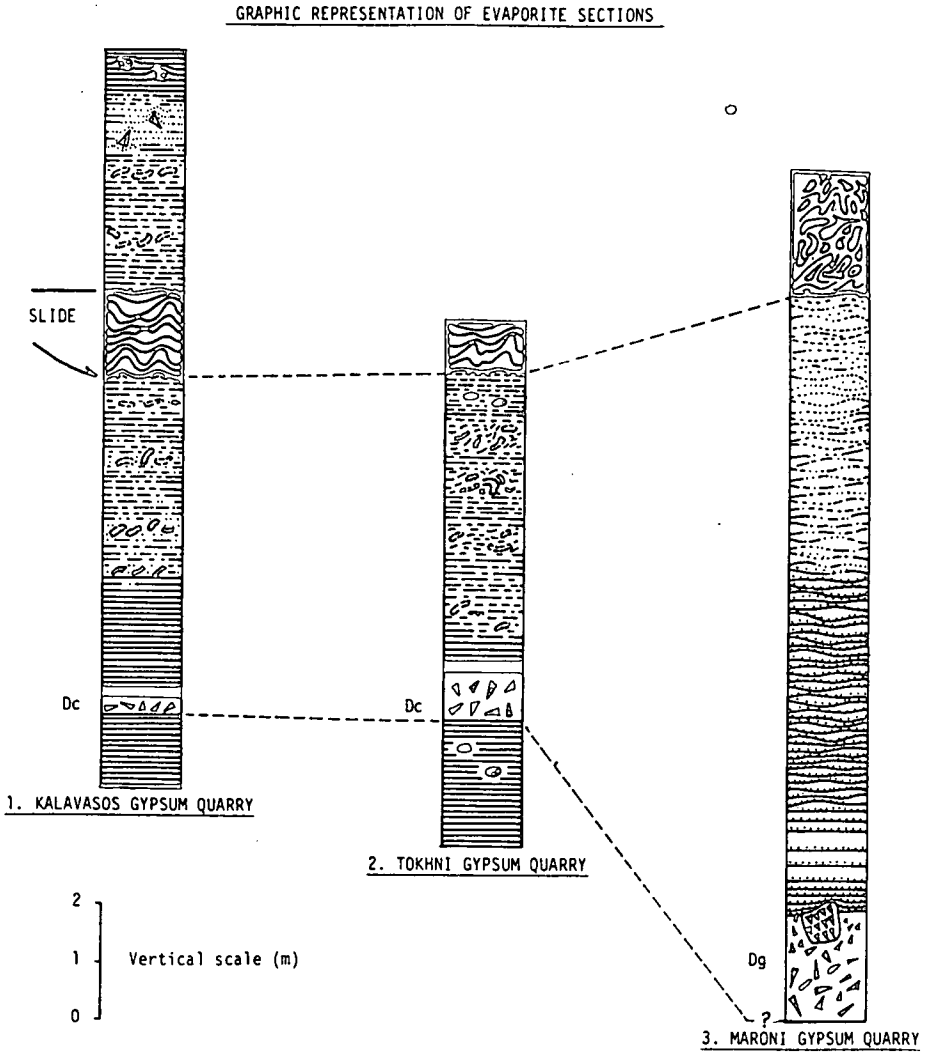
GRAPHIC REPRESENTATION OF EVAPORITE SECTIONS
SLIDE
Dc
Dc
Dg
?
1. KALAVASOS GYPSUM QUARRY
2. TOKHNI GYPSUM QUARRY
3. MARONI GYPSUM QUARRY
2
1
0
Vertical scale (m)

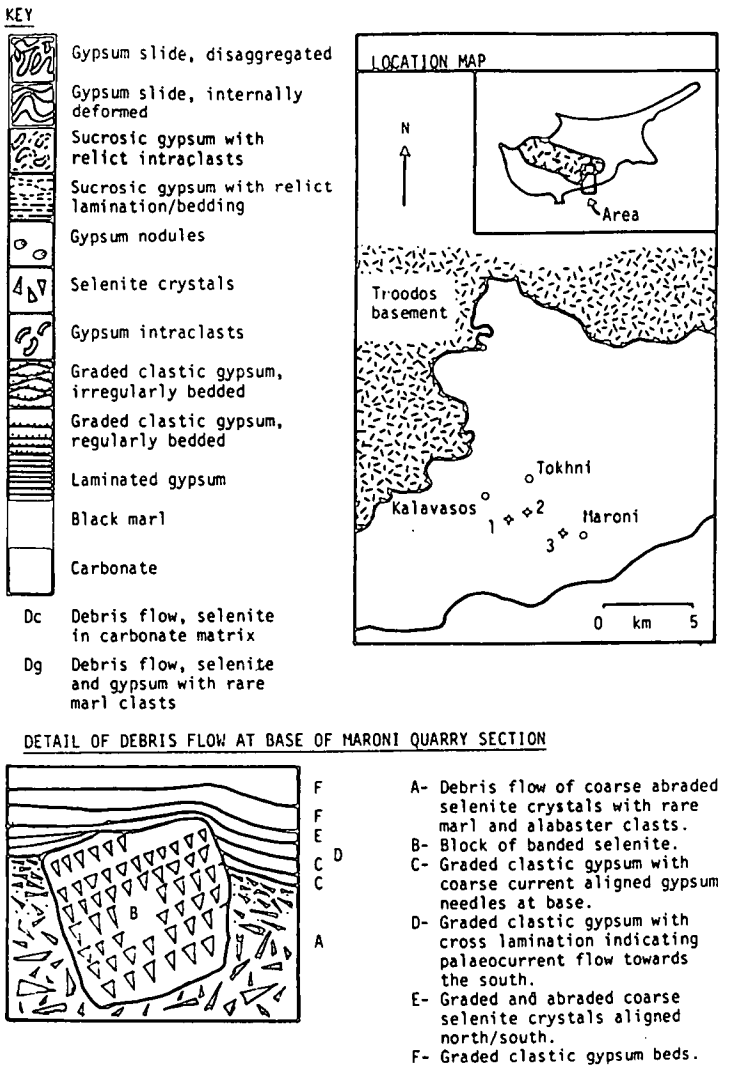
KEY
Gypsum slide, disaggregated
Gypsum slide, internally deformed
Sucrosic gypsum with relict intraclasts
Sucrosic gypsum with relict lamination/bedding
Gypsum nodules
Selenite crystals
Gypsum intraclasts
Graded clastic gypsum, irregularly bedded
Graded clastic gypsum, regularly bedded
Laminated gypsum
Black marl
Carbonate
Dc Debris flow, selenite in carbonate matrix
Dg Debris flow, selenite and gypsum with rare marl clasts
LOCATION MAP
N
Area
Troodos basement
Tokhni
Kalavasos
Maroni
1
2
3
0 km 5
DETAIL OF DEBRIS FLOW AT BASE OF MARONI QUARRY SECTION
F
F
E
C D
C
A
B
A- Debris flow of coarse abraded selenite crystals with rare marl and alabaster clasts.
B- Block of banded selenite.
C- Graded clastic gypsum with coarse current aligned gypsum needles at base.
D- Graded clastic gypsum with cross lamination indicating palaeocurrent flow towards the south.
E- Graded and abraded coarse selenite crystals aligned north/south.
F- Graded clastic gypsum beds.

FIG. 6.8

At Kalavasos quarry, the lower part of the section is predominantly parallel laminated gypsum, with a thin unit of coarse selenite laths supported in a micrite matrix. Above this, weathering has resulted in partial recrystallisation so that the finer detail is destroyed, but relict intraclasts are visible and testify to the reworking of gypsum. Within these bedded intraclast-bearing lithologies is a 1.2 m contorted band. A similar lithology was examined in more detail at Tokhni quarry, with which this unit is tentatively correlated, and interpreted as a slumped unit (section 6.3.7).

At Tokhni quarry a similar sequence is found. Gypsum nodules occur within the laminated unit at the base. The micrite-selenite debris-flow is here thicker. Above this are intraclast-bearing graded gypsum lithologies with small scale slumping of associated laminated gypsum. Brittle disaggregation and the "spooling off" of intraclasts is observed (Plate 17B).

A much thicker sequence is found closer to the inferred basin centre at Maroni quarry. The lowermost unit is a thick selenite debris flow, almost wholly composed of broken selenite laths and minor granular gypsum (section 6.3.5, Plate 16C). It is overlain by graded gypsum beds (Plate 16A). At the top is a unit of "marbled" black and white gypsum which is lithologically similar but internally more disorganised than the contorted gypsum (slumped) of Tokhni quarry.

These three sections convincingly demonstrate that gravity driven processes on a periodically unstable slope resulted in reworking of clastic gypsum into deeper water. Fold geometries in the contorted gypsum unit at Tokhni quarry indicate a palaeoslope towards the south east, ie away from the uplifted Limassol Forest Block. This is consistent with the occurrence of thicker turbidite dominated sequences in that direction (Maroni quarry). Furthermore, in-situ banded selenite (Plate 15B) and clastic gypsum beds with carbonate peloids and relict ooids (marginal lagoonal origin?, Plates 5C and 15D) are

observed near the western limit of outcrop, near Tokhni. This suggests evaporite deposition in a body of hypersaline water that shallowed, from a relatively deep area near Maroni, towards a shoreline in the north west on the margin of the uplifted Limassol Forest Block.

6.3.2 The Khalassa sub-basin

The gypsum sequences at Moutayiaka gypsum quarry (GR 097413) and near Pissouri (GR 716381) are illustrated in figure 6.9. They are dominated by clastic graded beds of selenite and gypsum needles. The exposure at Moutayiaka also contains a bed of banded selenite. The more massive, thicker bedding of these sequences, and the quantities of large selenite laths in coarsely graded units suggest deposition in proximity to a supply of banded large primary selenite crystals. Selenite banks have been described from Sicily (Hardie and Eugster, 1971) where they are interpreted as primary features, precipitated sub-aqueously in relatively shallow environments (see section 6.3.6). Possible analogues are also found elsewhere on Cyprus (in the Polis Graben, Plate 15A).

The direction in which clastic gypsum is reworked is dependant upon the processes involved. Two main possibilities exist (fig.6.10):

(1) Shoreward reworking by wave and storm action, from off-shore shallow selenite banks, as proposed by Hardie & Eugster (1971) for the Solifera Series in Sicily.

(2) Basinward reworking, by slope controlled processes, of marginal or exposed autochthonous selenite, as proposed by Vai & Ricci Lucchi (1977) for the Venna del Gesso basin in the Italian Appenines.

In the Maroni sub-basin gravity driven slope processes are clearly dominant, and basinward "cannibalistic" reworking is involved (see section 6.3.1).

In the Khalassa sub-basin the distinction on the basis of two widely separated exposures is not so clear, and more data are required. However, two points can be made;

MOUTAYIAKA GYPSUM QUARRY PISSOURI

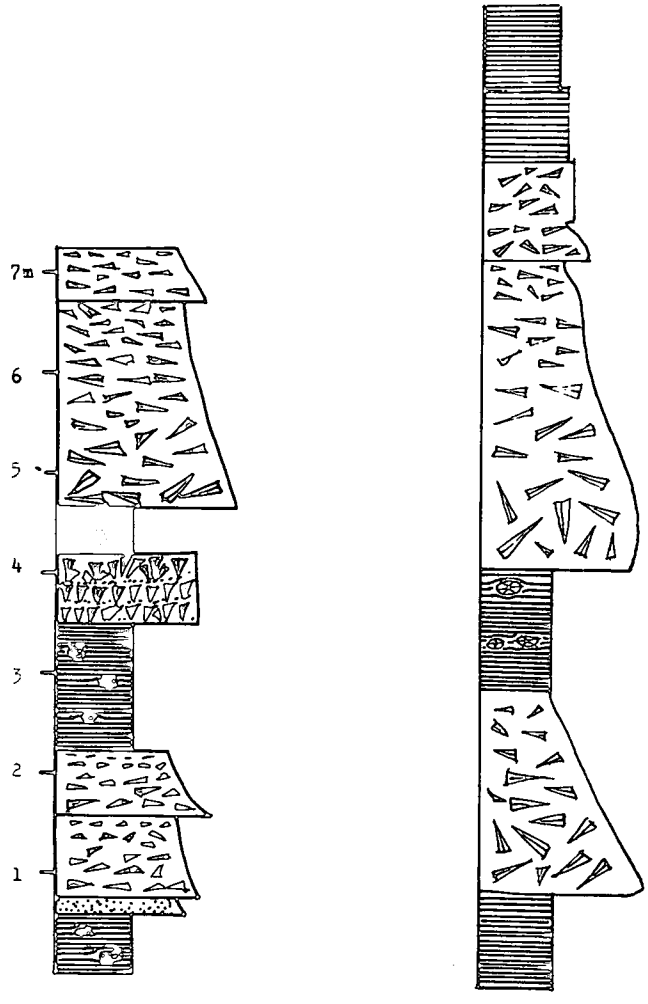

FIG. 6.9 Logged evaporite sections from the Khalassa sub-basin, draw to same scale. See Fig 6.8 for key.

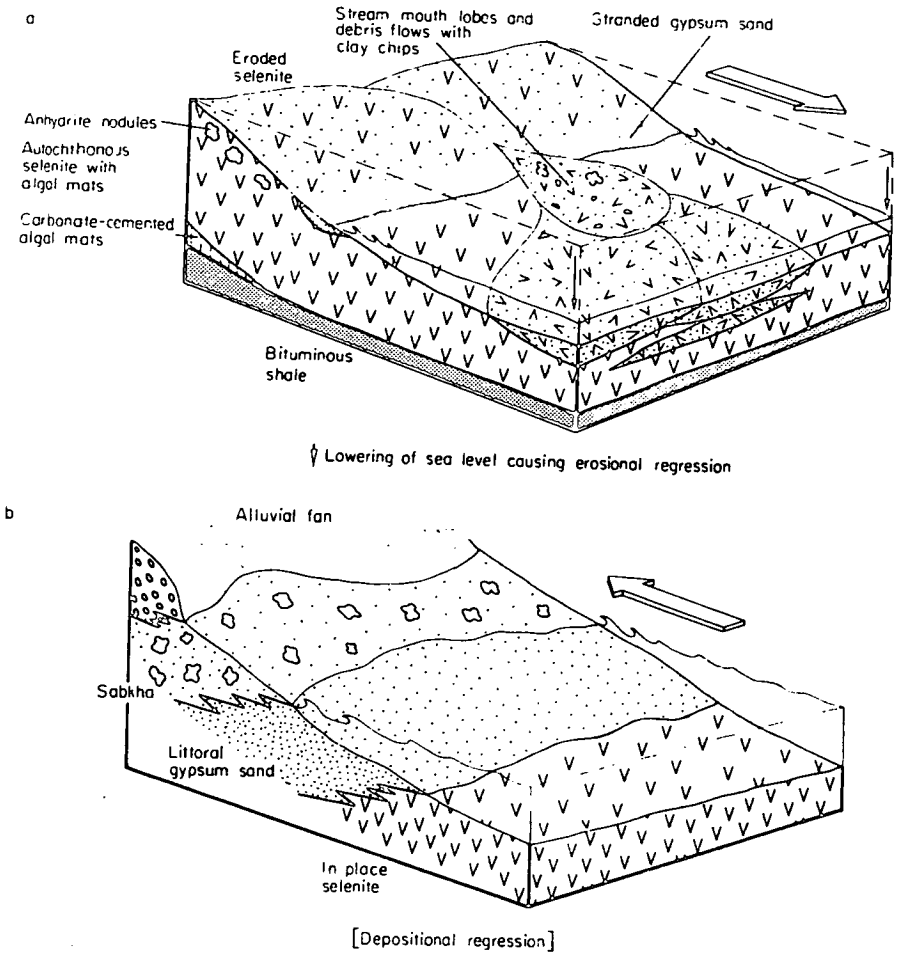

FIG. 6.10 Conceptual models for deposition of clastic gypsum, from Vai & Ricci-Lucchi (1977) above, and Hardie & Eugster (1971) below. Large arrows show dominant transport direction.

(1) Both localities appear to represent a more "marginal" position in a sub-aqueous evaporite basin (indicated by in-situ selenite growth and local clastic reworking) than the three sections described from the Maroni sub-basin.

(2) Borehole data from the Akrotiri Peninsula (Hadjistavrinou & Constantinou, 1977) indicates thickening of evaporites in the sub-surface to the south.

This suggests that the evaporite depocentre lay to the south of the exposures and was probably located beneath the middle of the Akrotiri Peninsular (as for the Pakhna Formation, see section 5.8.4).

6.5.3 Other evaporites of the circum-Troodos belt

The Kalavasos Formation also crops out on the north margin of the Troodos ophiolite (Gass, 1960; Wilson, 1959). Exposure is more patchy, and they have not been described in detail.

In the Polis Graben (see fig. 1.2) large areas of gypsum are exposed (Kluyver, 1969; Orszag-Sperber et al., 1980). Reconnaisance work (this study) found similar well developed subaqueous lithologies as in the Maroni and Khalassa sub-basins. For example, spectacular autochthonous selenite (Plate 15A), gypsum turbidites with flame structures (Plate 16B), gypsum conglomerates (Plate 16D), and minor slumping of laminated gypsum (Plate 17C). Gypsum deposition in the Polis Graben, therefore, appears to contain similar elements to those of the Khalassa and Maroni sub-basins. All in all, Cyprus contains some truly excellent clastic gypsum lithologies that would reward further study.

6.6 Depositional model

The subaqueous nature of the gypsum lithologies of the Kalavasos Formation requires deposition within a body of hyper-saline water. Parallel laminated gypsum indicates a low energy environment. Association with slumps, turbidites and debris flows, and lack of carbonate

material, suggests deposition in a relatively "deep" environment (below wave base), rather than in a protected shallow lagoon. Furthermore, the water body must have been deep enough to create the necessary relief on subaqueous slopes for gravity driven processes to transport clastic gypsum across a belt several kilometres wide (the region between Tokhni and Maroni). This is also suggested by the fact that gypsum deposition was continuous with gullied slope (and basin margin?) sedimentation of the Pakhna Formation (section 6.4.1), implying the pre-existence of significant depositional relief (i.e. an inherited bathymetry). Thus relatively deep conditions, tens of metres and probably more, certainly existed, and persisted during gypsum deposition.

To produce 30 m of gypsum by evaporation to dryness of normal sea water requires an initial water column in excess of 40000 m, and would also produce 530 m of associated halite (see Blatt, Middleton & Murray, 1980, page 539).

For these reasons a barred basin model model similar to that described by Schmalz (1969) is required (fig. 6.11). This model involves continuous refluxing of normal (or near normal) marine water across a shallow barrier in a basin where evaporation exceeds total fresh water input. Brine salinities are controlled by the balance between reflux and evaporation rates. Atmospheric humidity can also influence the equilibrium salinity developed in such a basin (Kinsman, 1976). During deposition of the Kalavasos Formation, these factors must have been such as to limit brine salinities within the range required for gypsum precipitation.

Consideration of these factors leads to the depositional model shown in figure 6.12. Near surface precipitation of gypsum, due to evaporation, supplies a continuous "fall-out" of fine acicular gypsum needles which accumulate as parallel laminated deposits in the "deep" parts of the basin. On the shallower basin margins, where salinities may be higher, banks of selenitic gypsum

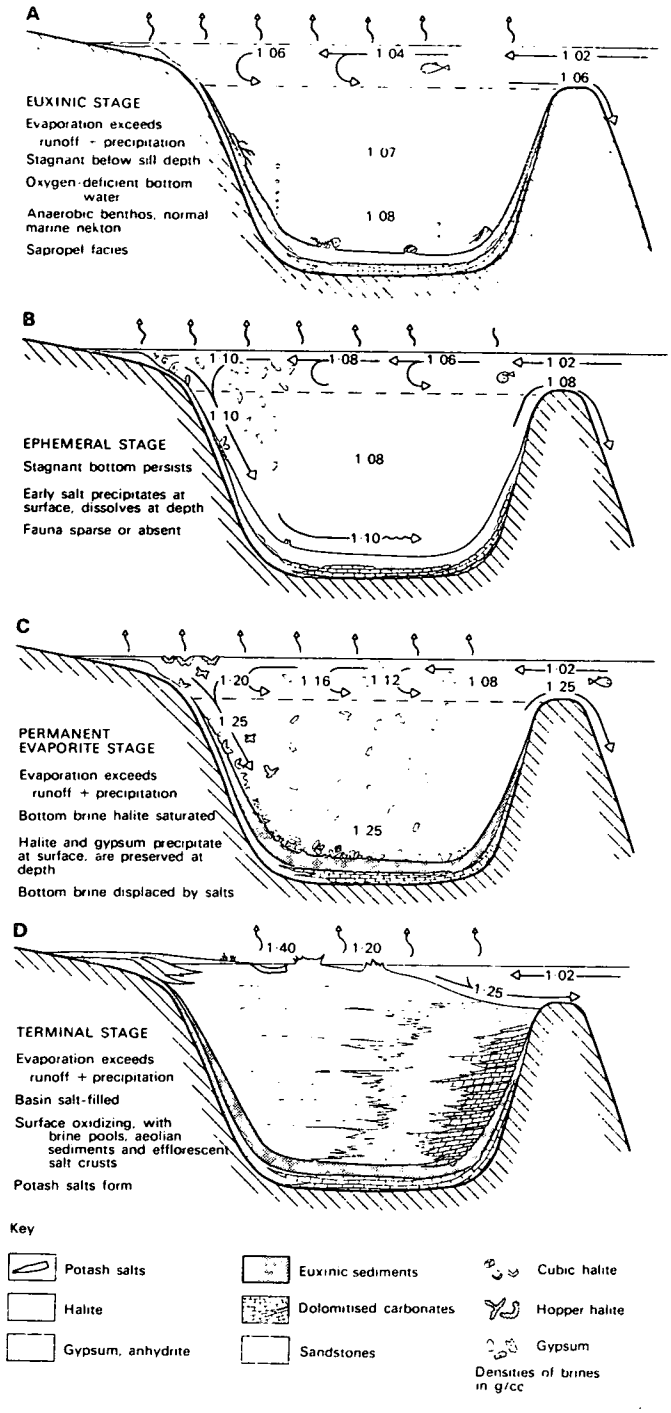

FIG. 6.11 A model for deep water evaporite deposits in a refluxing barred basin, showing four stages of basin infill. From Schmalz, (1969).

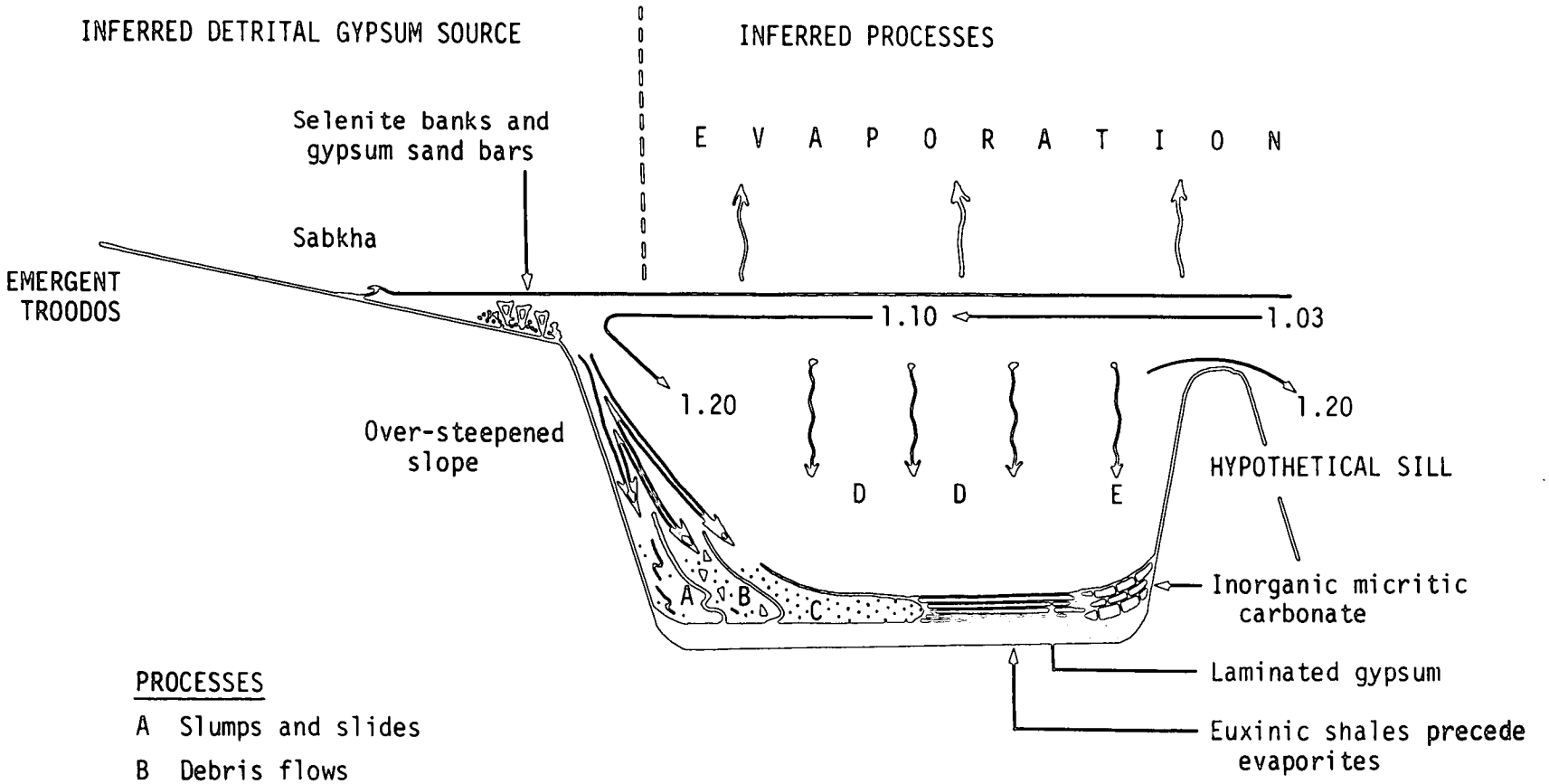

PROCESSES

A Slumps and slides

B Debris flows

C Turbidity currents

D Gypsum precipitation from the water column

E Inorganic precipitation of carbonate

Basin held in gypsum facies by atmospheric humidity (Kinsman 1976) and by extent of refluxing

Brine densities given in g/cc

FIG. 6.12 Diagram showing inferred depositional setting of evaporites in Maroni sub-basin.

develop by rapid vertical crystal growth from the substrate. These may be broken by wave action, supplying gypsum sand into protected hypersaline lagoonal environments (fig.6.10). However, the dominant sediment redistribution process is gravitational, with slumps, debris-flows and turbidites transporting gypsum from shallow areas into deeper parts of the basin. Slope instability is promoted by high sedimentation rates (see later), and increased sediment bouyancy due to the higher density of hypersaline water.

The existence of a sill limiting circulation between the Maroni and Khalassa sub-basins and the open proto-Mediterranean is implied, but has not been located. There is strong evidence from the Pakhna Formation for Late Miocene compressional tectonics (the uplift of the Limassol Forest block) and development of linear structural highs (e.g. the Akrotiri High, section 5.7). Cleintuar et al. (1977) also identified a series of Neogene structural highs in Cyprus. More specifically, linear structures active during the Late Miocene have been reported from northern Cyprus (Robertson & Woodcock, 1986) and from the off-shore areas immediately north and south of Cyprus (Mulder, 1973; Mulder et al., 1975). The development of a Late Miocene sill, as proposed to account for the gypsum deposits, is therefore perfectly consistent with the tectonic history of the area.

Few modern analogues for barred evaporitic basins exist. The most often quoted is the Gulf of Karaboghaz, which lies on the eastern side of the Caspian Sea (Twenhofel, 1950). More recently, evaporite sedimentation in a restricted estuary in Peru has been described (Brantley et al., 1984). However, water depths in both examples are very shallow, a matter of metres at the most. Selenite growth and gravity reworking, characteristic of the Kalavasos Formation in Cyprus, do not occur.

The best comparison from an ancient setting is found in the Romagna and Marche regions of the Italian Appenines. Here, Messinian evaporites are found which

contain similar lithologies to those in Cyprus. They are interpreted as deposited by gravity processes into deep brines in the foredeep of the rising Appenines (Ricci Lucchi, 1973), and are thus comparable in terms of lithologies, processes, and setting with the Kalavasos Formation in southern Cyprus (fig. 6.13).

6.7 Other aspects

6.7.1 Sedimentation rates

It is generally acknowledged that precipitation of thick sequences of dissolved salts from evaporating sea water can occur at rates which are effectively instantaneous on the geological timescale.

On Cyprus, poor biostratigraphic control and the relatively short period of time involved mean that sedimentation rates can only be approximated at. This is best done by "modelling" evaporite sedimentation rates on the basis of reasonable assumptions about evaporation rates.

According to Holser (1979) a nominal rate of evaporation of sea water in the present sub-tropics is 2 m/year, which corresponds to the deposition of 1.2 mm of anhydite per year, i.e. 120 cm / 1000 years. Correcting for a 38% volume reduction (Blatt, Middleton & Murray, 1980, pg.546) involved in the transformation from primary gypsum to secondary anhydrite gives:

$$120 \times 100/(100-38) = 194 \text{ cm} / 1000 \text{ yrs}$$

This compares with 1 cm / year and 18 cm / year calculated for the gullied slope and the basin margin associations of the Pakhna Formation. Admittedly evaporation rates from gypsum precipitating brines will be lower due to the reduction of vapour pressure with increasing salinity. However, cannibalistic reworking of gypsum from the margins will increase sedimentation rates significantly towards the depocentre, and though unquantified, might counter the effects of a reduced evaporation rate.

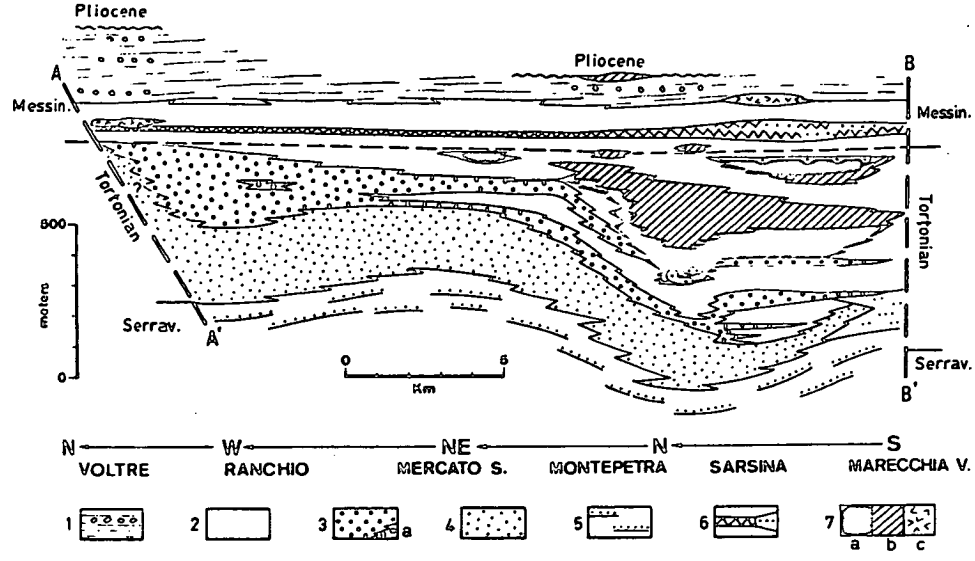

.. Miocene facies distribution between two major transversal tectonic lines of Romagna Apennines (A–A' = Forli line, B–B' = Marecchia line). The area of maximum subsidence adjacent to the Marecchia line is the Perticara Basin (minor evaporite basin).
1. prodelta clays, delta front sandstones and conglomerates; 2. slope mudstones and clays; 3. middle and inner fan, sandy turbidites (a = conglomerates); 4. outer fan, sandy/clayey turbidites; 5. basin plain, clayey/sandy turbidites; 6. "normal" evaporites and gypsarenites (dots); 7. chaotic levels (a = intraformational, b = allochthonous, c = slumped evaporites).

FIG. 6.13 Facies distribition in the Romagna-Marche basins, Italy. Note location of allochthonous evaporites in the foredeep area. From Ricci-Lucchi (1973).

The important conclusion is that it is quite feasible for gypsum sedimentation rates to be one or two orders of magnitude greater than for the underlying sediments of the Pakhna Formation.

6.7.2 The virtual absence of non-evaporitic input

Considering that sedimentation in the Pakhna Formation is characterised by clastic carbonate input from a productive neritic belt marginal to the uplifted Limassol Forest block (chapter 5), the evaporites of the Kalavasos Formation are surprisingly free of such sediments. Small amounts of entrained carbonate material were observed in a graded gypsum bed at one locality (6.3.4), and rare marl clasts were found in a gypsum debris flow at Maroni quarry (6.3.5). Four factors are thought to account for this. These are (1) reduced carbonate production, (2) high evaporite sedimentation rates, (3) early lithification of marginal exposed carbonates, and (4) peneplanation of emergent areas.

(1) Increasing salinities during evaporite deposition would have severely stressed carbonate producing biota in the basin. Intra-basinal supply of organicly derived carbonate would have been substantially reduced.

(2) As discussed previously (6.7.1), gypsum sedimentation rates were probably very high. With a reduced supply of intra-basinal carbonate (see above) gypsum sedimentaion rates could have exceeded carbonate input by two orders of magnitude or more.

(3) A sea level drop prior to initiation of evaporitic conditions would expose marginal marine carbonates (the "source areas" for clastic material in the Pakhna Formation, see section 5.9). These would then be vulnerable to early lithification, inhibiting erosion and reworking into the evaporite basin (Kendall & Schlager, 1981). The limestone conglomerates described in section 6.4.2 could represent a small volume of material derived from an exposed lithified carbonate belt immediately preceeding gypsum deposition. This belt could also serve

as a barrier to basinward transport of clastics derived from further inland.

Early lithification of Late Miocene carbonate sediments, exposed during evaporitic drawdown, is also recorded by Cita (1983, page 119) from the Malta escarpment. Hemi-pelagic sediments were protected from subaerial erosion by precipitation of protective crusts which "fossilized the pre-existing relief".

(4) The deposition of clean bioclastic limestones (Koronia Limestone member) over the eroded structures of the Yerasa fold and thrust belt (see section 7.2) suggests that the uplifted Limassol Forest block was largely peneplained, and not supplying large quantities of clastic material, before the onset of evaporite deposition

6.7.3 A final note on water depths

Depth of deposition is notoriously difficult to estimate from subaqueous evaporite lithologies. In this study two primary considerations have been used; (1) lithological indications for the energy conditions under which deposition took place, and (2) the assumption that gypsum precipitation only takes place under oxygenated conditions, and that in a density stratified brine body this is limited to the photic zone. Thus laminated gypsum associated with gravity flows is interpreted as deposited below wave base, and primary selenite is interpreted as grown on a substrate within the photic zone.

According to Friedman (1972) and Sonnenfeld (1984), gypsum which settles or is transported into anoxic brines beneath the photic zone will not be preserved due to the action of sulphate reducing bacteria. However, three factors may invalidate this assumption:

(1) Rate of supply of precipitated sulphate may exceed the rate of bacterial reduction (see Kendall, 1979, page 171).

(2) Rapid event deposition of gypsum by gravity controlled slope processes can "entomb" gypsum on an anoxic basin floor (Schreiber et al., 1976).

(3) Due to evaporation and concentration at the surface, there will be a continuous sinking of brines down through the water column, which could supply dissolved oxygen below the photic zone. Schreiber & Decima (1978) have reported selenite beds with no associated carbonate and interpreted as a primary precipitate from below the photic zone.

These three factors could remove a lower limit for the depositional depth of subaqueous gypsum.

In this study the absence of shallow water indicators, the assumption of an inherited bathymetry, and the association of laminated gypsum with slumps, turbidites and debris-flows have also been used to argue for a depositional setting below wave base.

Gravity-emplaced deposits, as seen in the Maroni sub-basin, clearly testify to slope-controlled processes. Maroni gypsum quarry is about 3000 m from Tokhni gypsum quarry in a down-palaeoslope direction (defined by slump data, section 6.3.7). Assuming a palaeoslope of only 1 degree between these locations, the brine depth during gypsum deposition must have been over 50 m greater at Maroni quarry than at Tokhni or Kalavasos quarries. 50 m must therefore be taken as a conservative minimum estimate for the brine depth at Maroni during evaporite deposition. There is no reason why the basin in which the Kalavasos Formation was deposited should not have been significantly deeper than this.

CHAPTER SEVEN
THE YERASA FOLD AND THRUST BELT

7.1 Introduction

Sedimentation in the Pakhna Formation in the study area is evidently influenced by the uplift of the Limassol Forest block. This is reflected in the compositional evolution of the sediments (section 5.2) and in the distribution of facies associations (section 5.6). Associated tectonic processes also led to the partitioning of sub-basins into which the clastic material was shed (section 5.8).

Deformation associated with this episode is limited in the sediments to a narrow linear belt about 2 km wide adjacent to the outcropping basement lithologies of the overthrust Limassol Forest block (fig. 1.3). This is known as the Yerasa fold and thrust belt. It extends from Ayios Mamas in the NW some 30 km towards Phinikaria and Ayios Tykhonas in the study area. Southeast of here, the structures plunge out towards Cape Dolos, where continuation is expressed as a broad anticlinal feature in the Moni and Lefkara Formations. These structures define the northern margin of the Khalassa sub-basin (section 5.8.2).

Previous work on this lineament has been associated mainly with studies on the ultramafic rocks (Searle & Panayiotou, 1980; Murton, 1986), and confirm that the thrusting originates in the basement. Published descriptions of deformation in the sedimentary cover are only of a general nature, referring to steep south facing or vertical folds in the Lefkara Formation (Morel, 1960; Robertson, 1977a).

In order to better understand the nature of the tectonics and its influence on sedimentation an area between the villages of Phinikaria and Ayios Tykhonas was mapped (figs. 7.1, 7.2). Faulting in the basement was also examined. Results have been combined with other observations made in the sedimentary cover to suggest that

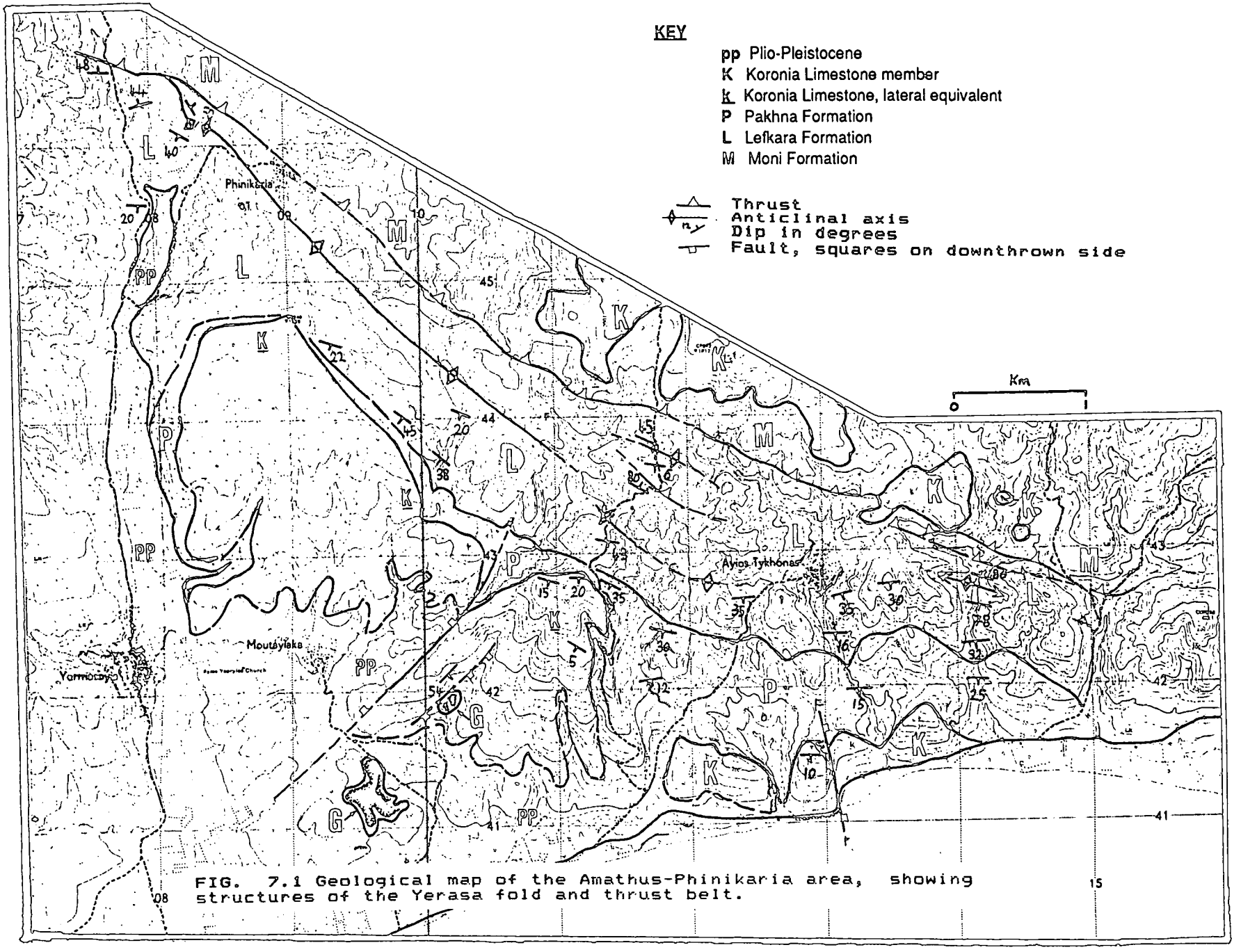

FIG. 7.1 Geological map of the Amathus-Phinikaria area, showing structures of the Yerasa fold and thrust belt.

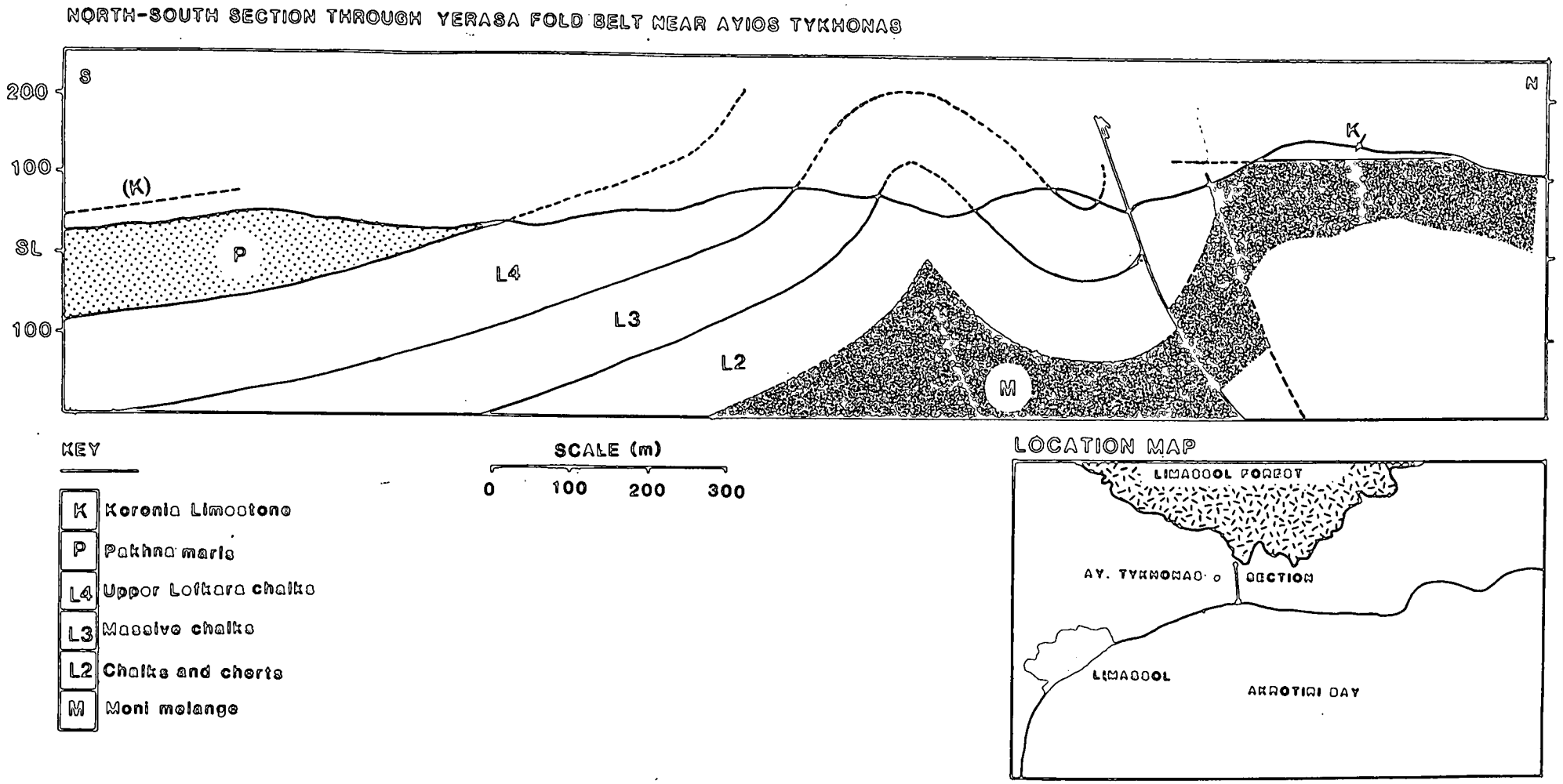
NORTH-SOUTH SECTION THROUGH YERASA FOLD BELT NEAR AYIOS TYKHONAS
S
N
200
100
SL
100
(K)
P
L4
L3
L2
M
K
KEY
K Koronia Limestone
P Pakhna marls
L4 Upper Lefkara chalks
L3 Massive chalks
L2 Chalks and cherts
M Moni melange
SCALE (m)
0 100 200 300
LOCATION MAP
LIMASSOL PORPOT
AY. TYKHONAS
SECTION
LIMASSOL
AKROTIRI BAY

FIG 7.2

the Yerassa fold and thrust belt originated by reactivation of basement faults in Tortonian or Messinian times.

7.2 Deformation style

7.2.1 The Moni Formation

This is an olistostrome unit, comprising Mesozoic olistoliths in an Upper Cretaceous matrix of in-situ bentonitic clays and deep water radiolarian siltstones (Robertson, 1977c). Matrix sediments are autochthonous with respect to the ophiolitic basement, and it is conformably succeeded by the Lefkara Formation, where preserved. Robertson's study was concerned with primary depositional aspects of this formation, and examination was deliberately limited to the relatively undeformed eastern parts of its outcrop area.

To the west of Parekklisha village this formation thins progressively from 200 m to 75-100 m at Phinikaria (Robertson, 1977c), and vanishes completely towards Apsiou. This is due to depositional thinning of the Moni Formation against the Troodos ophiolite (Limassol Forest block).

In a road cutting at Akrounda (GR 076470) a strong steep northerly dipping foliation in Moni Formation clays was seen (dip 60 degrees towards 000), of presumed tectonic origin. Otherwise, exposure is poor, and no other structurally significant observations were made.

This clay-rich formation is likely to have behaved in a plastic manner under deformation, and may have served to decouple the underlying basement from the overlying chalks of the Lefkara Formation. In this respect, it is probably significant that the intensity of folding and faulting in the sedimentary cover diminishes eastwards, beyond Moni village, as the Moni Formation thickens.

7.2.2 The Lefkara Formation

Deformation structures are most intense in the Lefkara Formation. The contact with the Moni Formation is

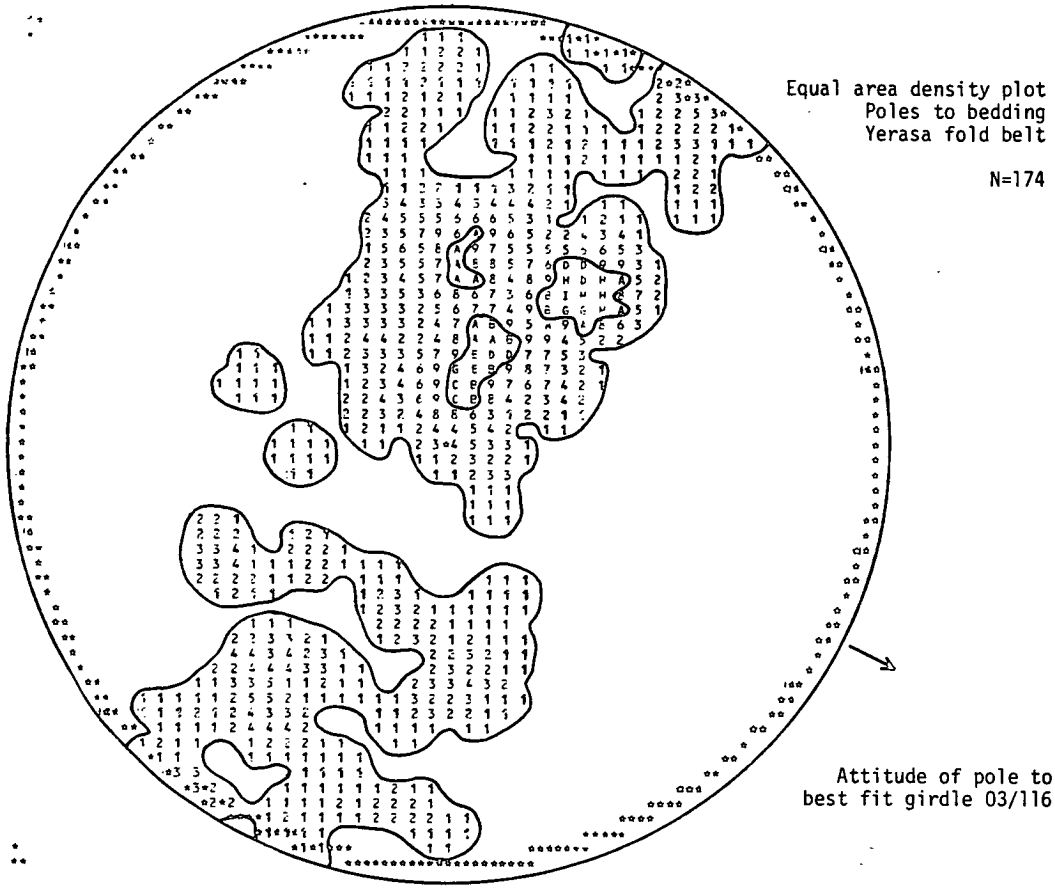

FIG 7.3 Equal area density plot of poles to bedding from area of Figure 7.1 (data from Pakhna and Lefkara Formation exposures). Alpha-numeric symbols give contoured density value, ranging from 1 (1) to 35 (Z) per 100/174% unit area.

sharp and steeply northward dipping, interpreted as a structural contact (eg. at GR Ø76466). Folding is tight, with steep northward dipping axial planes, and some overturned southern limbs (fig. 7.2). Axial planar cleavage is strongly developed, and steep northward dipping faults have been observed (eg. on the road section to Armenokhori village).

Towards the south, deformation intensity decreases rapidly, so that within a kilometre or so the chalks of the Lefkara Formation have gentle southerly dips and pass conformably upwards into the Pakhna Formation (eg. near Amathus).

7.2.3 The Pakhna Formation

With the exception of the Koronia Limestone member, the deposits of the Pakhna Formation are not preserved over the axis of the Yerasa fold and thrust belt.

The Koronia Limestone member crops out at numerous localities in the Yerasa fold and thrust belt, but in all cases it is undeformed. It rests unconformably upon the Moni Formation and (near Parekklisha) the pillow lavas of the Limassol Forest block.

7.2.4 Basememt lithologies

Thrust faults within the igneous lithologies of the Limassol Forest block have been reported by previous workers (Morel, 196Ø; Robertson, 1977a; Searle & Panayiotou, 198Ø; Murton, 1986). These thrusts are parallel to structures in the sedimentary cover, and dip north-north-east at angles which are generally steep (45 degrees or more), but occasionally as low as 3Ø degrees (Robertson, 1977c). These thrusts involve all levels of the igneous complex. Thrusting of pillow lavas over Lefkara Formation chalks at Akrounda is reported by Robertson (1977c). East of Apsiou (GR Ø245Ø7), microgabbros are thrust over lava breccias (plate 14A), and a sequence of pillow lavas, umbers and radiolarian cherts of the Perepedhi Formation is overturned (Plate

14B).

7.2.5 Orientation of structures

One hundred and seventy four dip readings from the Lefkara and Pakhna Formations, recorded during mapping in the Phinikaria-Ayios Tykhonas area, have been plotted (fig. 7.3). There is a strong clustering towards shallow southward dips, reflecting the areally extensive nature of the southern shallow limb. However, poles to bedding clearly define a girdle with a pole plunging 3 degrees towards 116 degrees (calculated by the Watson (1960) method on the STATIS programme).

7.3 A locally developed Miocene unconformity

The Koronia Limestone member at Amathus comprises channel-fill sequences of the gullied slope association of the Pakhna Formation (see section 4.5.3). Laterally-equivalent sheet-like bioclastic beds can be traced along the Armenokhori road as far as the saddle point at GR 113428. This location is closer to the axis of the Yerasa fold and thrust belt, and is on strike with steep southerly dipping chalks of the Lefkara Formation. At road level these chalks crop out with dips of 40 degrees towards the south-south-west, but they are here overlain a few metres above by shallow dipping beds laterally equivalent to the Koronia Limestone member at Amathus. Although the contact is not exposed, there is clearly an unconformity present, with upper Lefkara and lower Pakhna deposits missing. From this location, the view west along strike shows more clearly what is happening (Plate 14C). A thin (2 m) amalgamation of sheet like calcarenites, that are laterally equivalent to the Koronia Limestone at Amathus, defines the top of a north facing scarp. In the south, off-axis of the fold belt, these beds cap an apparently complete succession of Pakhna and Lefkara Formation deposits. Towards the north, this scarp transgresses the steeper dipping Lefkara Formation chalks, and older Pakhna and Lefkara Formation deposits are

progressively cut out (eroded prior to Koronia Limestone deposition). These relationships are illustrated in figure 7.4. Cross-sectional reconstruction indicates that at least 300 m of Lefkara chalks have been eroded on this unconformity (fig. 7.2), and this can be taken as a minimum estimate of the amount of vertical uplift involved.

2.4 Interpretation of observations

Several conclusions can be drawn from the observations described in the previous sections:

(1) Uplift of the Limassol Forest block involved steep thrusting of igneous basement against the overlying sediments, producing a narrow linear zone of deformation (the Yerasa fold and thrust belt).

(2) Uplift was accompanied by erosion (possibly submarine). Deepest stratigraphic erosion levels are found in the most structurally elevated areas, ie. furthest in towards the Limassol Forest block.

(3) The erosional unconformity passes southwards off structure into a continuous marine sequence, and may correlate with the cutting of marine channels in the gullied slope facies association of the Pakhna Formation.

(4) On the structural axis, erosion is followed by deposition of the Koronia Limestone member (peripheral sands association of the Pakhna Formation). Off-structure, uplift is accompanied by the influx of bioclastic material derived from the area of the peripheral sands, and transported through channels of the gullied slope.

Thus the level at which the unconformity passes into a conformable sequence south of the Yerasa fold and thrust belt can be used to accurately date the uplift of the Limassol Forest block. From the available data (age of Pakhna Formation marls into which channels are cut at Amathus) this appears to be within the Tortonian (see section 2.5.3).

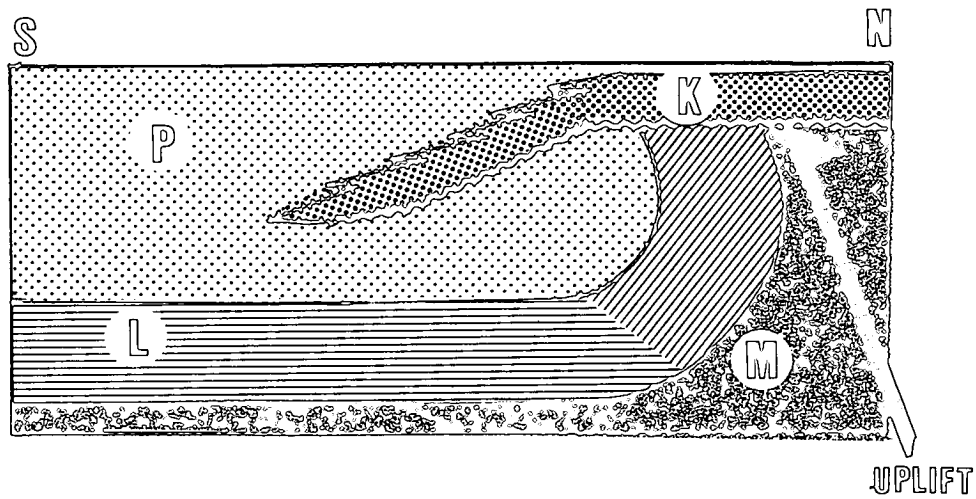

FIG. 7.4 Diagramatic representation of relationships in Tertiary sediments on south flank of Yerasa fold and thrust belt. M = Moni Formation, L = Lefkara Formation, P = Pakhna Formation, K = Koronia Limestone member. Not to scale.

7.5 Tectonic significance of the Koronia Limestone member

The Koronia Limestone member of the Pakhna Formation is characteristically a series of bioclastic calcarenites and calcirudites (section 2.3.2). An interpretation of field relationships in the Phinikaria-Ayios Tykhonas area (previous section) indicates that the cutting of by-pass channels in which the Koronia Limestone was later deposited (section 4.5.3) was related to uplift and erosion on the northern margin of the basin (the Yerasa fold and thrust belt). The sediments of the Koronia Limestone member in these channel deposits were probably fed from the peripheral sands which now comprise the Koronia Limestone deposits above the Yerasa fold and thrust belt. In this area, and probably elsewhere, the Koronia Limestone member is therefore of tectonic significance. It represents the first syn-tectonic (in basinward areas) or post-tectonic sediments.

7.6 Structures of the Limassol Forest block

Early geological maps of the Limassol Forest area (Bear, 1960; Pantazis, 1967) show large areas of serpentinite. This led Robertson (1977a) to suggest serpentinite diapirism as the driving mechanism for the Miocene uplift of the Limassol Forest block, in an analagous manner to that established for Mount Olympos in the Troodos area (Gass & Masson-Smith, 1963). However, Murton (1986) found that serpentinisation in the Limassol Forest block was an early sea-floor process associated with the initial formation of the ophiolite (Late Cretaceous), and does not represent late diapiric intrusion. This is confirmed by gravity studies (Vine, pers. com., 1984; Vine & Smith, in prep.), which indicate isostatic equilibreum. An alternative uplift mechanism must therefore apply.

To the North, the Limassol Forest block is bounded by the Arakapas fault - a major east-west fault - which separates it from the main Troodos massif (see fig 1.3). Moores & Vine (1971) suggested that this feature could be

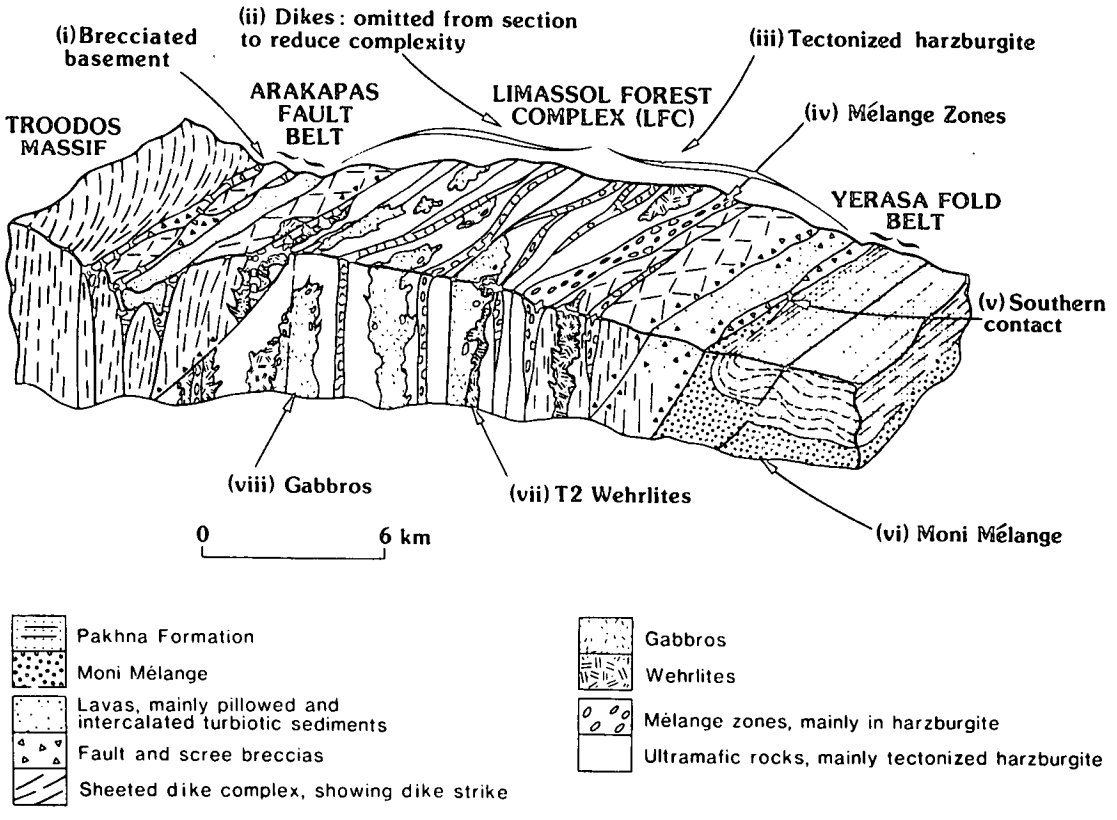

. North-south block diagram showing main petrological and structural features of western Limassol Forest complex. (i) *Arakapas fault belt*—Intensely brecciated basement of sheeted dikes overlain by scree deposits and mafic lavas intercalated with clastic basaltic sediments. For detailed cross section, see Simonian and Gass (1978, Fig. 3, p. 1223). (ii) *Dikes*—Three main trends, from oldest to youngest: 100°–110° near-vertical greenschist facies, commonly boudin-aged metabasalts; 030°–040° subvertical basaltic dikes, commonest trend in WLFC, associated with gabbro plutons (viii); several petrographic varieties identified; and 000°–040° sinuous brownstone facies dolerites. (iii) *Host lithologies*—Tectonized harzburgite, similar to other ophiolite mantle sequences, and mafic and ultramafic cumulates of high-level axis magma chamber(s). (iv) *Serpentinite shear zones*—East-west elongated, phacoidal blocks of tectonized harzburgite, dunite, and more rarely gabbro ranging from 0.1 to 100 m in totally serpentinized flakey matrix of comminuted harzburgite; contacts with adjacent rock types sharp. (v) *Southern contact*—Inverted unconformable contact with either umbers of Perapedhi Formation or Moni melange resting on basaltic scree breccias and/or pillow lavas of WLFC; identified in places as a north-dipping thrust (Panayiotou, 1977). (vi) *Moni melange*—Large allochthonous blocks of quartzose sandstone, Triassic limestone, jasper, chert, and basic volcanics in Upper Cretaceous bentonitic clay matrix. (vii) *Wehrlites*—Oldest phase of intrusive plutonism; small, irregular, 0.6–1.2-km diameter intrusive masses with sharp intrusive contacts that cut tectonic fabric of harzburgite host. (viii) *Gabbros*—Medium-grained, equigranular ol-opx-cpx-plag gabbros, petrographically similar to high-level gabbros of Troodos and other ophiolites; dike suites (ii) associated with major gabbroic masses.

FIG 7.3 Structure of the Limassol Forest block. From Murton & Gass (1986).

a fossil oceanic transform fault, and it was later proposed that the whole of the Limassol Forest block was formed within the same transform domain (Simonian & Gass, 1978). Recent detailed studies have confirmed this (Murton, 1986). Furthermore, Murton & Gass (1986) describe a series of east-west shear zones developed during early evolution of the Limassol Forest block, and related to transform tectonics. These impose a strong east-west trending tectonic fabric upon this basement block (fig. 7.5). Any interpretation of later deformation and uplift may need to take this into account.

7.7 Evidence for earlier fault activity

7.7.1 A parallel fault line in the Maroni sub-basin

In the area of the Ayia Mavri ruin, southwest of Kalavasos (GR 250442) a southeast striking fault zone has been mapped (fig. 7.6). Faults cut the Lefkara and Pakhna Formations and are downthrown to the northeast. Lithologies adjacent to the fault line tend towards steep fault-parallel dips. This is clearly shown by separating structural dip readings into two populations. One population consists of dip orientations taken from localities away from the fault line, and defines a regional dip of 16 degrees towards 106 (consistent with the uplift of the Limassol Forest block to the northwest). The other population is made up of dip readings taken from localities proximal to the fault line. This population, plotted as poles to bedding, defines a girdle with a best fit pole plunging 6 degrees towards 129. This deformation zone can be desrcibed as a fault-induced monocline striking towards the southeast.

In several respects the fault line at Ayia Mavri is similar to those associated with the Yerasa fold and thrust belt:

(1) Both structures strike towards the southeast (averaged azimuths of 116 and 129 degrees)

(2) Both structures involve Pakhna Formation deposits and may have been formed at the same time.

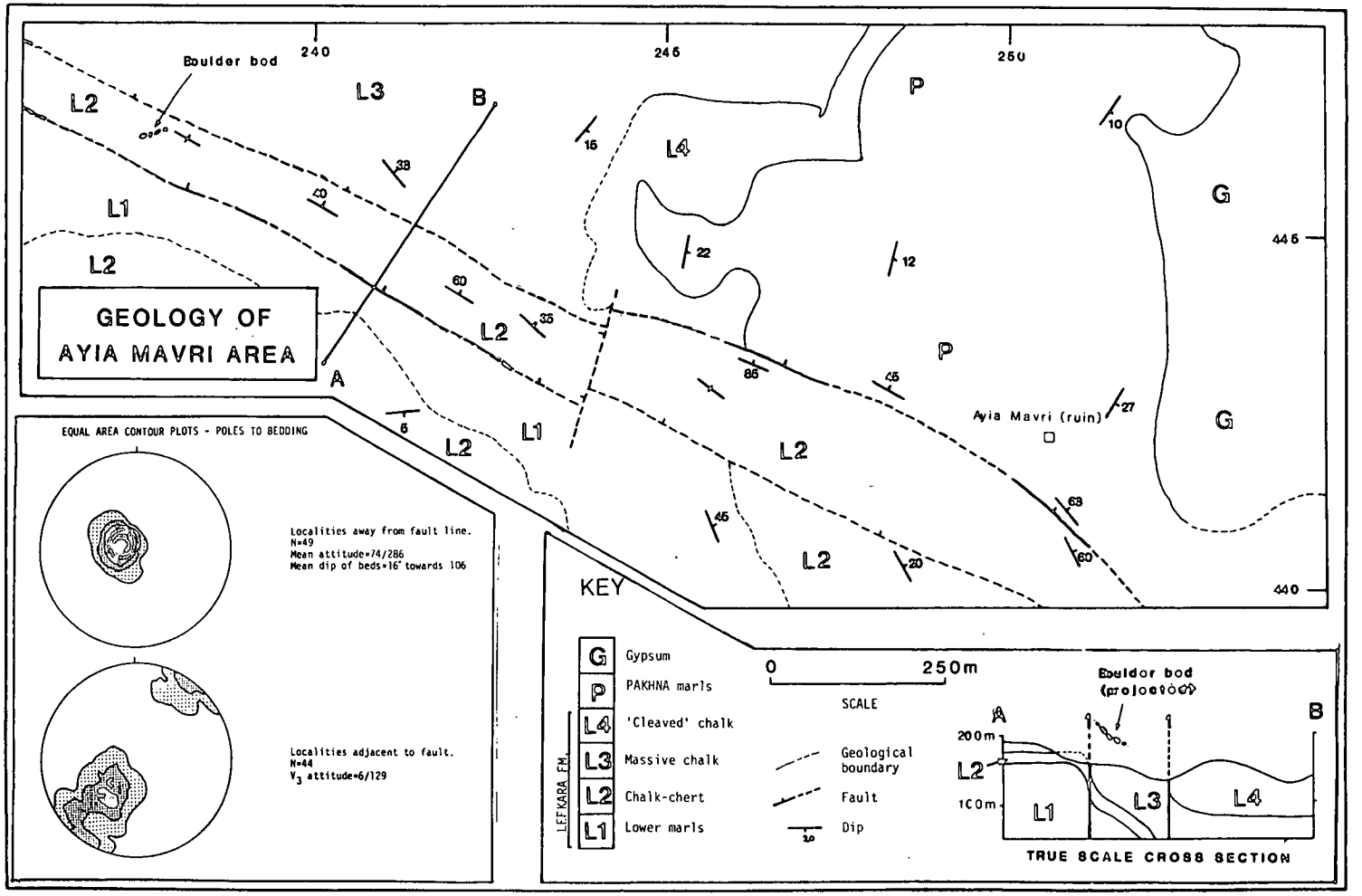

FIG. 7.6 Geological map of Ayia Mavri area. See fig. 2.1 for location.

(3) Both structures are associated with steep faults and dominantly vertical tectonics.

7.7.2 Evidence for earlier fault activity

Of particular interest in the Ayia Mavri area is evidence that the fault line was also active during deposition of the Lefkara Formation. At GR 238456 in a scarp above the track a thick (over 5 m) boulder bed is exposed (fig. 7.6). This contains large (over 1 m across) unsorted and randomly orientated blocks of cherty Lefkara chalks in a chalk matrix. These boulders form a clast-supported framework through most of the deposit. It is overlain by bedded calciturbidites, which are lithologically similar to the blocks in the boulder bed. This exposure occurs within the Middle Lefkara chalk-chert unit, which is of Paleocene to early Eocene age (Robertson, 1976). The only realistic interpretation for the origin, within a deep calciturbidite sequence, of this unit is by shedding of large blocks from a submarine fault scarp.

Further evidence for the tectonic disturbance of the sea floor during Middle Lefkara times is found a short distance away at GR 245438. Here, a depositional surface with several metres of relief occurs within the chalk-chert sequence (fig. 7.7). Numerous small faults cut the sediments beneath this surface, but do not extend upwards into the calciturbidites which drape and fill the relief. This outcrop may represent a ponded slump scar. It occurs within the same sequence as the boulder bed, and is probably related to the same episode of submarine fault activity.

Thus the Ayia Mavri area contains evidence for the creation of sea floor topography during Middle Lefkara times by basement faulting. In the same area, Pakhna Formation sediments have been deformed by subsequent reactivation of the faults. Orientation of these later structures is similar to those of the Yerasa fold and thrust belt, suggesting that thay may be of common origin.

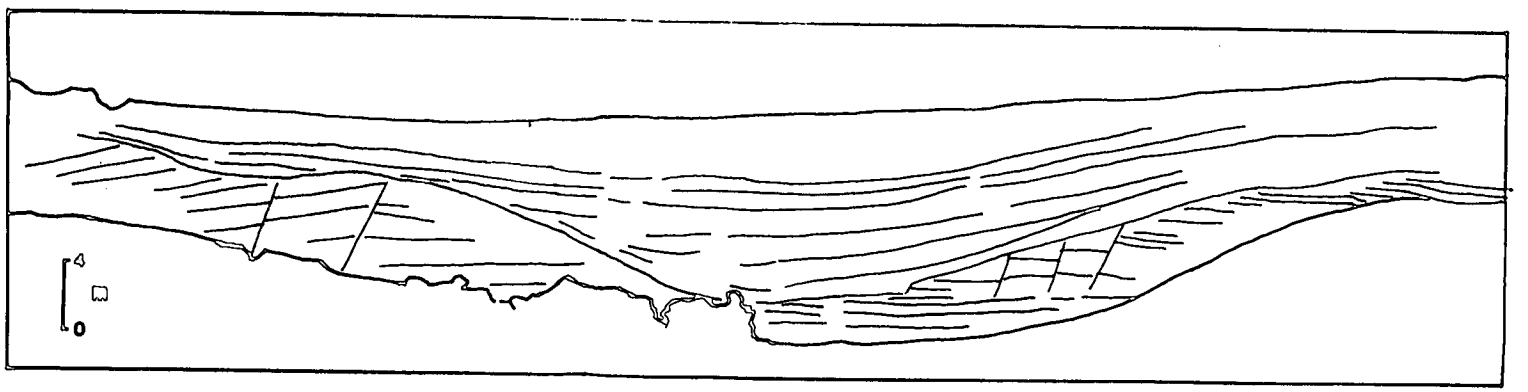

FIG. 7.7 Line drawing of exposure near Ayia Mavri, showing intraformational relief created and filled on the sea floor during deposition of the Lefkara Formation chalk-chert sequence.

7.7.3 Possible influence on calciturbidite deposition

Robertson (1976) recorded palaeocurrent data from the calciturbidites of the middle Lefkara chalk-chert unit. These data were collected from the area to the east of the Troodos massif (fig. 7.8), and cover the area of the Maroni sub-basin. It is interesting to note that at one locality, near Pano Lefkara, palaeocurrents deviate significantly from the general northeast to southwest trend. This location is along strike from a major east-west fault in the Troodos ophiolite - the Arakapas fault. The creation of sea floor topography by the reactivation of this fault during Palaeocene or early Eocene times could account for the anomalous palaeocurrent data.

7.8 Summary

The Yerasa fold and thrust belt is a narrow zone of steep thrusts and folds developed during uplift of the Limassol Forest block in Late Miocene times. Uplift is associated with the erosion of an unconformity which separates deformed sedimentary rocks beneath from undeformed clastic carbonates above. Basinwards, this unconformity passes into a conformable marine sequence. The Koronia Limestone member is locally developed at this level and represents the first syn- or post-tectonic deposit.

The steep nature of the faulting and the limitation of structures to a narrow belt indicates dominantly vertical tectonics.

A similarly orientated line at Ayia Mavri has been described. Sedimentological indications of earlier tectonic activity along the same fault line indicate that the location of Miocene faulting is controlled by the location of pre-existing faults.

It seems likely that faults in the igneous basement inherited from original formation of the ophiolite have been reactivated at various times. Exploitation of these faults during a Late Miocene compressional event might account for the steep nature of thrusts in the Yerasa fold

and thrust belt.

These conclusions are related to wider aspects of the Tertiary tectonic evolution of Cyprus in the following chapter.

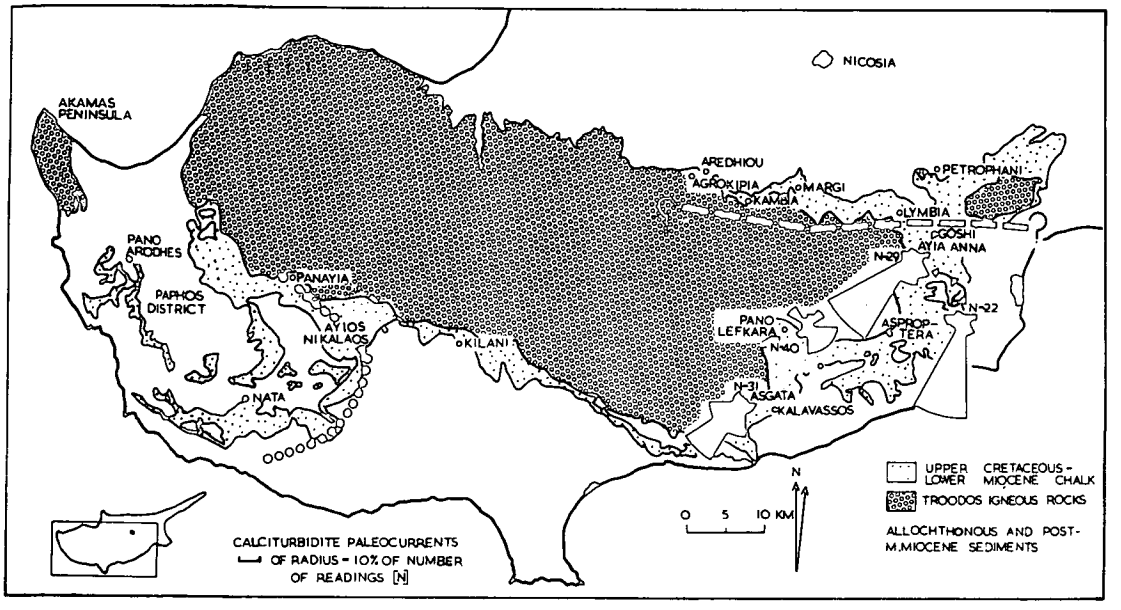

FIG. 7.8 Palaeocurrent data from the Lefkara Formation. Note anomalous data from Pano Lefkara location. From Robertson(1976).

CHAPTER EIGHT

SYNTHESIS

8.1 Introduction

Previous chapters have described how basin geometry and sedimentation during Pakhna Formation times have been strongly controlled by the evolution of local structural elements in the area studied. In this chapter it is intended to show how development of these structural elements may, in turn, be controlled by earlier basement structures. This is then placed in the context of the tectonic setting of Cyprus in the Eastern Mediterranean area.

Finally, the implications of the Miocene uplift history of southern Cyprus for the relationship of the Kalavasos Formation with other Mediterranean Messinian evaporites are considered.

8.2 Early development of the Troodos basement

Oceanic crust, formed along an active spreading axis, is subject to block faulting during migration to an off-axis position, and by further cooling and subsidence during its early evolution. These processes involve the development of grabens and half grabens by normal faulting parallel to the spreading axis (e.g. Rona et al., 1976).

Overall dyke orientation in the Troodos massif is north-south (Kidd & Cann, 1973), indicating a north-south orientated spreading axis. The development of half grabens, 0.5 to 3 km wide and parallel to the dyke trend, has been described from within the pillow lava sequence (Boyle & Robertson, 1984), with throws on normal and listric normal faults of up to 160 m. A prominent transverse fault was also described, and interpreted as a minor transform fault. Thus it is highly likely that the Troodos ophiolitic basement was dissected into a mosaic of fault blocks prior to accumulation of the overlying sediments. Furthermore, the Limassol Forest block was deformed within an oceanic transform zone, resulting in a strong east-west structural fabric (see section 7.6).

East-west block faulting of the Limassol Forest block has also been inferred (Murton & Gass, 1986; Vine & Smith, in prep.)

In addition to this structural fabric inherited from "normal" oceanic spreading processes, the basememt geology of Cyprus records a major Late Cretaceous structural reorganisation.

8.3 Late Cretaceous reorganisation of basement

As outlined in chapter one, the 90 degree counter-clockwise rotation of the Troodos ophiolite, originally thought to have occurred in Late Miocene times (Shelton & Gass, 1980), is now known to have been completed much earlier, with a substantial portion of the rotation occurring within the Late Cretaceous (Clube et al., 1985). This early rotation involved the juxtapositioning, by strike-slip faulting, of Troodos-type basememt with Mamonia lithologies (Swarbrick, 1980; Clube & Robertson, 1986), now exposed in southwest Cyprus (Robertson & Woodcock, 1979). A full account is found in Clube & Robertson (1986), but the important conclusions for the purpose of this study are:

(1) In southwest Cyprus, Late Cretaceous strike-slip faulting, associated with the rotation of the Troodos ophiolite, juxtaposed older crustal units (the Mamonia Complex) against Troodos-type oceanic crust along high-angle arcuate lineaments.

(2) Lineaments are characterised by the intrusion and extrusion of serpentinite, associated with fault activity.

(3) These steep lineaments closely parallel the arcuate southwest margin of Cyprus (fig. 8.1).

(4) The lineaments and both types of basement were subsequently buried by the Tertiary sedimentary cover.

With no expression in the Tertiary sediments, these lineaments cannot be traced into the areas of the Khalassa and Maroni sub-basins. However, two features of the Moni Formation cropping out within and along strike of the Yerasa fold and thrust belt, suggest the presence of a

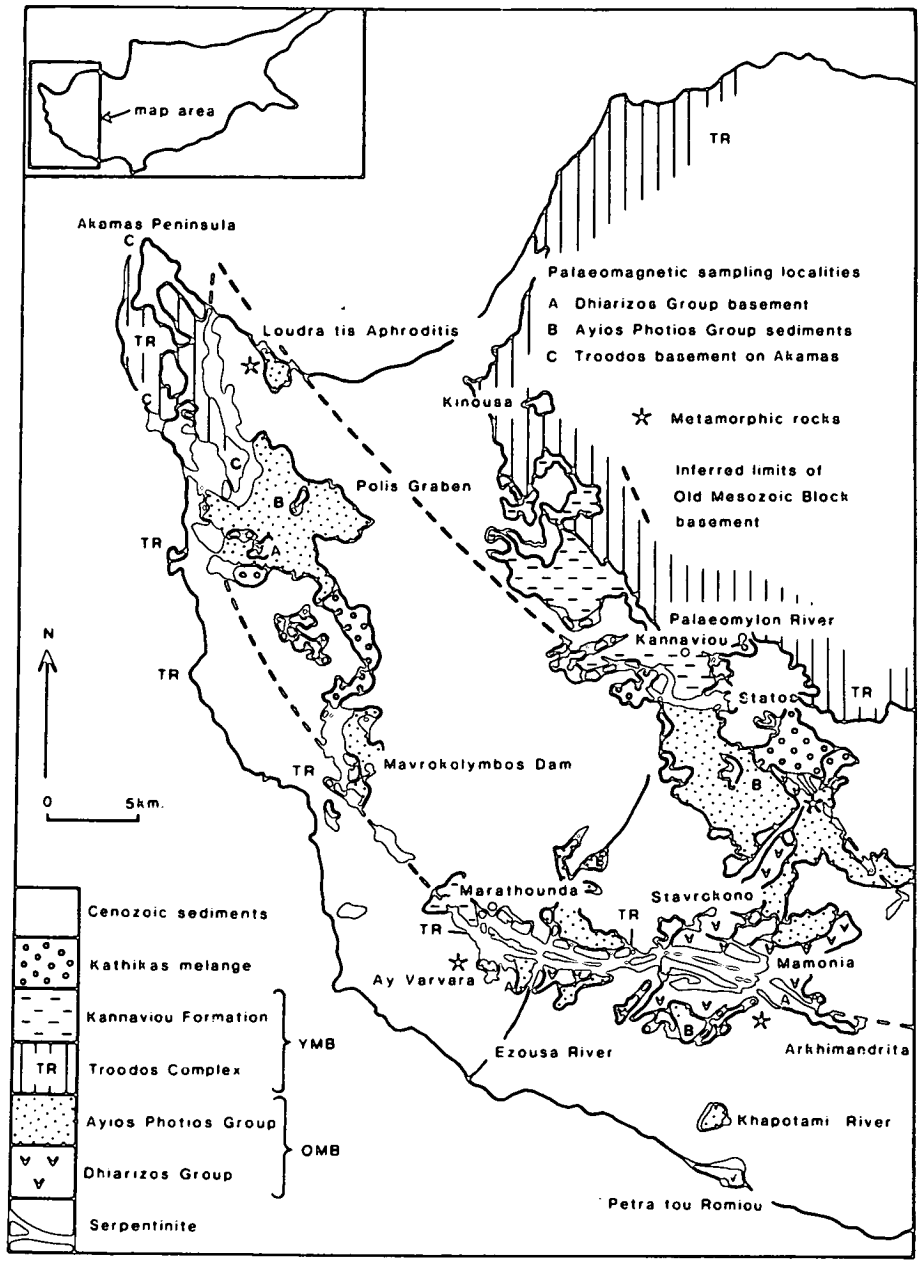

FIG. 8.1 Outline geology of southwest Cyprus, showing arcuate serpentinite-intruded fault lineaments. From Clube & Robertson (1986).

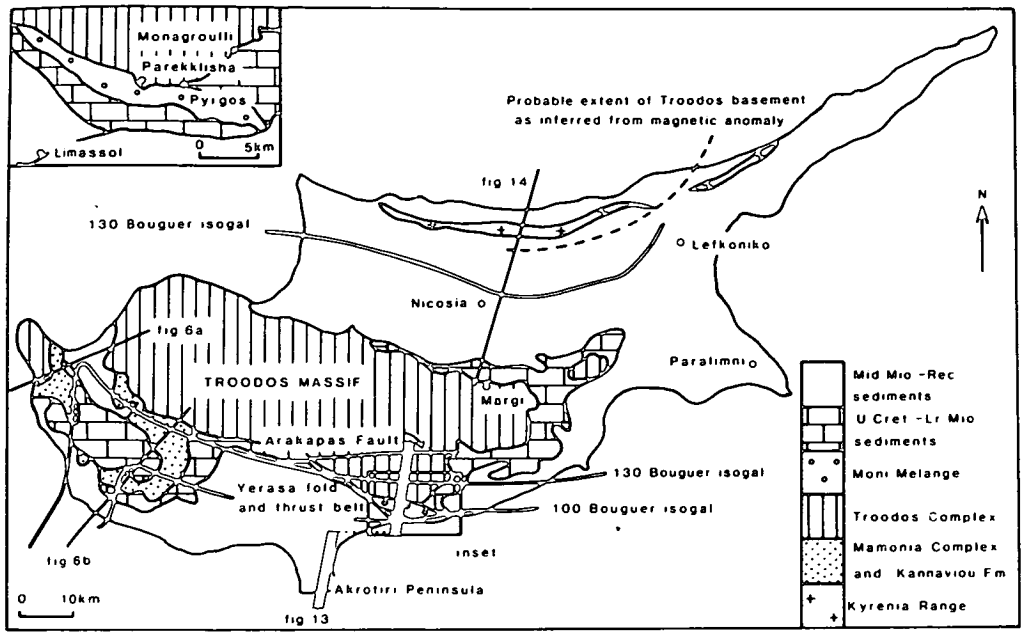

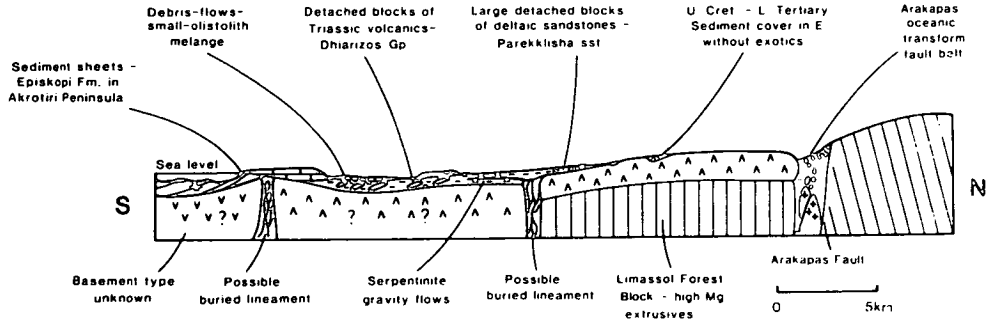

FIG. 8.2 Outline geological map of Cyprus (above), showing main basement features. Heavy lines show location of cross-section (below). This cross-section shows interpreted relationships between basement blocks beneath a thick Tertiary sedimentary cover. Note the possible buried lineament on the south side of the Limassol Forest block.

buried lineament. Firstly, massive serpentinite sheets, with steeply dipping shear fabrics, have been intruded vertically along a line immediately north of the present Moni Formation outcrop area (Robertson, 1977c). These serpentinites then flowed southwards across the Late Cretaceous ocean floor as a gravity flow, and were incorporated within the Moni Formation. They may be analagous to the serpentinites exposed along lineaments in southwest Cyprus.

Second, the inclusion of Mamonia-type olistoliths by gravity gliding and debris flow northwards into the Moni Formation implies that an uplifted block of Mamonia-type material existed to the immediate south of the Limassol Forest block (Robertson, 1977c; Swarbrick, 1980).

Thus it is possible that, as illustrated by Clube & Robertson (1986), a buried Late Cretaceous strike-slip lineament exists along the southern boundary of the Limassol Forest block (Fig. 8.2).

8.4 Tertiary uplift

As described in section 4.2, the Tertiary evolution of the Troodos ophiolite is characterised by generally continuous uplift, leading to localised emergence of the Troodos massif by Lower Miocene times. During the Middle and Upper Miocene uplift appears to have been centred on the Limassol Forest block. Recent field and gravity data rule out the presence of a rising serpentinite diapir as the driving mechanism for this apparently localised uplift (section 7.6). Instead, it now appears that the uplift of the Limassol Forest block may have been the local response to a general north-south directed compression that affected the whole island in Late Miocene times, and which can be related to the plate tectonic setting of the East Mediterranean region.

8.5 Miocene tectonics on Cyprus

Evidence has been presented to suggest that concommitant with the uplift of the Limassol Forest block

and the formation of the Yerasa fold and thrust belt, another linear structural feature, the Akrotiri High, was being uplifted and eroded to the south of the Khalassa sub-basin (section 5.7). Also, in the north of Cyprus, south directed thrusting of Mesozoic and younger sediments over lower Tertiary sediments occurred at the same time (the Kyrenia and Ovgos thrusts, Robertson & Woodcock, 1986). Off-shore, interpretation of seismic data indicates that both to the north of Cyprus (as the sub-sea extension of the Kyrenia Range) and to the south, arcuate thrust lineaments exist which involve deformation of the pre-evaporite (Messinian) sequences (Mulder, 1973; Mulder et al., 1975). See figure 8.3.

Other indications are more speculative. Murton (1986) shows the Arakapas fault, as well as the Yerasa faults, as a northward dipping steep thrust active during Late Miocene times (fig. 8.4). The block faulted anteformal structure of the Limassol Forest block (Murton & Gass, 1986) may originate from the same phase of compression. Various north dipping thrusts have also been recognised in the Troodos massif , which may have been active in Late Miocene times. Examples include the Kykko Thrust (Wilson, 1959), regarded by Dreghorn (1973) as contemporaneous with the thrusts of the Kyrenia Range, and the thrust near Platres, separating tectonised harzburgite above from gabbroic units below (fig. 8.5). This was described by Bortolotti et al., (1976) as being of Late Cretaceous age, but this is not constrained by any evidence, and it could conceivably have been active in Late Miocene times. It is particularly interesting in that it is roughly along strike of, and of similar orientation to, faults of the Yerasa fold and thrust belt.

The possibility that these structures, from across the whole island, may be related to one another was suggested by Bagnall (1964) (fig. 8.6). Although details (such as the significance given to wrench faulting) may be misleading, the basic concept fits in remarkably well with the plate tectonic setting of Cyprus.

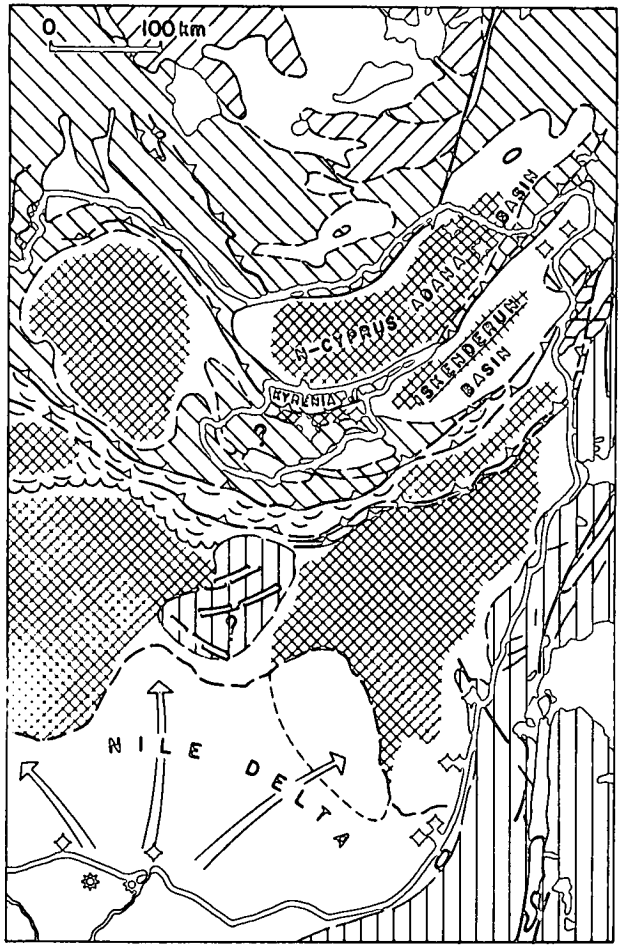

The easternmost part of the Mediterranean.
The allochthonous sediments of the East-Mediterranean ridge grade laterally into the little disturbed fill of late Cenozoic basins with thick Upper Miocene salt. Some of these basins are in a foredeep position, others are intra-orogenic basins, separated by narrow compressional belts.

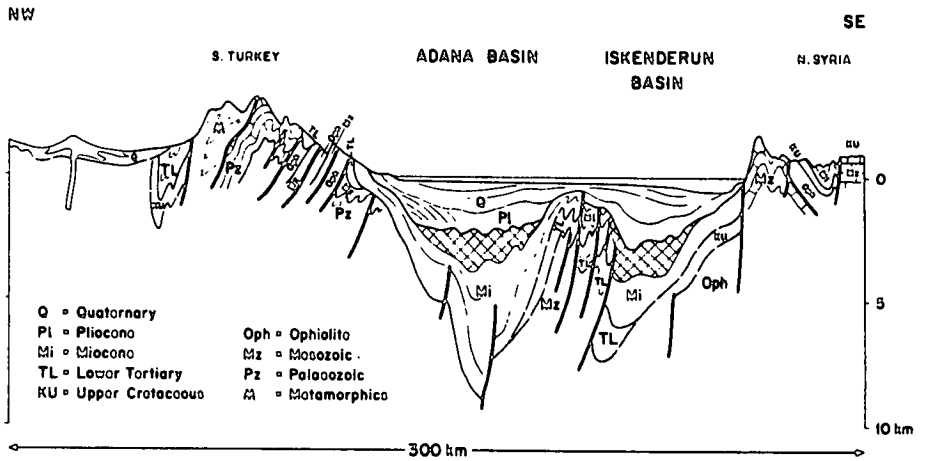

Schematic cross-section through the Adana and Iskenderun basins towards Northern Syria (Eastern Mediterranean). These two basins with thick Upper Miocene salt are separated by a relatively narrow belt of folding and outward thrusting (Kyrenia-Misis zone). A major unconformity is present below the Lower Miocene *Globigerina* marls.

Internal zones, including some smaller internal massifs.
External zones.
Areas of foreland folding and outer Alpine folded belts.
The foreland of Africa and Europe and some larger stable blocks.
Late Cenozoic basins with an appreciable basin fill.
Late Cenozoic allochthonous blankets.
Upper Miocene rock salt distribution.
Main occurrences of Cenozoic igneous rocks (mainly extrusives).

FIG. 8.3 Structural lineaments in the Eastern Mediterranean, as interpreted by Mulder (1973). Note Messinian evaporites post-date thrusting in the Adana and Iskendrum basins.

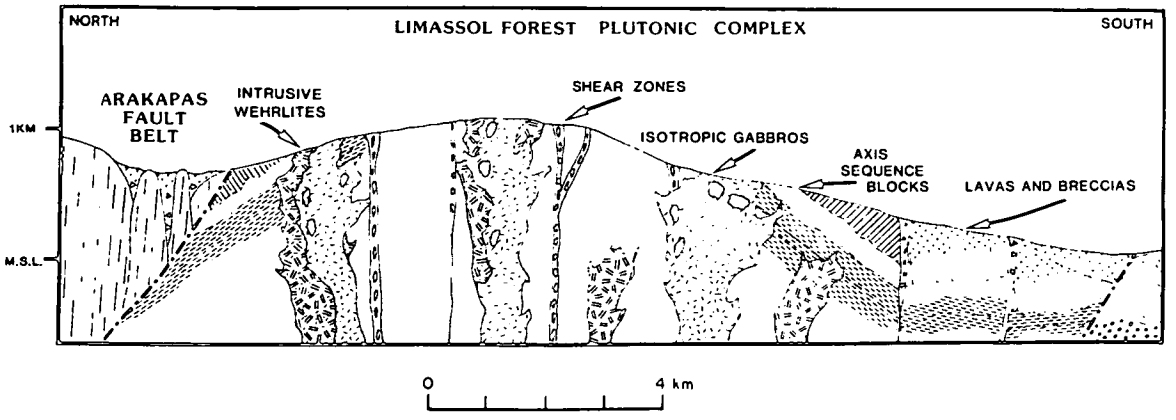

Schematic N–S cross-section showing the plutonic structure of the Western Limassol Forest Complex as one dominated by multiple intrusion. Troodos Axis Sequence blocks have been tilted and disaggregated prior to emplacement of the isotropic gabbros and intrusive wehrlites. High angle, Miocene thrusting (heavy broken lines) is apparent in both the north and the south.

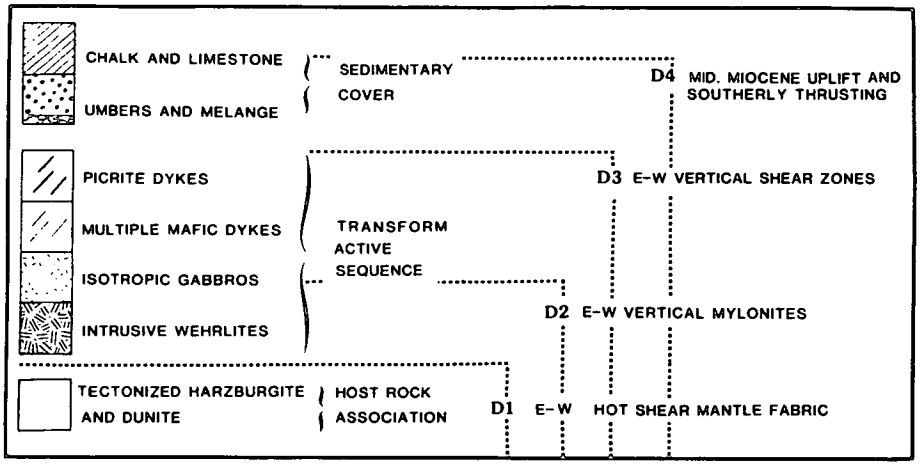

Ophiolitic stratigraphy and tectonic history of the Western Limassol Forest Complex. D_1 to D_3 are interpreted as seafloor formational events reflecting processes in an active transform domain. D_4 involves both uplift and high angle reverse faulting that was active until the Middle Miocene.

FIG. 8.4 Diagrams (above) from Murton (1986) showing Arakapas Fault interpreted as a reverse fault active in Miocene times (D4 phase of deformation, see lower diagram).

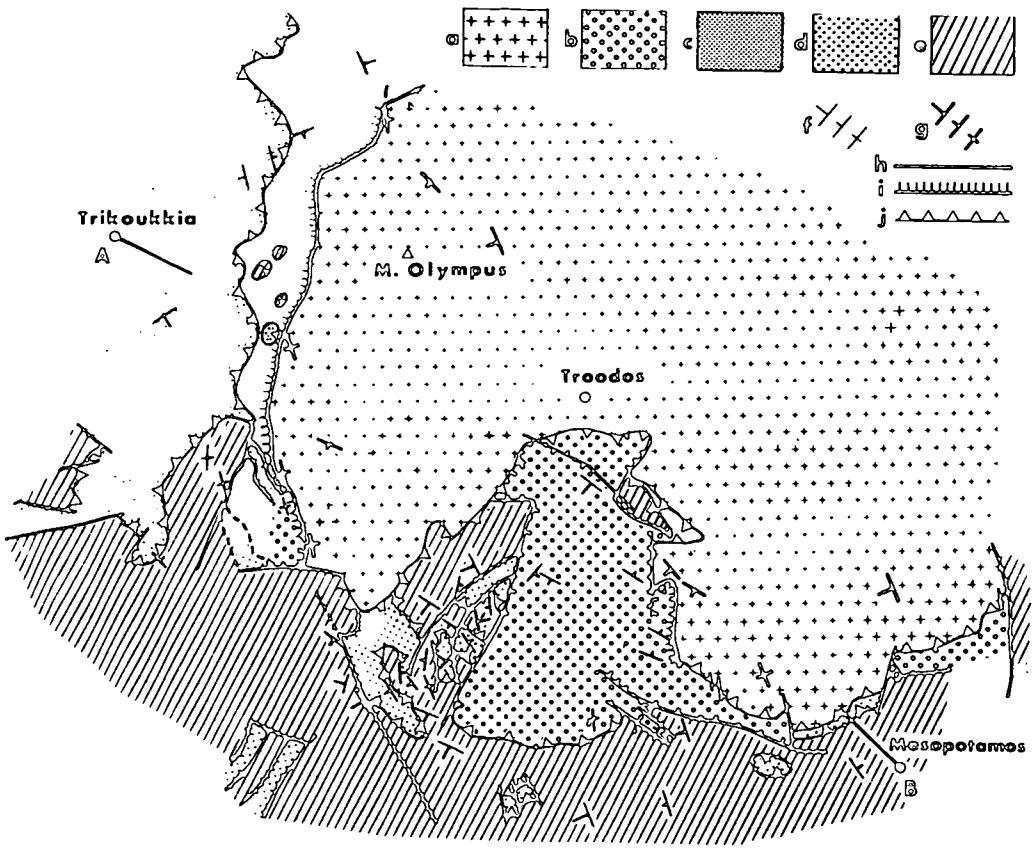

Sketch map of the southwest part of the Troodos Massif core.
Legend: *a* = tectonitic harzburgite—dunite unit (Mt. Olympus Unit), *b* = dunitic and wherlitic units, undifferentiated, *c* = dunitic units, *d* = wherlitic units, *e* = gabbroic units, *f* = magmatic layering, *g* = metamorphic banding and foliation, *h* = faults (dip unknown), *i* = normal faults, *j* = thrusts.

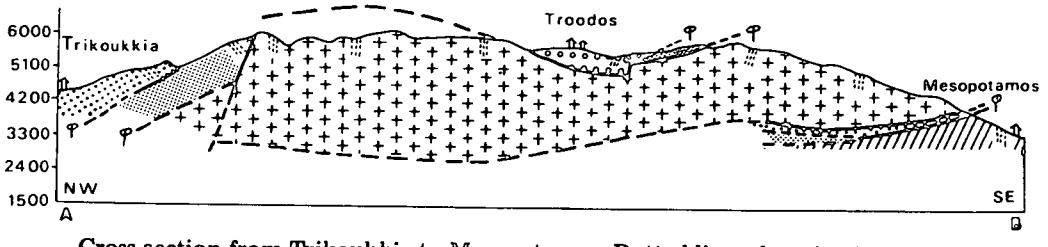

Cross-section from Trikoukkia to Mesopotamos. Dotted lines: layering in magmatic intrusives, banding and foliation in tectonitic ultramafics, φ = thurst surfaces.

FIG. 8.3 Northward dipping thrust in the Troodos igneous complex. From Bortolotti et al. (1976).

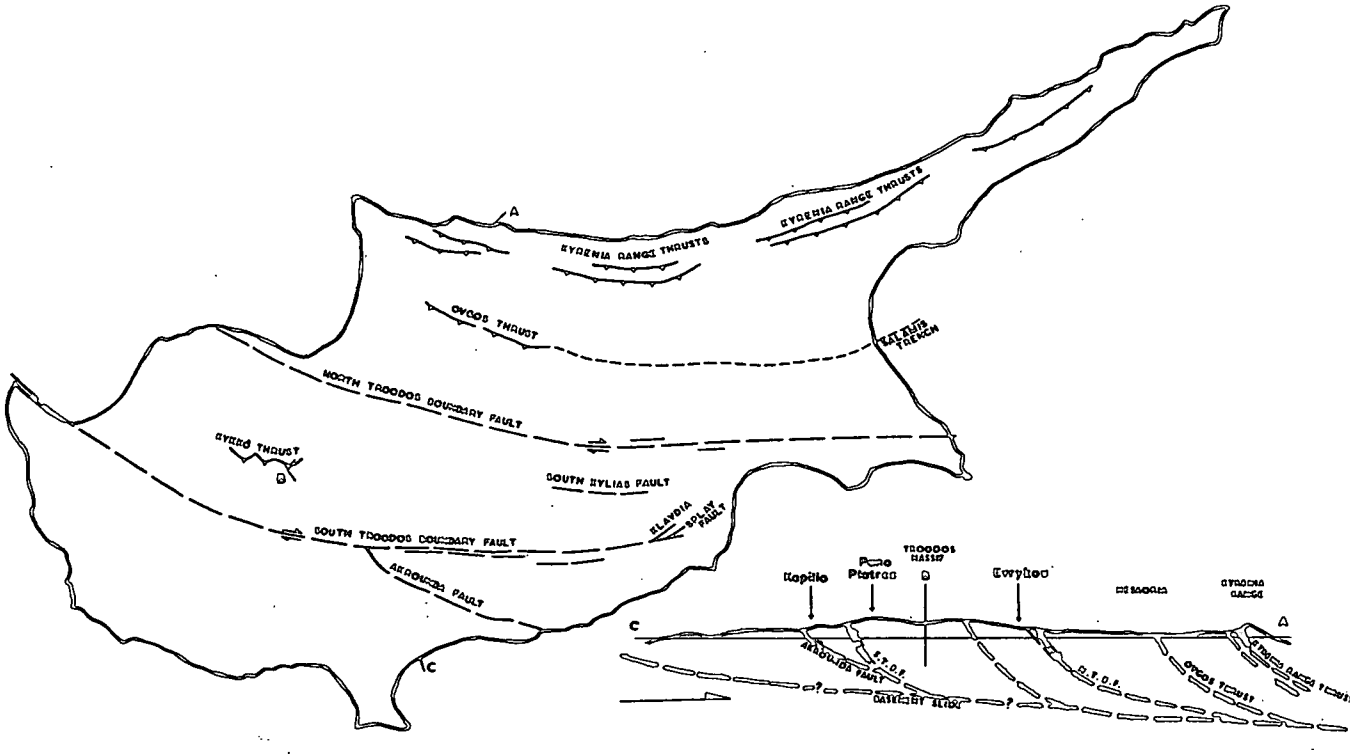

FIG. 8.6 Principle faults of Cyprus, an interpretive cross-section, from Bagnall (1964).

8.6 The plate tectonic setting of Cyprus

Palaeomagnetic data from the Eastern Mediterranean indicates that substantial convergence between the African and European plates has taken place during the Neogene (Livermore & Smith, 1985; see fig. 8.7). This convergent margin is well expressed seismically and bathymetrically to the south of Greece and the Aegean Sea, and corresponds to the Hellenic-Cretan trench (Mackenzie, 1970). East of Rhodes, however, the definition is less clear, though all authors agree in that it passes immediately south of Cyprus in a convex-southward arc (the Cyprus arc), and then links up eastward with the East Anatolia transform-Bitlis zones between the Arabian and Anatolian blocks (Ben-Avraham *et al.*, 1982; Biju-Duval *et al.*, 1978; Dewey *et al.*, 1973; Jackson & McKenzie, 1984; Papazachos & Comninakis, 1978; see fig. 8.8). This is supported by seismic reflection data, which show compressional deformation in sediments of the Florence Rise to the west of Cyprus (Woodside, 1978) and to the east (Mulder *et al.*, 1975).

Seismicity along the Cyprus arc is low. Recorded shocks are generally small, resulting in poor quality fault plane solutions for the region beneath Cyprus (Comninakis & Papazachos, 1972; Rotstein, 1984; Jackson & McKenzie, 1984). Although earthquake data selection and interpretation differ slightly, all authors agree on the consumption of northward travelling crust beneath Cyprus and along the Cyprus arc.

On the basis of gravity data, Gass & Masson-Smith (1963) concluded that the Troodos ophiolite is underlain by at least 30 km of high density mantle-type rock. In contrast, interpretation of more recent seismic refraction data, constrained by magnetic and gravity data, shows that Cyprus is underlain by 35 km of continental-type crust (Makris *et al.*, 1983; see fig. 8.9). This crust thins to the south, so that between Cyprus and the Israeli continental shelf, the Moho is overlain by 8 km of crystalline crust and 12 to 14 km of sediment. This may

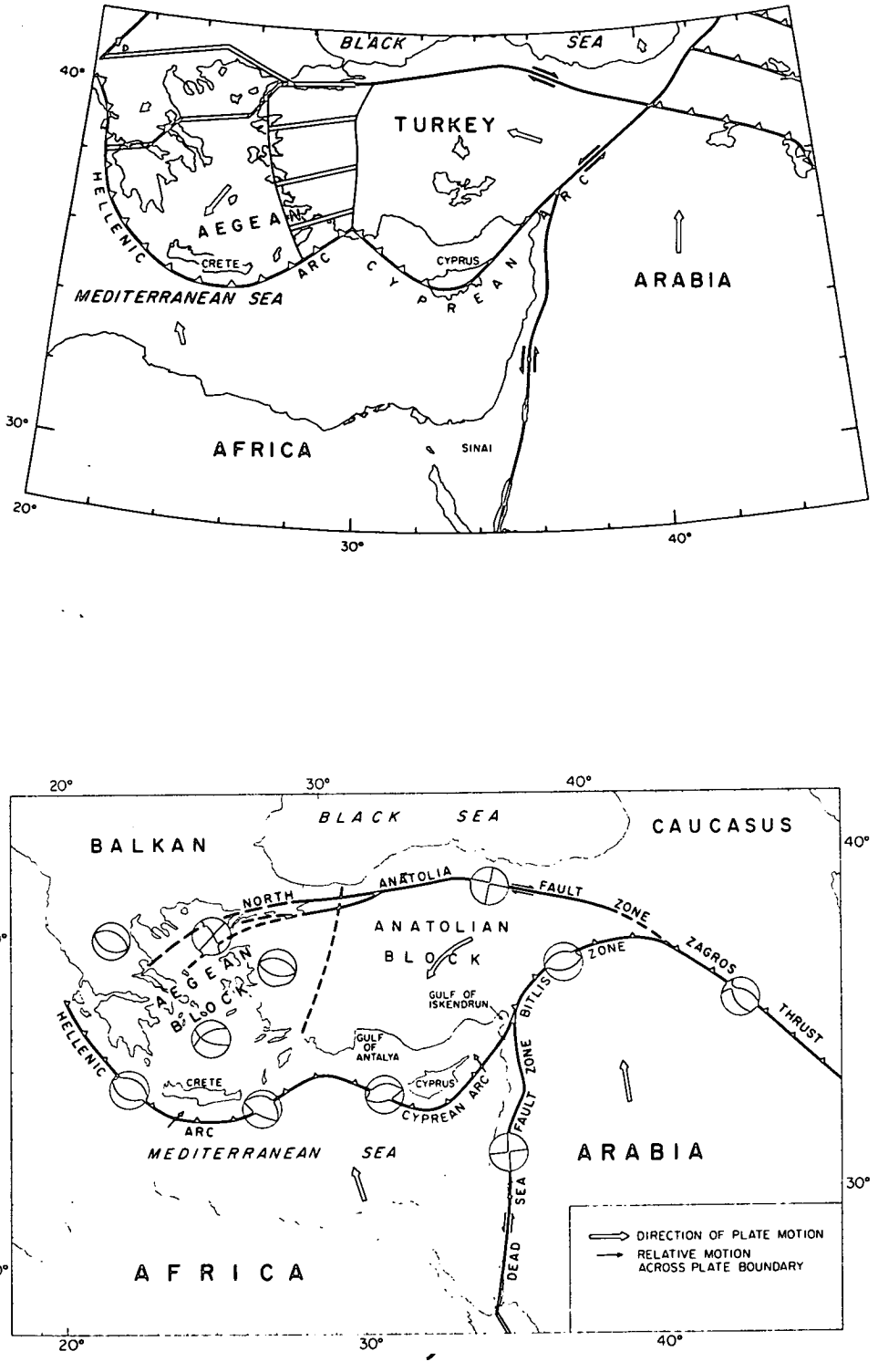

FIG. 8.7 Plate tectonic configuration in the East Mediterranean after McKenzie (1970) above, and Rotstein (1984) below.

(a) Decrease in oceanic areas with time.

Time interval (in m.y.)	Area lost[1] (in 10^6 km^2)	Total area	Av. rate (in 10^6 km^2 m.y.$^{-1}$)	Total rate
Cenozoic (0–65 m.y.)				
0– 9.6	0.71	0.71	0.07	0.07
9.6–37.1	1.96	2.67	0.07	0.07
37.1–48.1	1.21	3.88	0.11	0.08
48.1–51.7	0.18	4.06	0.05	0.08
51.7–52.7	0.06	4.11	0.05	0.08
52.7–66.1	<−0.01	4.09	<0.01	0.06

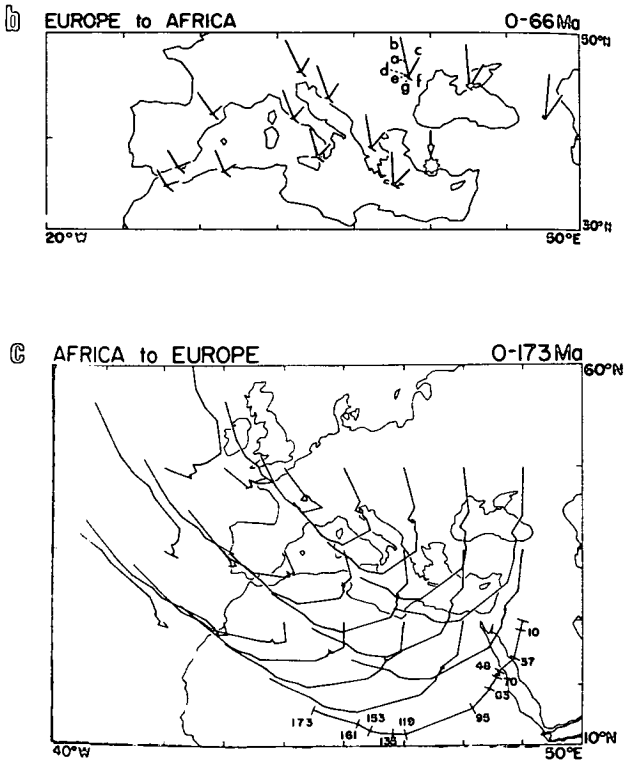

FIG. 8.8 Data from Livermore & Smith (1985). (a) Table of rates of consumption of oceanic crust in the Tethys area throughout the Cenozoic. (b) Vector diagram showing relative motion of Europe with respect to Africa. Nearest relevant data point (asterisked) represents approximately 400 km of convergence in the last 37 million years. (c) Motion of Africa relative to Europe for the past 173 million years. Diagram shows track of present day geographic grid rigidly fixed to Africa. Numbers on track give ages in million years.

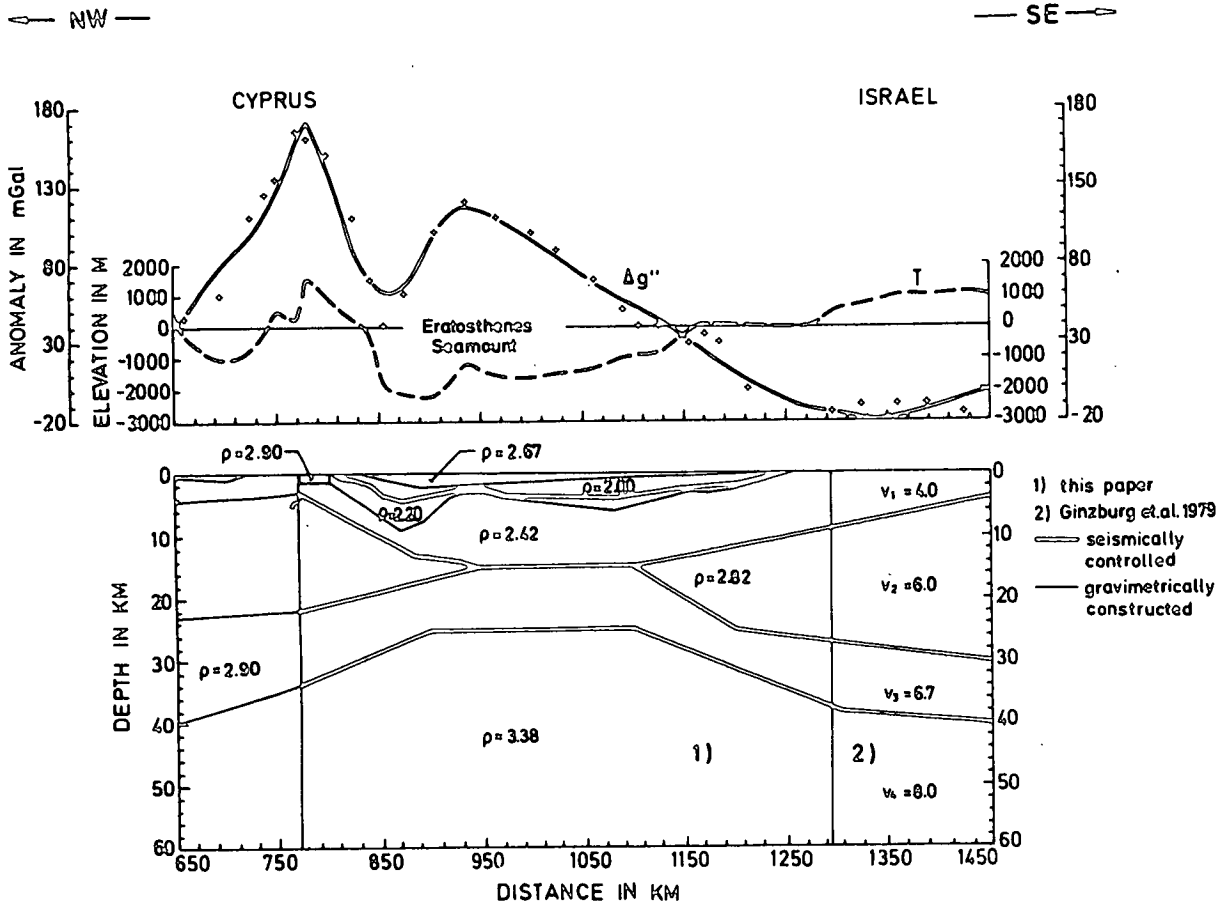

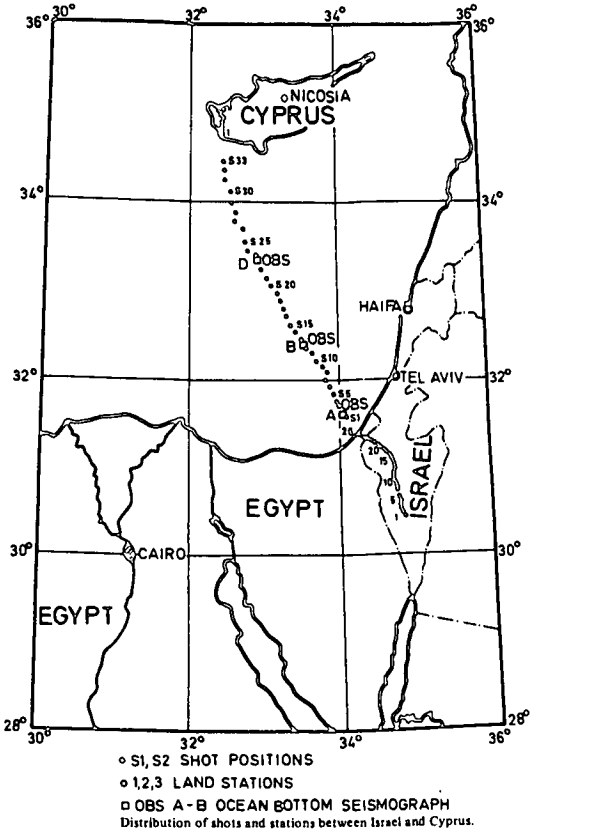

.. T = topography, Δg" = computed and interpolated Bouguer values, + = observed Bouguer values.

FIG. 8.9 Diagram shows crustal model between Cyprus and Israel, from Makris et al., 1983.

represent quasi-oceanic crust on the leading edge of the African continental margin.

8.7 A plate tectonic related uplift mechanism

In view of the plate tectonic setting of Cyprus, it is reasonable to attribute the Paleocene to Late Miocene uplift of the island to a continuous process of underplating during under-thrusting of the North African plate beneath Cyprus. Uplift due to underplating and crustal thickening could explain several features:

(1) The relatively undeformed nature of the Troodos ophiolite compared with other Tethyan ophiolites which are interpreted to have been emplaced as thrust sheets.

(2) The uninterupted nature of the autochthonous sedimentary cover, from abyssal depths (Perepedhi Formation) to shallow marine (Pakhna Formation).

(3) The thick nature of continental type crust beneath the ophiolite (Makris *et al.*, 1983).

Continuous uplift appears to have culminated in a major phase of tectonism in Late Miocene times. From the foregoing sections, it is now clear that:

(1) The convergent margin between the African and European plates is expressed in the Eastern Mediterranean by the Hellenic and Cyprus arcs, which run immediately south of Cyprus.

(2) Along these arcs, both to the east and west of Cyprus, Late Miocene thrusting of sediments is apparent on seismic reflection data.

(3) On Cyprus, Late Miocene compressional deformation is also evident in many areas.

It is possible that the Late Miocene event, involving uplift of the Limassol Forest block and the development of the Akrotiri High, resulted from underthrusting beneath Cyprus of the leading edge of the African continental margin, or of an isolated crustal unit ahead of this margin.

In this respect, it is interesting to note that a pause in spreading activity of the Red Sea occurred

between 6 and 4 mybp (ie. Late Miocene). This has been attributed to excessive resistance to deformation in the Aegean and Turkish areas (Le Pichon & Angelier, 1979). Tectonic resistance, it might be added in view of this synthesis, occurred also along the Cyprus arc.

8.8 Contrasting deformation styles

It has been argued in this work that the Late Miocene uplift of the Limassol Forest block was related to the same stress field across Cyprus that produced thrusting in the Kyrenia Range. If this is to be accepted then the differences in deformational style must be explained. As discussed earlier (section 7.2) the Yerasa fold and thrust belt is characterised by steep fault-induced folds occurring in a narrow belt, and involving relatively minor amounts of lateral shortening. In contrast, the Kyrenia Range was subject to strong southward thrusting representing significant north-south shortening (Robertson & Woodcock, 1986). Folds are generally subhorizontal. Thrusting over crustal ramps and the development of imbricate stacks are reported (fig. 8.10). These differences reflect differing degrees of lateral shortening, and can be explained by basement control on deformation style.

Geophysical evidence indicates that the southern limit of the (buried) Troodos ophiolite may lie a short distance beyond the southern coast of Cyprus, and that the northern limit runs obliquely beneath the Kyrenia range (Clube & Robertson, 1986), see figure 8.2. Under regional north-south directed compression the Troodos ophiolitic basement has remained essentially intact, with reactivation of previous steep faults as reverse faults. These have involved relatively small amounts of movement before locking up. The Yerasa fold and thrust belt may have been formed by reactivation of a buried Late Cretaceous strike-slip lineament (section 8.4). Reactivation would have been facilitated by the "lubricating" effect of associated serpentinite. A similar

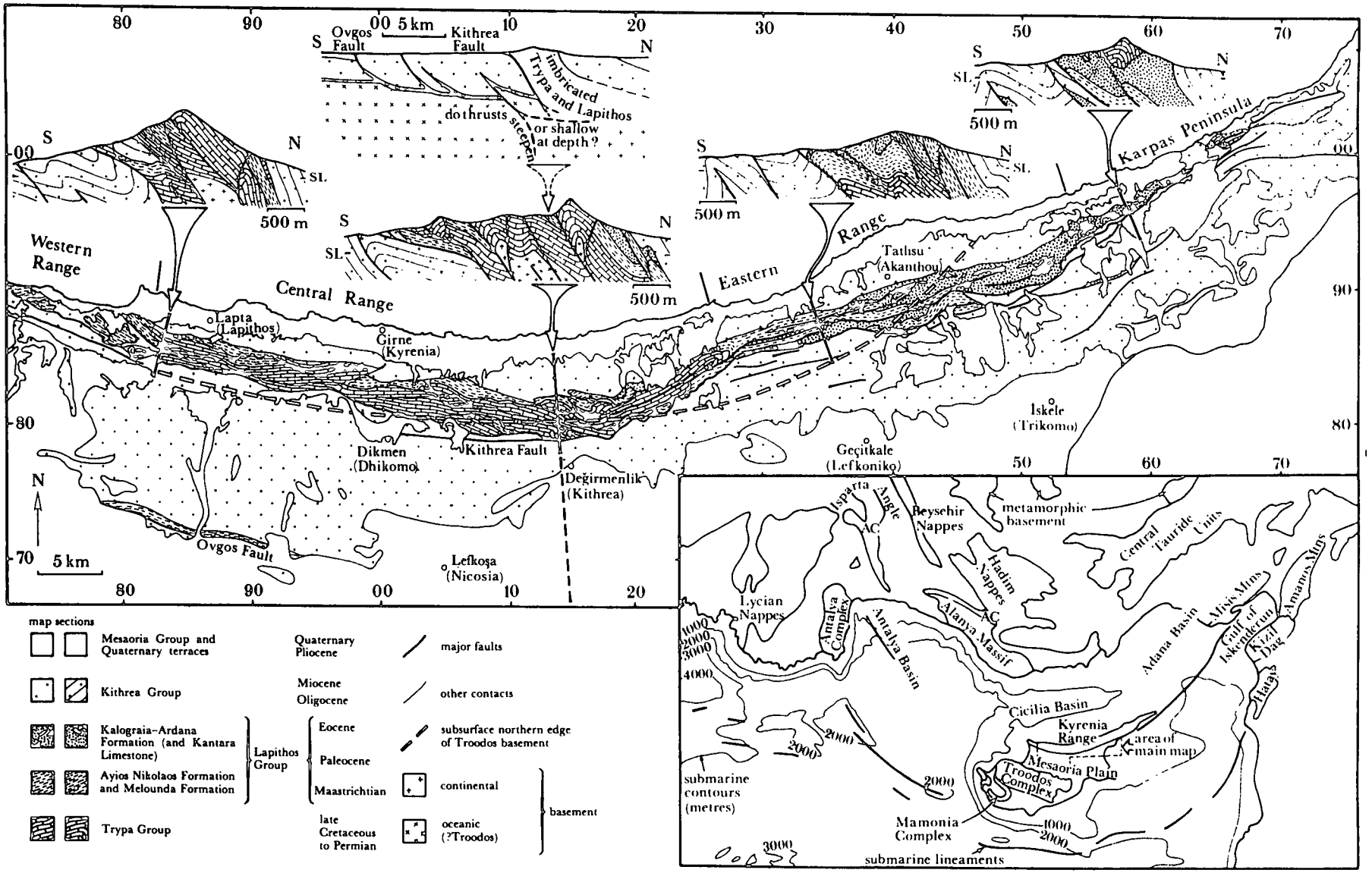

FIG. 8.10 Geological map of the Kyrenia Range showing interpreted true-scale structural cross sections. Location map inset. From Robertson & Woodcock (1986).

explanation may exist for the uplift of the Akrotiri High, and for reactivation of the Ayia Mavri fault (section 7.7), among others.

Thus deformation of the sedimentary cover to the Troodos ophiolite consists essentially of "drape folds" and faulting "forced" by reactivation of basement faults.

In contrast, the response to compression of lithologies which did not overly a competent basement unit was substantial lateral shortening, with the most intense deformation occurring where these lithologies butt against, and are thrust over, the northern edge of the Troodos basement, where the Kyrenia Range is now found.

The Troodos ophiolitic basement, therefore, has acted as a resistant foreland (Bishopp, 1952), protecting its autochthonous sedimentary cover from substantial lateral shortening under compressive stress.

8.9 Tectonics, sea-level changes, and evaporite deposition

During evaporation of normal sea-water, gypsum is first precipitated when the water is reduced to about one third of its original volume. According to the calculations of Debenedetti (1982) this corresponds to a sea-level fall of 1.5 km for an isolated Mediterranean Sea.

Prior to Messinian times, the Limassol Forest block and the Akrotiri High in southern Cyprus were already emergent and subject to erosion (section 5.10).

With the Messinian evaporitic drawdown of the Mediterranean, therefore, the Maroni and Khalassa sub-basins would have been left dry before evaporite deposition began. Deposition of the Kalavasos Formation must therefore have preceeded the main evaporitic drawdown of the Mediterranean.

This is consistent with the structural evolution of the area. Uplift across the Yerasa fold and thrust belt was completed before deposition of the Koronia Limestone member of the Pakhna Formation (section 7.5). Erosion products of the Akrotiri High in the Pakhna Formation also

indicate that in southern Cyprus, the Late Miocene tectonic events had already created a system of linear structural highs. This is also apparently the case for the off-shore continuation of these structures between Cyprus and Syria (Mulder et al., 1975). A system of narrow basins, defined by linear structural elements, was therefore in existence before evaporite deposition began.

However, it would be a remarkable coincidence if the evolution of these structural highs brought them to exactly the right configuration and elevation to promote gypsum precipitation in southern Cyprus, while normal pre-salinity crisis conditions continued in the surrounding proto-Mediterranean. Instead, preliminary sea-level fluctuations must have progressively lowered the head of water over these structural features, so that refluxing and evaporite deposition was inevitable at some point in time prior to complete isolation.

Evidence for progressive episodic sea-level falls prior to evaporite deposition are found in Spain, on the Nile cone, and (more speculative) on Cyprus itself.

In Spain, a series of Tortonian and Messinian reefs have been described, where younger reefs occur in successively lower topographic positions (Santisteban & Taberner, 1983). This is accounted for by the downslope migration of active reef growth concomittant with a falling sea-level. The upper and lowermost reefs are separated by more than 400 m vertically. The occurrence of a series of discrete reefs in successively lower positions indicates episodic sea-level fall, punctuated by periods of stability during which reefs established themselves at the new level.

Closer to Cyprus, in the Eastern Mediterranean, the basal Messinian unconformity has been mapped in the Nile Cone, by a combination of seismic analysis and borehole correlation, down to a present depth of 5 km (Barber, 1981). The presence of entrenched meanders, and impaired rejuvenation terraces on the Nile Canyon, imply that initial drawdown was gradual but with occassional sporadic

falls.

On Cyprus, the occurrence of distinctive platey-clast carbonate conglomerates immediately beneath the first evaporite deposits has been tentatively related to erosion of marginal carbonates exposed by a preliminary sea-level fall (section 6.4.2).

If it is accepted, by these arguments, that the evaporites of southern Cyprus were deposited in a barred basin before the main Mediterranean desiccation, then it follows that direct correlation with the evaporite sequences in the deep Mediterranean basins is not valid.

CHAPTER NINE

CONCLUSIONS

9.1 With rare exceptions, localised to the Yerasa fold and thrust belt, the Pakhna Formation has a conformable but diachronous lower boundary with the Lefkara Formation in the study area. The Koronia Limestone unit is a lateral bioclastic facies variation within the Pakhna Formation, and is attributed member status. The Kalavasos Formation conformably succeeds the Pakhna Formation, with no time-equivalence between the two units.

9.2 Two structurally controlled Miocene sub-basins have been recognised in the study area. These are the Khalassa sub-basin, bounded to the north by the Limassol Forest block, and to the south by the inferred Akrotiri High (now buried beneath Plio-Pleistocene sediments), and the Maroni sub-basin, to the east of the Limassol Forest block. These sub-basins are separated from each other by the eastward continuation of the Yerasa fold and thrust belt.

The geometry of these two sub-basins (and the existence of the Miocene Akrotiri High), has been determined by a combination of palaeocurrent and slump data, and by the arrangment of facies belts and sediment dispersal provinces.

9.3 The Pakhna Formation is a regressive marine basin-fill sequence recording the transition from bathyal pelagic to shallow shelf environments. It is characterised by hemi-pelagic marls and reworked bioclastic carbonate deposits. Clastic input is from a productive neritic carbonate environment fringing the adjacent uplifted Limassol Forest and Akrotiri areas. Erosional unroofing of these basin-bounding blocks is recorded in the compositional evolution of clastic lithofacies in the Pakhna Formation.

9.4 Four facies associations have been recognised in the Pakhna Formation. These are, in proximal to distal order, peripheral sands, gullied slope, basin margin, and basin plain. The gullied slope has acted as a bypass slope for clastic material transported from the peripheral sands association to the basin margin and basin plain associations.

9.5 Basin history (compositional evolution of clastic material, basin geometry and sediment dispersal patterns, development and migration of facies associations) has been strongly influenced by tectonic developments in the area. Uplift of basin-bounding blocks culminated in Late Miocene times with the south-directed thrusting of the Limassol Forest block over adjacent sediments, and the formation of the Yerasa fold and thrust belt. A series of linear structural highs, including the Akrotiri High and the submarine extension of the Kyrenia Range, was created at this time along the length of the Cyprus arc. Structural developments in the study area reflect the local response of underlying basement to a regional tectonic episode affecting the whole of the Cyprus arc, and related to the underthrusting of the African plate northwards beneath the European plate.

9.6 The Koronia Limestone member of the Pakhna Formation is transgressive over structures of the Yerasa fold and thrust belt, demonstrating that the main phase of Late Miocene uplift and deformation was completed prior to the deposition of the Kalavasos Formation. Seismic data also indicate that deformation terminated before evaporite deposition on other segments of the Cyprus arc.

9.7 The transition to evaporite sedimentation and the deposition of the Kalavasos Formation is marked by reduced benthic activity and the development of a laminated calcilutite facies in uppermost Pakhna Formation sediments. Locally occurring limestone conglomerates

immediately beneath the evaporites may represent marginal carbonate material that was exposed, lithified and eroded during preliminary sea-level fluctuations that heralded the onset of evaporitic conditions.

The gypsum deposits of the Kalavasos Formation are conformable upon the Pakhna Formation, with no evidence to suggest emergence or a break in sedimentation across the boundary.

9.8 Gypsum deposition was subaqueous, and occurred in a refluxing barred basin with brine depths in excess of 50 metres, and probably substantially deeper. Evaporitic refluxing conditions were brought about by the progressive lowering of sea-level over submarine linear structural highs developed during the Late Miocene tectonic episode (see 9.3).

Evaporite basin bathymetry was "inherited", and involved a similar geometry to that established for the underlying Pakhna Formation.

9.9 Clastic "cannibalistic" reworking of primary gypsum precipitates occurred by subaqueous, slope controlled gravity processes. Deposits are largely monomineralic due to high gypsum sedimentation rates and reduced carbonate production due to hyper-saline conditions.

9.10 With the complete isolation of the Messinian Mediterranean from the world ocean, and its rapid evaporitic draw-down, the refluxing barred basin(s) in the study area on Cyprus would have been "perched" and dry before the waters of the proto-Mediterranean were evaporated to the point at which gypsum deposition commenced. Thus the Kalavasos Formation of southern Cyprus is interpreted as immediately pre-dating the deposition of the Messinian evaporites now found beneath the Mediterranean abyssal plain.

REFERENCES

ADAMS,C.G. 1959. Geological distribution of Discospirina (foraminifera) and occurrence of D. italica in the Miocene of Cyprus. Palaeontology.London. 1, 364-368.

ADAMS,C.G. 1976. Larger foraminifera and the Late Cenozoic history of the Mediterranean region. Palaeogeogr. Palaeoclimatol.Palaeoecol., 20, 47-66.

ADAMS.C.G., BENSON,R.H., KIDD,R.B., RYAN,W.B.F. & WRIGHT,R.C. 1977 . The Messinian salinity crisis and evidence of Late Miocene eustatic changes in the world ocean. Nature, 269, 383-386.

BAGNALL,P.S. 1960. The geology and mineral resources of the Pano Lefkara-Larnaca area. Mem.geol.Surv.Dep.Cyprus, 5.

BAGNALL,P.S. 1964. Wrench faulting in Cyprus. J.Geol., 72, 327-345.

BANNER,F.T. & BLOW,W.H. 1960. Some primary types of species belonging to the superfamily Globigerinaceae. Contrib. Cushman Found.foramin.Res. 11, 1-41.

BARBER,P.M. 1981. Messinian subaerial erosion of the Proto-Nile Delta. Mar.Geol., 44, 253-272.

BAROZ,F. & BIZON,G. 1977. La couverture Tertiare du flanc nord du massif du Troodos et de la partie meridionale de la Mesaoria: etude stratigraphique et micropalaeontologique. Rev.Inst.Fr.Pet.Paris, 32, 719-759.

BEAR,L.M. 1960. The geology and mineral resources of the Akaki-Lythrodondha area. Mem.geol.Surv.Dep.Cyprus, 3.

BEAR,L.M. & MOREL,S.W. 1960. The geology and mineral resources of the Agros-Akrotiri area. Mem.geol.Surv. Dep.Cyprus, 7.

BELLAMY,C.V. & JUKES-BROWNE,A.J. 1905. The geology of Cyprus. W. Brendon and Son Ltd., Plymouth, Devon.

BEN-AVRAHAM,Z., NUR,A. & JONES,D. 1982. The emplacement of ophiolites by collision. J.geophys.Res., 87, 3861-3867.

BIJU-DUVAL et al., 1978. Structure and evolution of the Mediterranean basins. In HSU,K., MONTADERT,L. et al., (eds.) Initial Rep.Deep Sea drill. Proj., 43, 951-984.

BISHOPP,D.W. 1952. The Troodos Massif, Cyprus. Nature, 169, 489-492.

BIZON,G. & BIZON,J.J. 1972. Atlas des principaux foraminiferes planctoniques du bassin Mediterranean, Oligocene a Quaternaire. Editions Technip, Paris.

BIZON,G., CITA,M.B., MULLER,C. & WRIGHT,R. 1978. DSDP Leg 42A biostratigraphic range charts. In: HSU,K., MONTADERT,L. et al. (eds.) Initial Rep.Deep Sea drill. Proj., 42A, 1095-1138.

BLATT,H., MIDDLETON,G., MURRAY,R. 1980. Origin of sedimentary rocks. Prentice-Hall, USA.

BLOME,C.D, & IRWIN,W.P, 1985. Equivalent Radiolarian ages from ophiolite terrains of Cyprus and Oman. Geology, 13, 401-404.

BLOW,W.H. 1969. Late middle Eocene to Recent planktonic foraminiferal biostratigraphy. In: BRONNIMAN,P. & RENZ,H.H. (eds.) Proc.First Int.Conf.Plankt. Microfossils, Geneva, 1967, Vol. 1, E.J. Brill, Leiden, Netherlands, 199-421.

BORTOLOTTI,V, LAPIERRE,H. & PICCARDO,G.B. 1976. Tectonics of the Troodos Massif (Cyprus): preliminary results. Tectonophysics, 33, T1-T6.

BOYER,S.,E. & ELIOT,D. 1982. Thrust systems. Bul.Am.Assoc. Petrol.Geol., 66, 1196-1230.

BOYLE,J.F. 1984. The origin and geochemistry of the metalliferous sediments of the Troodos Massif, Cyprus. Unpub. PhD thesis, Edinburgh.

BOYLE,J.F. & ROBERTSON, A.H.F. 1984. Evolving metallogenesis at the Troodos spreading axis In Gass,G.I. et al. (eds.), Ophiolites and Oceanic Lithosphere, Spec. Pub.Geol.Soc.Lond., 13, 169-181.

BRANTLEY,S.L., CRERAR,D.A., MOLLER,N.E. & WEARE,J.H. 1984. Geochemistry of a modern marine evaporite: Bocana de Virrila, Peru. J.sed.Petrol. , 54, 447-462.

BRAUNE,K.F., FABRICIUS,F. & HEIMANN,K.O., 1973. Sedimentation and facies of Late Miocene strata on Cephalonia (Ionian Islands, Greece) In Drooger,C.W. (ed.) Messinian events in the Mediterranean. North-Holland, Amsterdam. 192-201.

BRINDLEY,G.W. & BROWN,G. 1980. Crystal structures of clay minerals and their X-ray identification. Min.Soc.London, Monograph 5.

BUTLER,R.W.H. 1982. Terminology of structures in thrust belts. J.struct.Geol., 4, 239-245.

CARR,J.M. & BEAR,L.M. 1960. The geology and mineral resources of the Peristerona-Lagoudhera area. Mem.geol. Surv.Dep.Cyprus, 2.

CHEVALIER,J.P. 1961. Recherches sur les Madreporaries et les formations recifal miocenes de la Mediterranean occidentale. Mem.soc.Geol.Fr., 93, 1-562.

CITA,M.B. 1983. The Messinian salinity crisis in the Mediterranean. A review. In Berckhemer,H. & Hsu,K. (eds.) Alpine-Mediterranean geodynamics. Geodynamics series, 7, 113-140.

CLEINTAUR,M.R., KNOX,G.J. & EALEY,P.J. 1977. The geology of Cyprus and its place in the East Mediterranean framework. Geol.Mijnbouw, 56, 66-82.

CLUBE,T.M.M. 1985. The palaeo-rotation of the Troodos microplate. Unpub. PhD. thesis, Edinburgh.

CLUBE,T.M.M., CREER,K.M. & ROBERTSON,A.H.F. 1985. Palaeo-rotation of the Troodos microplate, Cyprus. Nature, 317, 522-525.

CLUBE,T.M.M. & ROBERTSON,A.H.F. 1986. The palaeo-rotation of the Troodos microplate in the Late Mesozoic- Early Cenozoic plate tectonic framework of the Eastern Mediterranean. Surveys in geophysics, 8, 375-437.

COMNINAKIS,P.E. & PAPAZACHOS,B.C. 1972. Seismicity and some tectonic features of the Mediterranean ridge. Geol.Soc.Am.Bul., 83, 1093-1102.

COOK,H.E. 1982. Carbonate submarine fans versus carbonate debris aprons: facies patterns, depositional processes, and models (abs.). Bull.geol.Soc.Am., 14, 466-467.

COOK,H.E. 1983. Ancient carbonate platform margin, slopes, and basins. Soc.Econ.Palaeontol.Mineral. : Short course notes, 12, 5-1 to 5-189.

COOK,H.E. & MULLINS,H.T. 1983. Basin margin In Scholle,P.A., Bebout,D.G. & Moore,C.H. (eds.), Carbonate depositional environments, Mem.Am.Assoc.Pet.Geol., 33, 539-617.

COOK,H.E & TAYLOR,M.E. 1977. Comparisons of continental slope and shelf environment in the Upper Cambrian and lowest Ordovician of Nevada. In Cook,H.E. & Enos,P. (eds.). Deep water carbonate environments. Spec.Publ. Soc.econ.Paleontol.Mineral., 25, 51-82.

COOPER,D.J.W. 1984. The Hamrat Duru Group: evolution of a Mesozoic passive carbonate margin in the Oman mountains. Unpub.PhD thesis, Edinburgh.

CREVELLO,P.D. & SCHLAGER,W. 1980. Carbonate debris sheets and turbidites, Exuma Sound, Bahamas. J.Sed.Pet., 50, 1121-1148.

DABRIO,C.J., ESTEBAN,M. & MARTIN,J.M. 1981. The coral reef of Nijar, Messinian (uppermost Miocene) Almeria province, S.E. Spain. J.sediment.Petrol., 51, 521-539.

DEAN,W.D., DAVIES,G.R. & ANDERSON,R.Y. 1975. Sedimentological significance of nodular and laminated anhydrite. Geology, 3, 367-372.

DEAN,W.D. & ANDERSON,R.Y. 1982. Continuous subaqueous deposition of the Permian Castile evaporites, Delaware Basin, Texas and New Mexico In Handford,C.R., Loucks,R.G. & Davies,G.R. (eds.), Deposition and diagenetic spectra of evaporites - a Core Workshop: Calgary. 324-355.

DEBENEDETTI,A. 1982. The problem of the origin of the salt deposits in the Mediterranean and of their relations to the other salt occurrences in the Neogene formations of the contiguous regions. Mar.Geol., 49, 91-114.

DECIMA,A. & WEZEL,F.C. 1973. Late Miocene evaporites of the central Sicilian basin, Italy. In Ryan,W.B.F., Hsu,K.J. et al., Initial Rep.deep Sea drill. Proj., 13, 1234-1239.

DEWEY,J.F., PITMAN,W.C., RYAN,W.B.F. & BONNIN,J. 1973. Plate tectonics and the evolution of the Alpine system. Geol.Soc.Amer.Bull., 84, 3137-3180.

DREGHORN,W. 1973. Guide to the Troodos Mountains. Nicosia, Cyprus.

EINSELE,G. 1982. Limestone-marl cycles (periodite): Diagnosis, significance, causes - a review In: Einsele,G. & Seilacher,A. (eds.) Cyclic and event stratification, Springer-Verlag, Berlin.

ELION,P. 1983. Etude structurale et sedimentologique du bassin Neogene de Pissouri (Chypre). Thesis, Docteur 3em. Cycle, Univ. Paris-Sud, France (unpubl.)

EKDALE,A.A. 1978. Trace fossils in Leg 42A cores In; HSU,K.J. & MONTADERT,L. (eds.) Initial Rep.Deep Sea drill.Proj., 42A, 821-825.

ENGEL,W. 1974. Sedimentologische untersuchungen im flysh des Beckens von Ajdovscina (Slovenien). Gottinger Arb.Geol. Palaont., 16.

ENOS,P. & MOORE,C.A. 1983. Fore reef slope. In: Scholle,P.A., Bebout,D.G. & Moore,C.H. (eds.) Carbonate depositional environments. Mem.Am.Assoc.Petrol.Geol. 33, 507-537.

ESTEBAN,M. 1980. Significance of the Upper Miocene coral reefs of the Western Mediterranean. Palaeogeogr. Palaeoclimatol.Palaeoecol., 29, 167-188.

EVANS,G., MORGAN,P., EVANS,W.A., EVANS,T.R. & WOODSIDE,J.M. 1978. Faulting and halokinesis in the northeastern Mediterranean between Cyprus and Turkey. Geology, 6, 392-396.

FARRELL,S.G. 1984. A dislocation model applied to slump structures, Ainsa basin, south central Pyrenees. J.Struct.Geol., 6, 727-736.

FARRELL,S.G. & EATON,S. in press. Slump strain in the Tertiary of Cyprus and the Spanish Pyrenees. Definition of palaeoslopes and models of soft sediment deformation. In: Jones,M.E. & Preston,R.M.F. (eds.) 1987. Deformation of sediments and sedimentary rocks. Spec.Pub.Geol.Soc.Lond., 29, 181-196.

FRIEDMAN,G.M. 1972. Significance of the Red Sea in the problem of evaporites and basinal limestones. Bull.Am. Assoc.Petrol.Geol., 56, 1072-1086.

GARRISON,R.E. & KENNEDY,W.J. 1977. Origin of solution seams and flaser structure in Upper Cretaceous chalks of southern England. Sed.Geol., 19, 107-137.

GARRISON,R.E., SCHREIBER,B.C., BERNOULLI,D., FABRICIUS,F.H., KIDD,R.B. & MELIERES,F. 1978. In: HSU,K.J. & MONTADERT,L. (eds.) Initial Rep.Deep Sea drill.Proj., 42A, 571-611.

GASS,I.G. 1960. The geology and mineral resources of the Dhali area. Mem.geol.Surv.Dep.Cyprus, 4.

GASS,I.G. & MASSON-SMITH,E.M. 1963. The geology and gravity anomalies of the Troodos Massif, Cyprus. Royal Soc. London, Philos.Trans., ser.A, 255, 417-467.

GAWTHORPE,R.L. & CLEMMEY,H. 1985. Geometry of submarine slides in the Bowland Basin (Dinantian) and their relation to debris-flows. J.geol.Soc.London, 142, 555-565.

GIGNOUX,M. & FALLOT,P. 1927. Contribution a la connaisance des terrains Neogenes et Quaternaires marins sur les cotes Mediterraneennes d'Espagne. Congres geol. intern., C.R. 14e sess., Madrid, 1926. 413-521.

GREITZER,Y. & CONSTANTINOU,C. 1969. Report on the geology of the Kouris River area. Internal Report., Republic of Cyprus and Tahal Consulting Engineers Ltd., Israel.

HADJISTAVRINOU,Y. 1974. Ann.Rep.geol.Surv.Dep.Cyprus 1973.

HADJISTAVRINOU,Y. 1975. Ann.Rep.geol.Surv.Dep.Cyprus 1974.

HADJISTAVRINOU,Y. & CONSTANTINOU,G. 1977. Hydrogeology of the Akrotiri Peninsula. Cyprus Geol.Surv.Dept.Bull., 7.

HAMPTON,M.A. 1972. The role of sub-aqueous debris-flow in generating turbidity currents. J.sediment.Petrol., 42, 775-793.

HANSEN,E. 1965. Methods of deducing slip line orientations from the geometry of folds. Yb. Carnegie Instn. Wash. 1965. 387-405.

HANTZSCHEL,W. 1975. Trace fossils and problematica. In: Teichert,C. (ed.), Treatise on invertebrate palaeontology, part W, supp. 1, Univ. Kansas & Geol.Soc.Am. 1-269.

HARDIE,L.A. & EUGSTER,H.P. 1971. The depositional environment of marine evaporites: a case for shallow, clastic accumulation. Sedimentology, 16, 187-220.

HASKETT,M.J. 1984. Middle Miocene foraminifera of the Kissousa to Pakhna road section, southern Cyprus. Internal Report, Univ.Col.London (unpubl.)

HAYWARD,A.B. 1982. Coral reefs in a clastic sedimentary environment: fossil (Miocene, S.W. Turkey) and modern (Recent Red Sea) analogues. Coral reefs, 1, 109-114.

HAYWARD,A.B. 1985. Coastal alluvial fans and associated marine facies, Miocene, S.W. Turkey. In: Collinson,J.D. (ed.) Fluvial sedimentology. Spec.Publs.int.Ass. Sediment., 6, 323-336.

HEDBURG,H.D. 1976. International Stratigraphic Guide. John Wiley and Sons, New York.

HENSON,F.R.G., BROWNE,R.C. & McGINTY,J. 1949. A synopsis of the stratigraphy and geological history of Cyprus. Q.J. geol.Soc.London, 95, 1-41.

HERGUERA,J.C. 1982. Brief notes on the biostratigraphy and palaeobathymetry of some sections in the Kouris River valley near Khallasa (Cyprus). Internal Report, Univ. Col.London (unpubl.)

HOLSER,W.T. 1979. Mineralogy of evaporites In: Burns,R.G. (ed.), Marine minerals. Min.Soc.Am. Reviews in Mineralogy, 6, 211-235.

HSU,K.J., 1973. The dessicated deep basin model for the Messinian events In: Drooger,C.W. (ed.) Messinian events in the Mediterranean. North-Holland, Amsterdam. 60-67.

HSU,K.J., RYAN,W.B.F. & CITA,M.B. 1973. Late Miocene dessication of the Mediterranean. Nature, 242, 240-244.

HSU,K.J., MONTADERT,L., BERNOULLI,D., BIZON,G., CITA,M.B., ERIKSON,A., FABRICIUS,F., GARRISON,R.E., KIDD,R.B., MELIERES,F., MULLER,C. & WRIGHT,R.C. 1978. Introduction and explanatory notes. In: HSU,K.J. & MONTADERT,L. (eds.) Initial Rep.Deep Sea drill.Proj., 42A, 3-27.

HUDSON,J.D. 1977. Stable isotopes and limestone lithification. J.geol.Soc.London, 133, 637-660.

JACKSON,J. & McKENZIE,D. 1984. Active tectonics of the Alpine-Himalayan belt between western Turkey and Pakistan. Geophys.J.R.astr.Soc., 77, 185-264.

JONES,D.T. 1940. The geology of the Colwyn Bay district: study of submarine slumping during the Salopian period. Q.Jl.geol.Soc.London, 95, 335-382.

KENDALL,A.C. 1979. Subaqueous evaporites In: Walker,R.G. (ed.) Facies models. Geoscience Canada Reprint Series 1. 159-174.

KENDALL,G.St.C. & SCHLAGER,W. 1981. Carbonates and relative changes in sea-level. Mar.Geol., 44, 181-212.

KENNEDY,W.J. 1975. Trace fossils in carbonate rocks. In: Frey,K.W. (ed.) The study of trace fossils. Springer-Verlag, Berlin. 377-398.

KIDD,R.G.W. & CANN,J.R. 1974. Chilling statistics indicate an ocean floor spreadin origin for the Troodos Complex, Cyprus. Earth Planet Sci.Lett., 24, 151-155.

KINSMAN,D.J.J. 1976. Evaporites: relative humidity control of primary mineral facies. J.sediment.Petrol., 46, 273-279.

KLUYVER,H.M. 1969. Report on a regional geological mapping in Paphos District. Cyprus Geol.Surv.Dept.Bull., 4, 21-36.

LABOREL,J. 1961. La concretionnement algal coralligene et son importance geomorphologique en Mediterranee. Recl.Trav.Stn.Mar.Edoume Bull., 37, 37-60.

LAJOIE,J. 1972. Slump fold axis orientations: an indication of palaeoslope? J.sediment.Petrol., 42, 584-586.

LE PICHON,X. & ANGELIER,J. 1979. Hellenic arc and trench system. A key to the neo-tectonic evolution of the East Mediterranean. Tectonophys., 60, 1-42.

LEWIS,K.B. 1971. Slumping on a continental slope inclined at 1-4 degrees. Sedimentology, 16, 97-110.

LIVERMORE,R.A. & SMITH,A.G. 1985. Some boundary conditions for the evolution of the Mediterranean region. In: Stanley,D.J. & Wezel,F. (eds.), The geological evolution of the Mediterranean Basin, Springer-Verlag, Berlin.

LOWE,D.R. 1976a. Subaqueous liquified and fluidised sediment flows and their deposits. Sedimentology, 23, 285-308.

LOWE,D.R. 1976b. Grainflow and grainflow deposits. J.sediment.Petrol., 46, 188-199.

LOWE,D.R. 1982. Sediment gravity flows: II Depositional models with special reference to the deposits of high density turbidity currents. J.sediment.Petrol., 52, 279-297.

MAIKLEM,W.R. 1968. Some hydraulic properties of bioclastic carbonate grains. Sedimentology, 10, 101-109.

MAKRIS,J., BEN-AVRAHAM,Z., BEHLE,A., GINZBURG,A., GIESE,P., STEINMETZ,L., WHITMARSH,R.B. & ELEFTHERIOU,S. 1983. Seismic refraction profiles between Cyprus and Israel, and their interpretation. Geophys.J.R.astr.Soc., 75, 575-591.

MANTIS,M. 1970a. Upper Cretaceous-Tertiary foraminiferal zones in Cyprus. Epithris, 3, Cyprus Research Centre, Nicosia, 227-241.

MANTIS,M. 1970b. Composite stratigraphic range chart of foraminifera in the exploration boreholes from Ypsonas-Episkopi-Akrotiri area. Ann.Rep.geo.Surv.Dep.Cyprus 1969, Appendix 6.

MARTINI,E. 1971. Standard Tertiary and Quaternary calcareous nannoplankton zonation. In: FORINAL,A. (ed.) Proc. Second Plankt.Conf., Roma, 1970, Editioni Tecnoscienza, Rome, 739-785.

McILREATH,I.A. & JAMES,N.P. 1979. Carbonate slopes In: Walker,R.G. (ed.), Facies models, Geoscience Canada Reprint Series, 1, 133-143.

McKENZIE,D.P. 1970. Plate tectonics of the Mediterranean region. Nature, 226, 239-243.

MEULENKAMP,J.E. & ZACHARIASSE,W.J. 1973. Stratigraphic and structural framework of the Messinian deposits on Crete. In: Drooger,C.W. (ed.), Messinian events in the Mediterranean., North-Holland, Amsterdam. 202-205.

MONTADERT,L. LETOUZEY,J. & MAUFFRET,A. 1978. Messinian event: Seismic evidence. In; HSU,K.J. & MONTADERT,L. (eds.) Initial Rep.Deep Sea drill.Proj., 42A, 1037-1050.

MOORES,E.M. & VINE,F.J. 1971. The Troodos Massif, Cyprus, and other ophiolites as oceanic crust: evaluation and implications. Philos.Trans.R.Soc.London, A, 268, 433-466.

MOREL,S.W. 1960. The geography and mineral resources of the Apsiou-Akrotiri area. Mem.geol.Surv.Dep.Cyprus, 7, 51-88.

MULDER,C.J. 1973. Tectonic framework and distribution of the Miocene evaporites in the Mediterranean. In: DROOGER,C.W. (ed.) Messinian events in the Mediterranean, North-Holland, Amsterdam. 44-59.

MULDER,C.J., LEHNER,P. & ALLEN,D.C.K, 1975. Structural evolution of the Neogene Mediterranean salt basins in the Eastern Mediterranean and the Red Sea. Geol.Mijnbouw, 54, 208-221.

MULLINS,H.T. & NEUMAN,A.C. 1979. Deep carbonate bank margin structure and sedimentation in the northern Bahamas. Spec.Publ.Soc.econ.Paleontol.mineral., 27, 165-192.

MULLINS,H.T., HEATH,K.C., VAN BUREN,H.M. & NEWTON,C.R. 1984. Anatomy of modern open ocean carbonate slope: Northern Little Bahama Bank. Sedimentology, 31, 141-168.

MURTON,B.J. 1986. Anomalous oceanic lithosphere formed in a leaky transform fault: Evidence from the Western Limassol Forest Complex, Cyprus. J.geol.Soc.London, 143, 845-854.

MURTON,B.J. & GASS,I.G. 1986. Western Limassol Forest Complex, Cyprus: part of an Upper Cretaceous leaky transform fault. Geology, 14, 255-258.

MUTTI,E & GHIBAUDO,G. 1972. Un esempio di torbiditi di conoide sottomarina esterna: le arenarie di San Salvatore (Formazione di Bobbio, Miocene) nell' appennino di Piacenza. Mem.Acc.Sic.Torino, Cl., Sci.Fis.Mat.Nat.,16, 1-40.

MUTTI,E. & RICCI-LUCCHI,F. 1975. Turbidite facies associations. In: Mutti,E., Parea,G.C., Ricci-Lucchi,F., Sagri,M., Sanzucchi,G., Ghibaudo,G. & Jaccarino,S. (eds.), Examples of turbidite facies and facies associations from selected facies of the Northern Appenines., IX Int.Congr.Sedim., Nice, 1975. Field trip A2, 21-36.

MUTTI,E. 1977. Distinctive thin bedded turbidite facies and related depositional environments in the Eocene Hecho Group (South Central Pyrenees), Spain. Sedimentology, 24, 107-131.

NESTEROFF,W.D. 1973. Mineralogy, petrography, distribution and origin of the Messinian Mediterranean evaporites. In: RYAN,W.B.F., HSU,K.J. et al., Initial Rep.Deep Sea drill. Proj. 13, 673-694.

NEUGEBAUER,J. 1974. Some aspects of cementation in chalk. In: Hsu,K.J. & Jenkyns,H.C. (eds.), Pelagic sediments: On land and under the sea, Spec.Publ.Int.Assoc. Sedimentol., 1, 149-176.

OGNIBEN,L. 1957. Petrographia de la serie Solfifera Siciliana e considerazioni geologiche relative. Mem.Descr.Carta Geol. Italia, 33.

ORSZAG-SPERBER,F., ROUCHY,J.M., BIZON,G., BIZON,J.J., CRAVATTE,J. & MULLER,C. 1980. La sedimentation messinienne dans le bassin de Polemi (Chypre). Geologie Mediterraneene, 7, 91-102.

ORTIZ,P.A. 1982. Study of the Miocene planktonic foraminifera of the Pakhna Formation. Internal Report, Univ.Col.London (unpubl.)

OSGOOD,R.G. & SZUMUC,E.J. 1972. The trace fossil Zoophycus as an indicator of water depth. Bull.Am.Paleontol., 62, 1-22.

PAGNIA,H. 1978. Depth of deposition of Messinian selenitic gypsum in the basin of Sorbas, (S.E. Spain). Mem.Soc.geol.Ital., 16, 363-367.

PANTAZIS,Th.M. 1967. The geology and mineral resources of the Pharmakas-Kalavasos area. Mem.geol.Surv.Dep.Cyprus, 8.

PANTAZIS,Th.M. 1978. Cyprus evaporites. In: ROSS,D.A. & NEPROCHNOV,Y.P. (eds.) Initial Rep.Deep Sea drill.Proj., 42B, 1185-1194.

PAPAZACHOS,E.C. & COMNINAKIS,P.E. 1978. Deep structure and tectonics of the Eastern Mediterranean. Tectonophysics, 46, 285-296.

PAREU,G.C. & RICCI-LUCCHI,F. 1972. Residimented evaporites in the Peri-Adriatic trough. Israel J.Earth Sc., 21, 125-141.

PARKER,F.L. 1958. Eastern Mediterranean Foraminifera. Reports of the Swedish Deep Sea Expedition, R. 8., Sediment cores from the Mediterranean Sea and Red Sea, 4, 219-283.

PEDLEY,H.M. 1979. Miocene bioherms and associated structures in the Upper Coralline Limestone of the Maltese islands: Their lithification and palaeoenvironment. Sedimentology, 26, 577-591.

PEDLEY,H.M. 1983. The petrology and palaeoenvironment of the Sortino Group (Miocene) of S.E. Sicily: evidence for periodic emergence. J.geol.Soc.London, 140, 335-350.

PERES,J.M. 1967. Mediterranean benthos In: Barnes,H. (ed.), Oceanogr.mar.biol.ann.rev., 5, 449-533.

PERRODON,A. 1957. Etude geologique des bassins Neogene sublittoraux de l'Algerie occidentiale. Bull.serv.carte geol.Algerie, 12.

PETTIJOHN,F.J. 1975, Sedimentary rocks, Harper & Row, New York.

PHILPOTT,K. 1984. Micropalaeontological investigations of the Miocene of the Evdhimou-Pakhna area, Paphos District, southern Cyprus. Internal Report, Univ.Col. London (unpubl.)

POSTUMA,J.A. 1971. Manual of planktonic foraminifera. Elsevier, Amsterdam.

PRICE,I. 1977. Deposition and derivation of clastic carbonates on a Mesozoic continental margin, Othris, Greece. Sedimentology, 24, 529-546.

READ,J.F. 1985. Carbonate platform facies models. Bull.Am. Assoc.Petrol.Geol., 69,1-22.

READING,H.G. 1978. Sedimentary environments and facies. Blackwell Scientific Publications, Oxford.

RICCI-LUCCHI,F. 1973. Resedimented evaporites: indicators of slope instability and deep basin conditions in Peri-Adriatic Messinian (Appenines foredeep, Italy). In: DROOGER,C.W. (ed.) Messinian events in the Mediterranean, North-Holland, Amsterdam. 142-149.

RICKEN,W. & HEMELBEN,C. 1982. Origin of marl-limestone alternation in south west Germany. In: Einsele,G. & Seilacher,A. (eds.), Cyclic and event stratification, Springer-Verlag, Berlin. 63-71.

RICHTER-BERNBERG,G. 1973. Facies and palaeogeography of the Messinian evaporites in Sicily In: DROOGER,C.W. (ed.) Messinian events in the Mediterranean, North-Holland, Amsterdam. 124-141.

ROBERTSON,A.H.F. 1976. Pelagic shalks and calciturbidites from the Lower Tertiary of the Troodos Massif, Cyprus. J.sediment.Petrol., 46, 1007-1016.

ROBERTSON,A.H.F. 1977a.Tertiary uplift history of the Troodos massif, Cyprus. Bull.geol.Soc.Am., 88, 1763-1772.

ROBERTSON,A.H.F. 1977b. The origin and diagenesis of cherts from Cyprus. Sedimentology, 24, 11-30.

ROBERTSON,A.H.F. 1977c. The Moni Melange, Cyprus: an Olistostrome formed at a destructive plate margin. J.geol.Soc.London, 133, 447-466.

ROBERTSON,A.H.F. & HUDSON,J.D. 1974. Pelagic sediments in the Cretaceous and Tertiary history of Cyprus In: Hsu,K.J. & Jenkyns,H.C. (eds.), Pelagic sediments: on land and under the sea, Spec.Publ.Int.Assoc. Sedimentol., 1, 403-436.

ROBERTSON,A.H.F. & WOODCOCK,N.H. 1979. Mamonia Complex, southwest Cyprus: evolution and emplacement of a Mesozoic continental margin. Bull.geol.Soc.Am., 90, 651-665.

ROBERTSON,A.H.F. & WOODCOCK,N.H. 1986. The role of the Kyrenia Range lineament, Cyprus, in the geological evolution of the Eastern Mediterranean area. Philos. Trans.R.Soc.London, A 317, 141-177.

RODINE,J.D. & JOHNSON,A.M. 1976. The ability of debris, heavy freighted with coarse material, to flow on gentle slopes. Sedimentology, 23, 213-234.

RONA,R.A., HARBISON,R.H., BASSINGER,B.G., SCOTT,R.B. & NALWALK,A.J. 1976. Tectonic fabric and hydrothermal activity of the Mid-Atlantic Ridge, lat. 26N. Geol. Soc.Amer.Bull., 87, 661-674.

ROTSTEIN,Y. 1984. Counter-clockwise rotation of the Anatolian Block. Tectonophys., 108, 71-91.

ROUCHY,J.M. & MONTY,C.L.V. 1979. Stromatolites and cryptalgal laminites associated with Messinian gypsum of Cyprus. In: MONTY,C.L.V. (ed.) Phanerozoic stromatolites, Springel-Verlag, Berlin, Heidelberg, New York, 155-179.

RUIZ-ORTIZ,P.A. 1983. A carbonate submarine fan in a fault controlled basin of the Upper Jurassic, Betic Cordillera, southern Spain. Sedimentology, 130, 33-48.

RYAN,W.B.F., HSU,K.J. et al. 1973. Initial Rep.Deep Sea drill.Proj., 13. U.S. Government Printing Office, Washington.

RYAN,W.B.F., CITA,M.B., DREYFUS,M., RAWSON,.L.L., BURKLE & SAITO,T. 1974. A palaeomagnetic assignment of Neogene stage boundaries and the development of isochronous datum planes between the Mediterranean, the Pacific and Indian Oceans in order to investigate the response of the World Ocean to the Mediterranean "Salinity Crisis". Riv.ital.Paleontol.Stratigr., 80, 631-688.

RYAN,W.B.F. & CITA,M.B. 1978 (eds.). The nature and distribution of Messinian erosional surfaces indicators of a several kilometre deep Mediterranean in the Miocene. Mar.Geol., 27, 193-230.

SADLER,P.M. 1982. Bed thickness and grain size of turbidites. Sedimentology, 29, 37-51.

SANTISTEBAN,C. & TERBENER,C. 1983. Shallow marine and continental conglomerates derived from coral reef complexes after desiccation of a deep marine basin: the Tortonian-Messinian deposits of the Fortuna Basin, S.E. Spain. J.geol.Soc. London, 140, 401-411.

SCHILLING,A.V., STRADNER,H., CITA,M.B. & GAETANI,M. 1978. Stratigraphic investigations of the Late Neogene of Corfu, with special reference to the Miocene-Pliocene boundary, and the geodynamic significance. Mem.Soc.geol.Ital., 16, 279-317.

SCHLAGER,W. & BOLTZ,H. 1977. Clastic accumulation of sulphate evaporites in deep water. J.sediment.Petrol., 47, 600-609.

SCHLAGER,W. & JAMES,N.P. 1978. Low magnesium calcite limestones forming at the deep sea floor, Tongue of the Ocean, Bahamas. Sedimentology, 25, 675-702.

SCHLAGER,W. & CHERMAK,A. 1979. Sediment facies of platform-basin transition, Tongue of the Ocean, Bahamas. Spec.Publ.Soc. econ.Paleontol.Mineral., 27, 193-208.

SCHLANGER,S.O. & DOUGLAS,R.G. 1974. The pelagic ooze-chalk limestone transition and its implications for marine stratigraphy. In: Hsu,K.J. & Jenkyns,H.C. (eds.), Pelagic sediments:on land and under the sea. Spec.Publ.Int.Assoc. Sedimentol., 1, 117-148.

SCHOLLE,P.A. 1977. Chalk diagenesis and its relation to petroleum exploration - oil from chalks, a modern miracle?. Bull.Am. Assoc.Petrol.Geol., 61, 982-1009.

SCHOLLE,P.A., ARTHUR,M.A. & EKDALE,A.A. 1983. Pelagic environment. Mem.Am.Assoc.Petrol.Geol., 33, 619-691.

SCHMALZ,R.F. 1969. Deep water evaporite deposition: genetic model. Bull.Am.Assoc.Petrol.Geol., 55,791-823.

SCHREIBER,B.C. & KINSMAN,D.J.J. 1975. New observations on the Pleistocene evaporites of Montallegro, Sicily, and a modern analogue. J.sediment.Petrol., 45, 469-479.

SCHREIBER,B.C., FRIEDMAN,G.M., DECIMA,A. & SCHREIBER,E. 1976. Depositional environments of Upper Miocene (Messinian) evaporite deposits of the Sicilian basin. Sedimentology, 23, 729-760.

SCHREIBER,B.C. & DECIMA,A. 1978. Sedimentary facies produced under evaporitic environments: a review. Mem.Soc. geol.Ital., 16, 111-126.

SEARLE,D.L. & PANAYIOTOU,A. 1980. Structural implications in the evolution of the Troodos Massif, Cyprus. In: Panayiotou,A. (ed.), Ophiolites, Proc.Int.Ophiolite Symp., Nicosia, Cyprus. 50-60.

SEILACHER,A 1964. Biogenic sedimentary structures In: Imbrie,J. & Newell,N.D. (eds.), Approaches to palaeoecology, John Willey & Sons, New York. 296-316.

SHANMUGAM,G., DAMUTH,J.E. & MOIOLA,R.J. 1985. Is the turbidite facies association scheme valid for interpreting ancient submarine environments? Geology, 13, 234-237.

SHEARMAN,D.J. 1971. Marine evaporites: the calcium sulphate facies. Am.Assoc.Petrol.Geol. Seminar, University of Calgary, Canada.

SHELTON,A.W. & GASS,I.G. 1980. Rotation of the Cyprus microplate. In: Panayiotou,A. (ed.), Ophiolites, Proc.Int. Ophiolite Symp., Nicosia, Cyprus. 61-66.

SHINN,E.A. 1983. Tidal flat. Mem.Am.Assoc.Petrol.Geol., 33, 171-210.

SIMONIAN,K.A. & GASS,I.G. 1978. Arakapas fault belt, Cyprus: a fossil transform belt. Geol.Soc.Amer.Bull., 89, 1220-1230.

SLOSS,L.L. 1969. Evaporite deposition from layered solutions. Bull.Am.Assoc.Petrol.Geol., 53, 776-789.

SONNENFELD,P. 1979. Brines and evaporites. Geoscience Canada, 6, 83-90.

SONNENFELD,P. 1984. Brines and evaporites. Academic Press, London.

STANLEY,D.J. 1982. Welded slump-graded sand couplets: evidence for slide generated turbidity currents. Geo-marine Letters, 2, 149-155.

STONE,B.D. 1976. Analysis of slump slip lines and deformation fabric in slumped Pleistocene lake beds. J.sediment.Petrol., 46, 313-325.

STURANI,C. 1978. Messinian facies in the Piedmont Basin. Mem.Soc.geol.Ital., 16, 11-25.

SWARBRICK,R.E. 1980. The Mamonia Complex of S.W. Cyprus: a Mesozoic continental margin, and its relationship with the Troodos Complex. In: Panayiotou,A. (ed.), Ophiolites: Proc.Int.Ophiolite Symp., Nicosia, Cyprus. 86-92.

SWARBRICK,R.E. & ROBERTSON,A.H.F. 1980. Revised stratigraphy of the Mesozoic rocks of southern Cyprus. Geol.Mag., 117, 547-563.

TWENHOFEL,W.H. 1950. Principles of sedimentation, McGraw-Hill, New York.

UNDERHILL,J. 1985. Neogene and Quaternary tectonics and sedimentation in Western Greece. Unpub. PhD thesis, University College, Cardiff.

URQUHART,E. 1984. Miocene foraminifera from the Pakhna Formation, Cyprus. Internal Report, Univ.Col.London (unpubl.)

VAI,G.B. & RICCI-LUCCHI,F. 1977. Algal crusts, autochthonous and clastic gypsum in a cannibalistic evaporite basin: a case history from the Messinian of north Appenines. Sedimentology, 24, 211-244.

WALKER,R.G. 1975. Generalised facies models for resedimented conglomerates of turbidite association. Bull.geol. Soc.Am., 86, 737-748.

WALKER,R.G. 1978. Deep water sandstone facies and ancient submarine fans: models for exploration for stratigraphic traps. Bull.Am.Assoc.Petrol.Geol., 62, 932-966.

WALKER,R.G. & MUTTI,E. 1973. Turbidite facies associations In: Middleton,G.V. & Bouma,A.H. (eds.), Turbidites and deep water sedimentation. Soc.econ.Paleontol.Mineral. Short Course Notes. 119-157.

WARREN,J.K. 1982. The hydrological setting, occurrence and significance of gypsum in Late Quaternary salt lakes in south Australia. Sedimentology, 29, 609-638.

WATSON,G.S. 1966. The statistics of orientation data. J.Geology, 74, 786-797.

WILSON,R.A.M. 1959. The geology of the Xeros-Troodos area. Mem.geol.Surv.Dep.Cyprus, 1.

WILSON,R.A.M. & INGHAM,F.T. 1959. The geology of the Xeros-Troodos area, with an account of the mineral resources. Mem.geol.Surv.Dep.Cyprus, 1.

WOODCOCK,N.H. 1976. Structural style in slump sheets: Ludlow series, Powys, Wales. J.geol.Soc.London, 132, 399-415.

WOODCOCK,N.H. 1979a. The use of slump structures as palaeoslope orientation indicators. Sedimentology, 26, 83-99.

WOODCOCK,N.H. 1979b. Size of submarine slides and their significance. J.Struct.Geol., 1, 137-142.

WOODSIDE,J.H. 1978. Tectonic elements and crusts of the Eastern Mediterranean Sea. Mar.Geophys.Res., 3, 317-354.

WRAY,J.L. 1979. Palaeoenvironmental reconstructions using benthic calcareous algae. Bull.Cent.Rech.Explor.Prod. Elf-Aquitaine, 3, 873-879.

WRIGHT,V.P. & WILSON,R.C.L. 1984. A carbonate submarine-fan sequence from the Jurassic of Portugal. J.sediment. Petrol., 54, 394-412.

PLATE 1 SEM PHOTOGRAPHS SHOWING SOME FEATURES OF THE CALCILUTITES

A. Globigerinid foraminiferal test, extracted from pelagic lime mudstone.

B. Globigerinid foraminiferal test, extracted from pelagic lime mudstone.

C. Close-up of globigerinid test, showing good preservation of detail.

D. Close-up of rugose globigerinid test, showing calcite overgrowth.

E. Close-up of rugose globigerinid test, showing extensive calcite overgrowth.

F. General view of calcilutite, showing compactionally crushed foraminiferal test in coccolithic matrix.

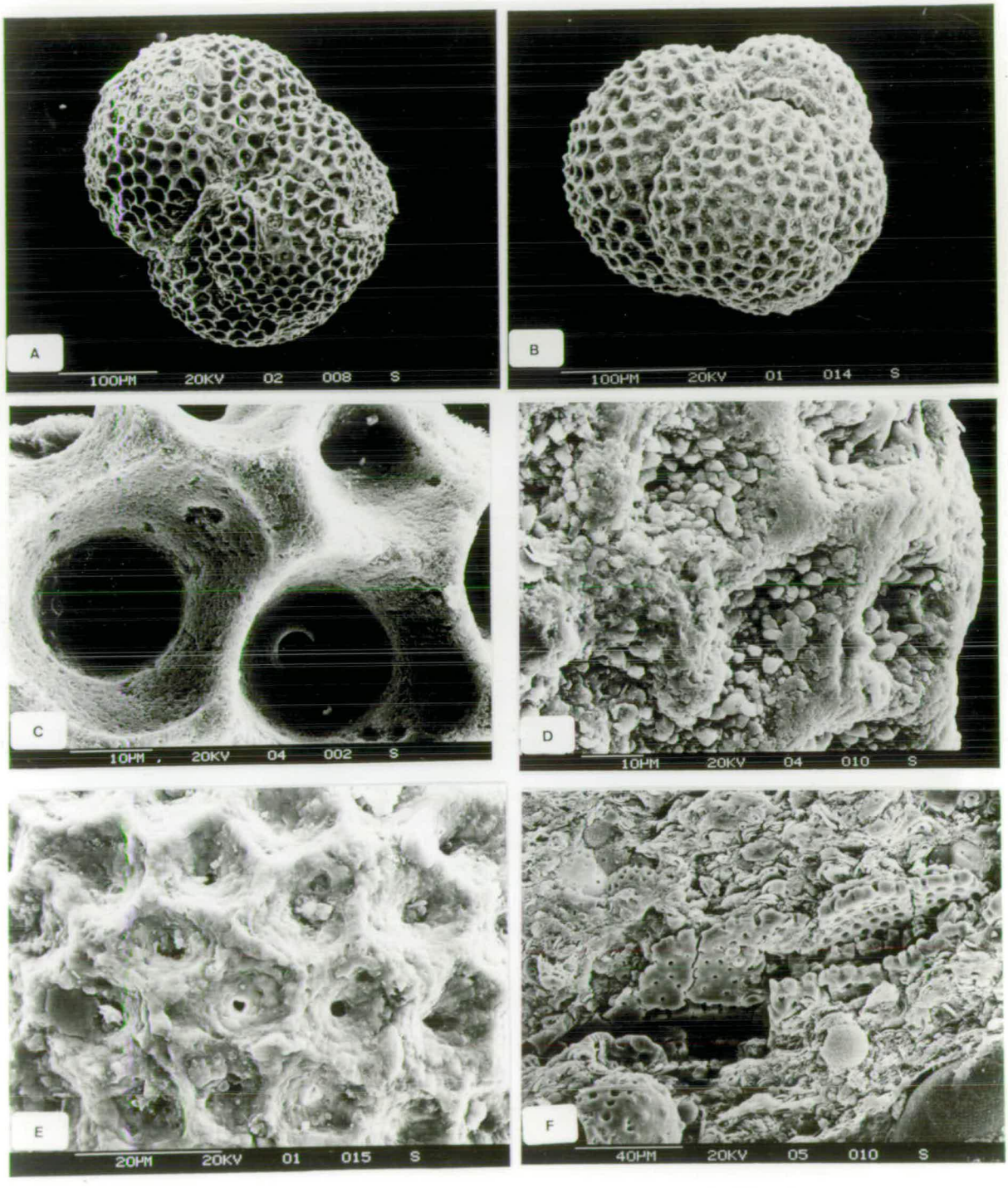
A
100UM 20KV 02 008 S
B
100UM 20KV 01 014 S
C
10UM 20KV 04 002 S
D
10UM 20KV 04 010 S
E
20UM 20KV 01 015 S
F
40UM 20KV 05 010 S

PLATE 1

PLATE 2 PETROGRAPHIC FEATURES OF THE CALCILUTITES

A. Photomicrograph of globigerinid mudstone. Scale bar is 1 mm long. Plane polarised light.

B. SEM photograph of lime mudstone showing coccolithic nature.

C. Recrystallised lime mudstone, with no preservation of original texture. From a sample high up in the Pakhna Formation stratigraphy, and possibly originally rich in shallow water derived aragonitic muds with a high diagenetic potential.

D. SEM photohraph showing coccosphere preserved in a state of partial collapse, as suggested by the arrangement of coccolithic shields.

E. Framboidal pyrite growing in the aperture of a benthic foraminifera.

F. Framboidal pyrite on plant fragment.

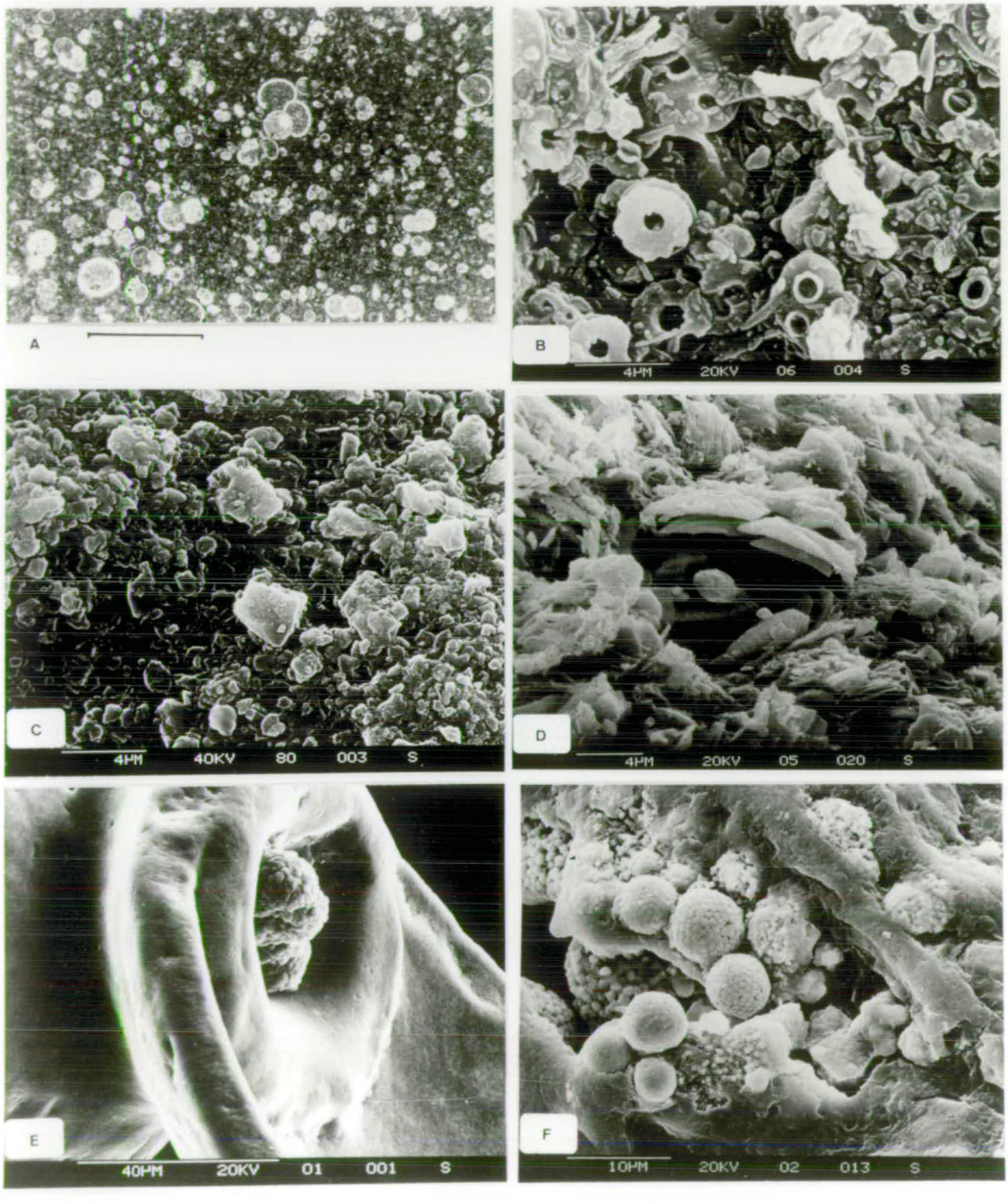
A
B
4μM 20KV 06 004 S
C
4μM 40KV 80 003 S
D
4μM 20KV 05 020 S
E
40μM 20KV 01 001 S
F
10μM 20KV 02 013 S

PLATE 2

PLATE 3 PHOTOMICROGRAPHS OF CALCARENITES

A. Foraminiferal grainstone, from a thin-bedded calcarenite, deposited by a turdidity current and indicating reworking of pelagic chalks from upslope. Sample CYY-185, from the Kisoussa road section, Khalassa sub-basin. Plane polarised light. Short side of photograph is 1 mm across.

B. Turbidite containing bioclastic grains of neritic origin, including branching coralline algae fragments, large benthic foraminifera and echinoderm debris. Sample CYY-116, plane polarised light, short side of photograph is 1.5 mm across.

C. Bryozoan fragment (b) encrusted by coralline algae (a). From a bioclastic grainstone of the Koronia Limestone, sample CYY-126. Plane polarised light, short side of photograph is Ø.7 mm across.

D. Shell fragment (S) with micritic envelope has been exsolved and partially replaced with sparry calcite cement. Uncompacted nature of exsolved shell and coated peloids (P) indicates early cementation. Sample CYX-3Ø, Koronia Limestone, Khalassa sub-basin. Plane polarised light. Short side of photograph is 1 mm across.

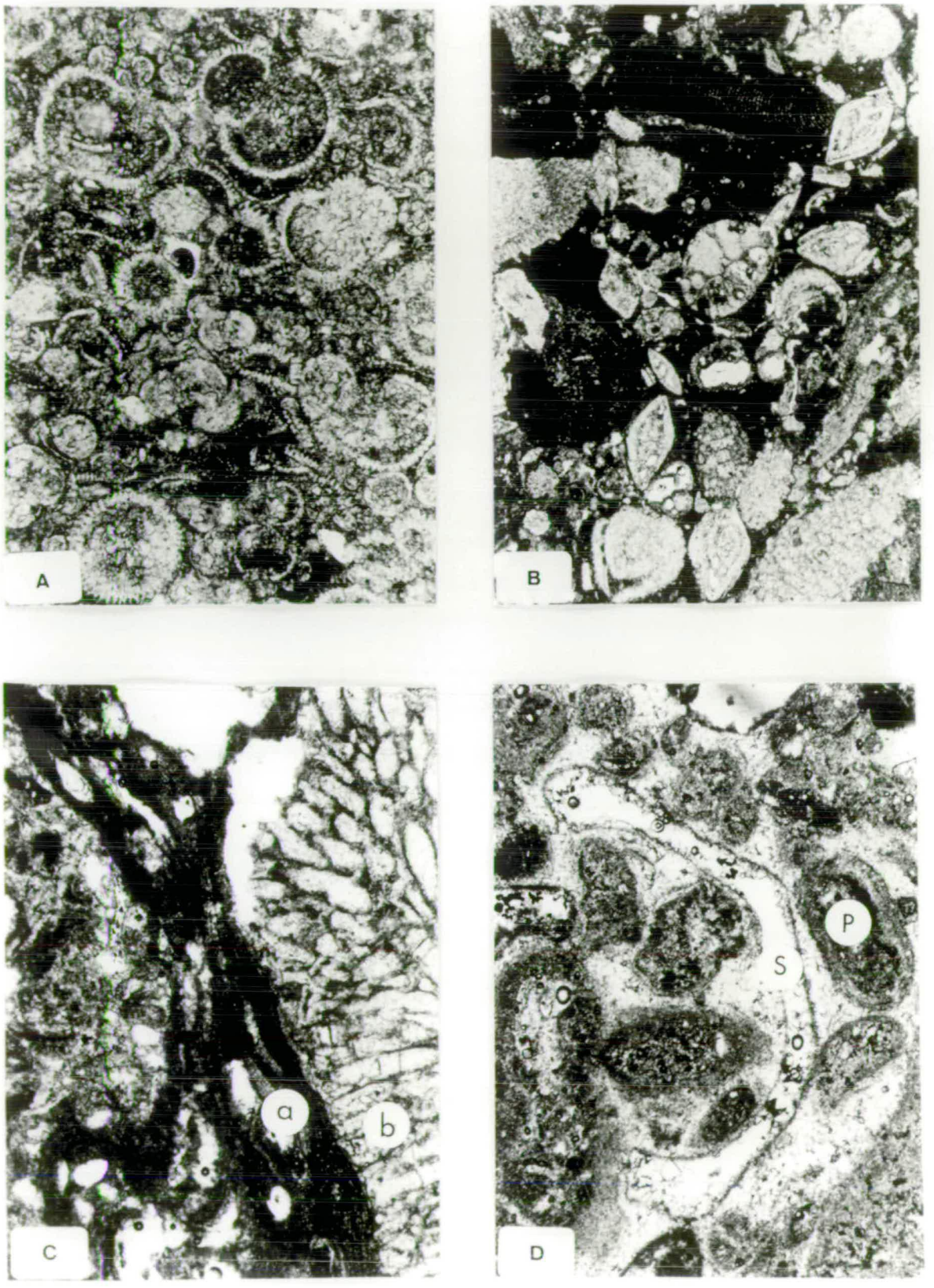

PLATE 3

PLATE 4 PHOTOMICROGRAPHS OF THE KORONIA LIMESTONE.

A. Coral fragment (C) has been infilled with carbonate mud and fine carbonate debris similar to the matrix (M), and encrusted with serpulids (S) and coralline algae (A). Subsequently, dissolution of the aragonitic coral fragment has created a secondary mouldic porosity. Sample CYZ-98, Maroni sub-basin. Plane polarised light. Short side of photograph is 3 mm across.

B. Geopetal fill within shell in peloidal mudstone. Sequence of void-filling events is: precipitation of fringing fibrous calcite cement (I), in-filtering of geopetal fill (II). The shell fragment was then exsolved prior to the deposition of a void filling coarse sparry calcite cement (III). Sample CYY-112, Maroni sub-basin. Plane polarised light. Short side of photograph is 1.5 mm across.

C. As for A above (and from the same sample), but showing encrustation of coral fragment by coralline algae, both of which have been bored (B), possibly by a bivalve. The boring organism was later itself encrusted by coralline algae. Plane polarised light. Short side of photograph is 2.5 mm across.

D. As for B above (and from the same sample), but showing section through serpulid worm tube (S) with early fibrous calcite cement (I), micritic peloidal geopetal fill (II), and later void-filling sparry calcite cement. Plane polarised light. Short side of photograph is 2 mm across.

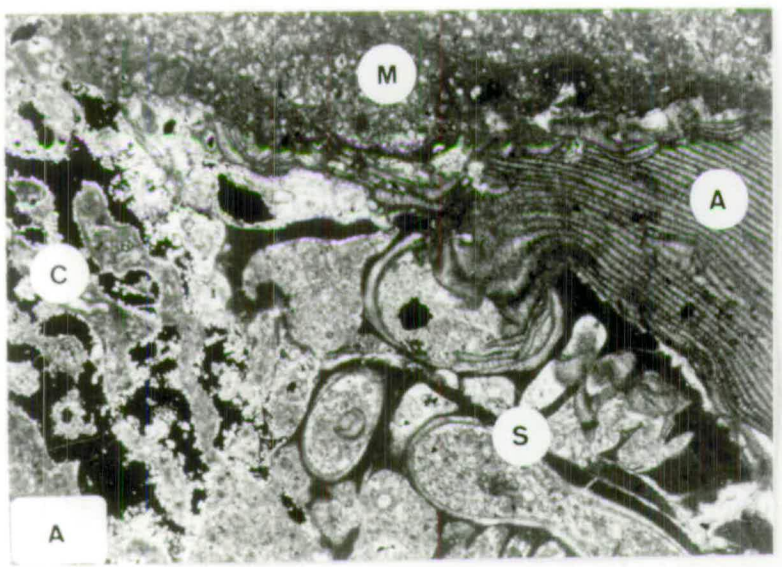

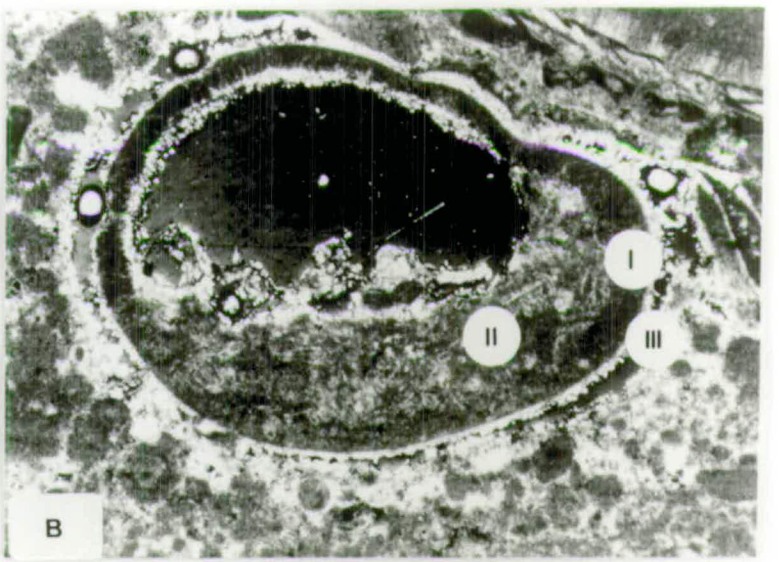

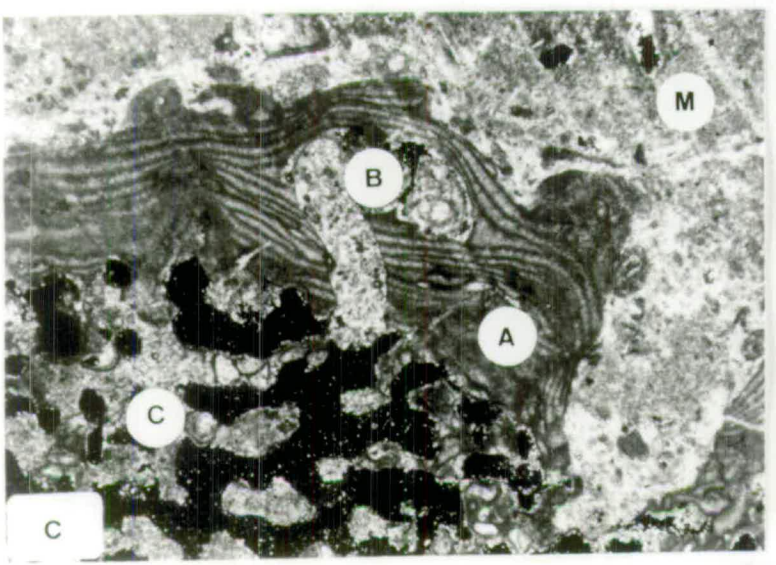

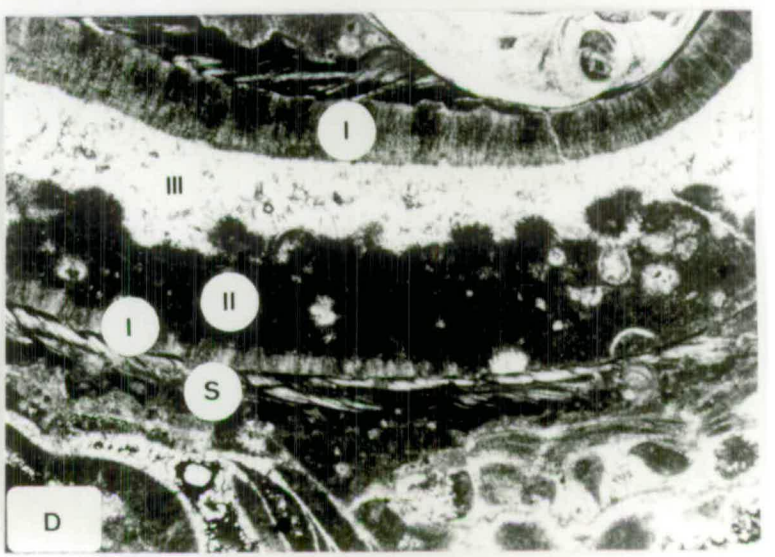

PLATE 4

PLATE 5 PHOTOMICROGRAPHS

A. Plagioclase-phyric lava clast derived from the Troodos ophiolite. From calcirudite CYY-76, Maroni sub-basin. Plane polarised light. Short side of photograph is 2 mm across.

B. Laminated pelsparite. From sample CYZ-45, Maroni sub-basin. Plane polarised light, short side of photograph is 1 mm across. See also Appendix 3 for isotope data.

C. Clastic gypsum deposit, with granular gypsum grains and admixed coated carbonate grain (O) and foraminiferal test (F). Sample CYY-10Ø, Maroni sub-basin. . Crossed polars. Short side of photograph is 1 mm across. See also plate 15D.

D. Parallel laminated gypsum with longitudinal sections through some acicular crystals. No carbonate material. Sample CYY-9Ø, Maroni sub-basin. Crossed polars. Short side of photograph is 1 mm across.

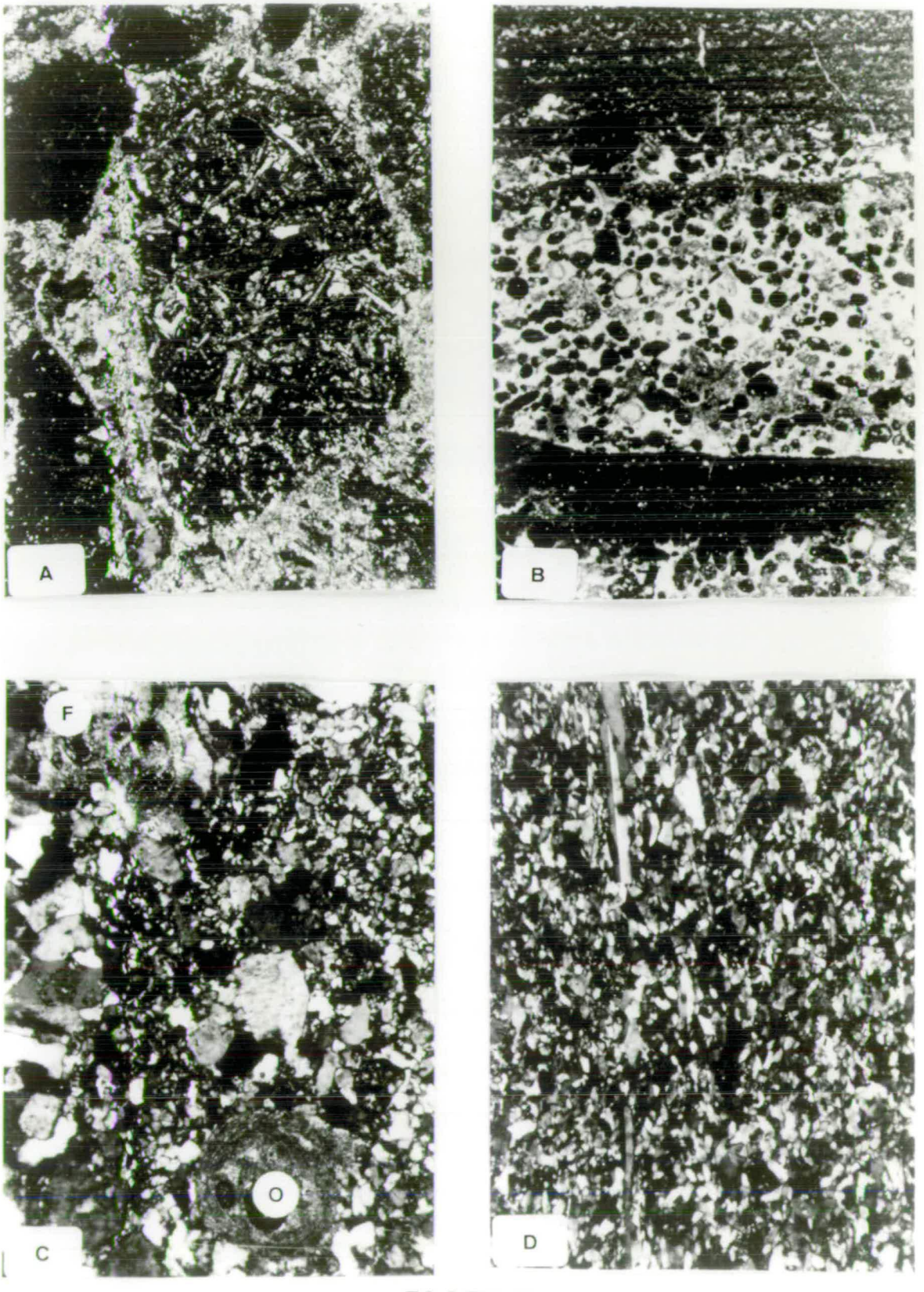

PLATE 5

PLATE 6 FIELD PHOTOGRAPHS

A. Road section near Kisoussa, showing monotonous lime mudstone sequence of the basin plain facies association. Khalassa sub-basin.

B. Bioturbated thin-bedded calcarenites in lime mudstone sequences. Basin plain facies association, Khalassa sub-basin.

C. Erosion of lime mudstone substrate by pebbly calcarenite. Soft substrate-derived lime mudstone clasts are incorporated into the calcarenite (behind hammer). Kouris River, Khalassa sub-basin.

D. Channelised graded calcarenites thinning towards channel margin. Basin margin facies association, Khalassa sub-basin.

E. Amalgamated graded calcarenites with "floating block" of Lefkara chalk (behind hammer). Basin margin facies association, Khalassa sub-basin.

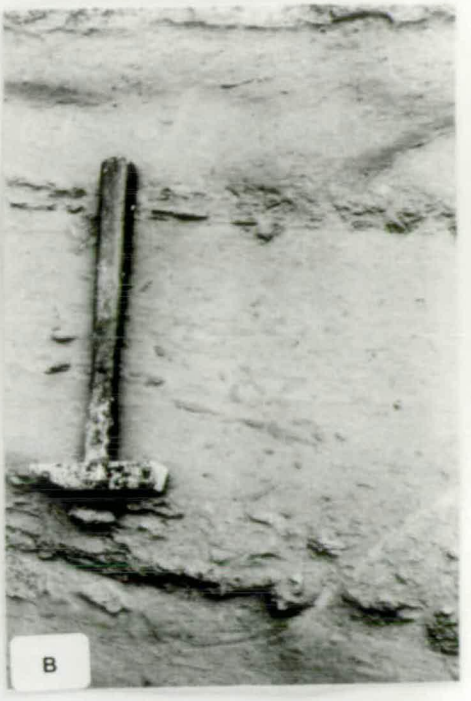

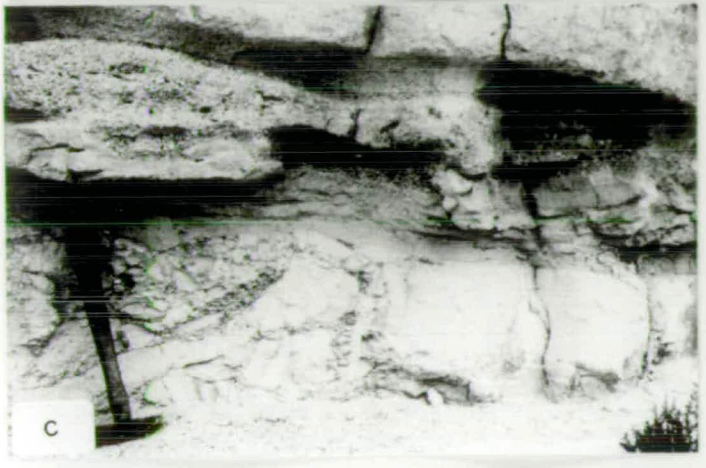

PLATE 6

PLATE 7 GULLIED SLOPE FACIES ASSOCIATION

A. Khirokitia gorge section, showing calcirudites (C) infilling deep channel eroded into marls of the Pakhna Formation (M). Coarse lag (L) marks the base of a second (compounded) channel fill sequence. Trees on sky line are about 2 m high.

B. Inverse grading in a reworked conglomerate of carbonate and igneous clasts. Near Tokhni, Maroni sub-basin.

C. Massive channellised calcarenites at Tokhni.

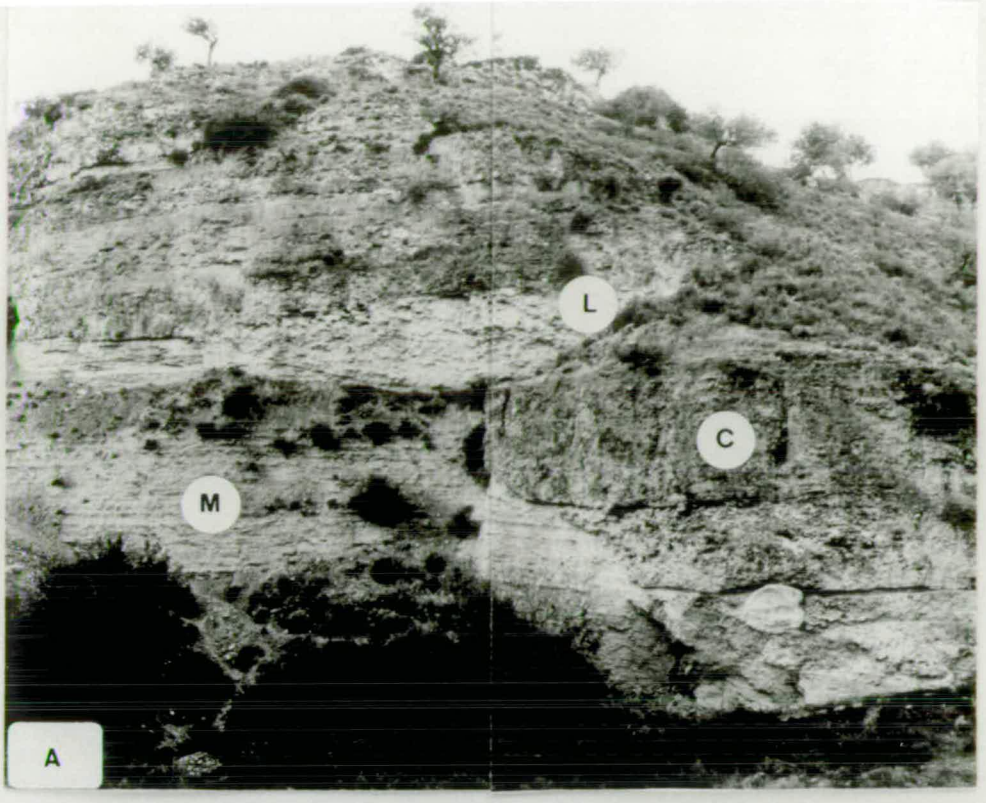

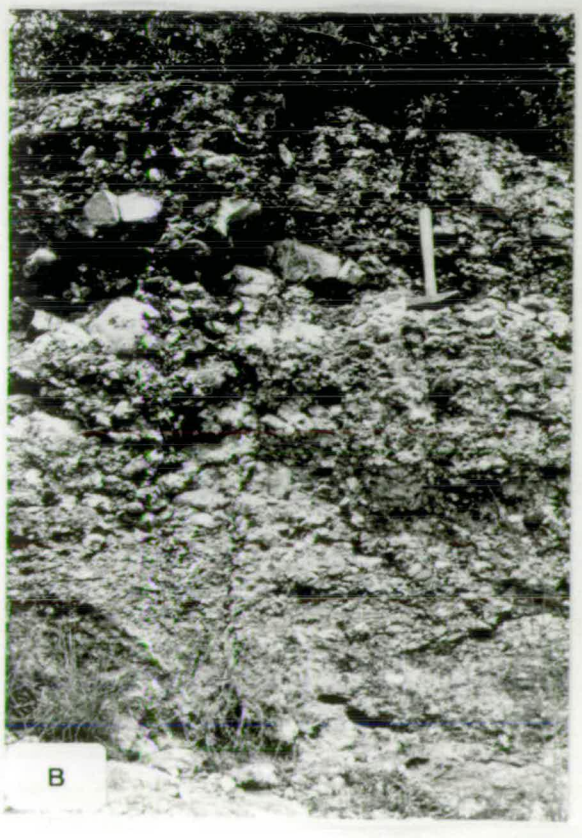

PLATE 7

PLATE 8 FIELD PHOTOGRAPHS

ABOVE - Photo-montage of toe of debris-flow at Happy Valley, with associated small thrusts in the lime mudstone substrate. See Fig. 5.4 for line drawing.

BELOW - Slumped unit passing northwards into a debris-flow, at Ayia Phyla, Khalassa sub-basin. Quarry face is about 10 m high. See Fig. 5.3 for line drawing.

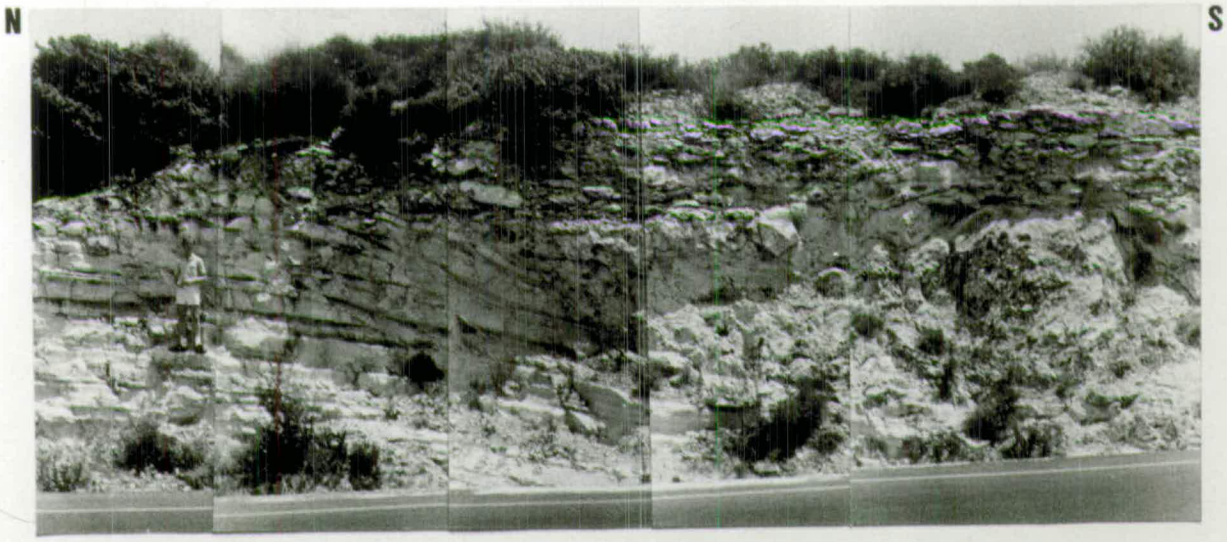

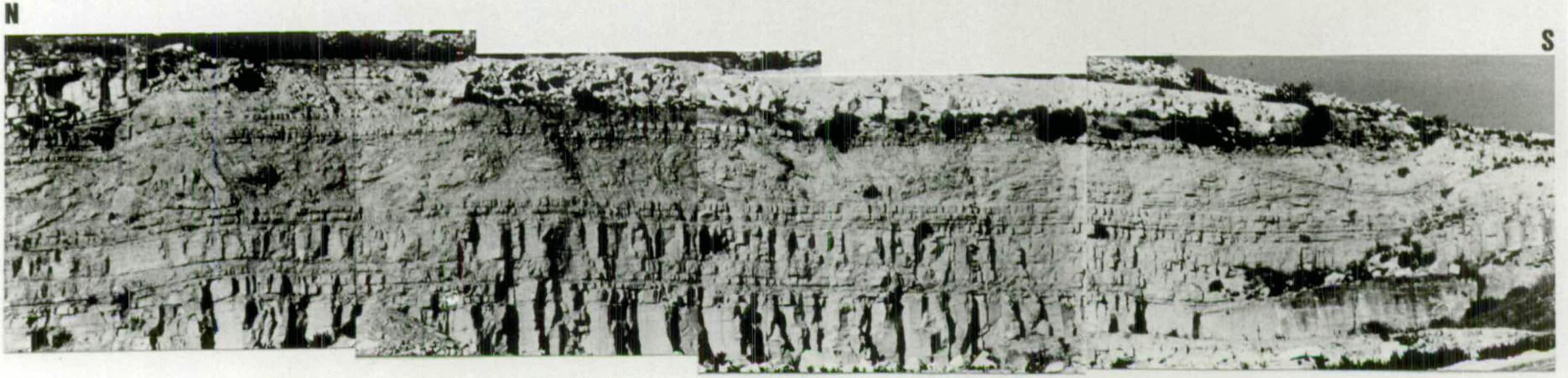

PLATE 8

PLATE 9 SLUMPS

A. Slumped unit at Amathus.

B. Extensional faulting within slumped unit at Amathus.

C. Compressional micro-faulting of slump fold limb, Amathus.

D. Slumped unit exposed at Petrouda Point. Cliff face is 12 m high.

E. Sections through sheath folds in Petrouda Point slump sheet.

F. Slump fold at Ayios Theodhoros. Steve Farrell for scale.

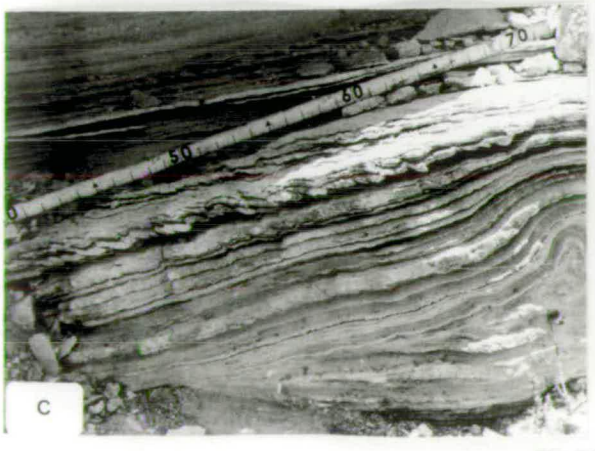

PLATE 9

PLATE 10 FIELD PHOTOGRAPHS

A. Loaded base of massive calcirudite unit deposited upon pelagic chalks. From the basin margin to basin plain transition, Happy Valley, Khalassa sub-basin.

B. Graded calcarenite with pebbly base showing loading. From Ayia Phyla, basin margin facies association, Khalassa sub-basin.

C. View down axis of a channel-fill sequence (Koronia Limestone), cut into marls of the Pakhna Formation. Gullied slope facies association, Amathus, Khalassa sub-basin.

D. Thinning upwards channel-fill sequence of massive calcarenites at Tokhni (quarry face, foreground). Scarp slope in the distance is of Pakhna Formation marlstones and laminated calcilutites capped conformably by gypsum of the Kalavasos Formation.

PLATE 10

PLATE 11 MAMONIA DERIVED CHERT PEBBLES

Photomicrographs illustrating the main pebble varieties found in Pakhna Formation deposits. See section 5.7.3 for discussion.

A. Crossed polars. Short side of photograph is 5 mm across.

B. Crossed polars. Short side of photograph is 5 mm across.

C. Plane polarised light. Short side of photograph is 3 mm across.

D. Crossed polars. Short side of photograph is 2 mm across.

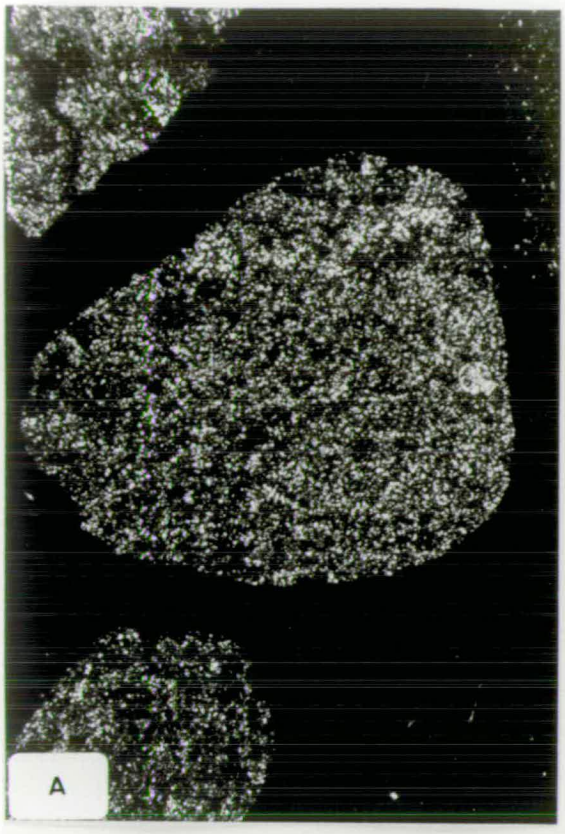

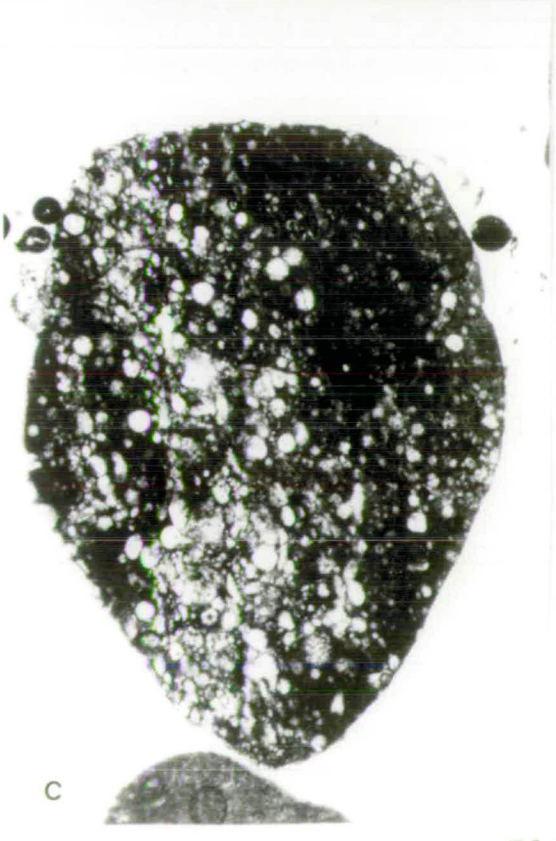

PLATE 11

PLATE 12 MAMONIA DERIVED CHERT PEBBLES

Photomicrographs showing the main varieties of chert pebbles found in Pakhna Formation deposits. See section 5.7.3 for discussion.

A. Crossed polars. Short side of photograph is 2 mm across.

B. Black metalliferous chert pebble (M). Plane polarised light. Short side of photograph is 5 mm across.

C. Crossed polars. Short side of photograph is 5 mm across.

D. Crossed polars. Short side of photograph is 5 mm across.

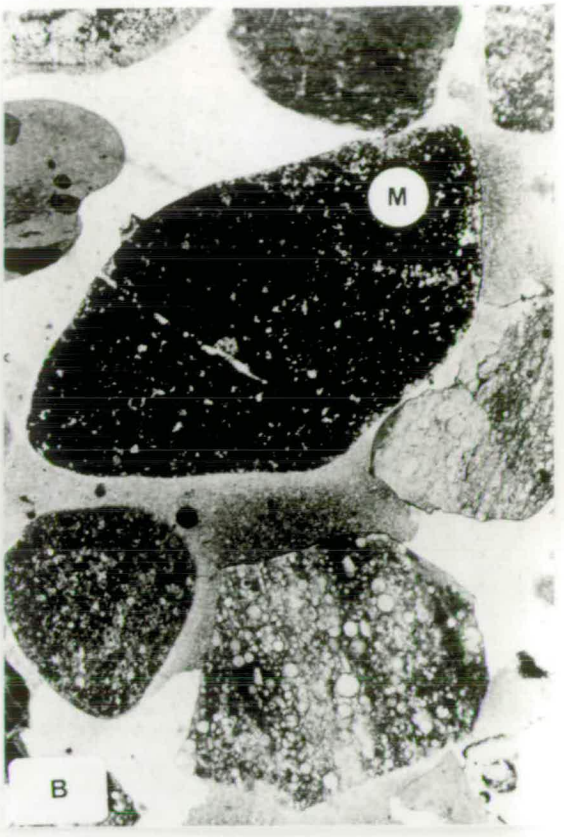

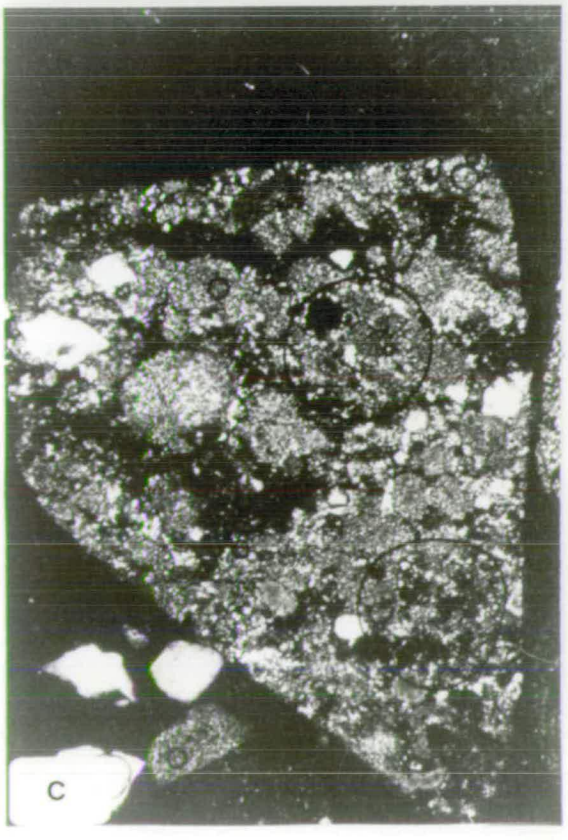

PLATE 12

PLATE 13 MAMONIA COMPLEX CHERT BEARING LITHOLOGIES

Thin sections of Mamonia Complex lithologies collected from outcrops in southwest Cyprus. For comparison with Plates 11 and 12. Samples collected by A.H.F. Robertson and I. Price. All photographed with crossed polars, and all with short side of photograph 5 mm across.

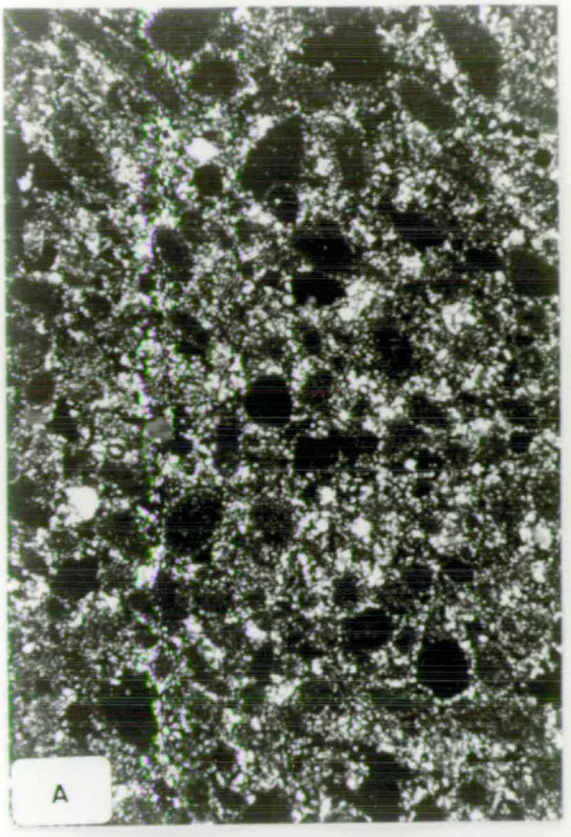

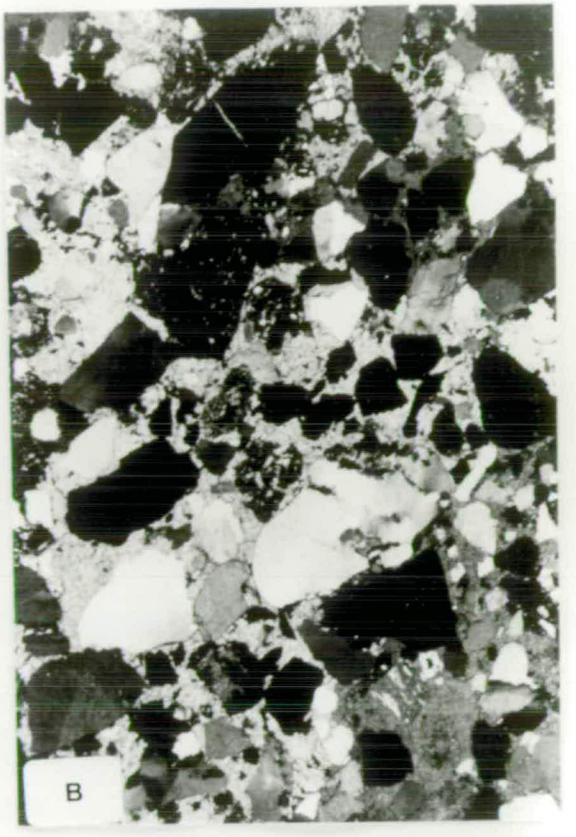

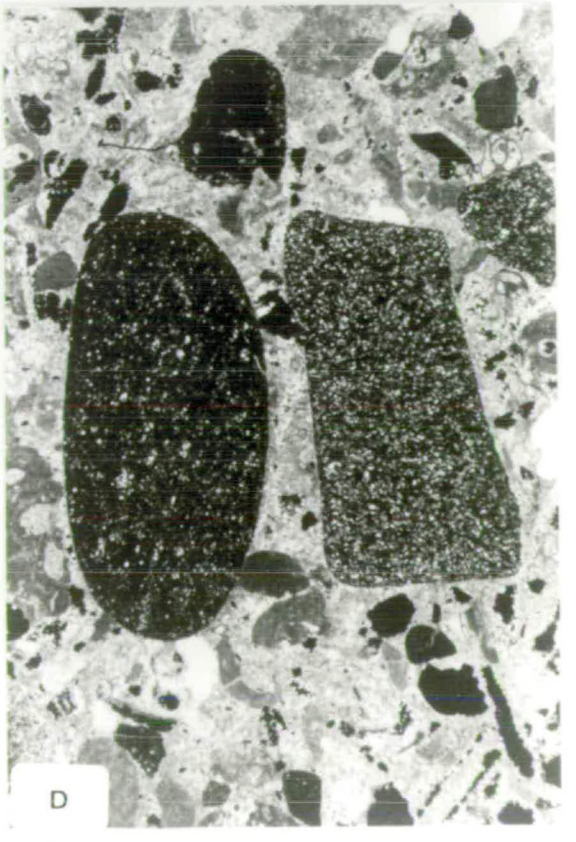

PLATE 13

PLATE 14 THE YERASA FOLD AND THRUST BELT

A. North dipping thrust (F) in the Limassol Forest block, juxtaposing microgabbros (G) over pillow breccias (L). East of Apsiou village.

B. Overturned sequence of pillow lavas (L), umbers (U) and radiolarian cherts (R) of the Perepedhi Formation. East of Apsiou village.

C. View west from high point on the Armenokhori road, showing expression of Miocene unconformity on southern flank of the Yerasa fold and thrust belt. Shallow dipping Pakhna Formation sediments overstep across steeper dipping Lefkara sediments to the north (right hand side of photo).

D. View east from same location. Steep dipping Lefkara Formation sediments form hills on left side. On the sky line (right) are north facing scarps capped with Koronia Limestone as channel-fill sequence of the gullied slope facies association (Amathus).

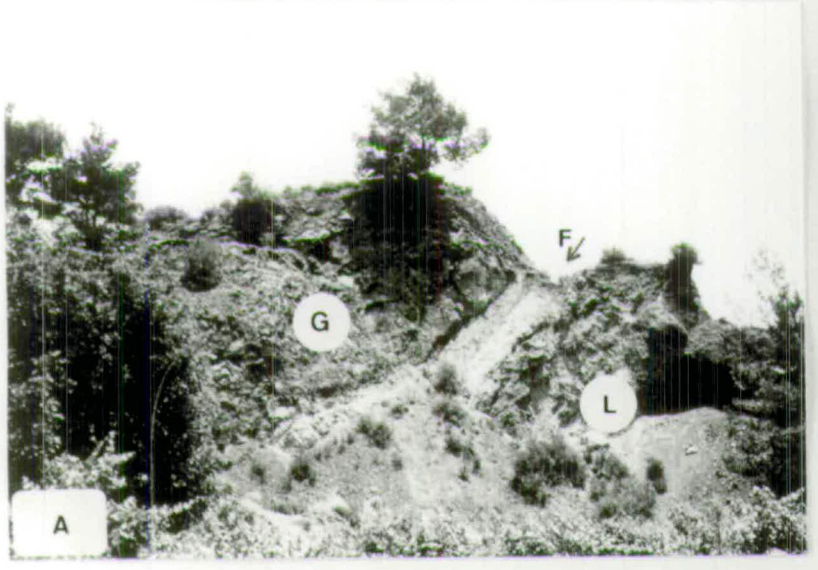

PLATE 14

PLATE 15 EVAPORITES OF THE KALAVASOS FORMATION

A. Spectacular development of selenite, regarded as primary and in-situ (from the Polis Graben)

B. Banded selenite, comprising upwardly radiating twinned selenite crystals with thinly interbedded micritic carbonate. From gypsum surface south of Tokhni, Maroni sub-basin.

C. Freshly exposed parallel laminated gypsum. Kalavasos gypsum quarry, Maroni sub-basin.

D. Clastic gypsum with admixed carbonate peloids and coated grains. Fom west of Tokhni, Maroni sub-basin.

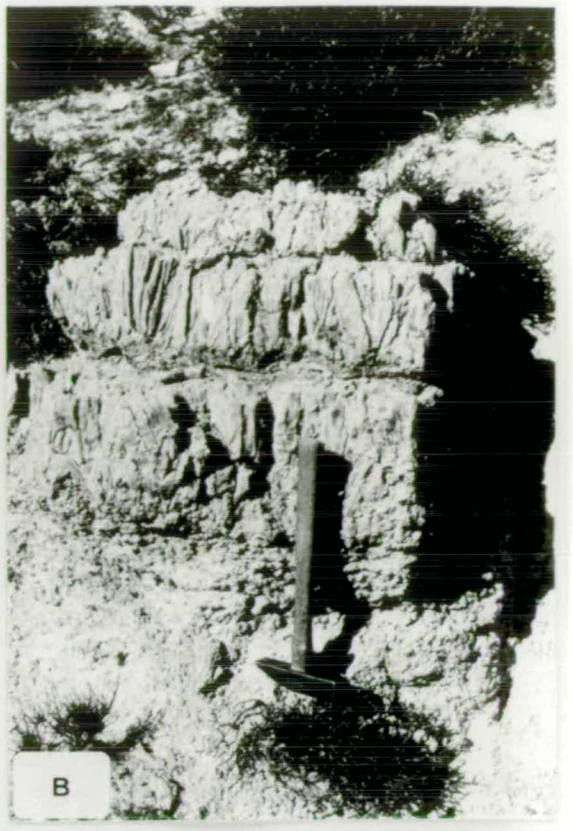

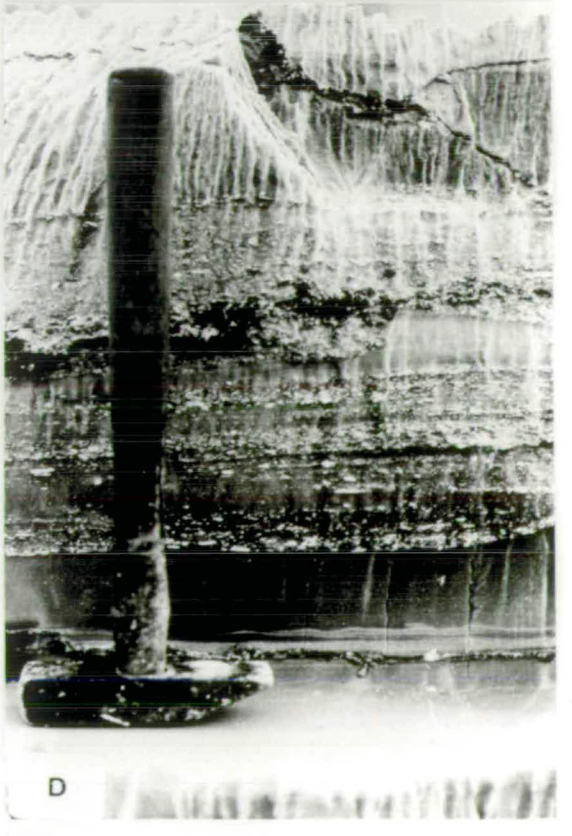

PLATE 15

PLATE 16 EVAPORITES OF THE KALAVASOS FORMATION

A. Graded gypsum beds (turbidites). Maroni gypsum quarry.

B. Loading structures at the base of a graded gypsum bed (turbidite). Polis Graben. Hand lens for scale.

C. Gypsum turbidites draping protruding block of banded selenite at the top of a chaotoc selenite bed (debris-flow). Hammer for scale, centre right. Maroni gypsum quarry. See Fig. 6.8 for line drawing.

D. Gypsum conglomerate overlying laminated gypsum. Polis Graben area.

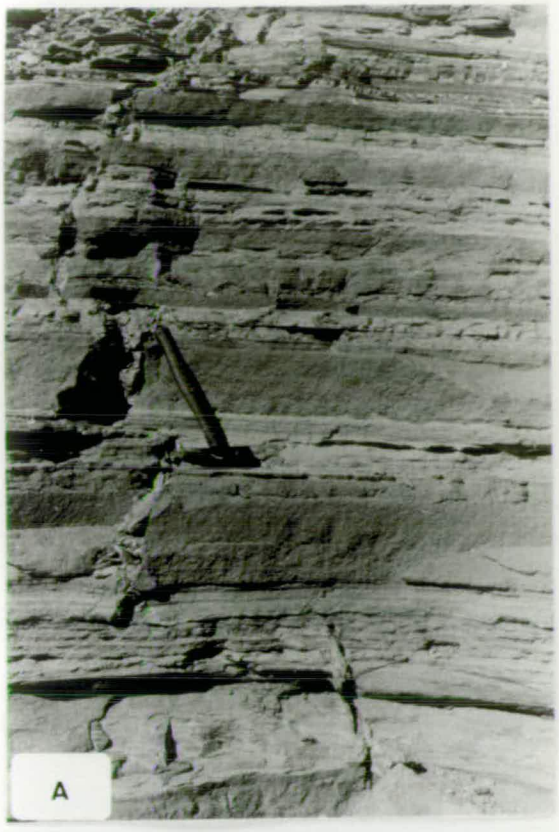

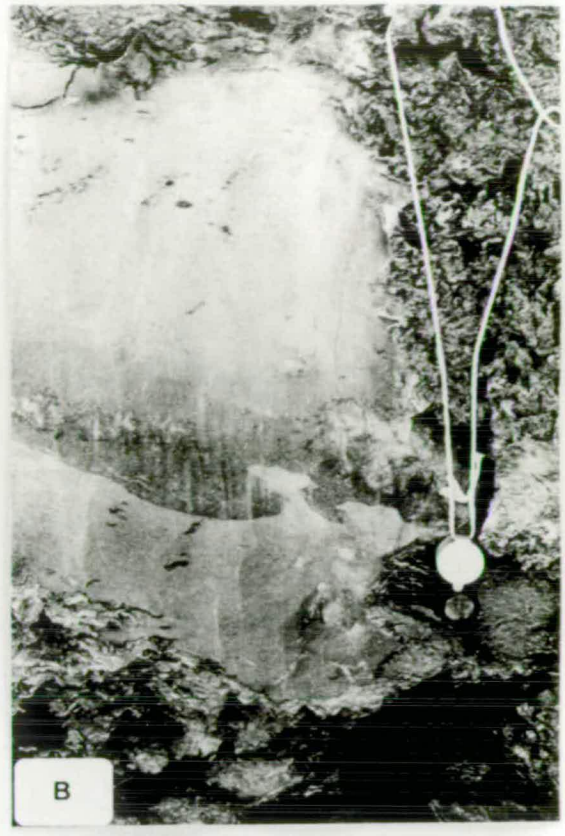

PLATE 16

PLATE 17 EVAPORITES OF THE KALAVASOS FORMATION

A. Nodular laminated gypsum. Kalavasos gypsum quarry.

B. Disaggregated slump fold of laminated gypsum incorporated into clastic gypsum bed. Tokhni gypsum quarry, Maroni sub-basin.

C. Slump folds in laminated gypsum. Polis Graben.

D. Contorted gypsum (slump) at Tokhni qypsum quarry.

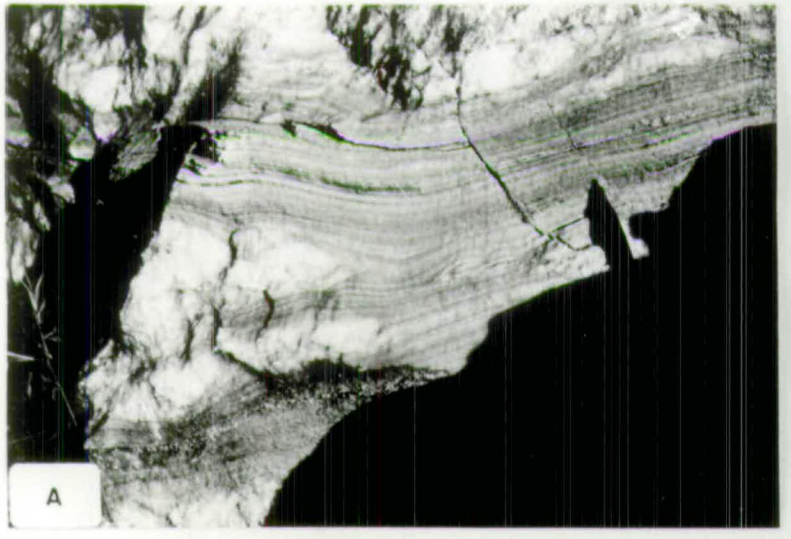

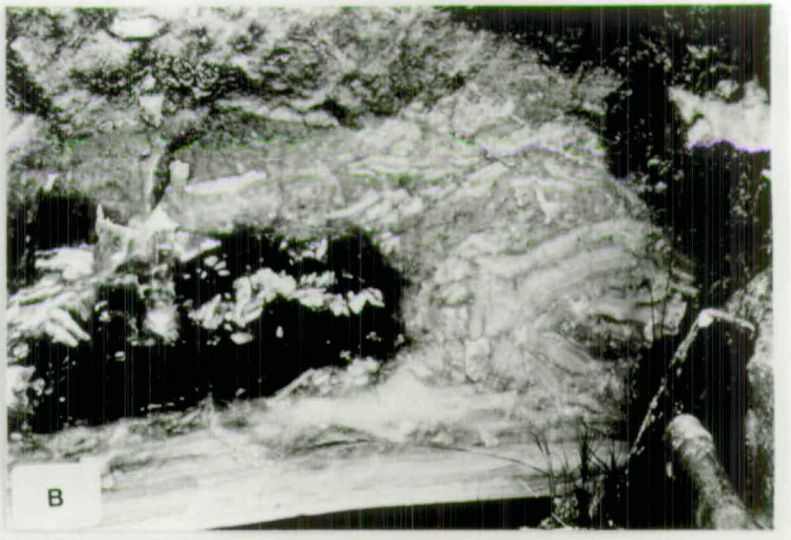

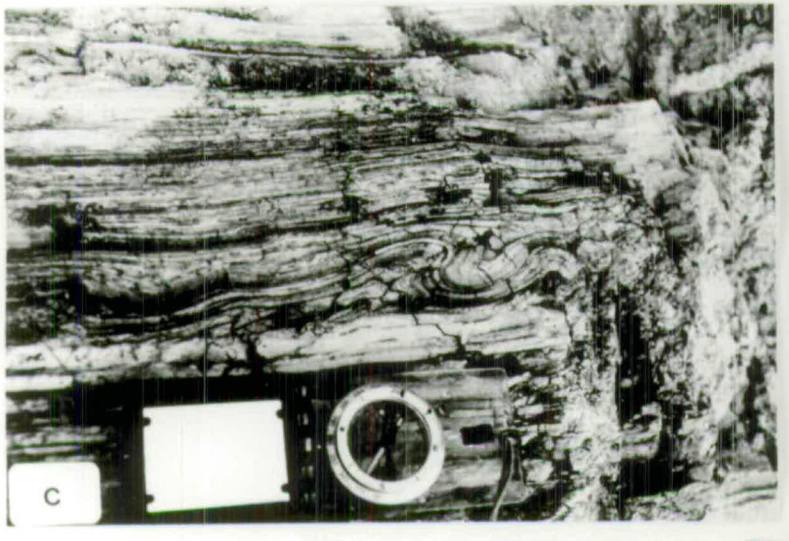

PLATE 17

APPENDIX 1
RANGE CHARTS

The following pages (239-244) contain Neogene foraminiferal range charts from Blow (1969), used for biostratigraphic dating of samples as discussed in chapter two.

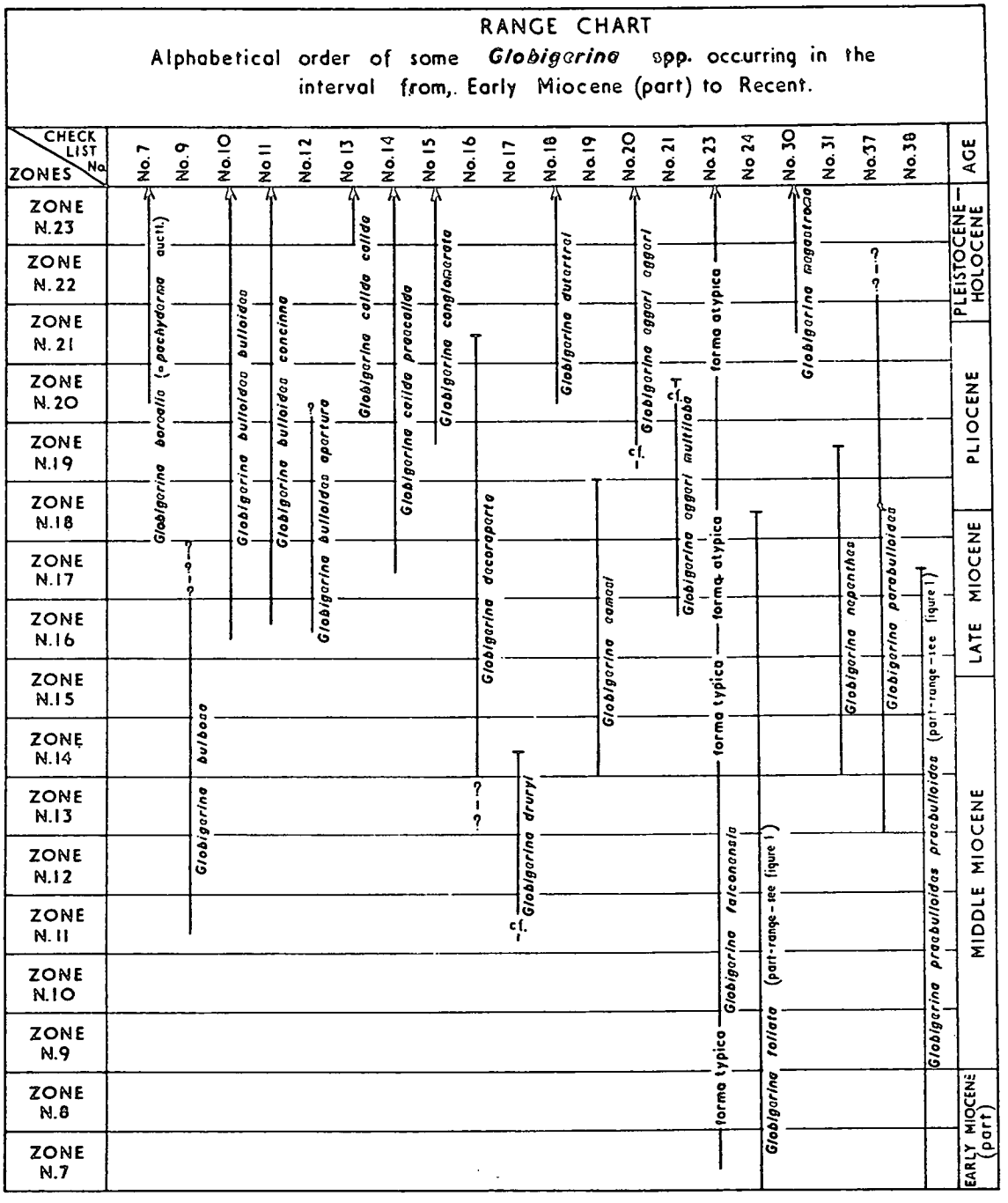

NOTE: – The range of *G. nepenthes* should continue to near the Zone N. 20/Zone N. 19 boundary.

ERRATA: For *G. megastroma* read *G. megastoma*.

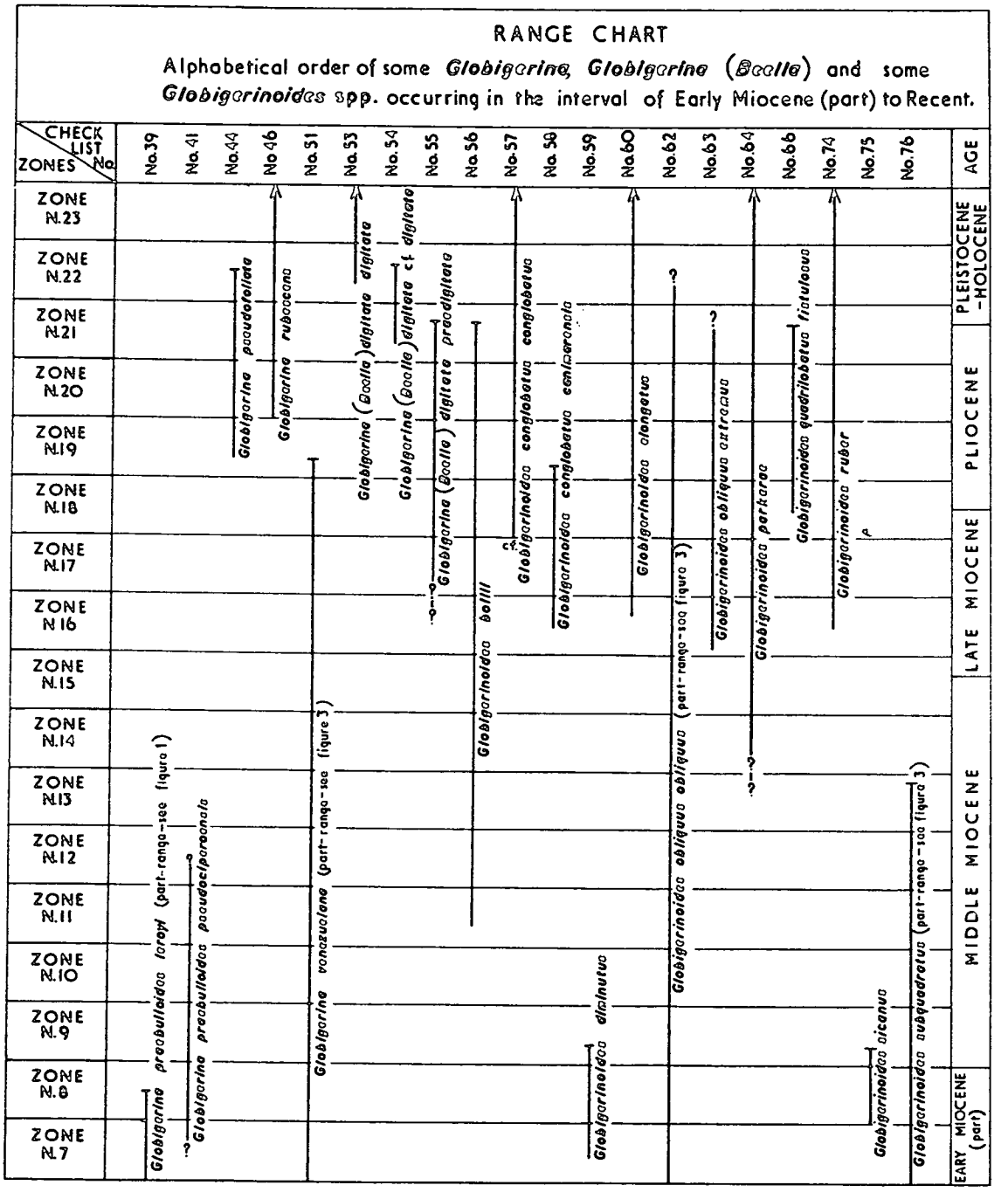

ERRATUM: The range of *Globigerinoides conglobatus conglobatus* as given on Figure 4 was incorrectly drawn. The first occurrence of this form is, as given in the text, within about the middle part of Zone N.17.

RANGE CHART

Alphabetical order of some *Globigerinoides*, *Globigerinita*, *Globigerinatella*, *Praeorbulina*, *Orbulina*, *Candeina*, *Sphaeroidinella* and some *Sphaeroidinellopsis* spp. occurring in the interval from Early Miocene (part) to Recent.

RANGE CHART

Alphabetical order of some *Sphaeroidinellopsis*, *Globoquadrina* and some *Globorotalia* (*Turborotalia*) spp. occurring in the interval from Early Miocene (part) to Recent.

RANGE CHART

Alphabetical order of some *Globorotalia* (*Turborotalia*) , *G.* (*Clavatorella*) and some *Globorotalia* (*Globorotalia*) spp. occurring in the interval of the Early Miocene (part) to Recent

ZONES \ CHECK LIST No.	No.145	No.147	No.148	No.149	No.152	No.153	No.156	No.157	No.158	No.159	No.160	No.161	No.163	No.164	No.165	No.166	No.167	No.168	No.169	No.170	AGE
ZONE N.23																					PLEISTOCENE-HOLOCENE
ZONE N.22																					
ZONE N.21																					
ZONE N.20																					PLIOCENE
ZONE N.19																					
ZONE N.18																					
ZONE N.17																					LATE MIOCENE
ZONE N.16																					
ZONE N.15																					
ZONE N.14																					MIDDLE MIOCENE
ZONE N.13																					
ZONE N.12																					
ZONE N.11																					
ZONE N.10																					
ZONE N.9																					
ZONE N.8																					EARLY MIOCENE (part)
ZONE N.7																					

Globorotalia (*T.*) *aegyri*

Globorotalia (*T.*) *aimica*

Globorotalia (*T.*) *ainulitoidea* (part-range – see figure 9)

Globorotalia (*T.*) *obesa* (part-range – see figure 9)

Globorotalia (*T.*) *peripheroacuta*

Globorotalia (*T.*) *peripheroronda* (part-range – see figure 9)

Globorotalia (*T.*) *acitula gigantea* (part-range – see figure 9)

Globorotalia (*T.*) *acitula praeacitula* (part-range – see figure 9)

Globorotalia (*T.*) *acitula acitula*

Globorotalia (*T.*) cf. *acitula acitula*

Globorotalia (*T.*) *crotonensis* (part-range – see figure 9)

Globorotalia (*T.*) *puncticulata*

Globorotalia (*T.*) *suberotacea*

Globorotalia (*T.*) *subacitula*

Globorotalia (*T.*) *tosaensis tosaensis*

Globorotalia (*T.*) *tosaensis tosaensis*

Globorotalia (*C.*) *berravatazi*

Globorotalia (*G.*) *cultrata cultrata*

Globorotalia (*G.*) *cultrata cultrata*

Globorotalia (*G.*) *cultrata azilia*

Globorotalia (*G.*) *cultrata limbata*

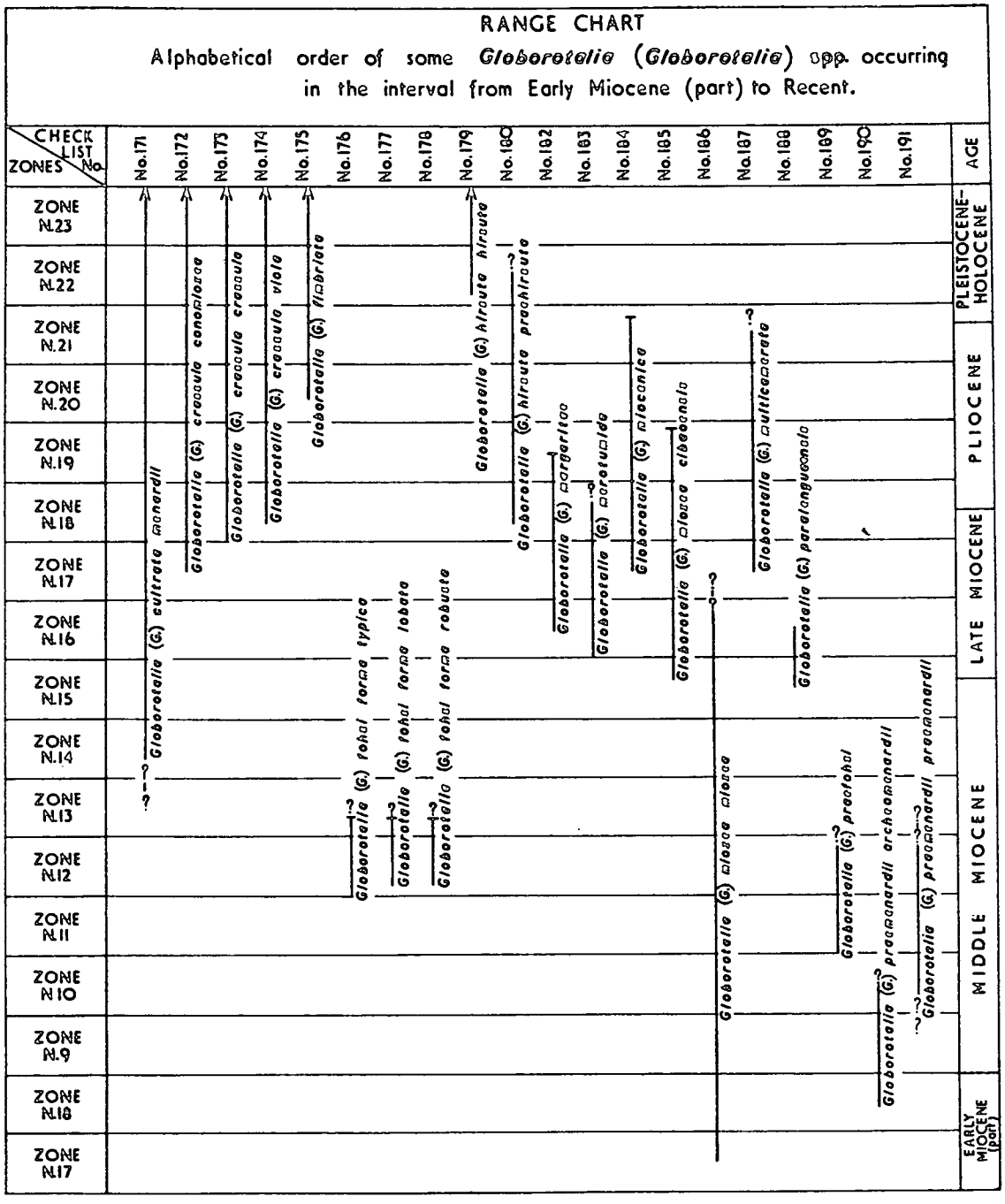
RANGE CHART
Alphabetical order of some Globorotalia (Globorotalia) spp. occurring in the interval from Early Miocene (part) to Recent.
CHECK LIST No.
ZONES
No.171
No.172
No.173
No.174
No.175
No.176
No.177
No.178
No.179
No.180
No.182
No.183
No.184
No.185
No.186
No.187
No.188
No.189
No.190
No.191
AGE
ZONE N.23
ZONE N.22
ZONE N.21
ZONE N.20
ZONE N.19
ZONE N.18
ZONE N.17
ZONE N.16
ZONE N.15
ZONE N.14
ZONE N.13
ZONE N.12
ZONE N.11
ZONE N.10
ZONE N.9
ZONE N.8
ZONE N.7
Globorotalia (G.) cultrata menardii
Globorotalia (G.) crassula conomiozea
Globorotalia (G.) crassula crassula
Globorotalia (G.) crassula viola
Globorotalia (G.) humerosa
Globorotalia (G.) peripheroronda
Globorotalia (G.) peripheroacuta
Globorotalia (G.) scitula scitula
Globorotalia (G.) scitula praescitula
Globorotalia (G.) margaritae
Globorotalia (G.) partimlabiata
Globorotalia (G.) miozea miozea
Globorotalia (G.) miozea conoidea
Globorotalia (G.) miozea archaeomiozea
Globorotalia (G.) miozea praemiozea
Globorotalia (G.) fohsi fohsi typica
Globorotalia (G.) fohsi fohsi lobata
Globorotalia (G.) fohsi fohsi robusta
Globorotalia (G.) fohsi praefohsi
Globorotalia (G.) fohsi praemenardii
Globorotalia (G.) acostaensis
Globorotalia (G.) obesa
Globorotalia (G.) multicamerata
Globorotalia (G.) paralenguaensis
PLEISTOCENE-HOLOCENE
PLIOCENE
LATE MIOCENE
MIDDLE MIOCENE
EARLY MIOCENE (part)

APPENDIX 2

NANNOFOSSIL EXTRACTIONS

Two samples have been analysed for nannofossils by Hilary Stowe of the Micropalaeontology Unit, University College, London. Both samples were collected from laminated calcilutite lithologies at a high stratigraphic position in the Pakhna Formation.

Sample CYZ-122. Collected from top of logged section near Moutayiaka, GR. 100423. Contains an abundant but poorly preserved nannofossil assemblage, with a low identifiable diversity. Identifiable species are:

Umbilicosphaera tenuis
Cyclococcolithus macintyrei
Reticulofenestra pseudoumbilica
Sphenolithus moreformis

These are relatively long ranging species (Middle Miocene to Lower Pliocene).

Sample CYZ-37 This sample was collected from laminated calcilutites at GR 277474, near Kalavasos. Identifiable species include:

Reticulofenestra pseudoumbilica
Cyclococcolithus macintyrei
Cyclococcolithus anisotrema
Sphenolithus moreformis
Coccolithus pelagicus
Helicosphaera kamptrien
Umbilicosphaera mirabilis
Rhabdosphaera clavigera
Reticulofenestra minutula
Scyphosphaera apsteini
Braanidosphaera bigelowi
Discoaster adamanteus
Discoaster challangeri
Discoaster brouwely
Discoaster variabilis

Hilary Stowe writes "Of these Cyclococcolithus macintyrei is very abundant, probably forming about 60% of the total number of specimens, and Sphenolithus moreformis is surprisingly rare. The first and last occurrences of these species suggest a date of between NN11 and NN15

(Martini, 1971). Negative evidence i.e. absence of diagnostic species, further refines this to NN12 to NN13, however, this is not conclusive as species such as Discoaster quinqueranus (NN11) and Discoaster asymmetricus (NN14 and above) may be absent for palaeoenvironmental or preservation reasons. The Ceratoliths, which are usually used to define the two zones over the Miocene-Pliocene boundary, are deeper water genera, and so are likely to be absent for palaeoenvironmental reasons. In conclusion, sample CYZ-37 gives a nannofossil date of NN11 to NN19 (Tortonian to Piacenzian), possibly NN12 to NN13 (latest Messinian to Zanclian).

APPENDIX 3
OXYGEN AND CARBON ISOTOPE DATA

Three samples were analysed for oxygen and carbon isotopes (samples run by K.M. Greig and J. Andrews). These samples are:

CYX-11 A powdered whole-rock sample from a 20 cm gypsiferous white marl bed within the evaporite sequence at Tokhni gypsum quarry.

CYY-37 A powdered whole-rock sample of matrix material supporting disorganised selenite laths, from the Kalavasos formation near Ayia Mavri.

CYZ-45 A laminated pelsparite limestone from the top of the Pakhna Formation near Kalavasos, at GR 277474. Four samples were extracted and analysed separately from this one specimen. These are SE1, SE2, SE3 (each consisting of micrite drilled from peloids) and SE4 (consisting of spar drilled from the specimen).

Results are:

SAMPLE	DELTA C13 (PDB)	DELTA O18 (PDB)
CYX-11	-1.76	+0.01
CYY-37	+0.95	+2.31
SE1	-1.70	-0.36
SE2	-1.57	-0.02
SE3	-1.41	-0.34
SE4	-1.46	-2.12

APPENDIX 4

SELECTED LOGS

The following pages illustrate selected sedimentary logs from the Pakhna Formation. All lithologies are carbonates. With the exception of the Kalavasos road section, the calcilutites have been inked in to emphasize the relative proportions of clastic and hemi-pelagic material. Calcilutites are all bioturbated unless otherwise indicated.

Locations are illustrated in fig. A4.1 (page 258), which also shows the present day outcrop of the facies associations of the Pakhna Formation.

KEY

Loading
Bioturbation
Cross lamination
Marl intraclasts
Carbonate cobbles and boulders
Non-carbonate clasts
Neritic clastic components
Slumping

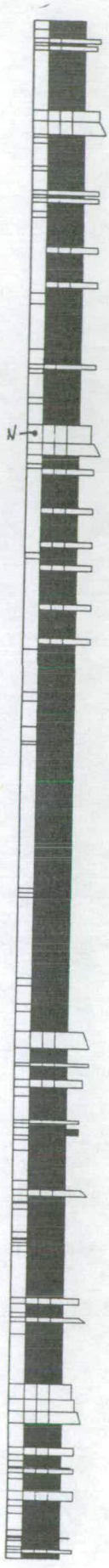

VERTICAL SCALE

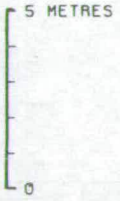

GRAIN SIZE

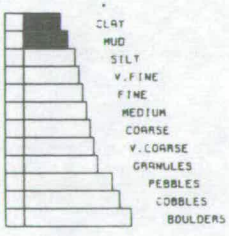

LOG: Kisoussa (road section)
GRID REF: 808516
FACIES ASSOC. Basin plain

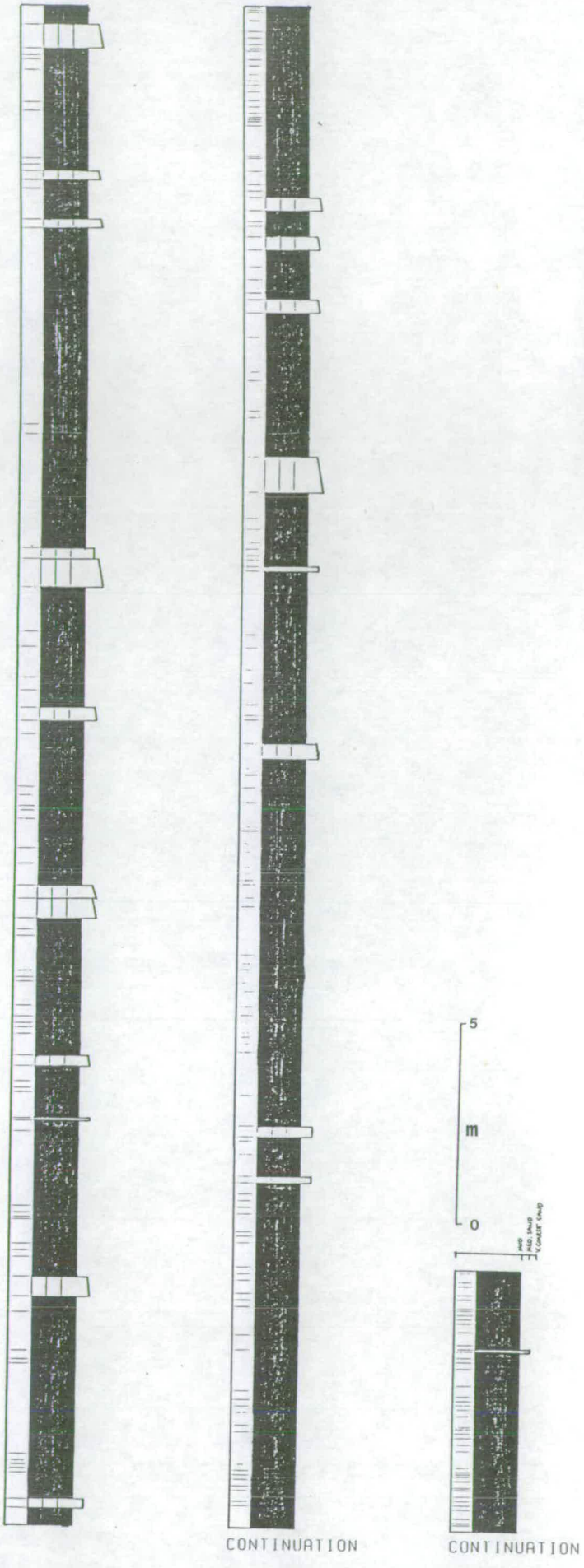

LOG: Ayios Therapon (road section)
GRID REF. 846503
FACIES ASSOC. Basin plain

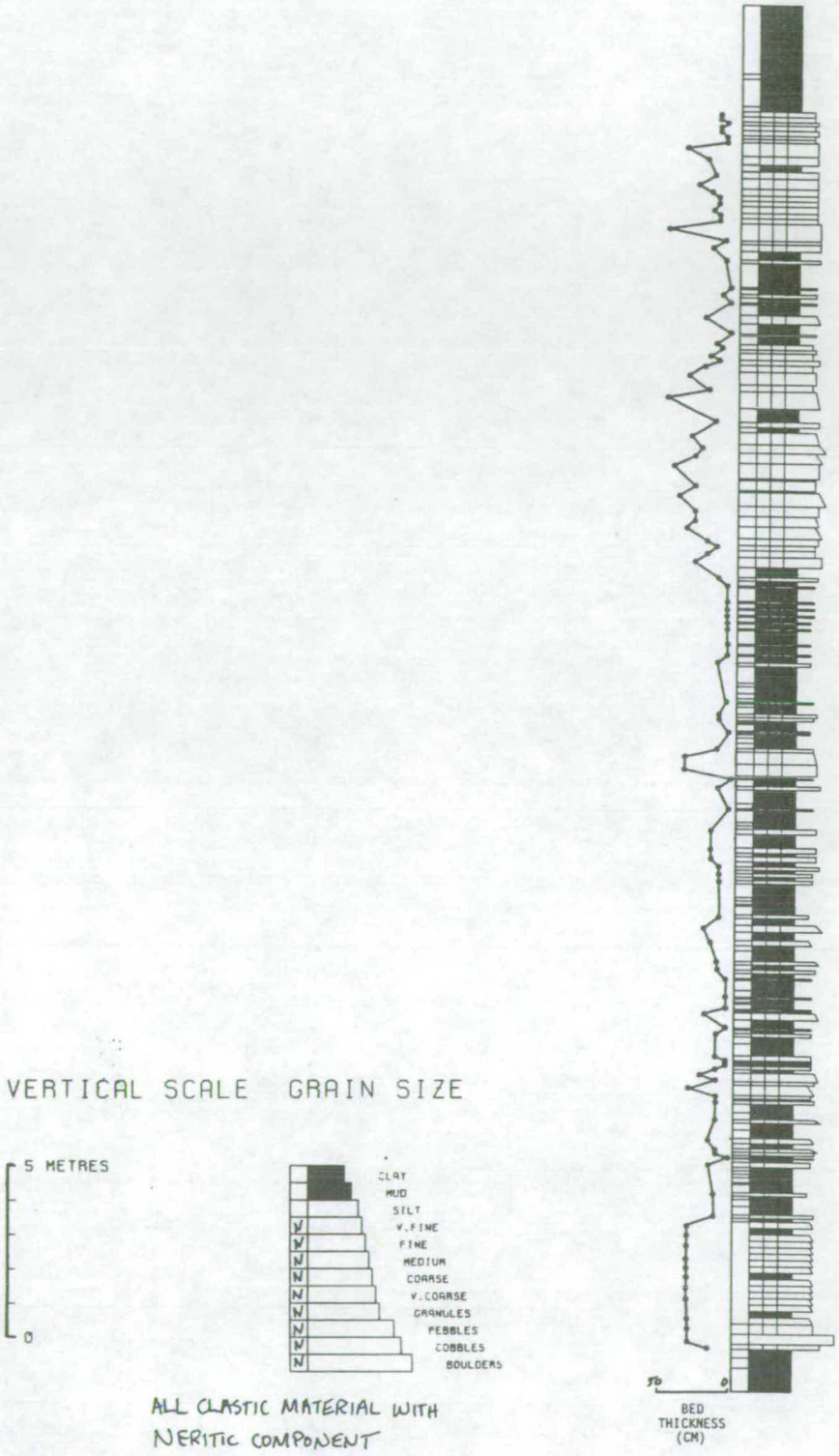

LOG: Kouris River (road section)
GRID REF. 927431
FACIES ASSOC. Basin margin

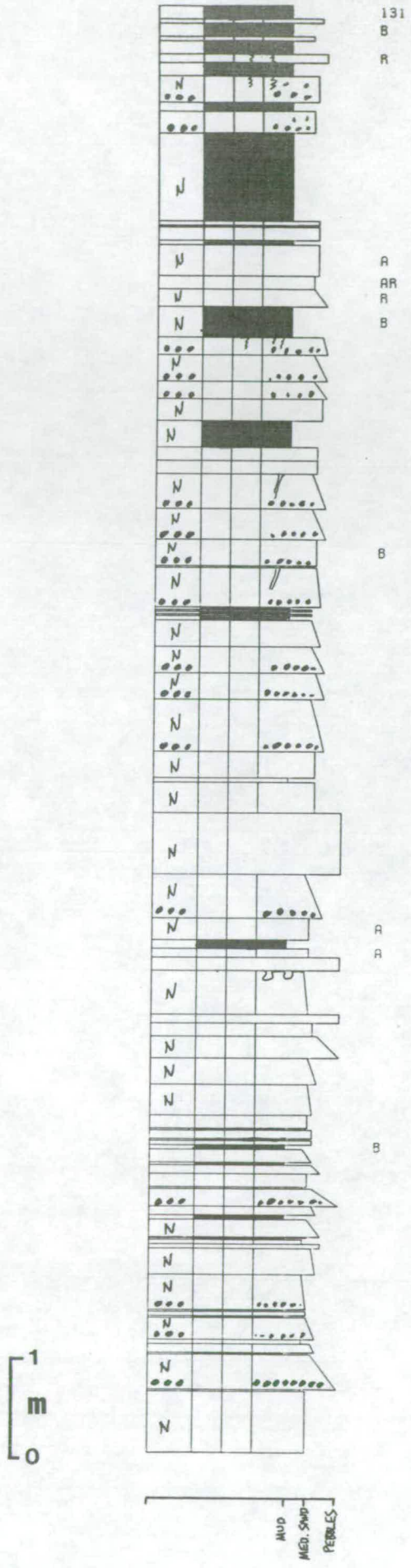

LOG: Ayia Phyla
GRID REF. Ø15425
FACIES ASSOC. Basin margin

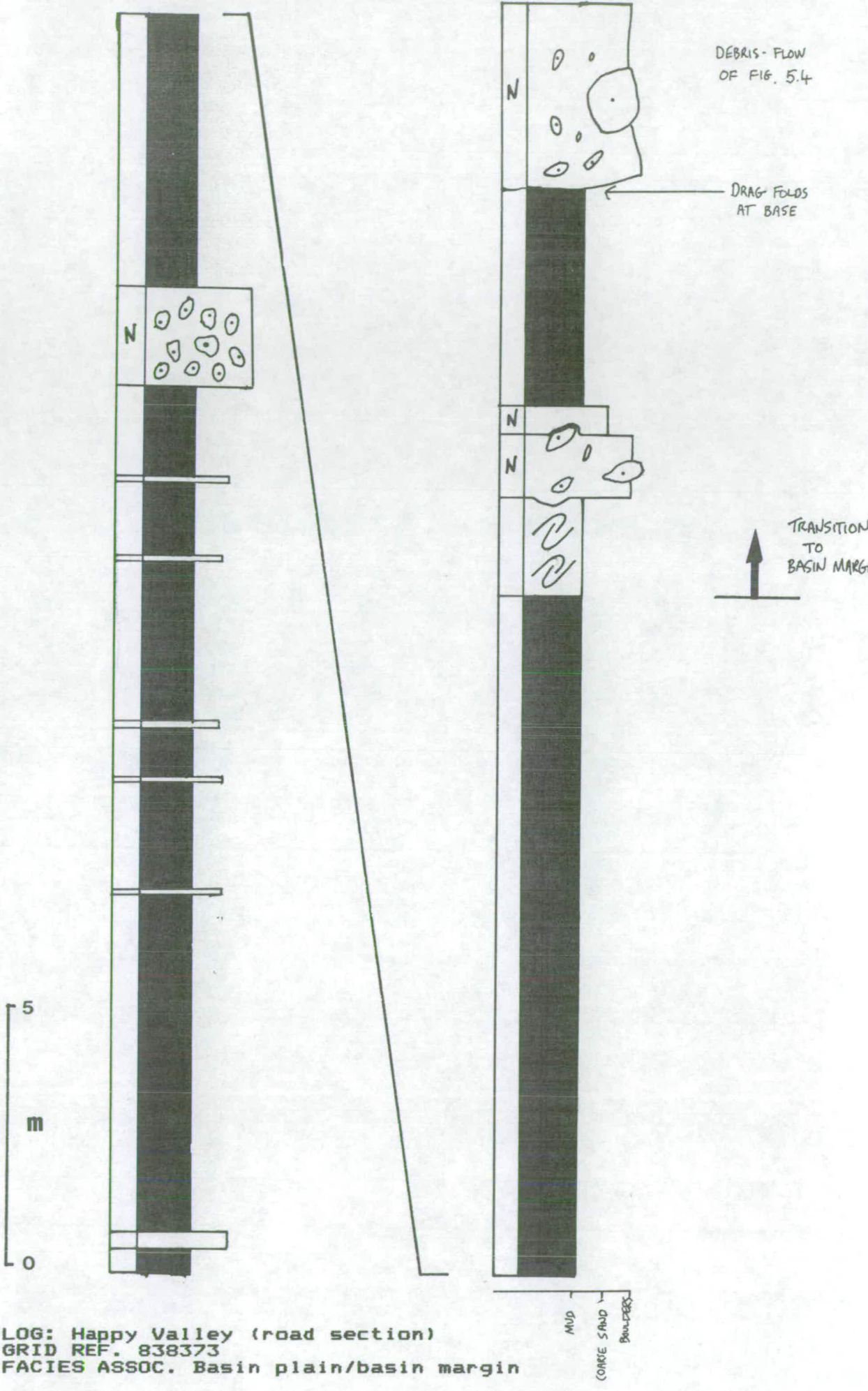

LOG: Happy Valley (road section)
GRID REF. 838373
FACIES ASSOC. Basin plain/basin margin

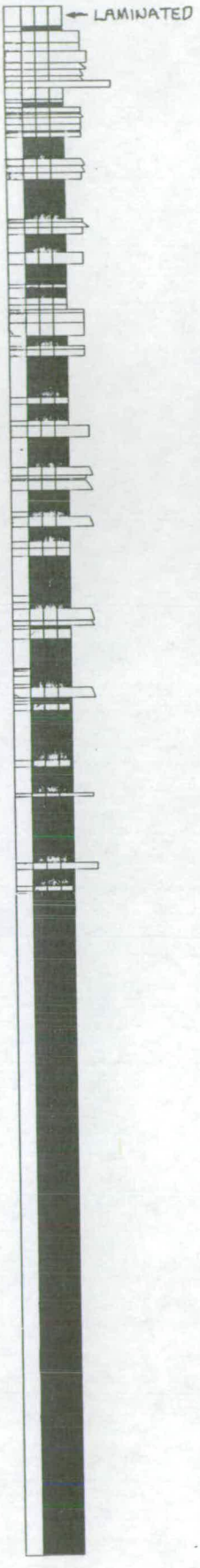

VERTICAL SCALE

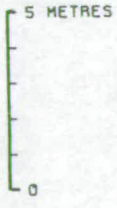

GRAIN SIZE

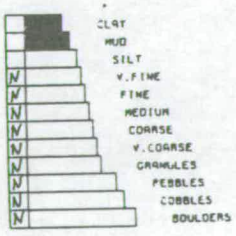

ALL CLASTIC MATERIAL WITH NERITIC COMPONENT

LOG: Moutayiaka
GRID REF. 1Ø2425
FACIES ASSOC. Gullied slope

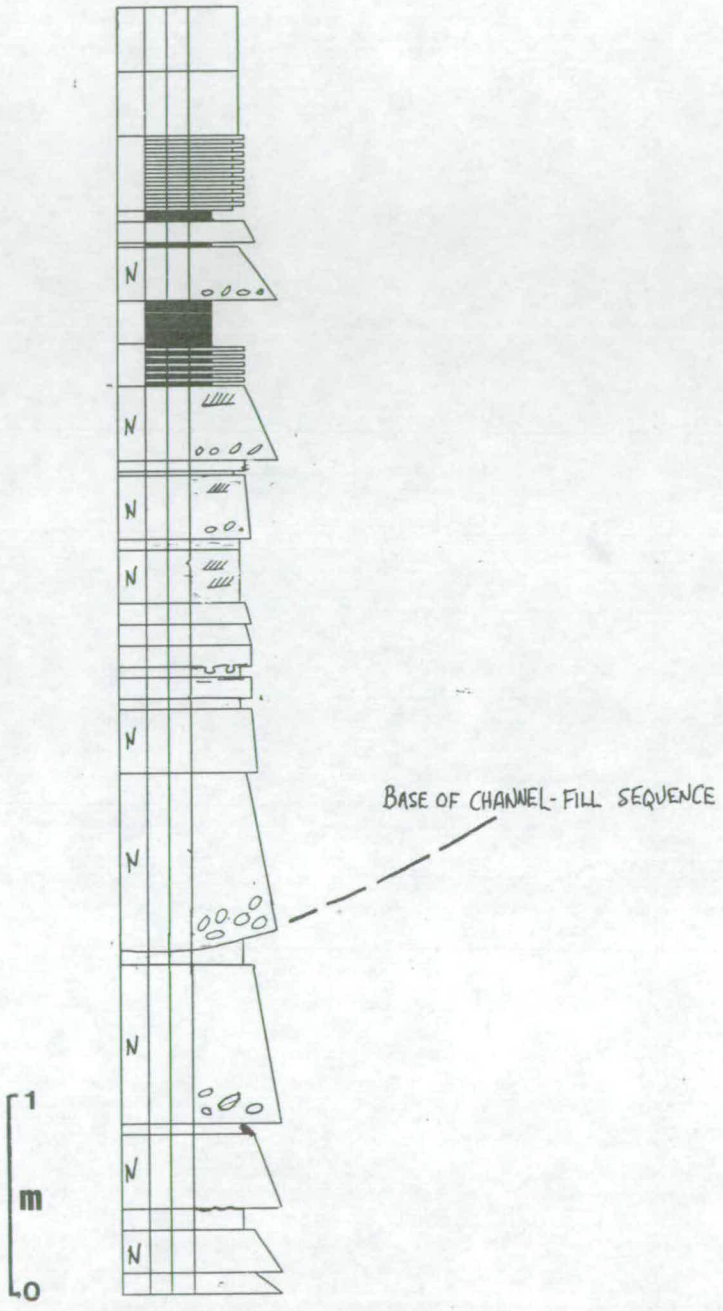

LOG: Amathus
GRID REF. 136418
FACIES ASSOC. Gullied slope (channel-fill)

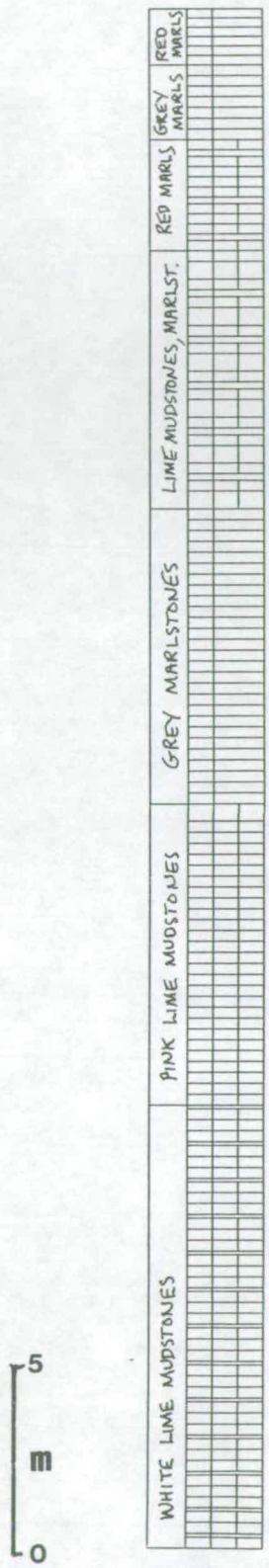

LOG: Kalavasos (road section)
GRID REF. 274474
FACIES ASSOC. Gullied slope (hemi-pelagic)

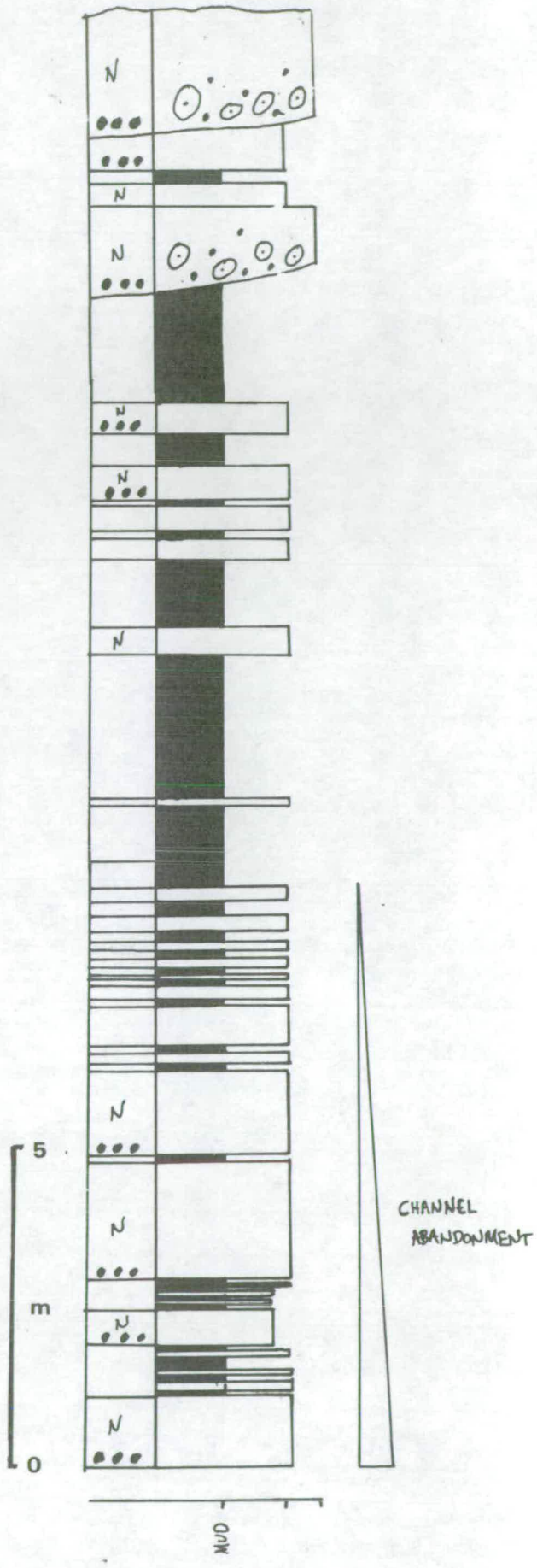

LOG: Tokhni quarry
GRID REF. 295493
FACIES ASSOC. Gullied slope (hemi-pelagic sequence)

FIG. A4r

Locatio

Formati

KEY

LOGS

A

B

C

D

E

F

G

H

I

0 SCALE (km) 20

33°00' E

33°30' E

FIG. A4.1

Location map and facies association outcrop pattern, Pakhna Formation.

KEY

1 Peripheral sands facies association
2 Gullied slope facies association
3 Basin margin facies association
4 Basin plain facies association

LOGS

A Kissousa
B Ayios Therapon
C Kouris River
D Ayia Phyla
E Happy Valley
F Moutayiaka
G Amathus
H Kalavasos
I Tokhni

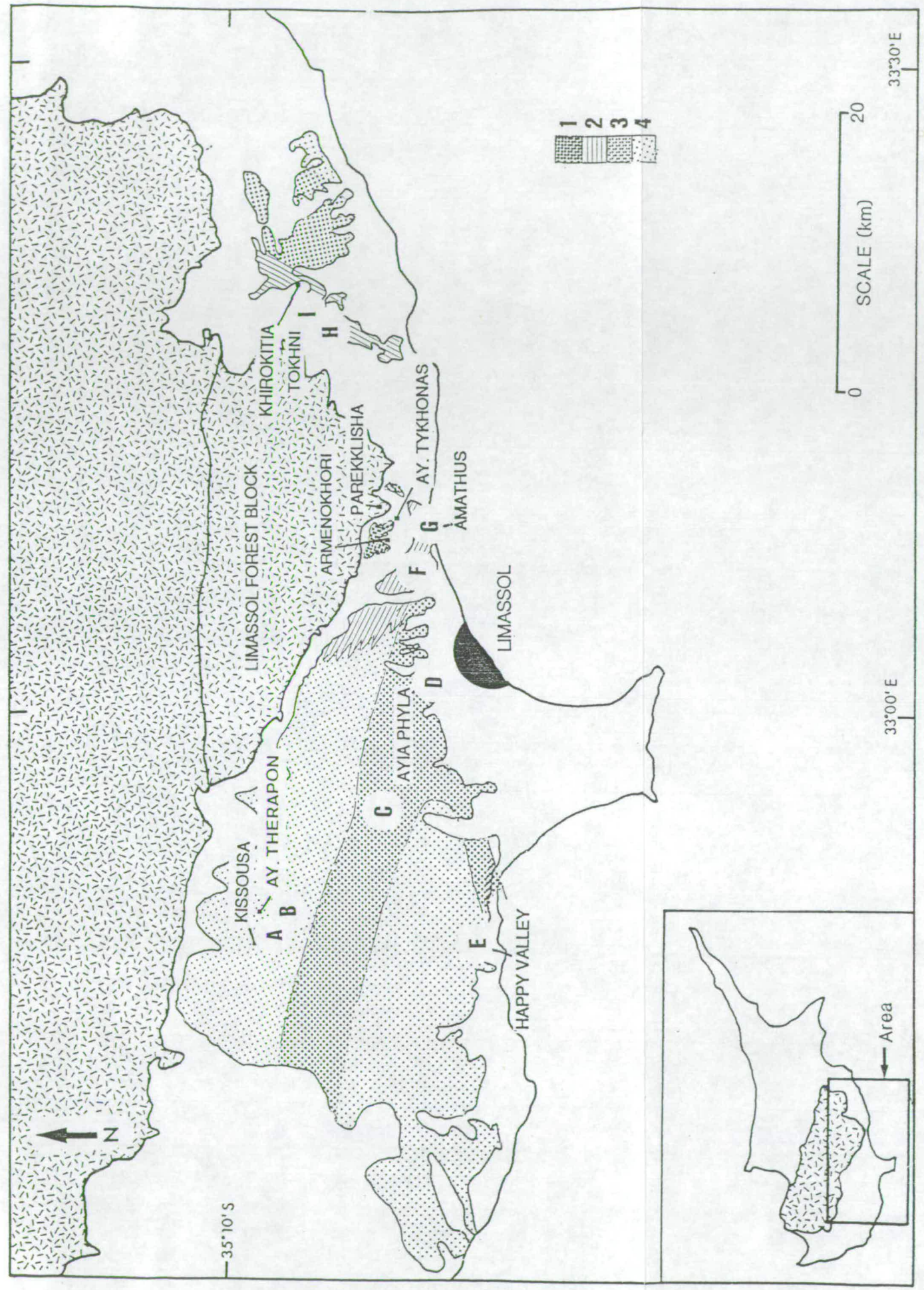

APPENDIX 5

PUBLISHED PAPER

Included is a reprint of the article referred to in this thesis as "Farrell & Eaton (in press)", which came into print during the final stages of compilation.

Slump strain in the Tertiary of Cyprus and the Spanish Pyrenees. Definition of palaeoslopes and models of soft-sediment deformation

S. G. Farrell* & S. Eaton

SUMMARY: Slumps exposed in Tertiary sediments in Cyprus and the Spanish Pyrenees vary in inferred translation distance from metres to hundreds and possibly thousands of metres. Contractional strain initiates open to tight upright to inclined folds with hinges that are sub-parallel to the strike of the palaeoslope. This strain is produced mainly by pure shear layer parallel shortening as the slump detachment propagates, but may involve a component of simple shear strain. Downslope translation of the failed unit commonly imparts a simple shear strain which tends to tighten folds and rotate fold hinges and fold axial surfaces. Fold hinges rotate towards the downslope direction, and fold axial surfaces rotate towards parallelism with the upper and lower surfaces of the slump. Coaxially refolded folds and sheath folds may also develop. Steeply plunging folds may initiate in slumps, due to the development of steeply dipping shear zones with margins sub-parallel to the downslope direction which accommodate differential downslope movements of segments of the slump. Fold axial surface attitude and fold profile may be used as a rough estimate of the degree of fold rotation.

In studies of sedimentary basins, slump fold hinge orientations are routinely used to infer palaeoslopes (Jones 1937; Woodcock 1976a; Naylor 1981). Palaeoslope estimations are usually made with the assumption that the mean fold hinge orientation is parallel to the strike of the palaeoslope (Woodcock 1976b). However, fold hinge rotation during slumping may complicate the interpretation of palaeoslope orientation (Lajoie 1972; Woodcock 1979), and with small data sets may give rise to highly inaccurate inferred palaeoslope orientations. The aim of this paper is to describe a variety of slump strain geometries from Tertiary rocks in the Spanish Pyrenees and Cyprus and through a consideration of fold genesis to infer and interpret possible rotations of fold hinge orientations during slumping.

Definition of palaeoslopes

Palaeoslopes in the basins investigated have been defined by assuming that slump folds with gently plunging fold hinges initiate with a mean azimuth plunge that is sub-parallel to the palaeoslope on which failure occurred (Jones 1937; Woodcock 1979; Farrell 1984a). The direction of palaeoslope dip has been made assuming that folds predominantly verge downslope (Woodcock 1976a; Naylor 1981; Farrell 1984a). Basin palaeogeography defined by palaeocurrents and sediment dispersal and distribution patterns has been used to corroborate palaeoslope estimates made using slump folds.

*Steve Farrell died on 30 January 1987 after a brave two-year fight against cancer.

Geological setting

The Ainsa Basin, Spanish Pyrenees

Deep marine Paleocene and Eocene rocks in the south Pyrenees were deposited in the South Pyrenean basin during the Pyrenean orogeny (Séguret 1970; Séguret *et al.* 1983; Nijman & Nio 1975). The Ainsa basin is a compartment of the Palaeogene South Pyrenean basin and contains numerous slump horizons (Van Lunsen 1970; Mutti 1977) which are up to 120 m thick (Farrell 1984a). Slumped units in the Spanish Pyrenees, described in this paper, crop out in the NE of the Ainsa basin in the Marina and San Vicente formations (Van Lunsen 1970) (Fig. 1).

In the NE Ainsa basin, slump strain has been observed in a variety of turbidite and hemipelagic lithologies. These include massive sandstones, thinly bedded sandstones and marlstones, interlaminated marlstones and siltstones and laminated marlstones. Slump strain is most easily observed in thinly interbedded (10–100 mm) sandstones and marlstones. Slump units preserve evidence of various states of slope failure. Some slumps are traceable to units of undeformed sediment showing that movement on the basal

From: JONES, M. E. & PRESTON, R. M. F. (eds), 1987, *Deformation of Sediments and Sedimentary Rocks*, Geological Society Special Publication No. 29, pp. 181–196.

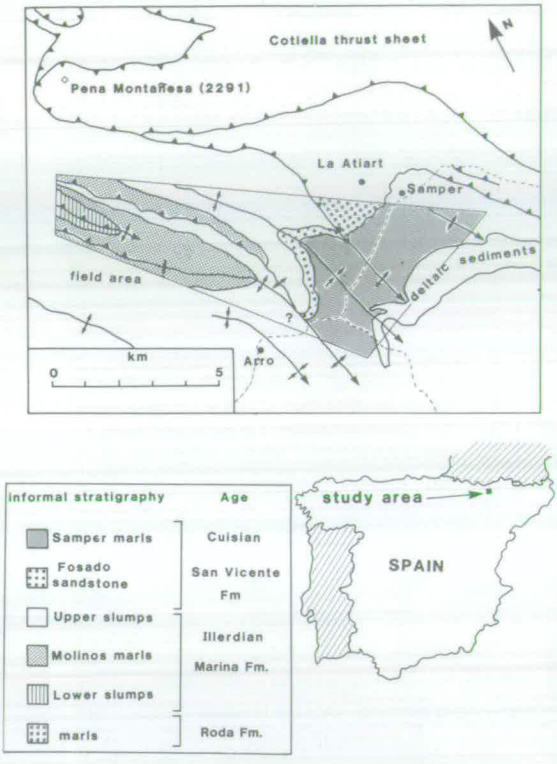

FIG. 1. Geological setting of the Ainsa basin showing the general stratigraphy and the position of the study area in the NE of the basin.

detachment was limited (Farrell 1984a) and that the basal detachment did not cut up to the seafloor to delineate a discrete failed unit. Estimates of translation on the basal faults of these slumps can be made by graphically restoring a cross-section through the slump and is usually found to be less than 50 m (shortening is generally less than 25%). Many slumps of this type occur in the Molinos marls member and have been used to define the palaeoslope (Farrell 1984a). This inferred palaeoslope towards the SW is supported by palaeogeographical reconstructions of the basin (Nijman & Nio 1975). Slumps in other members are traceable over larger areas (up to 8 km^2) and represent major slope failure events (Farrell 1984b). Where slumps can be shown to have travelled only short distances, coherent trains of folds tend to be open to tight, with axial surfaces that dip more than 30° with respect to the underlying undisturbed bedding. In the larger slumps, translation distances are inferred to be one or two orders of magnitude greater than slumps in the Molinos marls member. The larger slumps contain isolated intrafolial folds of sandstone, siltstone or marlstone in a matrix of marlstone. These folds have fold limb lengths of up to 3 m and are usually tight to isoclinal, with limbs that are sub-parallel to underlying undisturbed bedding. High slump strains in these units have partially obliterated bedding and both extensional and contractional strain overprinting features are commonly developed. Fold hinge orientations are variable but are often sub-parallel to the inferred down-palaeoslope direction.

The Khalassa and Maroni Basins, Cyprus

Slumped horizons from southern Cyprus, described in this paper, occur in the Miocene sedimentary cover to the Troodos massif in the area to the east of the town of Limassol (Fig. 2). Miocene sediments have been divided into the Pakhna and Kalavasos formations (Fig. 2), and consist of marine chalks, marls, calcarenites, polymict conglomerates and gypsum beds (Bagnall 1960; Pantazis 1967). Miocene sedimentation was strongly influenced by the uplift of the Troodos ophiolite culminating in late Miocene times with the southward overthrusting of the Limassol Forest igneous block on to the sedimentary cover of the ophiolite (Robertson 1977). Southward thrusting generated the Yerasa fold and thrust belt and was accompanied by the development of the Khalassa and Maroni basins to the south and east of the Limassol Forest block. Slumps were examined at Amathus in the Khalassa basin and at Petrounda Point, Ayios Theodhoros and Tokhni Quarry in the Maroni basin (Fig. 2).

A variety of fold styles and intensities of deformation and bedding disaggregation have been observed in Cyprus. Fold styles are similar to those observed in slumps in the Ainsa basin. The slumped unit at Amathus forms part of the Koronia Limestone (Pakhna Formation) and consists of channelized debris flows and graded bioclastic calciturbidites. The slump unit investigated (Fig. 3A) is 0.8–1.0 m thick and consists of thinly interbedded medium to coarse carbonate sands and silts. Slump folds are generally asymmetrical with axial surfaces that have a mean dip of 32° with respect to the underlying bedding. Rare recumbent sheath folds are also present (Figs 7B and 8A).

The Lefkara Formation which crops out at Petrounda Point is Miocene in age and consists of chalks, marls, foraminiferal sands and lignitic marls which have been incorporated into a slumped unit with an exposed thickness in excess of 12 m. Slumps with similar deformation styles and in a similar stratigraphic position (Bagnall 1960) occur at localities up to 35 km apart, suggesting extensive development of major slope

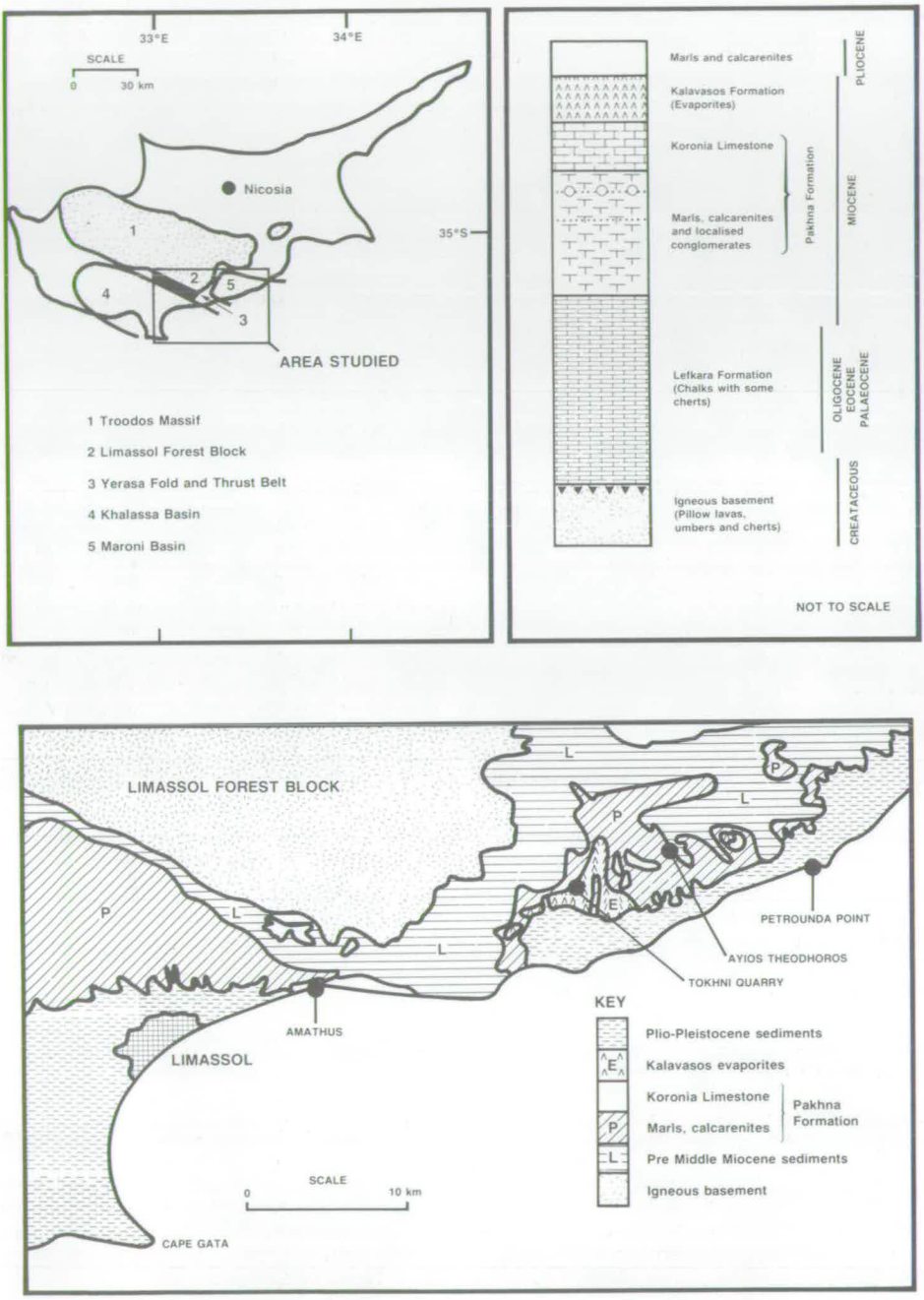

FIG. 2. Geological setting and stratigraphy of the Khalassa and Maroni basins, Cyprus.

failure units. A variety of fold geometries is developed (Table 1) in the Petrounda slumps, with early thin slumps and debris flow deposits folded by later open to tight, upright to inclined, large scale folds which have fold limb lengths of up to 8 m. The early thinner slumps contain isolated recumbent folds with curvilinear hinges that may take the form of recumbent sheath folds (Figs 7A and 8D).

Another slumped unit in the Pakhna Formation crops out 750 m south of Ayios Theodhoros. This 5 m thick unit is composed of medium

(A)

(B)

FIG. 3. (A) Asymmetrical slump folds at Amathus in the Pakhna basin (Cyprus). This slump has a basal failure and extensional strain of gently dipping fold limbs. (B) Isoclinal recumbent slump folds exposed at Ayios Theodhoros, Maroni basin, Cyprus. (C) Upright symmetrical slump folds developed in gypsum at Tokhni Quarry in the Maroni basin, Cyprus. (D) Upright symmetrical folds, Molinos marls, Ainsa basin, Spain.

TABLE 1. *Summary of slump data from the Pakhna, Ayios Theoderos and NE Ainsa basins*

	Ainsa basin Spanish Pyrenees		Cyprus			
	Molinos Marls	Upper Slumps	Amathus	Petrounda	Tokhni	Ayios Theodhoros
Thickness of Slump units	Up to 3m	Up to 25m	1.0m	over 12m	1.5m	5m
Upright to Inclined Early Folds	✓	✓	✓		✓	
Recumbent Isoclinal Folds	✓	✓		✓		✓
Sheath Folds		✓	✓	✓		
Refolded Folds		✓		✓		
Late Upright Folds		✓		✓		

bedded foraminiferal chalks with thin marly interbeds. Asymmetrical folds have gently dipping axial surfaces and curvilinear hinges (Figs 3B, 8C and 9D). Slump faults are common and cut many folds so they occur as isolated recumbent intrafolial folds.

Slumped gypsum deposits at Tokhni Quarry (Figs 3C and 8B) are part of the Kalavasos Formation which has been correlated with Messinian evaporites elsewhere in the Mediterranean (Gass & Cockbain 1961; Baroz & Bizon 1974; Baroz & Bizon 1977; Pantazis 1978). The 1.2–1.5 m buckle folded slump sheet exposed at this quarry can be correlated with exposures up to 5 km distant.

Fold styles in Cyprus and the Ainsa basin

Coherent trains of symmetrical and asymmetrical folds occur in slumps where slump strain and the degree of bedding disaggregation is low to moderate. Near symmetrical folds with steep axial planes have been observed in both Cyprus and the Spanish Pyrenees (Figs 3C, D). Fold hinges plunge up to 26° and axial surfaces are approximately planar. These folds have a predominantly parallel geometry (class 1B of Ramsay 1967) with some flowage of sediment into the cores of the folds. Asymmetrical folds are also common in both the Ainsa slumps and the Miocene slumps on Cyprus. The steep limbs of folds may be overturned and fault splays from the slump basal detachment commonly terminate as tip lines (in the sense of Elliott 1976) in the cores of these folds (Fig. 4A). Some asymmetrical folds have extensionally strained shallow limbs. Fig 4(B) from the Ainsa basin shows boudinage of the gently inclined limb of an asymmetrical fold with boudin axes that are sub-parallel to the slump fold hinge. Some gently dipping fold limbs at Amathus are cut by normal micro-faults. The steep limbs of folds may be reverse faulted, either by micro-faults or by larger listric reverse faults which root into the basal detachment. Fold style is generally parallel (class 1B of Ramsay 1967) although some folds may be similar in style (class 2). Folds which approach a similar geometry are generally tight and recumbent and often have attenuated lower limbs (Figs 5A, 6A).

There is a general correlation of fold interlimb angle and the attitude of fold axial surfaces for folds with gentle hinge plunge azimuths (less than 30°). Tighter folds tend towards a recumbent geometry which bears out observations made by Naylor (1981). Folds with steeply plunging hinge azimuths (30–90°) show no good correlation of fold tightness and dip of axial surfaces.

Refolded folds

Recumbent folds and refolded folds generally occur in slumps with a moderate to high degree of bedding obliteration. This is commonly the case in thicker, more aerially extensive slumps (Table 1). Refolded folds observed in slumps in the Ainsa basin are commonly either: (i) recumbent, tight to isoclinal early folds with flat lying axial surfaces folded by upright, generally open, later folds with sub-vertical axial surfaces (Fig. 5B), or (ii) plane, non-cylindrical, approximately coaxial refolded folds with flat lying axial surfaces (Figs 5C, 6C and 7D). Both of these refolded fold

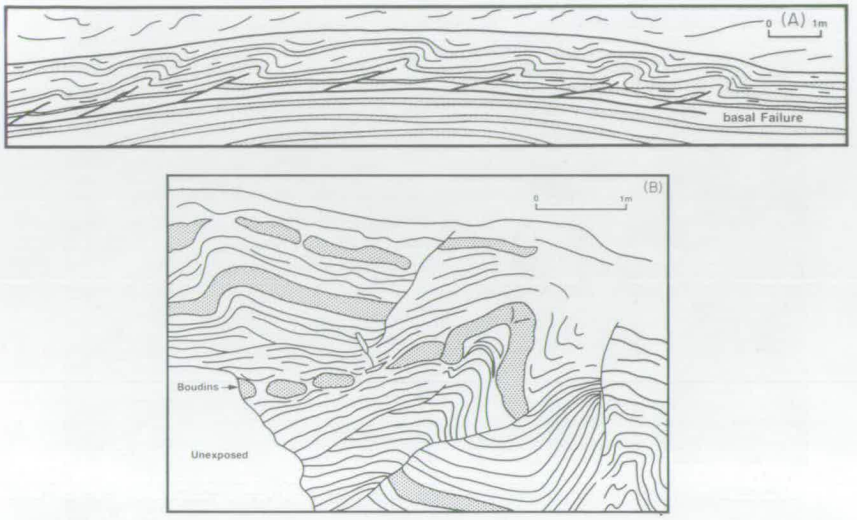

FIG. 4. (A) Asymmetrical slump folds developed in interbedded sandstones and marlstones, NE Ainsa basin (Spanish Pyrenees). The basal fault to this slump terminates as tip lines in the cores of asymmetrical folds. (B) Asymmetrical slump fold, NE Ainsa basin (Spanish Pyrenees). The gently dipping limb of the fold is extensionally strained (boudinage).

styles have been observed in the Ainsa basin slumps and at Petrounda Point in Cyprus (Fig. 7D). They correspond to type two and type three refolded folds, defined by Ramsay (1967), and are similar to refolded slump folds described in California by Tobisch (1984).

Fold hinge curvature is commonly observed in tight to isoclinal recumbent folds and varies from gentle undulations of the fold hinge to isoclinally bent hinges (sheath folds) (Figs 6B and 7A–C). Folds with strongly curvilinear hinges have hinge azimuth orientations that are consistently subparallel to the inferred down-palaeoslope direction (Fig. 8D, F). Plots of axial surface dip against fold hinge azimuth orientation, indicate that rotation of fold hinge azimuths towards parallelism with the gross transport direction often results in a tendency for folds to become recumbent (Fig. 9A, C, D, E). However, some slumps in the Ainsa basin contain folds with a variety of fold hinge azimuth orientations which show no correlation between fold hinge azimuth orientation and axial surface dip (Fig. 9B). Slumps with steeply plunging fold hinges also show no correlation of fold orientation and dip of axial surfaces.

Interpretation

Fold development

The presence of boudinage in some slumps (e.g. Fig. 4B) indicates that competency contrasts existed between layers during slumping. Where there is a competency contrast between layers undergoing deformation, strain is accommodated by buckling (Ramsay 1967) and suggests that slump folds developed actively by buckling rather than passively by shear or flow folding. The comparative rarity of class 2 (similar folds) in slumps also indicates that during slumping folds develop principally by buckling (Woodcock 1976b). However, the occurrence of some similar folds indicates that although buckling may initiate folding, homogeneous or heterogeneous simple shear may modify some fold geometries by flow or shear folding during fold growth and rotation (Woodcock 1976b).

However, the occurrence of some similar folds indicates that although buckling may initiate folding, homogeneous or heterogeneous simple shear may modify some fold geometries by flow or shear folding during fold growth and rotation (Woodcock 1976b).

Upright, near symmetrical folds probably developed as buckle folds reflecting predominantly pure shear deformation during longitudinal shortening of the failed unit. These upright folds indicate that the x–y plane of the finite strain ellipsoid for the slump deformation was perpendicular or nearly perpendicular to bedding, and involved layer parallel shortening. Although asymmetrical folds can develop during either a bulk pure shear or simple shear deformation, asymmetrical folds developed during slumping are often a manifestation of tip strain associated

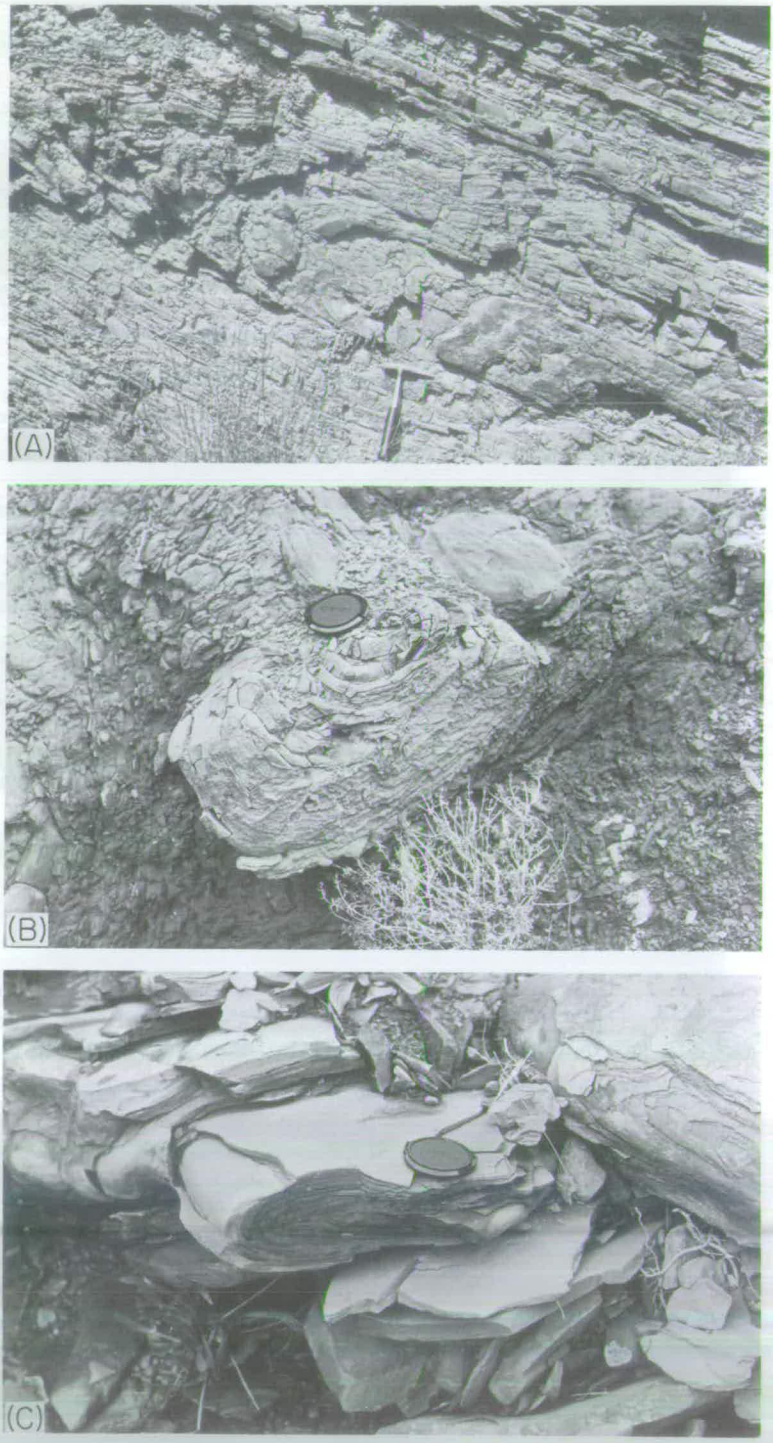

FIG. 5. (A) Similar style recumbent isoclinal slump fold, NE Ainsa basin (Spanish Pyrenees). (B) Refolded fold. An early tight to isoclinal recumbent fold with a gently dipping axial surface refolded by a later open upright fold with a steeply dipping axial surface. Upper slumps, Ainsa Basin, Spain. (C) A plane non-cylindrical approximately coaxial refolded fold. Lower slumps, Ainsa basin, Spain.

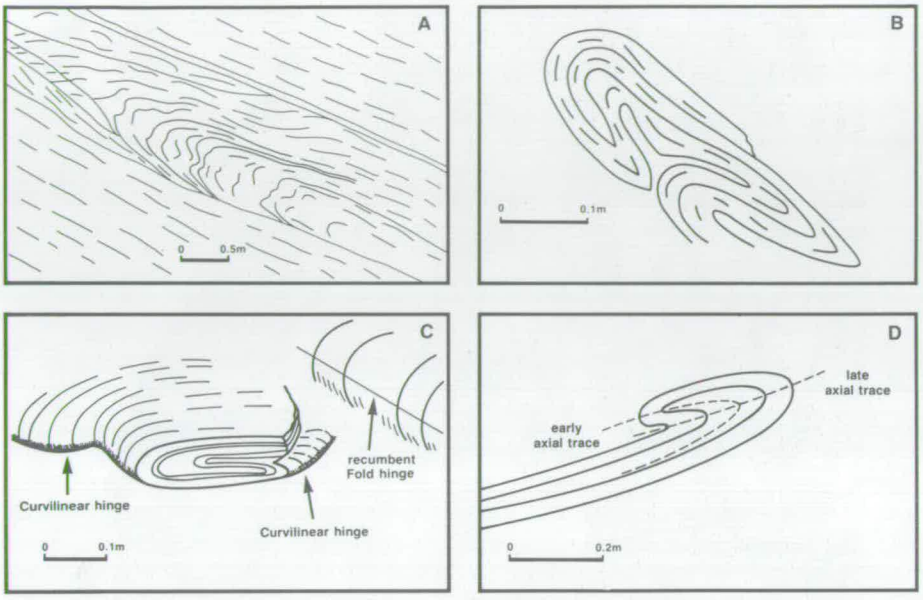

FIG. 6. (A) Line drawing of Fig. 5(A); (B) Line drawing of Fig. 7(C). (C) Line drawing of Fig. 5(C). (D) Line drawing of Fig. 7(D).

with reverse fault imbricate fans (Farrell 1984a) produced during pure shear layer parallel shortening.

Asymmetrical tectonic folds with long limbs showing extensional strain, and short limbs showing contractional strain, have been described by Ramsay *et al.* (1983) (Fig. 10) and interpreted as having developed principally by buckling during simple shear deformation. During simple shear deformation, material lines, such as fold limbs, lying in the contractional field of the incremental strain ellipsoid, will shorten. Material lines initially lying in, or subsequently rotated into, the extensional field of the incremental strain ellipsoid will extend (Ramsay 1967). The angular relationship of the shallow limbs of asymmetrical folds with the margins of the shear zone in which they are developed is such that they commonly lie in the extensional field of the incremental strain ellipsoid (Ramsay *et al.* 1983). Although the steep limbs of asymmetrical folds commonly begin to develop in the contractional field of the incremental strain ellipsoid, during progressive simple shear deformation and active buckling they may become rotated into the extensional field of the finite strain ellipsoid (Ramsay *et al.* 1983). Slump folds which show extensionally and/or contractionally strained fold limbs that are not the product of a separate overprinting deformation can be interpreted as developing during simple shear deformation (Fig. 4B). If slump fold limbs are extensionally strained the limbs may extend by normal faulting, boudinage or ductile thinning, depending on the rheologies and competency contrasts of the sediments that are slumping. Ductile thinning and attenuation of the lower limbs of folds may produce folds with a similar style (Figs 5A and 6A).

The development of sheath folds has been linked to the accentuation of curvature of initially curved fold hinges during simple shear deformation (Escher & Waterson 1973; Ramsay 1980; Ghosh & Sengupta 1984). During simple shear deformation, linear elements such as fold hinges are progressively rotated towards the x-direction of the finite strain ellipsoid (Escher & Waterson 1974; Williams 1978; Ramsay 1980) and planar surfaces such as axial surfaces are progressively rotated towards the x–y plane of the finite strain ellipsoid. Plane coaxial non-cylindrical refolded folds (see Figs 5C and 7D) (type three of Ramsay 1967) have also been interpreted as having developed during progressive simple shear deformation (Ghosh & Sengupta 1984).

From these observations of slumps it is suggested that slump folds initiate as open to tight parallel style folds with axial surfaces that dip at 30–90° with respect to the slump basal detachment. Fold hinges initiate sub-parallel to the palaeoslope (Jones 1937), although some initial curvature to the fold hinges may be generated as

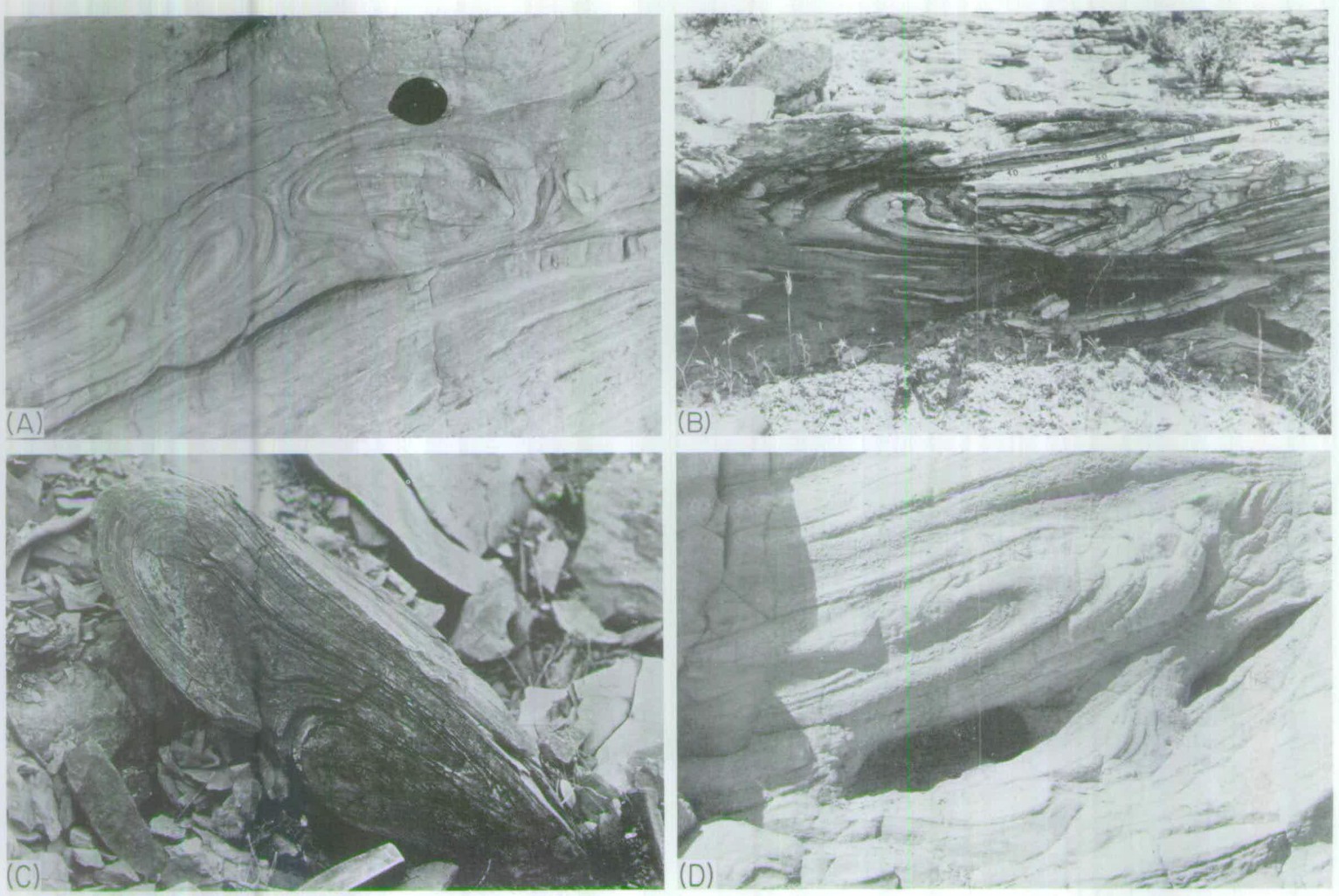

FIG. 7. (A) Sheath fold, Petrounda Point, Maroni basin, Cyprus. (B) Sheath fold, Amathus, Khalassa basin, Cyprus. (C) Isoclinal fold refolded by a sheath fold, Lower slumps, Ainsa basin, Spain. (D) An early tight fold refolded by a later tight recumbent fold. Petrounda Point, Maroni basin, Cyprus.

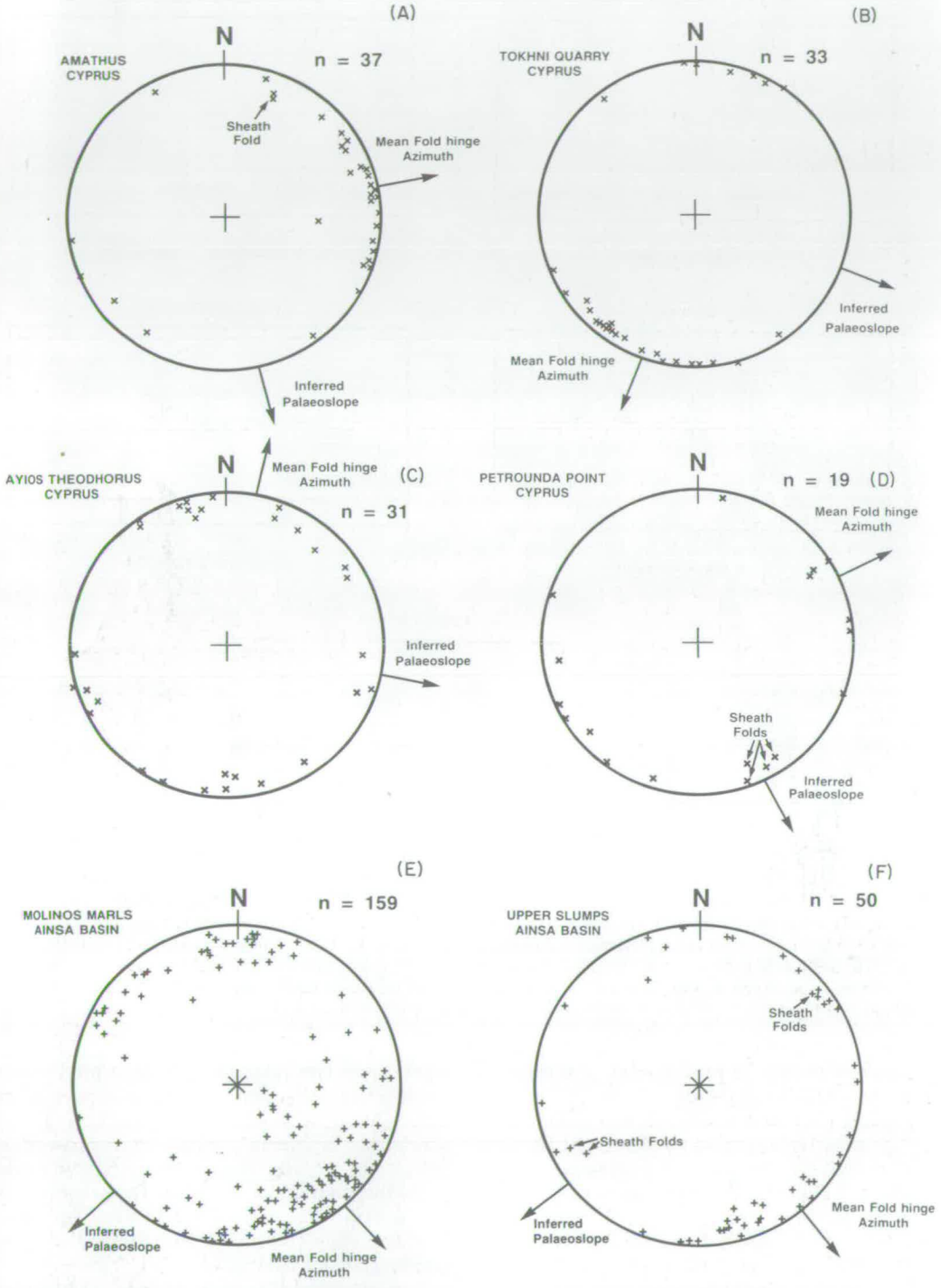

FIG. 8. Equal area stereoplots of fold hinge azimuths from slumps in the N.E. Ainsa basin (Spanish Pyrenees) and the Khalassa and Maroni basins (Cyprus).

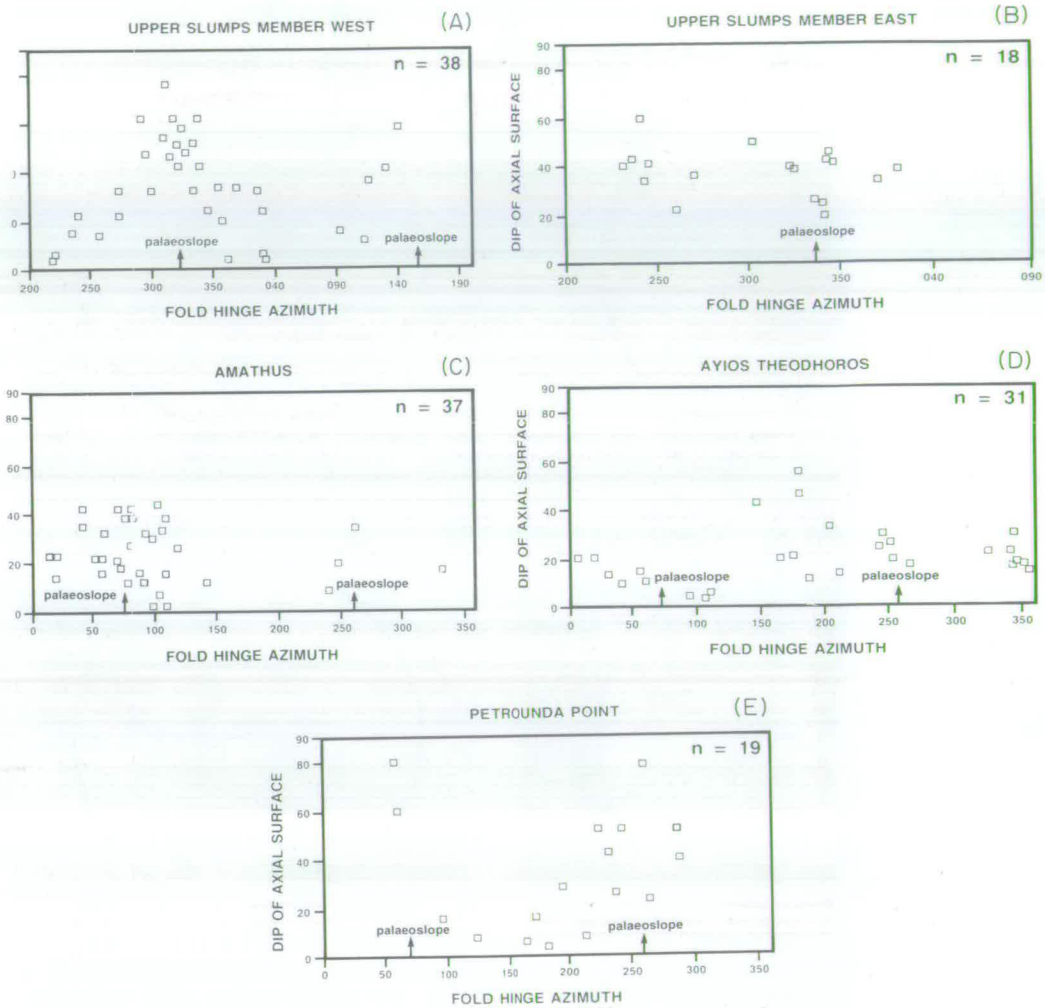

FIG. 9. Plots of dip of slump fold axial surface and fold hinge azimuth. Plots (A) and (B) are from the Upper slumps, NE Ainsa basin (Spanish Pyrenees); plot (C) is from Amathus, Khallasa basin (Cyprus); plot (D) is from Ayios Theodhoros, Maroni basin (Cyprus) and plot (E) from Petrounda Point, Maroni basin (Cyprus). Plots (A), (C), (D) and (E) show a decrease in dip of fold axial surface as the fold hinge azimuth tends towards the downpalaeoslope direction. Plot (B) shows no decrease in dip of fold axial surface with change of fold hinge azimuth.

a result of the radial propagation of the slump basal failure (Farrell 1984a).

During internal deformation of a slump, folds are progressively rotated so that axial surfaces become sub-parallel to the slump basal detachment and folds are tightened so that they may become isoclinal. Concomitant with the tendency for folds to be rotated towards a recumbent geometry, fold hinges tend to be rotated towards the downslope direction (gross transport direction).

Curvilinear hinges may be accentuated into sheath folds. Refolding of folds producing upright, open late folds suggests that final minor strain increments may be due to a pure shear deformation with the slump thickening and shortening. Sediment compaction imparts a flattening strain on the slump. This strain will tend to rotate fold axial surfaces further towards parallelism with undisturbed bedding and may modify parallel recumbent folds so that they have similar geometries (Fig. 11).

This proposed scheme for the genesis of slump folds can be interpreted as fold initiation during layer parallel shortening, and pure shear deformation followed by strain which is predominantly

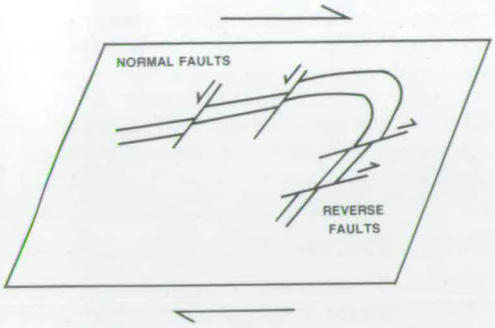

FIG. 10. Strain in the shallow limb (normal faults) and steep limb of an asymmetrical fold developed in a shear zone (after Ramsay *et al.* 1983).

due to simple shear deformation. In slumps with basal detachments that did not cut up to the seafloor (see Fig. 4A), contractional slump strain is predominantly in the form of folds and faults, indicating that deformation principally involved pure shear layer parallel shortening of the failed unit. This strain develops as a consequence of the propagation of the slump basal detachment (Farrell 1984a). Slip on the basal fault is accommodated as internal strain in the hanging wall to the detachment (Fig. 12A) and will take the form of a predominantly pure shear strain with a sub-vertical x–y plane to the finite strain ellipsoid. However, simple shear strains may also be developed during propagation of the basal detachment and will be superimposed on the pure shear strains (Fig. 12B). It is possible that some slumps initiate as zones of slope parallel simple shear, but unless a basal detachment develops, translation of the slumped unit will be limited.

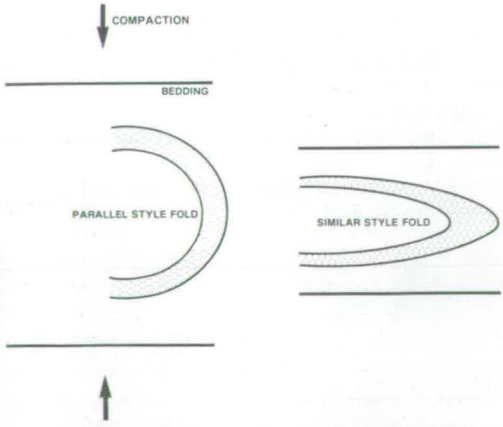

FIG. 11. Change of fold profile from a parallel to similar style by the superposition of a compactional flattening strain on a recumbent slump fold.

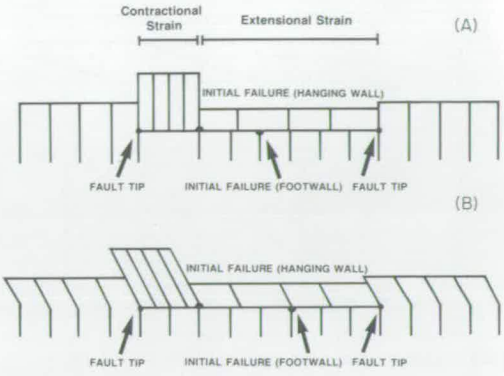

FIG. 12. (A) Contractional pure shear strain developed downslope of the initial slope failure as a consequence of the propagation of the basal slump detachment. Movement on the fault is taken up as strain in the hanging wall to the detachment. (B) Propagation of a basal slump detachment with a superimposed component of simple shear strain.

The development of extensional slump strain upslope of an initial slope failure and contractional strain downslope of the failure in many slumps and Holocene to recent submarine slope failures (Farrell 1984a), indicates that development of a basal fault and associated pure shear strain is a common mode of slope failure. It is likely that much of the variation in observed slump strain is due to the development of a spectrum of failure styles dependent on the mechanical properties of the sediment and the relative importance of the components of pure and simple shear. During translation of the failed unit, thickening or thinning (pure shear strain with a sub-vertical x–y plane) of the slump will occur whenever there are sequential up or downslope propagating velocity changes. These sequential velocity changes will be expected to develop during translation over changes in slope and when friction increases on the basal detachment by localised dewatering of the slump (Fig. 13) (Farrell 1984a). Final strain increments may be in the form of open buckle folds if the toe of the slump comes to rest before the rest of the failed unit.

Where slumps are inferred to be far travelled, the common occurrence of fold rotation and coaxial refolding shows that simple shear is often an important consequence of downslope translation. Simple shear strains are likely to occur in a slumped body as a result of dewatering of the slump and loss of fluid from the basal fault. The shear strength of a sediment body is a function of pore-fluid pressure; high pore-fluid pressures are often considered to lead to a loss of shear strength

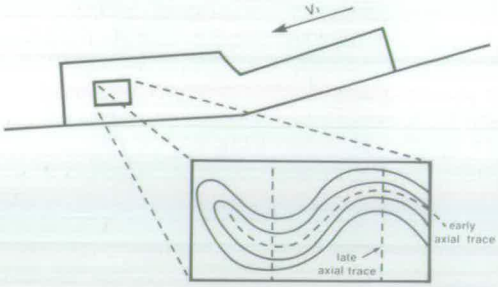

FIG. 13. Pure shear strains develop in slumps during sequential velocity changes. Deceleration on the front of a slump generates contractional strains and may lead to the development of late upright folds which refold earlier structures.

and subsequent failure of the unit (Mandl & Crans 1981). Deceleration of a slump by recovery of shear strength may be caused by loss of excess pore fluid pressure. Recovery of shear strength will eventually result in significant friction on the detachment, and momentum and gravitational potential of the failed body may be expended in internally deforming the slump. If general dewatering occurs by upwards movement of water through the slump, the shear strength of the base of the slump may be recovered while the upper layers of the slump are still moving. This differential movement will generate simple shear strains.

The movement of salt (Talbot 1981) and ice (Nye 1953) glaciers over obstructions in the glacier floor generates simple shear strains in the glacier and may be analogous to the movement of slumps over an irregular seafloor topography. The first irregularity encountered on the sea floor by the slump is the frontal toe scar to the slope failure (Schwartz 1982). Strain imparted to the slump as it moves over this scar may be analogous to the simple shear strains imparted to thrust sheets as they move over frontal thrust ramps (Fischer & Coward 1982).

Gravitational collapse of unlithified sediments during translation may generate significant strains in the failed unit. Ramberg (1981) has suggested that gravitational collapse of long thin bodies will generate simple shear strains as the upper parts of the collapsing unit moves further than the lower parts. If differential downslope movements occur in segments of the slump then strike-slip and oblique faults and steeply dipping shear zones may develop. Differential downslope velocities are likely to occur because of local pore-fluid pressure related variations in friction on the slump basal fault. The development of steeply plunging folds and fold rotation without a decrease in axial surface dip may occur in such steeply inclined shear zones. The strain ellipsoid for steep shear zones will have a sub-vertical x–y plane and folds initiated in such steep shear zones will tend to be steeply plunging. Fold rotation in such steep shear zones will tend to steepen the dip of fold axial surfaces.

Definition of palaeoslopes

The initial development of slump folds is related to the shortening of the slump as the basal fault propagates. This produces a strain ellipsoid with an x–y plane that is sub-parallel to the strike of the palaeoslope, and therefore slump folds initiate with a mean fold hinge azimuth sub-parallel to the strike of the palaeoslope. Therefore, small data sets of upright symmetrical or inclined asymmetrical folds may be used with more confidence to define a palaeoslope strike than data sets composed of recumbent isoclinal folds that may have been rotated during translation of the slump. Fold rotation may result in a wide spread of hinge azimuths, and therefore a palaeoslope defined from a small data set of recumbent isoclinal folds may be highly inaccurate. Large data sets recorded from many slump units eliminate many of the problems of having relatively unclustered fold hinge azimuth data. If it is not possible to measure a large data set, a rule of thumb estimate of the possibility of a particular fold having been rotated may be made by considering the fold shape. Recumbent isoclinal folds are likely to have rotated significantly in comparison with upright symmetrical folds.

Unfortunately, it is not possible to equate the observed strain in a slump directly with the amount of translation that the slump has undergone. Translation on the basal detachment of a slump may not generate slump strain and relatively unstrained slumps may be translated for considerable distances on the sea bed. However, slumps which can be demonstrated to have been translated only small distances commonly have much less internal deformation than slumps which are inferred, from their size and lateral continuity, to be far travelled.

Conclusions

Slumps in the Khalassa and Maroni basins in Cyprus, and the Ainsa basin in the Spanish Pyrenees, contain folds with a wide variety of fold styles. Fold style can be related to the inferred translation distance of a slump. Translation distance has been inferred by consideration of slump size, the degree of bedding disaggregation

and whether a slump is transitional into unslumped sediment. Upright and inclined folds with fold hinges sub-parallel to the palaeoslope are frequently observed in slumps where translation distances are small. Recumbent isoclinal folds, sheath folds and refolded folds are common in slumps where translation distances are large. Fold hinge rotation towards a down-palaeoslope trend is also common in far travelled slumps. Slump strain can develop during the initiation, translation and termination phases of slump development. Contractional slump strain, initiated during the propagation of the basal failure to a slump, is predominantly buckle folding related to the longitudinal shortening of the slump. Folds produced during this initiation phase of slump development are generally upright to inclined and open to tight. During translation of the slump, strain is principally in the form of simple shear which may rotate and tighten folds and lead to the development of sheath folds and refolded folds. Deceleration of a slump may impart a final pure shear strain to the slump producing upright open to tight folds. Fold rotation is, therefore, a common consequence of slump translation and small sets of fold orientation data measured from far travelled slumps may indicate spurious palaeoslope orientations. Thus the internal deformation of a slump should be taken into account when deciding the degree of confidence with which palaeoslope orientation estimates are made.

ACKNOWLEDGEMENTS: S. Farrell acknowledges British Petroleum for permission to publish this paper. Diagrams were drafted by B.P. special reprographics section. S. Farrell was supported by a Shell Postgraduate Scholarship at University College Cardiff. S. Eaton was supported by a NERC studentship under the supervision of A. H. F. Robertson. He also thanks the Cyprus Geological Survey Department, particularly C. Xenophontos and A. Panayiotou for their help in Cyprus.

References

BAGNALL, P. S. 1960. The geology and mineral resources of the Pano Lefkara-Larnaca area. *Cyprus Geol. Survey Dept. Mem.* **5**, 116 pp.

BAROZ, F. & BIZON, G. 1974. Le Neogene de la Chaine du Pentadaktylos et de la partie nord de la Mesaorie (Chypre). *Etude stratigraphique et micropaleontologique*. Inst. Francais Petrole, Rev. **29**, 327–59.

—— & BIZON, G. 1977. La couverture Tertiaire du flanc nord du massif du Troodos et de la partie meridionale de la Mesaoria. *Etude stratigraphique et micropaleontologique*. Inst. Francais Petrole. Rev. **32**, 719–59.

ELLIOTT, D. 1976. The energy balance and deformation mechanisms of thrust sheets. *Philos. trans. Roy. Soc.* **A283**, 289–312.

ESCHER, A. & WATERSON, J. 1974. Stretching fabrics, folds and crustal shortening. *Tectonophysics*, **22**, 223–31.

FARRELL, S. G. 1984a. A dislocation model applied to slump structures. Ainsa basin, South Central Pyrenees. *J. struct. Geol.* **6**, 727–36.

—— 1984b. *Slope processes and tectonism in Eocene marine sediments of the Ainsa basin, Spanish Pyrenees*. Unpubl. Ph.D. thesis, Univ of Wales.

FISCHER, M. W. & COWARD, M. P. 1982. Strains and folds within thrust sheets. An analysis of the Hellam thrust sheet, north western Scotland. *Tectonophysics*, **88**, 291–312.

GASS, I. G. & COCKBAIN, A. E. 1961. Notes on the occurrence of gypsum in Cyprus. *Overseas Geol. Min. resources*, **VIII**. 269–87.

GHOSH, S. K. & SENGUPTA, S. 1984. Successive development of plane noncylindrical folds in progressive deformation. *J. struct. Geol.* **6**, 703–9.

JONES, O. T. 1937. On sliding and slumping of submarine sediments in Denbighshire, North Wales, during the Ludlow period. *Q. J. geol. soc. Lond.* **93**, 241–83.

LAJOIE, J. 1972. Slump fold axis orientations, and indication of palaeoslope. *J. sed. Pet.* 584–6.

LUNSEN VAN, H. A. 1970. Geology of the Ara-Cinca region, Spanish Pyrenees, province of Huesca. *Geol. Ultraectina*, 1–119.

MANDL, G. & CRANS, W. 1981. Gravitational gliding in deltas. *In:* MCCLAY, K. R. & PRICE, N. J. (eds) *Thrust and Nappe Tectonics*. Spec. Publ. geol. Soc. London, **9**, 41–54.

MUTTI, E. 1977. Distinctive thin bedded turbidite facies and related depositional environments in the Eocene Hecho Group (South Central Pyrenees). *Sedimentology*, **24**, 107–31.

NAYLOR, M. A. 1981. Debris flow (olistostromes) and slumping on a distal continental margin; the Palombini limestone-shale sequence of the northern Apennines. *Sedimentology*, **28**, 837–52.

NIJMAN, W. J. & NIO, S. D. 1975. The Eocene Montanana delta (Tremp-Graus basin, province of Lerida and Huesca, South Pyrenees, N. Spain). *In:* ROSELL, J. & PUIGDEFABREGAS, C. (eds) *Sedimentary Evolution of the Palaeogene South Pyrenean Basin*, 9th congress Sedim, Part B, 1–9, Nice, 1975, Field trip 19.

NYE, J. R. 1953. The motion of ice sheets and glaciers. *J. Glaciol.* **3**, 493–507.

PANTAZIS, T. M. 1967. The geology and mineral resources of the Pharmakas-Kalavasos area. *Cyprus Geol. Survey Dept. Mem.* **8**, 190 pp.

—— 1978. Cyprus evaporites. *In:* ROSS, D. A., NEPROCHNOV, Y. P., *et al*, 1978. Initial reports of the Deep Sea Drilling Project, **42**, part 2, 1185–94 pp, *Washington (U.S. Government Printing Office)*.

RAMBERG, H. 1981. The role of gravity in orogenic belts. *In:* MCCLAY, K. R. & PRICE, N. J. (eds) *Thrust and Nappe Tectonics*. Spec. Publ. geol. Soc. London, **9**, 125–40.

RAMSAY, J. G. 1967. *Folding and Fracturing of Rocks*. McGraw-Hill, New York.

—— 1980. Shear zone geometry: a review. *J. struct. Geol.* **2**, 83–99.

—— CASEY, M. & KLIGFIELD, R. 1983. Role of shear in development of the Helvetic fold, thrust belt of Switzerland. *Geology*, **11**, 439–42.

ROBERTSON, A. H. F. 1977. Tertiary uplift history of the Troodos massif, Cyprus. *Geol. Soc. Am. Bull.* **88**, 1763–72.

SCHWARTZ, H. U. 1982. Subaqueous slope failures, experiments and modern occurrences. *Contrib. Sediment.* **11**, 116 pp.

SEGURET, M. 1970. Etude tectonique des nappes et series decollees de la partie centrale du versant sud des Pyrenees, Publ Ustella, Montpellier. *Ser. Geol. Struct.* **21**, 1–155.

——, LABAUME, P. & MADARIAGA, R. 1983. Eocene seismicity in the Pyrenees from megaturbidites in the South Pyrenean basin (N. Spain). *Mar. Geol.* **55**, 117–31.

TALBOT, C. J. 1981. Sliding and other deformation mechanisms in a glacier of salt, S. Iran. *In:* MCCLAY, K. R. & PRICE, N. J. (eds) *Thrust and Nappe Tectonics*. Spec. Publ. geol. Soc. London, **9**, 173–83.

TOBISCH, O. T. 1984. The development of foliation and fold interference patterns produced by sedimentary processes. *Geology*, **12**, 441–4.

WILLIAMS, G. D. 1978. Rotation of contemporary folds into the X-direction during overthrusting, Processes in Lakesfjord, Finnmark. *Tectonophysics*, **48**, 29–40.

WOODCOCK, N. H. 1976a. Ludlow series slumps and turbidites of the Montgomery trough, Powys, Wales. *Proc. Geol. Ass.* **87**, 169–82.

—— 1976b. Structural style in slump sheets, Ludlow series, Powys, Wales. *J. geol. Soc. Lond.* **132**, 399–415.

—— 1979. The use of slump structures as palaeoslope orientation estimators. *Sedimentology*, **26**, 83–99.

S. G. FARRELL, BP Petroleum Development Ltd, Farburn Industrial Estate, Dyce, Aberdeen, Scotland.

S. EATON, Grant Institute of Geology, The University of Edinburgh, Edinburgh EH9 3JW, Scotland.